University of Salford MANCHESTER

SCHOOL OF SCIENCE, ENGINEERING & ENVIRONMENT

Investigation of genetic and epigenetic mechanisms of iNOS gene expression in infection of natural populations of *Apodemus sylvaticus* with the parasite *Toxoplasma gondii*.

Asem Hassan AbdAlsalam Eshenshani.

Submitted in Fulfilment Requirements for the degree of Doctor Philosophy

February 2020

Table of contents

Table of Figures:

Acknowledgements

This work has been sponsored by the Libyan Government, I would like to express my gratitude to them, Thank you very much for my Government. I would like to extend my special appreciate to my God, and to extend my gratitude to my supervisor Professor (Geoff Hide), and his confidence in considering me as one of his students, and all my gratitude to my family (my Father , My Mother, Sister Asma/ Brothers: Ibrahim, Bashier, Mohammed, and My wife, Daughters Balqees and Hoor, Sons Mohamed and Abdalsalam & one on the way), as well my Colleagues Bader Alwafi & Al-Ammeen Mohamed, last but not least, my Tutor, relative, and the best friend, Dr, Musa Abohisa

Abbreviations

Toxoplasma gondii (T. gondii)

Surface antigen gene (SAG)

Deoxyribonucleic acid (DNA)

Ribonucleic acid (RNA)

Cytosine next to Guanidine island (CpG)

Polymerase chain reaction (PCR)

Single Nucleotide polymorphism (SNP)

Hot Start (HS)

Cycle threshold (CT)

Toll-Like receptor (TLRs)

Pathogen -Associated Molecular Patterns (PAMPs)

Declaration

I hereby announce and declare that this work has been presented in this thesis is my own work, unless otherwise stated herein.

Any other bibliography has been paraphrased and then referenced as the Academic referencing system Using a Mendeley referencing free software

I declare that this work has not been submitted for a degree or any qualification at University of Salford other university.

Abstract:

Toxoplasma gondii is a ubiquitous parasite that infects all warm blooded animals. It can cause pathology in both infected humans and infected animals. There have been many studies investigating the factors the affect infection of laboratory animals, with *T. gondii*, but relatively few that have studied mechanisms of infection in natural populations. Laboratory studies have shown that the host gene iNOS influences sensitivity and resistance to *T. gondii* infection. This study sets out to investigate the role of genetic and epigenetic mechanisms of iNOS gene expression in the outcome of infection of natural populations of *Apodemus sylvaticus* with *T. gondii*.

Collections of *Apodemus sylvaticus* were made from the Malham Tarn region of the Yorkshire Dales in the UK. These were tested for *T.gondii* infection using PCR based detection and each collection showed a significant prevalence ranging between 20 -40% of infected animals. This provided useful sample sets for investigating the role of iNOS gene expression in relation to infected or uninfected animals.

The DNA sequences of the iNOS and Arginase genes of *A. sylvaticus* were not available in the DNA databases. PCR amplification, based on development of primers, from related rodent sequences were used to build up a partial sequence of both genes. Additional use of a partial genome sequence was used to determine the sequences of several exons and introns in the *Apodemus* iNOS and Arginase genes. This also included a detailed analysis of the iNOS gene promoter and Exon 1.

Gene expression of the iNOS and Arginase genes were measured by quantitative PCR from mRNA derived cDNA. When the iNOS and Arginase gene expression was measured, uninfected *Apodemus* showed significantly higher ratio of iNOS/Arginase expression compared to infected animals.

Analysis of single nucleotide polymorphisms and epigenetic polymorphisms (methylated and non-methylated cytosines), were carried out on 144 animals within the iNOS gene promoter and exon 1. Interesting differences between infected an uninfected animal were observed that could potentially be linked to expression differences in iNOS gene expression.

The conclusions of this work are that there are both genetic and epigenetic differences in expression of the iNOS gene in wood mice and that these differences influence infection with *Toxoplasma gondii*.

Chapter 1: Introduction

1.1 Introduction:

The broad aims of this thesis are to investigate the influence of the immune regulating proteins, inducible nitric oxide synthase (iNOS) and L-Arginase, on infection of natural populations of wood mice, *A. sylvaticus*, with the protozoan parasite, *Toxoplasma gondii*. An understanding of infection in this example wild animal system could help to understand the roles of these regulators in other natural populations of animals, including humans.

Toxoplasma gondii is widely prevalent in humans and animals. It is a member of the group of organisms in the phylum Apicomplexa, a large group of protozoon parasites that includes the causative agents of cryptosporidiosis, malaria and *Toxoplasmosis* (Vannier and Krause, 2012). This group of parasites is responsible for major global health issues. *Toxoplasma gondii* can potentially infect all warm-blooded animals and birds. The definitive host of the parasite are cats, as they are the only hosts where the parasite can complete its full sexual life cycle. The main source of infection in humans is thought to be through eating contaminated food, that contains bradyzoites, which is undercooked (Dubey et al 2009). However, it is generally thought that the source of that infection in livestock comes from contaminated water, grass and soil, containing *Toxoplasma* oocysts. Another potential route of transmission is by congenital infection where the parasite is passed from the mother to her foetus during of pregnancy. In humans, this route of transmission can cause miscarriage, foetal damage or severe neuromuscular disease. There is also a high risk of serious infection in immunocompromised hosts which can occur during transplantation of organs, cancer chemotherapy or infection with HIV. The frequency of congenital transmission, is controversial with some authors reporting it to be very low, such as 1 in 10,000 live births in humans (Tenter and Weiss, 2001), and generally rare in sheep (Innes, 2010), while other studies show rates of about 75% in mice (Marshall, 2004), 69% in Sheep (Duncanson *et al*, 2001; Williams, 2005) and, more recently, 9.9% in humans (Hide, 2009, ; Yarovinsky, 2014a; Haq *et al.*, 2016).There

are several techniques used to detect *Toxoplasma* infection including conventional methods such as histological, serological and bioassay methods. Molecular approaches, such as PCR amplification from DNA, offer other diagnostic approaches and these can differentiate between strains of parasite, in more precise detail. These approaches can identify and recognise specific genotypes and strains (Johnson and Savva, 1990; Howe *et al.*, 1997), and a number of different *T. gondii* genetic markers are used for this. These include markers such as the SAG1 gene, the SAG2 5' end and the SAG2 3' end of that gene.

During infection of the human or animal body, the defence systems are activated by recognition of the infection and trigger a complex set of responses (Takeuchi and Akira, 2010). Two types of the immune system are evoked, to tackle and resolve the infection. The first response is the innate immune response which consists of sensors, such as the family of molecules known as the Toll-like Receptor (TLRs), which act by sensing Pathogen-Associated Molecular Patterns (Takeuchi and Akira, 2010), PAMPs, which are released from *T. gondii* . Secondly, there is the adaptive immune response that gets subsequently triggered to generate an antibody and cellular response. A wide variety of molecular mechanisms are involved in the innate immune response but one of the key components is Nitric Oxide (NO) which is generated by the enzyme iNOS. This molecule is an important inhibitor of intracellular pathogens. A related enzyme, L-Arginase, utilising the same substrate as iNOS (arginine), is antagonistic to iNOS and reduces the production of NO. The balance of iNOS and L-Arginase expression has been shown to have an important influence in experimental infection of laboratory mice and rats with *Toxoplasma gondii* (Li *et al.*, 2012; Zhao *et al.*, 2013; Wang *et al.*, 2015). Little is known about the influence of these enzymes on natural infection of natural populations of rodents. The broad aim of this thesis is to investigate this question.

1.2 Life cycle and Reproduction

Toxoplasmosis is considered to be one of the most frequently transmitted diseases amongst warm-blooded animals and , for birds (including humans) (Tenter, … and 2001; Philip and Michel, 2014). *Toxoplasma* was first discovered in Tunis in 1908 in a rodent, the Gundi (‘’(*Ctenodactylus gundi*), by Nicolle and Manceaux (1908). A year later Splender (1909) reported it in South America in Rabbits. Human *Toxoplasmosis* was unknown until its discovery by Wolf & Cowen (Dubey, 2009)’’) and the acknowledgement that it caused a human disease (Thomasson, 2011; Bajnok *et al.*, 2015). This is a zoonotic disease and transmission cycles can involve a wide range of both carnivores and herbivores by ingesting contaminated foodborne cysts or oocysts shed in cat faeces. Rodents considered to be an important intermediate host, to transfer the infection to other animals but specifically between cats., In 1970, a complete understanding of the life cycle was established (Dubey 1970). There are three transmission routes of the disease starting out with the definitive host the cat. Infection by *T.gondii*, can happen by ingesting oocysts produced in cat faeces which have contaminated food sources and the environment. The second method is via ingestion of undercooked meat cysts reach the stomach and duodenum and the cyst wall is breaks down to release tachyzoites. Tachyzoites infect the epithelial layer of the intestinal, then become systemic and lodge to form a cysts where it differentiates into the slowly growing bradyzoite stage (Black and Boothroyd, 2000). Liver, lung, heart can be infected but the and the optimal organ for *Toxoplasma* is the brain (Dubey, 2014; Bajnok *et al.*, 2015), Sexual reproduction is completed in the cats intestinal epithelial tissue (Su *et al.*, 2012). The third route of transmission is congenital transmission where the parasite is transmitted directly from mother to offspring. Figure1.1 shows the life cycle.

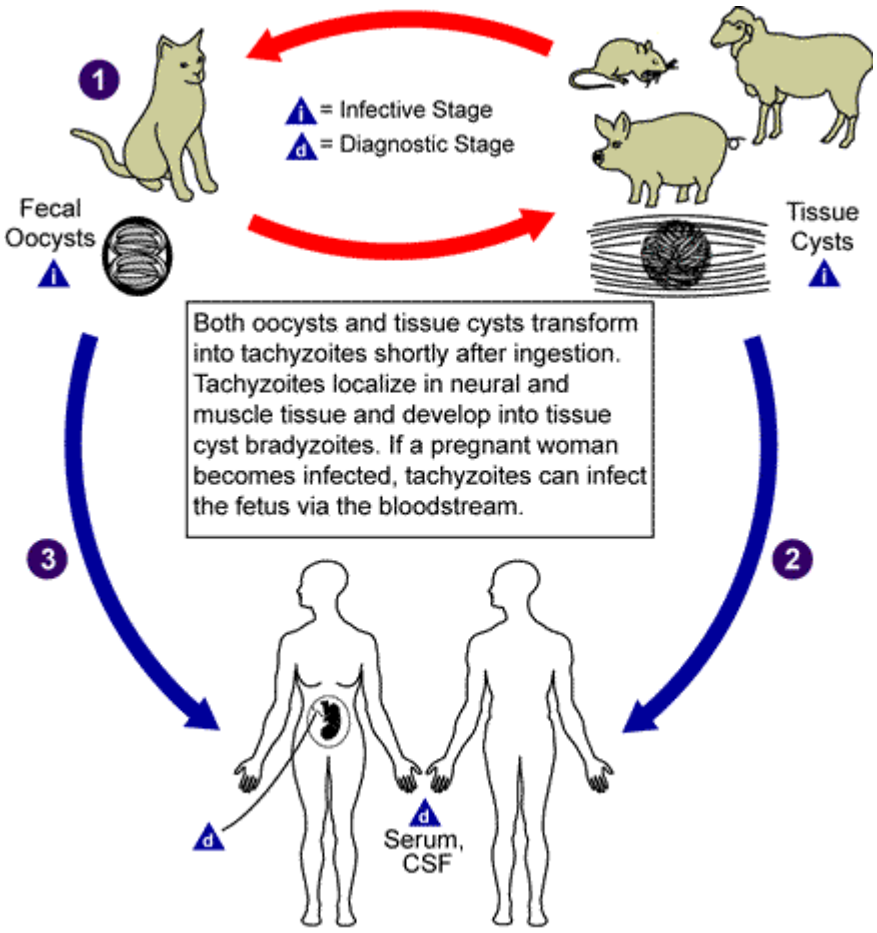

Figure 1-1 Life cycle of *Toxoplasma*.

1 Sexual reproduction is only performed in the definitive host, the cat. Oocysts develop from the male & female gametes, which are then excreted in cat faeces. Ingested oocysts infect secondary hosts such as *A. Sylvaticus,* then tachyzoites form cysts containing bradyzoites. 2. Infection can occur by carnivory – ingestion of infected meat. 3 .Congenital transmission can also occur in the secondary hosts. In the case of *Apodemus sylvaticus,* found in the region relatively free of cats at Malham, it is likely that transmission route 1 (oocysts) is reduced but that routes 2 (carnivory, perhaps by scavenging dead infected carcasses) or 3 (congenital infection) are more important. The figure is taken from the following website and also used in the following references: **(**https://web.stanford.edu/group/parasites/ParaSites2006/Toxoplasmosis/references.html**)** (Dubey et al 2009; Hunter and Sibley, 2012; Murphy *et al.*, 2008; Wen *et al.*, 2016;Dubey *et al.*, 1995; Dubey, Lindsay et al., 2009; Innes *et al.*, 2009)**.**

1.3 Morphology

Toxoplasma gondii has a typical apicomplexan structure with the dominating key feature being the apical complex. This structure comprises the conoid, that is thought to be involved with host cell invasion and motility as the parasites becomes intracellular (Graindorge *et al.*, 2016), the rhoptries and the micronemes. The latter two are thought to be the cellular machinery that manufactures and stores the enzymes necessary for cell invasion and remodelling of the cell membrane (Dlugonska, 2008). Other features typical of eukaryotic cells (e.g. nucleus and mitochondrion) are also present. These structures are shown in Figure 1.2.

The parasite exists in several different life cycle stages (Figure 1.3). The tachyzoite (rapidly diving stage) is the main trophic stage of the parasite and invades host cells, reproduces and spreads around the human or animal body. The tachyzoite becomes intracellular and can most often be seen within cells such as macrophages. The tachyzoites transform into the bradyzoite stage (slow/non-dividing stage) as the immune system starts intervening and this results in the formation of a cyst which encapsulates the bradyzoites.

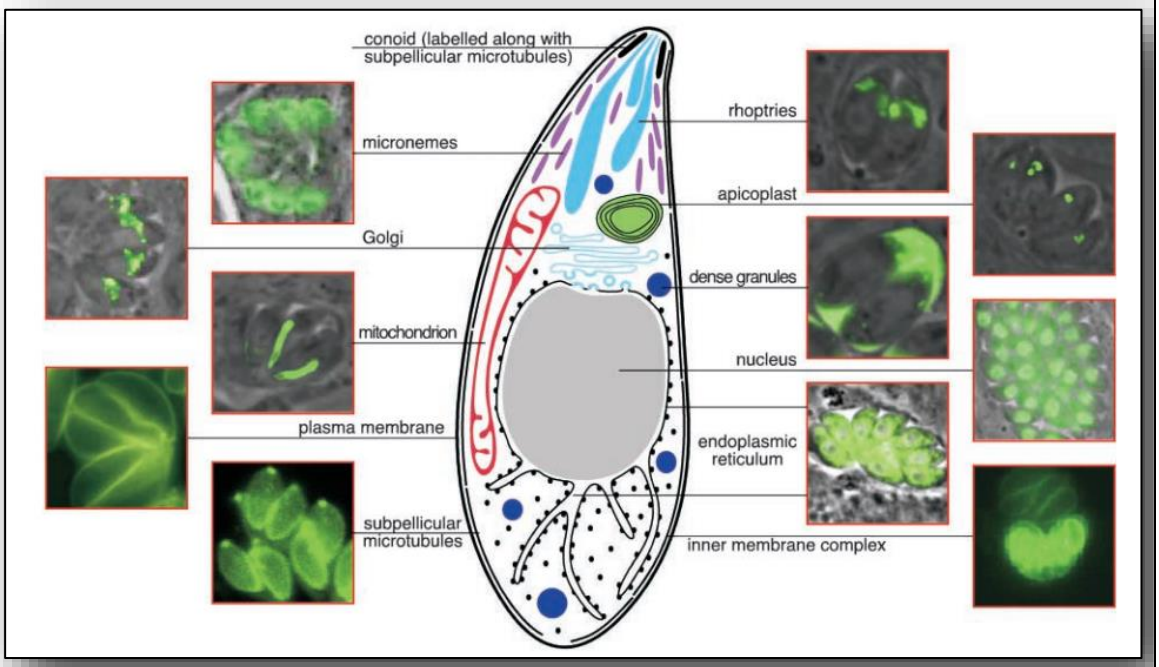

Figure 1-2 structure of *Toxoplasma*.

The parasite is pear shaped, a single cell approximately ~8µm long. The figure shows the key cytoplasmic structures as defined using specific antibodies. (Taken from: (Joiner and Roos, 2002)).

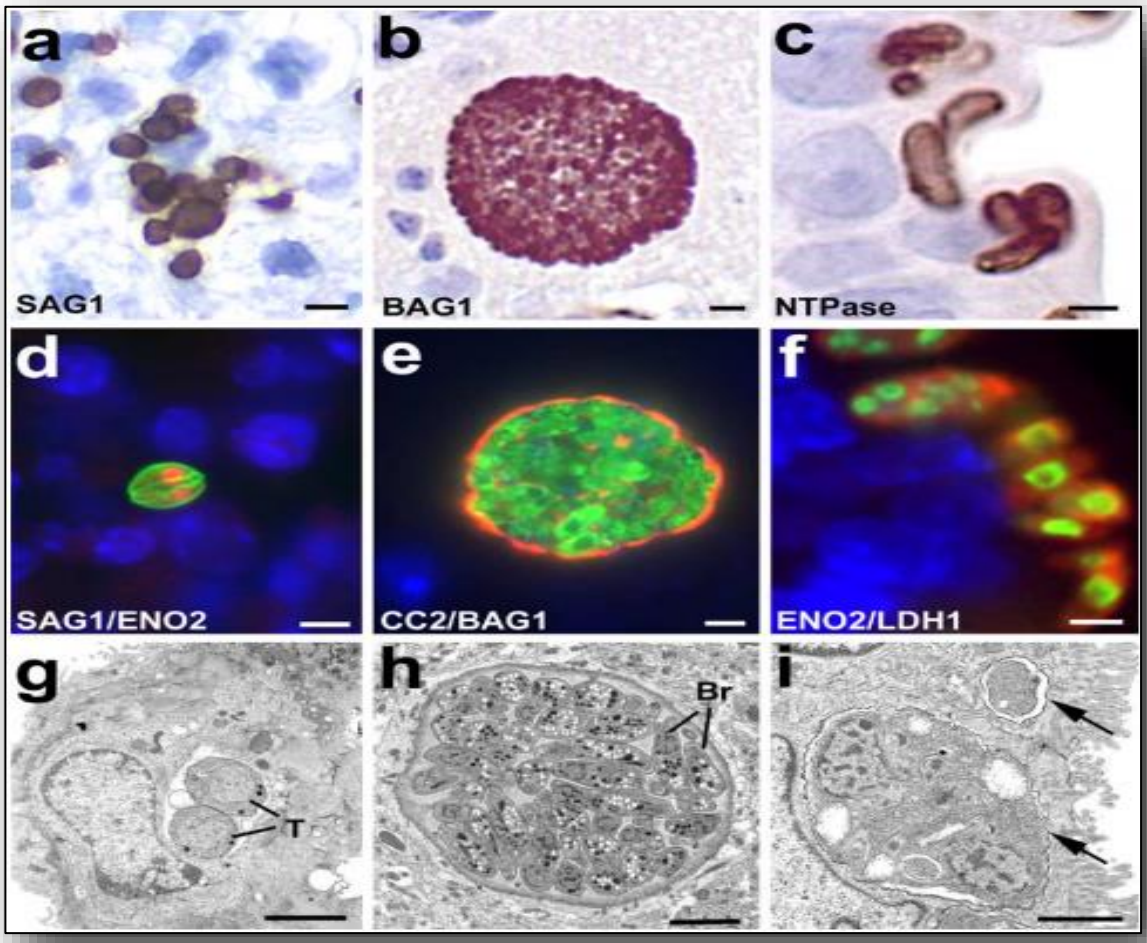

Figure 1-3 varied form stages of *Toxoplasmosis.*

Toxoplasmosis are Illustrations of life cycle stages using electron microscopy, immunocytochemistry and staining of infected tissue samples. (A), (d) and (g) are the Tachyzoite stages showing the anti SAG1 antibody shown in brown (a), (b) shows the nuclei and endoplasmic reticulum red-stained with antibody ENO2 and the anti SAG1 antibody in green; and (g) shows a phagocytosis of two tachyzoites by a Macrophage. While (b), (e) and (h) show tissue cysts: (b) stained brown using the anti Bag1 antibody which specifically recognises the bradyzoite stage, (e) shows the cyst wall stained in red with antibody CC2 and the anti BAG1 antibody staining green (Bradyzoites); (h) shows a tissue cyst containing a high number of Bradyzoites. (c), (f) and (i) show an early stage host cell invasion, (c) the Tachyzoite stages showing the anti SAG1 antibody shown in brown, (f) shows the nuclei and endoplasmic reticulum red-stained with antibody ENO2 and the anti SAG1 antibody in green; and (i) shows a phagocytosis of a tachyzoite by a Macrophage. (Taken from: (Ferguson, 2004; Prandovszky *et al.*, 2011)).

1.4 **Taxonomy**

The traditional taxonomy of *Toxoplasma* has it classified as belonging to the phylum Apicomplexa. This classification is based on the protein complex, the apical complex, which is found in all species in this phylum (Figure 1.4).

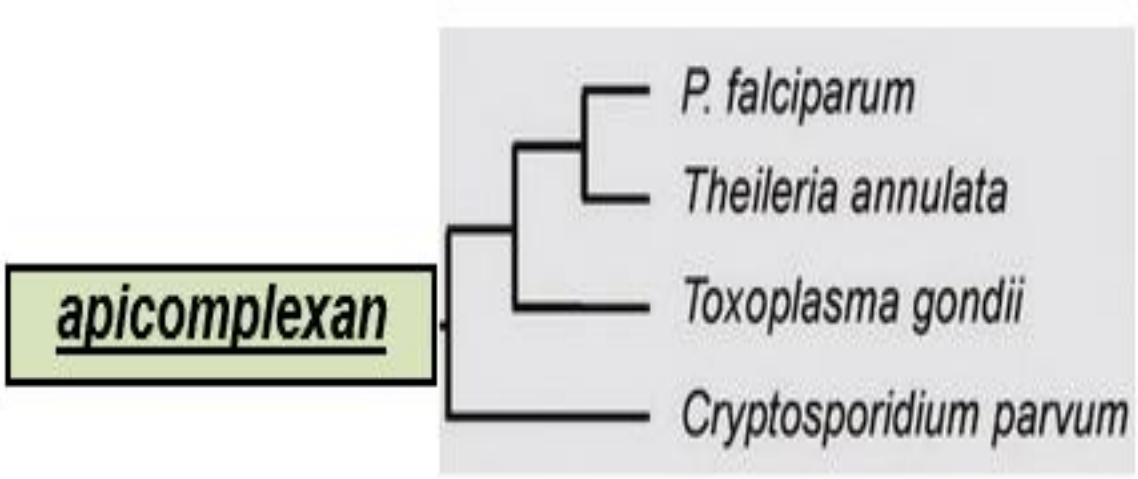

Figure 1-4 phylogenetic tree of some of the important parasites within the phylum Apicomplexa. (Taken from: (Ajioka and Soldati, 2007)).

Toxoplasma can be classified in three basic strain types based on the genotypes and nucleotide polymorphisms. These are *Toxoplasma* I,II, and Type III, and are defined using a range of different PCR markers based on RFLP analysis (Sibley and Boothroyd, 1992). In humans in the European region and North America strain type strain II is the most commonly seen genotype (Khan *et al.*, 2009). A wide range of studies have explored the genotypes in different locations. *Toxoplasma* strain types have often been described as clonal and this can be seenwhen comparing a wide range of isolated strains. For example, in Tunisia an isolate has been compared to existing isolates and is shown to be nearly identical to strains collected from many different species and locations (Figure 1.5).

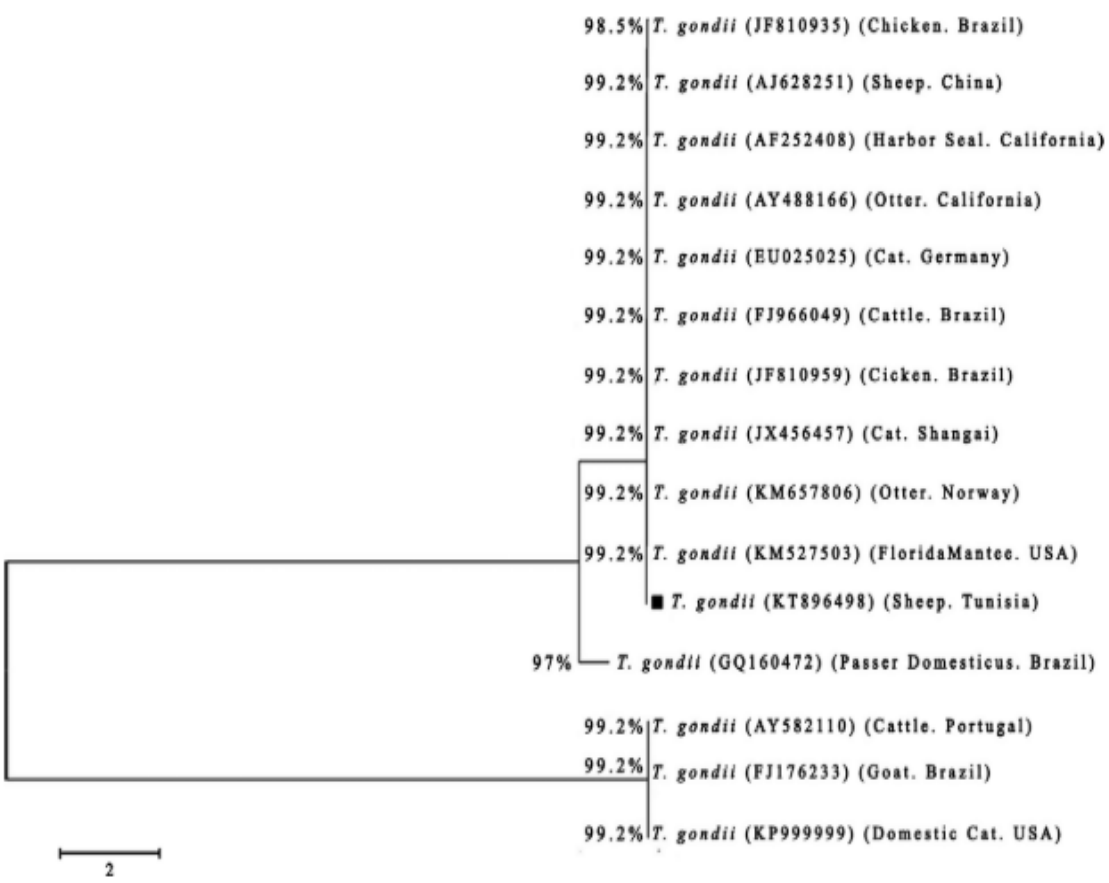

Figure 1-5 Phylogenetic tree of *Toxoplasma*.

a *Toxoplasma* isolate from a ewe in Tunisia and compares it with a number of other annotated isolates (Taken from: (Rouatbi *et al.*, 2017)).

More recent studies have shown that the number of strains is now much greater than the 3 basic strains. These are recorded in the *ToxodB* database (Bahl *et al.*, 2003; Kissinger *et al.*, 2003; Gajria *et al.*, 2008). In the wild animal of host, *A.sylvaticus* in the U.K, the subject and location on which this thesis is based, for all strain types are present but type II & III, predominate (Bajnok *et al* 2015).

1.5 Diagnosis

Toxoplasma infection is considered to cause chronicle and acute disease It can be screened and detected using a number of techniques: serological testing which recognises the presence of antibodies against *T. gondii* is the most widely used approach (Nowakowska *et al.*, 2006; Montoya and Remington, 2008; Calderaro *et al.*, 2009). Other methods comprise various types of ELISA methods, isolating *Toxoplasma* from tissue using mouse-specific inoculation, using Immune histochemistry, Immune cytochemistry with individual anti-SAG1/ENO1 antibodies (Ferguson, 2004). Genetic techniques using DNA and the polymerase chain reaction (PCR) are also available and a wide variety of markers can be used (Ferreira *et al.*, 2011; Khanaliha *et al.*, 2014). RNA detection can also be used as a method which measures gene expression but this is rarely used diagnostically (Calderaro et al., 2009).

1.6 Treatments & Vaccine

The only vaccine against *T. gondii* is an live attenuated vaccine called *Toxovax* (Dlugonska, 2008; Innes *et al.*, 2009; Bolhassani and Zahedifard, 2012). This is valid for goats and sheep in veterinary use. It is not licenced for human use due to the concerns that it might revert to a pathogenic form. There are no drugs that specifically kill *T. gondii* however sulphonamides, & pyrimethamine are reasonably effective at eliminating an infection and are typically the drugs used when a mother becomes infected during pregnancy (Araujo and Remington, 1974; Denkers *et al.*, 1993; Elsheikha, 2008).

1.7 Background to the Immune system and the interaction with *Toxoplasma gondii*

The human and animal body has several processes which make up the immune system. Each one interacts with its neighbouring system. The immune system is presented in this summary. This system defends our bodies from diseases and pathogens and it has two essential parts: the innate immune system and the adaptive immune system. The innate immune system can be divided into two types (Johnson and Savva, 1990; Gavrieli and Ben-Sasson, 1992; Furuta *et al.*, 2006), The first is an hereditary system which is an essential subsystem within the overall immune system. It includes the cells which prevent infections are a first line of defence against pathogens. A deeper look at these cells, highlights the most important receptors of this system, for example, the Toll-Like receptors. These consist of about thirteen types in mice which have been identified, and ten types in humans. They recognise a variety of pathogens. Some of them recognise gram-negative bacteria, or gram-positive viruses, fungi and eukaryotic parasites (Table 1). The essential principle behind these receptors is that they do not recognise specific antigens from specific pathogens but instead recognise generic molecular identities that are produced by pathogens but not by the host itself. The molecular signatures are know as Pathogen Associated Molecular Patterns (PAMPs) and include molecules such as Lipopolysaccharide (LPS) and various forms of nucleic acids.

Table 1-1 **varied types of TL-Like receptors**

Table 1. PRRs and Their Ligands

PRRs	Localization	Ligand	Origin of the Ligand
TLR			
TLR1	Plasma membrane	Triacyl lipoprotein	Bacteria
TLR2	Plasma membrane	Lipoprotein	Bacteria, viruses, parasites, self
TLR3	Endolysosome	dsRNA	Virus
TLR4	Plasma membrane	LPS	Bacteria, viruses, self
TLR5	Plasma membrane	Flagellin	Bacteria
TLR6	Plasma membrane	Diacyl lipoprotein	Bacteria, viruses
TLR7 (human TLR8)	Endolysosome	ssRNA	Virus, bacteria, self
TLR9	Endolysosome	CpG-DNA	Virus, bacteria, protozoa, self
TLR10	Endolysosome	Unknown	Unknown
TLR11	Plasma membrane	Profilin-like molecule	Protozoa

Examples of Toll-like receptors (TLRs). This table shows the various types of TLRs with their locations and ligands. It also shows the associated foreign bodies, which can cause disease. TLR12 and TLR 13 , from mice are not show as they were discovered later than this paper This table was taken from (Takeuchi and Akira, 2010)

Secondly, the acquired immune system is the stage in the immune reaction. It requires signals from the innate immune system and generates a specific immune response consisting of T-cell and B Cell production. Both of these cell types are produced in the bone marrow, but T-cells are then transferred to the lymph nodes and develop to become more specific in the medulla of the node. While B-cells can grow in the cortex of the lymph node, T-cells can be separated into a number of types. One key type is called CD8, or cytotoxic T-cell, another is called CD4 or helper T-cells. Figures 1.6, 1.7 and 1.8 illustrate a summary of the defence system and how it works.

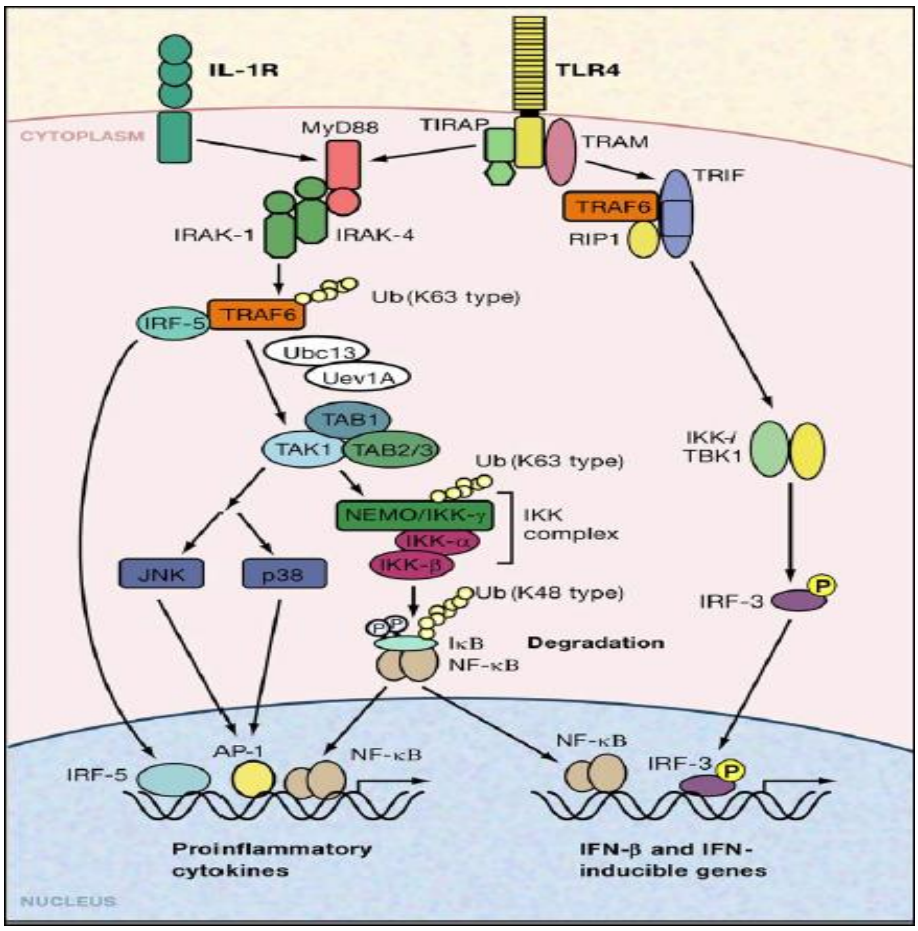

Figure 1-6 **single TLR-4**

This diagram illustrates the single TLR-4, IFN-β & IFN inducible gateway which triggers the transcription factor NFkB. Taken from: (Akira et al 2006)

Diagram (1.6) above summarises how pro-inflammation can be activated, which consists of many pathways. Firstly when LPS, a lipoprotein of a negative gram of bacteria binds to TLR4, it can cause it to dimerise with TLR6. This consists of four molecular adaptors: MYD88, then IRAK1-IRAK4, through several links to the ultimate transcriptional key molecular activator which is NF-Kb. This acts in producing a cytokine as an inflammatory response, while the type 1 IFNs cannot include MYD88 as a molecular adaptor. However, the sensing of DAMP OR PAMP, by the Toll-like receptor activates the factors of the inflammatory response, which consist of cytokines such as IFN-α,β. These produce an adaptive response. The studying of the relationship of the innate immunity TLR ("TOLL-LIKE receptors"), infected transmitting diseases by parasite, [the engagement between both of them, and which one of the

TLRs can be with specific sort of parasites] and the gene excretion of the immunity response of producing the pro-inflammatory cytokine- IFN, ILs, chemokines. These could be offering advantages to treating dangerous diseases, for instance, cancers, growth factors (GF), as disadvantages of losing control in which the overproduction of it might be vital in itself.

These Toll-Like receptors are located in the cell surface or on the surface of the endosome of DCs. Natural killer cells, macrophages, of the mammalian cell, as has been mentioned above and can be explained here in much detail. There is some ability of these receptors to recognise SSRNR (TLR7), dsRNA (TLR3), ssDNA, dsDNA (TLR9), it depends on which Toll-Like receptor. E.g. the dimerization of TLR1/TLR2,& TLR2/TLR6 recognise teichoic lip acid of gram-positive bacteria, & bacterial lipoprotein. While TLR4 h can realise LPS, of gram-negative bacteria, TLR5 can be combined with a specific target such as flagella of the bacteria which occurs, while the link activation factors between the T and B cells of the adaptive system and the innate immunity system are activating or switching on these transcription factors. The nuclear element of activated T cells (NFAT), and NF-κB, IRF, IFR factor3, besides, can be activated by a combination between TLRs and mitochondrial antiviral signal (MAVA). This combination can detect 5' triphosphate of SSviral RNA.

Finally, the Toll-like receptors are the 'first line in the immunity system against invaders, which can cause dangerous or vital diseases (Ruan and Zheng, 2011; Ruan *et al.*, 2012).

In contrast, the Focalin's: [Focalin's: which consist of collagen-Like, fibrinogens] are the molecule of the TLRs, which bind to the specific components of the strains, and they can activate the phagocytosis process by, DCS, or Natural Killer Cells to start phagocytosis or endocytosis. The cells then start processing it, and after that introducing the pathogen as simple data as an epitope, to confirm T, cells by cytokines pathway, or by MHC major histocompatibility (Johnson and Savva, 1990; Matsushita and Fujita, 2002).

Figure 5 and 6, illustrates TLRs that are located on the surface of the dendritic cell, which combines with the pathogen (PAMP) (coloured blue). It can start the process for phagosome/endosome. Upon this process, the phagosome appears as a cell compartment in which the pathogen can be eliminated (in Figure 1.7, the process is done via MHC II).

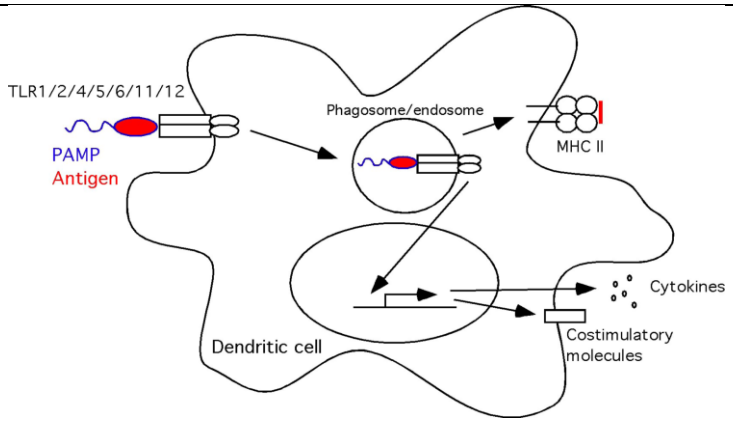

Figure 1-7 **Dendritic cell**

Dendritic Cells triggered by a PAMP. This summarises the mechanism of TLR activity and how they sense PAMPs from the pathogens. This activates phagocytosis, inflammation and activation of the adaptive immune system. The blue represents the PAMPs which are recognised by the TLRs, they are then phagocytosed and digested into key components. These are then presented on the cell service as a type II major histocompatibility molecule (MHC II) Taken from: (Iwasaki and Medzhitov, 2010).

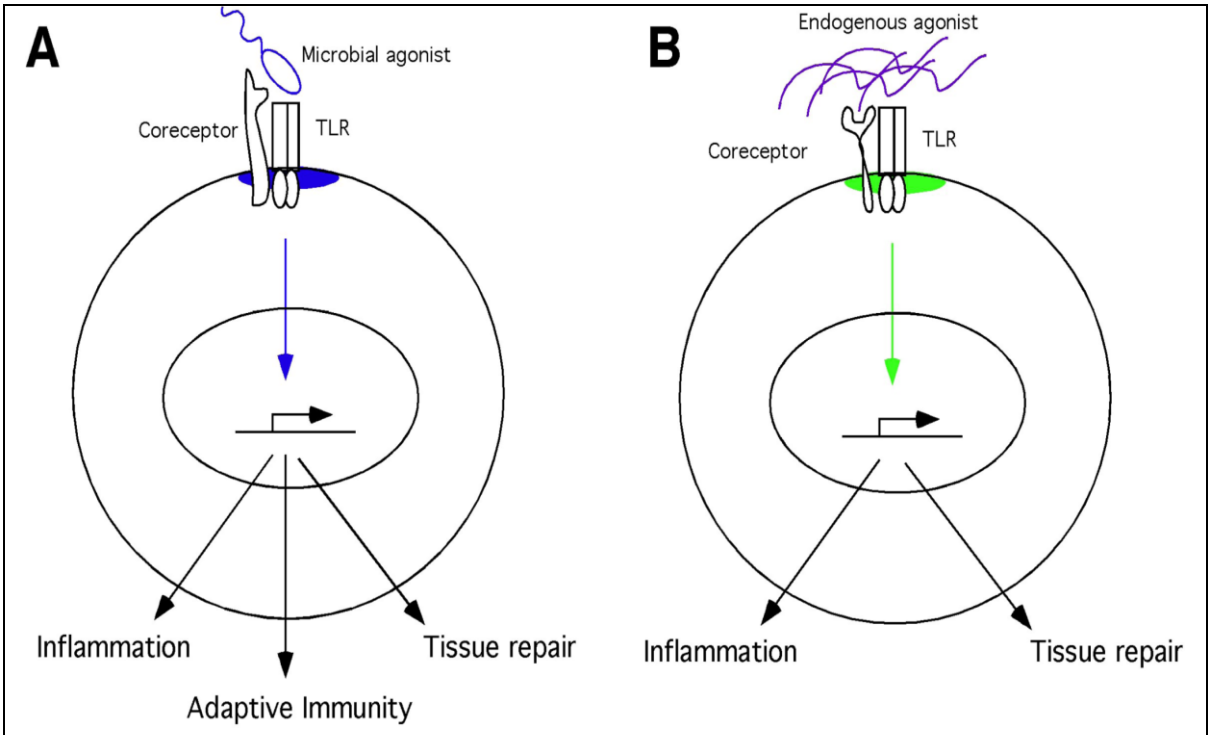

Figure 1-8 **Dendritic cells**

Effect of microbial and endogenous (host) agonists on the stimulation of Dendritic Cells via Toll-Like Receptors Taken from: (Iwasaki and Medzhitov, 2010).

In the case of *Toxoplasma gondii* the TLRs have a role in detection of the parasite. Laboratory created transgenic mice which were TLR11 deficient were highly susceptible to *T. gondii* infection (Pifer and Yarovinsky, 2011; Yarovinsky, 2014). Furthermore, it was shown that profilin, a parasite specific molecule, from *T. gondii* was required for resistance to *T. gondii* infection by means of its interaction with both TLR11 and TLR12 (Kucera *et al.*, 2010; Koblansky *et al.*, 2013) However, while studies in laboratory animals have shown the role of TLRs, little is known about what happens in wild animals. (Morger *et al.*, 2014) investigated polymorphism in both TLR11 and TLR 12 in wild wood mice, *A. sylvaticus* but were unable to detect haplotypes that were under-represented (resistance associated haplotypes) in *T. gondii* infected animals.

Another key influencer of growth in *T.gondii* is interferon gamma (IFNγ). This is released as a consequence of detection of PAMPS by Toll-like Receptors as a result of infection. Tn acts as a signal which inhibits *T. gondii* growth. This is summarised on

Figure 1.9. IFNγ binds to the surface of infected cells and can promote expression of both inducible nitric oxide synthase (iNOS) and Indoleamine 2,3-dioxygenase (IDO). The first essential inhibitory factor (iNOS) needs to metabolise Arginine to Nitric Oxide (NO), and produces substantial metabolic toxicity, which reduces the growth of *Toxoplasma* (Wilson *et al.*, 2010; Sturge and Yarovinsky, 2014; Yarovinsky, 2014).

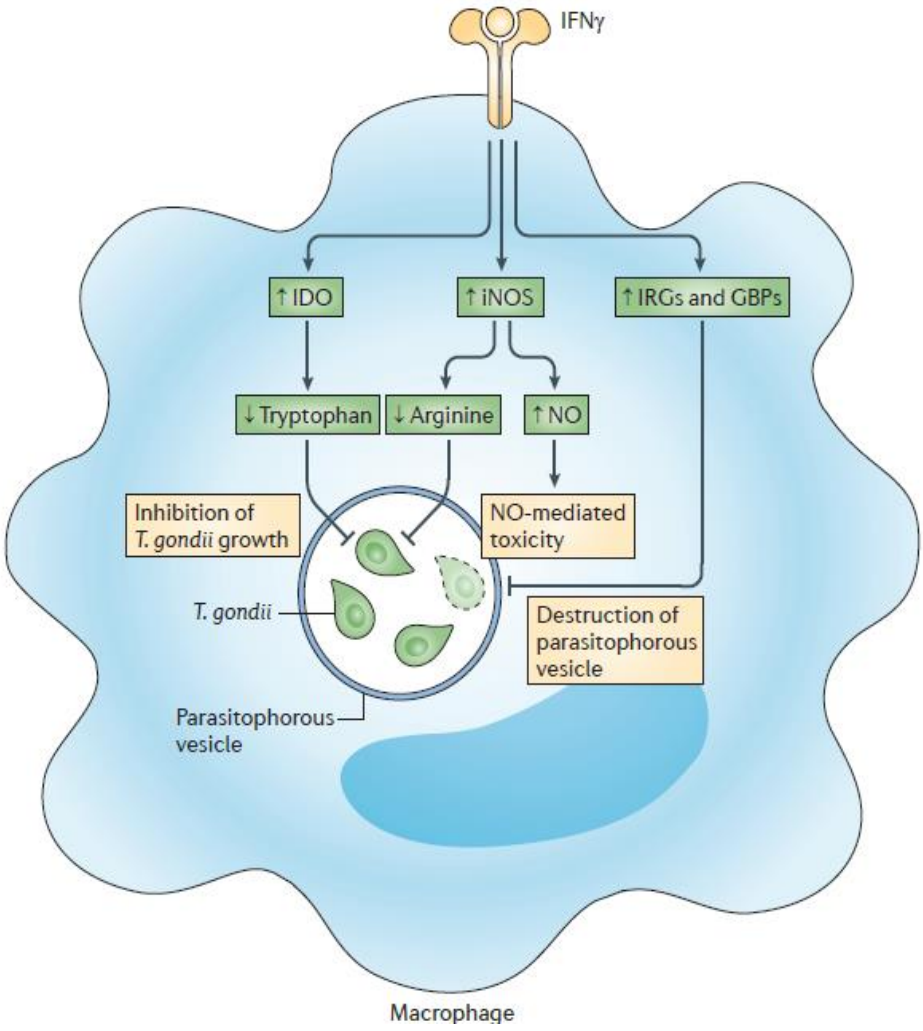

Figure 1-9 Macrophage

Action of IFNγ on infected macrophages. IFNγ prevents *Toxoplasma gondii* by activating iNOS which in turn generates the highly toxic NO. Photo Taken from : (Yarovinsky, 2014b).

The macrophage's ability to tackle the *Toxoplasma* infection is based on the expression of iNOS (Li *et al.*, 2012), which increases the toxicity and blocks

Toxoplasma metabolism. It does this by increasing NO production, reducing the essential amino acid Arginase as well as activating other highly critical factors IRGs/ GBPs that can destroy the parasite parasitovorous vacuole that protects the *Toxoplasma*, (Yarovinsky, 2014)

Previous studies (Li *et al.*, 2012; Zhao, *et al.*, 2012; Zhao *et al.*, 2013), have shown that resistance to *Toxoplasma* in rats is linked to the ability of the rats to produce high iNOS expression and low Arginase expression. The susceptibility of infection in mice (Zhao *et al.*, 2013; Hargrave *et al.*, 2019; Zhu *et al.*, 2019)is linked to high levels of Arginase and low levels of iNOS expression produced in peritoneal macrophages. Furthermore, in rat alveolar macrophages, the opposite effect is seen to rat peritoneal macrophages where there is a higher level of infection and this is associated with lower levels of iNOS and high Arginase (Zhao *et al.*, 2013). This is interesting because it shows different susceptibilities of rat peritoneal and alveolar macrophages to parasite infection despite these cells coming from genetically inbred lines of rats. Furthermore, the correlation of iNOS and Arginase expression with infection suggests that these differences in iNOS expression and protection against infection might be caused by epigenetic differences between this cell type. This raises an important question – to be explored in this thesis – as to whether the epigenetic control of iNOS and/or Arginase expression could be responsible for determining resistance or susceptibility to *T. gondii* infection.

During acute *T.gondii* infection, production of NO reduces growth of *Toxoplasma* and other intracellular pathogens however, a down side is that overproduction of NO can harm the host cells (Khan *et al.*, 1997). Nitric oxide is synthesized from arginine which increases the cytotoxicity of the macrophage as has been demonstrated in cultured tumour cell lines using the inhibitor L-N-methyarginase. There are a wide range of iNOS homologues known in a wide range of animals although the chromosomal locations of these genes varies (Murad, 2006). Knowledge of the mechanisms of how nitric oxide production is activated will be important in understanding the mechanisms of resistance (Dupont, et al 2012). Key mechanisms that need to be considered are the involvement of the transcription factor NF-kB and its role in increasing Nitric oxide levels and the reduction of *T. gondii* infection. Both TLR4 and NFkB can enhance expression of NOS2 (iNOS) and are clearly involved (Jorge, Duarte and Silva, 2010). While, mice with active TLR2, signal through IFN- gamma, combined with Tumour

Necrosis Factor alpha (TNFα) and secondary LPS alone can enhance MyD88 which can activate the transcription factor of NFkB. This is responsible for transcription activation of nitric oxide that activates mediated immunity and prohibits growth of a *Toxoplasma* (Mun *et al.*, 2003). However, as demonstrated in both cellular murine models in vivo, high arginase levels which are synthesised by M2 macrophages, hydrolyse arginine to Urea and Ornithine, and arginase is considered to be vital for *T.gondii*. A wide range of factors have been demonstrated to enable *Toxoplasma* replication in macrophages (Araujo and Remington, 1974; Li *et al.*, 2012, 2012; Li, Zhao, *et al.*, 2012; Zhao *et al.*, 2013).

1.8 DNA Methylation, epigenetics and the iNOS structure.

One of the main methods of control of gene expression is the methylation of DNA. Specifically, these epigenetic effects occur in the CpG Islands (Bird, 1986). These are runs of CG residues where the cytosine becomes methylated causing the gene to be switched on or off or to modulate expression). This form of gene control is associated with more permanency for longer term control.

The iNOS gene is located on chromosome 17 in humans (Qidwai & Jamal, 2010), and chromosome 11 in the mouse (*Mus musculus*) (Glomerulonephritis *et al.*, 1994). The *Mus musculus* iNOS gene is a large gene that has 27 exons spanning 45-50kB of genomic sequence on chromosome 11 and it expresses a mRNA of about 3700bp (Guo *et al.*, 2007). The promoter region and the 5' untranslated region (5'UTR) has been investigated (Lowenstein *et al.*, 1993). There are similarities with the human iNOS gene (called NOS2 in humans) and has a length of approximately 4200bp and occupies about 45-50kB of genomic DNA spanning 27 introns (Charles *et al.*, 1993; Mehrabian *et al.*, 1994). The promoter and 5'UTR have been characterised (e.g. Chu et al 1998) and annotated in the DNA data bases. A summary of the gene structure of the promoter, 5'UTR and Exon is shown in figure 1.10

Figure 1-10 Schematic Diagram of the iNOS gene of *Mus musculus.*

There are no published data on the iNOS gene of *Apodemus sylvaticus* however a partially completed genome is available and this could be used to convert bioinformatic information from *Mus musculus* studies to enable parallel studies in *Apodemus sylvaticus*.

It has been shown that DNA methylation can modulate gene expression (Hmadcha *et al.*, 1999; Chan, et al., 2005) with increased methylation causing lower expression and vice-versa (Kuriakose and Miller, 2010). Methylation of the iNOS promoter has been shown to be modified by exposure to environmental pollutants in humans (Tarantini *et al.*, 2009), with suppressed methylation and a consequent increase in expression of iNOS. Furthermore, evidence suggests that methylation is acting as an epigenetic method of silencing the human NOS2 gene (Gross *et al.*, 2014).

Development of tools for analysing DNA methylation patterns in *A. sylvaticus* offers the potential to develop a model system in wild animals to investigate the relationship between methylation and infection status.

1.9 Wild rodent infection with *Toxoplasma gondii* in the collection site (Malham Tarn, Yorkshire, UK).

Mice probably play an important role in *T. gondii* transmission as the cat is the definitive host and mice form a major source of prey. Surprisingly little is known about *T. gondii* prevalence in wild populations of rodents in general. Typically, epidemiological studies on mice are based on serological diagnostic methods which detect both current and historical infection (Franti *et al.*, 1976; Jackson et al., 1986;

Dubey *et al.*, 1995; Wei *et al.*, 1995; Hejlíček 1997; Jakubek *et al.*, 2001; Yin *et al.*, 2010; Bajnok *et al.*, 2015). However, studies have also been conducted using PCR–based methods (Li *et al.*, 2004; Marshall, 2004; Hughes *et al.*, 2008; Kijlstra *et al.*, 2008; Murphy *et al.*, 2008; Thomasson, 2011; Bajnok *et al.*, 2015a; Thomasson *et al.*, 2019). In the Malham Tarn area of Yorkshire, prevalence's of infection have been typically quite high: for example, 30 – 40% has been reported (Thomasson, 2011; Bajnok *et al.*, 2015a; Thomasson *et al.*, 2019). This makes this an ideal sampling site to investigate host-parasite interactions between *T. gondii* and the most common rodent, *A. sylvaticus*. The availability of samples (Bajnok *et al.*, 2015a) was utilised, alongside new collections of mice, to build a substantive collection of samples for use in this project.

1.10 **Aims of the project**

Most studies on the basis of resistance and sensitivity to infections by pathogens like *Toxoplasma gondii* have been carried out on laboratory strains of mice and rats. While these studies are highly controllable and hugely informative, they give us little insight into what happens in natural populations of animals. These lab strains are highly inbred and, in reality, probably only represent a very small sample of the wild immunological variation seen in natural populations. Furthermore, using controlled parasite doses – while helpful for reproducibility in the lab – probably do not mirror the trickle infections experienced by wild animals. The aims of this study are to try to bridge these gaps by utilising key information gained from laboratory work and address specific questions of wild animal populations. A key aspect of this is the study of iNOS and Arginase gene expression in relation to *T. gondii* infection in wild populations of wood mice, *A. sylvaticus*. The iNOS gene has a complex structure and there are 27 iNOS exons covering 50Kb of the mouse genome. Laboratory based studies have demonstrated that there is evidence that differences in the expression of these genes could be linked to resistance and susceptibility (Murphy *et al.*, 2008; Li *et al.*, 2012; Zhao *et al.*, 2013; Lun *et al.*, 2015).

To investigate iNOS / Arginase expression in *A. Sylvaticus*, new approaches need to be developed to enable analysis of these large genes. To focus this study, two key aspects were considered. Firstly, the notion that control of gene expression is often

co-ordinated through the upstream promoter regions of genes. For this reason, these areas will be focussed upon. Secondly, the studies of (Zhao *et al.*, 2013), demonstrated that epigenetic control might be important in controlling the expression of these genes. For this reason, there will be a focus on epigenetic modifications within the promoter region that might be responsible for influencing gene expression. CpG islands are key parts of the genome that can be involved in gene expression. These regions can readily become methylated at the cytosine residues, which in combination with the binding of other proteins can result in either the switching off or on of the relevant gene. The broad aims of this study are to use an existing collection of wood mice and new collections to develop a model system for investigating the roles of these genes in wild populations. A collection of *Apodemus sylvaticus* DNA samples was available from the Malham Tarn area in Yorkshire in the U.K (Bajnok *et al.*, 2015a). These have been tested for *Toxoplasma* infection and a wide range of other features. There will also be the need for new collections to enable the extraction of RNA, for expression studies, and to build up a further collection of samples. It will be necessary to develop, optimise and update protocols for reliable analysis of these genes from *Apodemus sylvaticus* which are currently poorly characterised from a genetic perspective.

The overall aim of this thesis is to investigate whether the roles of iNOS and Arginase on resistance/sensitivity to *T. gondii* infection, as defined in laboratory rodent studies, have a similar level of importance in determining infection in wild populations of rodents. There are two basic hypotheses to be tested. Firstly, an expectation of the lab results is that wild infected rodents should have a low iNOS/Arginase expression balance to enable infection with *T. gondii*. The approach to testing this will be to measure iNOS and Arginase expression levels in infected and uninfected *Apodemus sylvaticus*. The second hypothesis is that epigenetic mechanisms control the expression of iNOS and that epigenetic mechanisms may therefore control infection with *T. gondii*. The approach to investigating this will be to look for different profiles of epigenetic mutations in infected and uninfected *A. sylvaticus*.

1.11 **Objectives:**

To make a collection of *A. sylvaticus* and to investigate the prevalence of *T. gondii* in these samples. using PCR amplification protocols. Furthermore, to create a sample set to augment existing samples for subsequent analyses.

Additionally, to develop tools to investigate iNOS and Arginase genes of *A. sylvaticus*. also, measure the expression of these genes using quantitative PCR

Finally, to develop tools for investigating epigenetic differences between *T. gondii* infected and uninfected *A. sylvaticus*.

Chapter 2: Material and Methods

2.1 Sample collection

This study involves the analysis of *Toxoplasma gondii* infection and expression of host genes in the wood mouse *A. sylvaticus*. This study received ethical approval at the University of Salford, No: STR1718-32 and involves collections of wood mice made from the Field Studies Council Centre grounds at Malham Tarn in North Yorkshire England (see Figure 2.1). Permissions and collection methods have been described previously (Boyce *et al.*, 2012, & 2019; Morger *et al.*, 2014; Bajnok *et al.*, 2015). The study makes use of DNA extracted from the brains of 116 wood mice, *A. sylvaticus*, that were collected between 2012 and 2014 (Bajnok *et al.*, 2015; Duncanson *et al.*, 2001; Morley *et al.*, 2005; Thomasson *et al.*, 2011; Boyce *et al.*, 2012). A further 38 and 12 wood mice brains collected in 2014 (Hide G, personal communication) and 2017 (Eshenshani A. and Hide, G), respectively, were also used. Animals were collected and killed using the 'Code of Practice for the Humane Killing of Animals under Schedule one of the Animals (Scientific Procedures) Act 1986 as previously described (Bajnok *et al.*, 2015). The 116 wood mice DNA samples have been previously tested for *Toxoplasma* infection (Bajnok *et al.*, 2015), and the remaining 50 were extracted and tested for *T. gondii* infection by the author of this thesis.

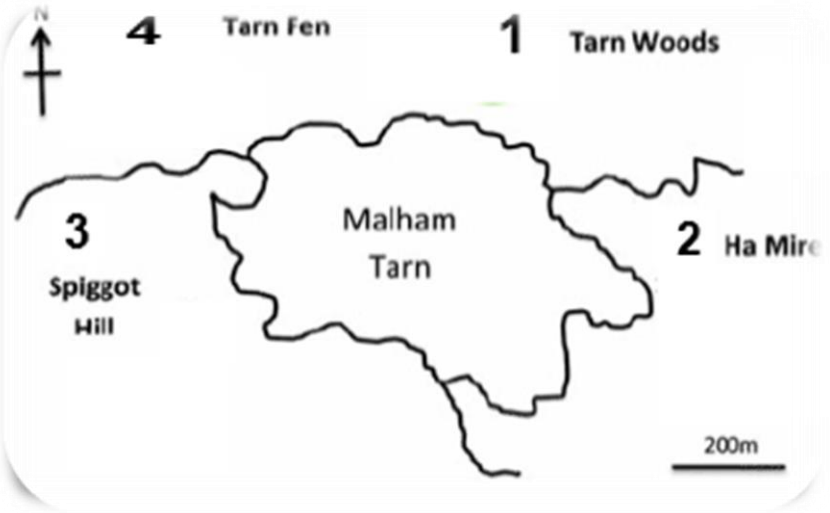

Figure 2-1 Location of collection of *A. sylvaticus* populations at the Malham Tarn Field Centre, North Yorkshire, UK. Four sampling sites were used for population 1 (Table 2-1, Bajnok, 2017) (Tarn Woods, Ha Mire, Spiggot Hilland Tarn Fen). All other samples (populations 2, 3 and 4, Table 2-1) were collected from Tarn Woods (Location 1). (Photo Taken from Bajnok *et al*., (2015)).

The Malham Tarn Field Centre occupies a periaquatic location in North Yorkshire, England, at 375m above sea level and is reputed to be the highest lake in England (Spiro *et al.*, 2002), This location has been owned by the National Trust since 1947 and has been the location of a number of scientific studies (Society, 2016)

Table 2-1. 1 Different Sample collections from Malham Tarn used in this thesis.

Population	Source	Year	Species	Number
1	Bajnok , 2017	2012	*A. Sylvaticus*	**116**
2	Malham Tarn Collection	2013	*A. Sylvaticus*	**16**
3	Malham Tarn Collection	2014	*A. Sylvaticus*	**38**
4	A. ESHENSHANI, Collection	2017	*A. Sylvaticus* *Myodes glareolus* (vole)	**8** **4**

All mice were necropsied at Malham Tarn Field Centre and brain tissue (and on occasions heart tissue) was taken, and collected in 400ul lysis buffer (100mM NaCl, 25mM EDTA, 0.5% SDS, 20mM Tris pH 8.0). For some samples, brain tissue was additionally collected in RNA Latter, for subsequent RNA extraction, and collected according to the manufacturer's instructions. The DNA (and RNA) was stored at -20^{c}0 until use.

2.2 Extraction of DNA

Phenol-chloroform extraction from mouse brain tissue was carried out as described (Morley, 2005). Briefly, samples were thawed, and proteinase K was added to a final concentration of 50µg/ml and incubated overnight at 56^{o}C. Samples were then extracted three times using 500µl Tris buffered phenol/chloroform pH8.0 with mixing for 10 minutes at each stage. The final collected supernatant was precipitated by the addition of 2 volumes of ice-cold ethanol and 0.3M sodium acetate and left overnight at -20^{o}C. Following centrifugation, pellets were resuspended in 100µl TE buffer (Yang *et al.*, 1998; Lynch and Tsai, 2002; Cheng and Jiang, 2006).

Samples were analysed by gel electrophoresis using a 1% agarose TBE mini gel system as described (Morley, 2005; Bajnok *et al.*, 2015). Briefly, 0.3 grams of agarose was added to 30 ml of 1x TBE and melted by boiling. To include the stain, 30µl of GEL RED (1000x) was added and mixed by swirling gently. Gels were allowed to set, and then covered with 1x TBE buffer (approximately 200ml) for running. Samples were loaded in loading buffer and run at 70V until the dye front had migrated 2/3 down the gel. Larger size gels were used also and reagents scaled up appropriately. Quantification of the phenol-chloroform extracted DNA, and the purity was measured using a nanodrop 2000. Using 1µl of DNA free water as a standard solution. Measurements were carried out at 260nM and 280nm to determine the concentration and purity of the DNA. Additional *Apodemus sylvaticus* Brain and Heart samples were used to extract DNA & RNA, by using commercial kits purchases from Qiagen. Protocols were followed as the recommended by the manufacturer.

2.3 PCR Amplification

PCR using universal Mouse Tubulin primers, which amplify all mammalian DNAs was carried out to investigate the quality of the extraction (Terry *et al.*, 2001). (Mouse Tubulin Forward: (5'CGT GAG TGC ATC TCC ATC CAT 3'). Mouse Tubulin Reverse: (5'-GCC CTC ACC CAC ATA CCA GTG-3'). PCR reactions were carried out using Biotaq TM DNA polymerase 5u/ul Bio21060, Master Mix, (2.5 µl of Bioline NH_4 PCR Buffer without $MgCl_2$, 1µl of 50Mm Mgcl2, with 0.25µl of dNTPs, 0.5µl of each forward & reverse primer, 18.75µl water, and of 5µl (5units Taq), 1µL of DNA. The PCR reactions were run for 40 cycles (94^0C for 40 seconds, 60^0C , for 40 seconds and 72^0C for 1:30 minutes). An initial denaturing step of 5 minutes at 94^oC and a final elongation step of 72^oC for 10 minutes was carried out to ensure complete denaturation and complete elongation. Other PCR amplifications were carried out using the same approaches but with other primer pairs, modified annealing temperatures and other modifications as listed (Wang *et al.*, 1997; Terry *et al.*, 2001).

2.3.1 Detection of *Toxoplasma gondii* DNA by SAG1 and SAG2 PCR.

The majority of the *Apodemus* samples were tested for infection with *Toxoplasma* by Dr Jaroslav Bajnok as described (Bajnok *et al.*, 2015b). In the remainder of the samples, which were tested by the author, diagnosis of the presence of *Toxoplasma* DNA was carried out by detection of the SAG1 or SAG2 genes using PCR. Detection was carried out using protocols as described (Bajnok *et al.*, 2015b). Briefly, the SAG1 protocol follows the above protocol for the mouse tubulin PCR except for the following. The annealing temperature used was 63^oC and the master mix was as follows: 2.5 µl of Bioline NH_4 PCR Buffer without $MgCl_2$, 1µl of 50Mm $MgCl_2$, 2.5µl β-Mercaptoethanol (50mM) with 0.25µl of dNTPs, 0.5µl of each forward & reverse primer, 18.75µl water, and of 5µl (5units Taq polymerase). The reaction is a two stage nested PCR. The first round follows the above protocol and uses the following primers: DS29 Forward: 5'TTGCCGCGCCCACACTGATG3', and DS30 Reverse: 5'CGCGACACAAGCTGCGATAG3' producing an expected band size of 914 bp, (Johnson and Savva, 1990). One microlitre of the first round reaction was transferred to a new tube and the above reaction was then replicated but using the following primers: DS38 Forward 5' CGACAGCCGCGGTCATTCTC 3'; DS39 Reverse

5’ GCAACCAGTCAGCGTCGTCC 3’, producing an expected band size of 522 base pairs.

The second diagnostic approach was to use the SAG2 gene. The SAG2 locus comprises two locations, the first position at 3’ end while the second location is placed at the 5’ end of the gene (Howe et.al, 1997). The SAG2 ‘3 end PCR was carried out as previously published (Bajnok et al. 2015). Briefly, the following nested primers were used in the first and second round PCRs. 1st Round: Forward: SAG2.F3 (5’ TCTGTTCTCCGAAGTGACTCC 3’) and Reverse: SAG2.R3 (5’ TCAAAGCGTGCATTATCGC 3’). The same protocol was used as for the SAG1 PCR reaction. The second-round primers that were used were: Forward, SAG2.F2 (5’ ATTCTCATGCCTCCGCTTC 3’) and Reverse SAG2.R2 (5’ AACGTTTCACGAAGGCACAC 3’).

Similarly, the SAG2 5’ end reactions were carried out under the same conditions as the SAG1 nested PCR. The following primers were used: 1st Round: Forward: SAG2. F4 (5’ GCT ACC TCG AAC AGG AAC AC 3’) and Reverse: SAG2. R4 (5’ GCA TCA ACA GTC TTC GTT GC 3’), The second round (nested PCR) used the following primers: Forward: SAG2.F (5’ GAA ATG TTT CAG GTT GCT GC 3’), Reverse: SAG2.R2 (5’ GCA AGA GCG AAC TTG AAC AC 3’) and the PCR conditions remain the same (Schumacher *et al.*, 1993; Lafay *et al.*, 1994; Follmann et al, 1996; Frank et al., 1996; Lekutis, Ferguson and Boothroyd, 2000; Mishima *et al.*, 2001; Orciari *et al.*, 2001; Grbić, 2003; Huang *et al.*, 2004; Cliquet *et al.*, 2007; Ling et al., 2008; Chong *et al.*, 2011; Rummel *et al.*, 2014; Mähl *et al.*, 2014).

2.3.2 PCR Amplification of the Arginase and iNOS gene from *Apodemus sylvaticus*

PCR amplification of the Arginase gene from *Apodemus* PCR was carried out as follows. Primers were selected from a previous publication (Li *et al.*, 2012) which used them to amplify the Arginase gene from *Mus musculus* (Forward :5’ AAG AAA AGG CCG ATT CAC CT 3’ and Reverse: 5’ CAC CTC CTCTGC TGT CTT CC 3’) which is expected to produce an expected band size of 201 bp. The reaction was carried out in 12.5 ul ready-mix Taq (Bioline, BIO-25044) (Béji-Hamza *et al.*, 2015; Berrens *et al.*, 2017; Iaconelli *et al.*, 2017; La Rosa *et al.*, 2017; Tallei, Fatimawali and Pelealu, 2019) which included $MgCl_2$, this called ready mix Taq buffer technology, 1 ul of each forward

and reverse primer10pm, 9.5 µl water, and 1 µl DNA. The PCR reactions total volume 25 ul were run for 40 cycles (94^{0}C for 40 seconds, 600C for 40 seconds and 72^{0}C for 1:30 minutes). An initial denaturing step of 5 minutes at 94^{o}C and a final elongation step of 72^{o}C for 10 minutes was carried out to ensure complete denaturation and complete elongation.

PCR amplification of the iNOS gene from *Apodemus* PCR was carried out as follows. Primers were selected from a previous publication (Glomerulonephritis *et al.*, 1994; Li *et al.*, 2012; Li, Zhao, *et al.*, 2012), which used them to amplify the iNOS gene from *Mus musculus* (Forward :5' GCCTCGCTCTGGAAAGA 3' and Reverse: 5' TCCATGCAGACAACCTT 3') which is expected to produce an expected band size of 419 bp. The reaction was carried out in 25µl PCR total volume ready-mix Taq (Bioline, BIO-25044) with 12.5 µl buffer technology which includes a 50Mm $MgCl_2$, 1 ul of each forward and reverse primer, 9.5 ul water, and 1µl DNA. The PCR reactions total volume of 25 ul, were run for 40 cycles (94^{0}C for 40 seconds, 60 C^0 for 40 seconds and 72^{0}C for 1:30 minutes). An initial denaturing step of 5 minutes at 94^{o}C and a final elongation step of 72^{o}C for 10 minutes was carried out to ensure complete denaturation and complete elongation. As these primers were unsuccessful in amplifying the iNOS gene from *Apodemus*, further sets of primers (Table 2.1) were designed (see later in the bioinformatics section for methods), based on access to the partial genome sequence of *Apodemus* (http://www.ebi.ac.uk/ena/data/view/GCA_001305905.1). Primers were designed that would be capable of distinguishing cDNA and genomic sequences by inclusion of intron sequences within the target sequence (see Chapter 4 for strategy and results). PCR reactions were carried out in 12.5 µl ready-mix Taq (Bioline, BIO-25044) buffer technology with all the PCR essentials reagents 1µl of each forward and reverse primer, 9.5µl water, and 1µl DNA. The PCR reactions were run for 40 cycles (94^{0}C for 40 seconds, 54^{0}C for 40 seconds and 72^{0}C for 1:30 minutes). An initial denaturing step of 5 minutes at 94^{o}C and a final elongation step of 72^{o}C for 10 minutes was carried out to ensure complete denaturation and complete elongation.

Table 2-2 Summary of primers used for PCR amplification of the iNOS genes in *A. sylvaticus*

Primer name	Forward	Reverse	Band Size
iNOS AF1/AR1:	5/AATGTTCCAGAA TCCCTGGAC/3	5/GCCCCTCGCTGC ATCGG/3	410bp in *Mus*
iNOS B, F2/R2:	5/AGCTCATCTTTG CCAC/3	5/AAGTACGAGTGGT TCCAGG/3	468bp in *Mus*
iNOS C, F3/R3:	5'AGAGGACAACAT CCCAAGAAG-3'	5'-TCCCAGGAG GCTAGGATAAA-3'	604bp in *Mus*
iNOS, cDNA F1/R1:	5'GAGAAGCTGAAG CCCAAGAA3'	5'GCTTGTCACCACC AGAAGTAG3'	620 bp DNA mRNA 263bp
iNOS, cDNA F2/R2:	5’ CACATCTGGCA GGATGAGAAG 3’	5’ ACCTTGGTGTT GAAGGCATAG 3’	619bp DNA mRNA 200bp

2.3.3 DNA sequencing of PCR amplicons.

PCR amplicons were sent for commercial sequencing at Source Bioscience. Amplicons were cleaned up using a Bioline Isolate II Gel kit, Bioline, BIO-52060) purification, prior to sequencing and concentrations of DNA and sequencing primers were sent as described in the instructions provided by Source Bioscience. Data was provided as an interpreted sequence (files labelled file's) and as the raw chromatogram (files labelled file.ab1). Forward and reverse sequences were generated where possible, raw chromatograms were used to check ambiguities or identify heterozygotes and forward and reverse sequences were used to generate a consensus sequence.

2.4 **Bioinformatics**

The key bioinformatics tool used to read the chromatograms was Finch TV (https://en.freedownloadmanager.org/Windows-PC/FinchTV-FREE.html) (Finch, 1956; Bruno, 2019). is the results from the sequencing come back as a chromatogram coloured in Green, Blue, Red, Black (for each base), these are used to view and to correct the sequence. Using forward and reverse sequences, where possible, or multiple replicates of sequences, sequences were corrected by checking and correcting ambiguous bases and deleting poor quality ambiguous sequences which could not be corrected with confidence. Once sequences were corrected, their identity was determined using the programme BLAST. The NCBI database (https://blast.ncbi.nlm.nih.gov/Blast.cg) (Ganley and Kobayashi, 2007; Wheeler and Bhagwat, 2007; Madden, 2013), was searched using BLAST to identify related sequences and the extent and degree of similarity was used to assess whether the correct amplicons had been generated by PCR. When comparison of sequences was required from the partial *A. sylvaticus* genome sequence, BLAST was carried out via the following web link (https://blast.ncbi.nlm.nih.gov/Blast.cgi?PAGE_TYPE=BlastSearch&PROG_DEF=blastn&BLAST_SPEC=Assembly&ASSEMBLY_NAME=GCA_001305905.1).

The programme Clustal Omega (https://www.ebi.ac.uk/Tools/msa/clustalo/) was used to create multiple sequence alignments of sequences. Sequences were formatted in the FASTA format for data entry.
In order to generate PCR primers, the Integrated DNA Technology (IDT), website was used as described in the instructions:
To check if there is any self-dimerization in the primer or production of primer dimers with the reverse primer, may or there are free tools can be used online for this purpose (Web address: https://www.idtdna.com,https://www.idtdna.com/pages/tools/oligoanalyzer).

To check for primer dimer a free website from Fisher used:(https://www.thermofisher.com/uk/en/home/brands/thermo-scientific/molecular-biology/molecular-biology-learning-center/molecular-biology-resource-library/thermo-scientific-web-tools/multiple-primer-analyzer.html)

Free calculating a copy number for the Realtime Q-PCR (www.scienceprimer.com/copy-number-calculator-for-realtime-pcr.), additionally another website used to converts a sequence to reverse sequence is (https://www.bioinformatics.org/sms/rev_comp.html)

2.5 RNA Extraction

RNA Extraction was carried out using the Qiagen kit, RNeasy Fibrous Mini Kit (50)- Cat No./ID: 47704 Kit (cat. no. 74034) as directed by the the manufacturers recommendations (Osterholzer *et al.*, 2013). During RNA extraction, DNase Digestion was carried out using an RNase-Free DNase Kit (The QIAGEN Kit, catalogue no. 79254, contains RNase-Free DNase Set (50) DNase I, RNase-Free (lyophilised) 1500 Kunitz units* Buffer RDD 2 x 2 ml RNase-Free Water 1.5 ml to set up a working solution. The kit was used as in the manufacturers protocol recommendations (He *et al.*, 2016; QIAGEN, 2018; Swiderski *et al.*, 2019).

2.5.1 Quantitative PCR (qPCR).

However, RNA extraction performed on the remaining piece of the Brain samples, taken out of the RNA later, using kit called Fibber RNeasy from Qiagen, the kit used as the manufactory recommendations, and DNA digested in the spin Column , final volume of the extraction 30µl of total RNA saved in three PCR tubes, 10µl each two of them saved in -80c^0, then the first group called A group used in Nanodrop to measure the quality and the quantity of the RNA extracted, and the result represented in the quality of the RNA extracted using RNase Fibrous kit, gives an excellent yield of the 18S & 28S RNA, However, this extraction went well as the nanodrop & agarose gel, which can perform a good q-PCR, in addition, it confirms that the gDNA digested and there is no any DNA bands can appear beside of the tow RNA bands.
Before establishing the q-PCR, there is a step which is converting all the RNA to cDNA, has been applied using a QuantiNova Reverse Transcriptase, Cat No./ID: 205410, From Qiagen (Chen *et al.*, 2016; Asumda *et al.*, 2018), contains all the important components for instances dNTPs, the enhancer the, RNase inhibitor, which can converts a total RNA consist of a poly AAA tail to a cDNA (Cho *et al.*, 2014; Kluess *et al.*, 2015; Ahmadipour et al., 2018).

"SensiFAST™ SYBR® & Fluorescein Kit BIO-96005, SYBER, all needed for qPCR, which consist a buffer chemistry technology , with the enhancer all in one, this regents considered as a Hot-Start DNA polymerase system, additionally this system called a2x master mix compromises all the necessary reagents for performing, a technology of florescent marking the taq, and when the amplification started and the taq binds the primer with the cDNA companioned sequence amplicon, it made a reflected florescent can be q-PCR detector, then it recorded with a time measurement to each amplification, logarithmic calculation via the machine shows the real time of the CT of each sample (Mehta et al., 2013; Jiménez and Forero, 2018). while used as the recommendation protocol recommendations, in addition to that a specific cDNA primer required to quantifying a specific expressed gene, two specific primers has been used for the gene expression measurements, biased for this study the are iNOS & Arginase both are ready for quantification, and measurement applied via using a Rotor-Gene Q, Cat No./ID 9001550, from Qiagen (Figueroa-López *et al.*, 2017; Kim *et al.*, 2018; Stevens *et al.*, 2019).

2.6 Bisulphite treatment of DNA, design of bisulphite primers and bisulphite sequencing.

For the epigenetic studies, the genomic location (ID: GenBank: L23806.1) of the *Mus musculus* NOS2 gene (inducible nitric oxide synthase) was searched in order to get the sequence of the promoter region 5'UTR and exon 1. This sequence was compared with the partial *Apodemus* genome to get a sequence for designing iNOS primers which covered the promoter and exon 1 of *Apodemus*. Using bioinformatic analysis, a family of primers were designed to amplify the regions of this gene as follows:

AF1:5' TGATTTGTAATTCATTTATTC3', AR1: 5'ACTAGGCTACTCCGTGGAGTGA3' expected band size 1253 bp,

primer BF2: 5'TCTTTCTGTTTGTTCCTTTTCCCCTAA3', BR2: 5'AGTATTCCAAC-GCCCAGGAAACCT'3, expected band size: 458 bp.

CF3: 5' TCTTTCTGTTTGTTCCTTTTCCCCTAA 3', CR3:5': CTAGGCTACCTAGG-CTACTCTGTGGAGTGAAC 3', expected band size1075 bp.

In order to amplify bisulphite treated DNA regions of the iNOS promoter and Exon1, special bisulphate primers need to be designed to account for the changes of Cs to Ts when they are unmethylated. Using the *Apodemus* sequence for this region, programme Bisulfited Primer Seeker (Website https://www.zymoresearch.com/pages/bisulfite-primer-seeker) was used to suggest atotal of 12 predicted primers, were chosen in the Tm range: 55-60^{o}C. These primers were confirmed by using web tools on the ZymoResearch website (http://www.zymoresearch.com/tools/bisulfite).

The following primers were chosen: BIOS F1:

5'TATTGGTTATTTGGAATTTGGATTTTTTTTTTTAG 3'

BIOS R1: 5' ATAATCCCCAATTAAATATACAAATTAACTCATTCAC 3'

expected band size 338 bp. BIOS

F2: 5' TATTGGTTATTTGGAATTTGGATTTTTTTTTTTAG 3' BIOS

R2: 5' CAATATTCCAACATACCCAAAAAACCTTCA 3' expected band size 771 bp.

BIOS F3: 5' TGAAGGTTTTTTGGGTATGTTGGAATATTG 3' BIOS R3:

5' TTTTACATAAAATCACTATTCCCCAAAAAATAATCCCC 3'

expected band size 421 bp.

BIOS F4: 5' GTTATTGAGGGAAAAAGAAAAGAAAAAGGTTG 3', BIOS R4:

5’ CCACTCCTAATCTATATACTATAACATCACTC 3’ expected band size 514 bp
BIOS F5: 5’ AGATAGTATTTTAGGGGTTTTTTTGTTTTTATAGTTTG 3’
BIOS R5: 5’ CAAAACCCRAACCTAAAAAACCTC3’ expected band size 680 bp.
Bisulphite treatment of DNA, has been carried out using a Kit called EZ DNA Methylation-Gold Cat:D5031 size 200 Rxns, from a ZYMO RESEARCH the U.S (D, no date; Gruntman *et al.*, 2008; Igarashi *et al.*, 2008; Vaitkiene *et al.*, 2013), supplied via Cambridge Bioscience, the protocell participated as the manufactory recommendation, after adding the amount of DNA 3 ul plus 17 ul of H2o, to justify it to 20 ul, a CT conversion reagent of 130 ul added in the same tube, to make a total reaction volume up to 150 ul, then the tubes carried out on the thermocycler Robo-cycler, which consist of on denaturation step at 98^{c0} for a 8 mints, aneling temperature 53^{c0} one Sycle for one hour, storage at 4^{c0}.

PCR Amplification, of DNA, applied using the one ul of non-bisulphate threated DNA, amplified with Hot Start Taq polymerase from Bioline, MyTaqHS Red Mix Bio-25047 (Laqqan *et al.*, 2017; Al Khaled *et al.*, 2018), a PCR total reaction 25ul, of 12.5 of the HS Red mix taq, 1ul of each iNOS Primers CF3

CR3, finally 9.5 ul of H2o, carried out on the 200UL PCR tube, using a Robo-cycler the U.S the temperature condition like a Tubulin condition, and the annealing temperature is 60^{c0}

Sequencing of Bisulphite PCR amplicons of bisulphite treated DNA, applied using the 3ul of bisulphate threated DNA, amplified with Hot Start Taq polymerase from Bioline, MyTaqHS Red Mix Bio-25047, a PCR total reaction 25ul, of 12.5 of the HS Red mix taq, 1ul of each PRIMERES BIOS F5/BIOS R5, finally 7.5 ul of H2o, carried out on the 200UL PCR tube, using a 96 well Robo cycler The U.S the temperature condition like a Tubulin condition, and the annealing temperature is $60^{c0,}$

2.7 Gel electrophoresis and Sequences Preparation.

Final PCR products has been separated of both of bisulphates and non-bisulphate, via 1.5 agarose gel electrophoresis FOR 1 hour 100v, and bands have been extracted from the gel using a Bioline gel extraction, BIO-52060, purification

methods, the protocol has been a participated as recommended a Nanodrop used to quantifying the PCR products, justified PCR products have been prepared as Source-Biosciences recommendation, samples 1ng/ul bear 100 bps, have packaged in the PCR tube and 3.2 pmol/ul primers has been used to amplifying a both PCR reaction sent with the samples to Commercial sequencing company (Source-Biosciences, Nottingham The U.K branch), (https://www.sourcebioscience.com/)
An account constricted with them, and a result then received via email

2.8 Statistical Analyses

Microsoft excel, has been used for the graphs construction, and whisker blots, additionally a contingency table 2x2 & 2x4 has been used online: (http://www.physics.csbsju.edu/stats/contingency_NROW_NCOLUMN_form.html) P-Value <0.05 = significant, >0.05= not significant (McCulloch, 1981; Kallianpur, 2006; Matchima, Vongprasert and Chutiman, 2018)

GraphPad prism 8 free trial downloaded from the website(https://www.graphpad.com/demos/) (Swift, 1997), University of Salford licence MATLAB R2018A software use as well (Shiue *et al.*, 2018; Hwang, Mitz and Murray, 2019).

Chapter 3: Investigation of the prevalence of *Toxoplasma gondii* infection in wild wood mice (*Apodemus sylvaticus*)

3.1 **Introduction**

A fundamental principle of any clinical and pathological study of parasitic infection is proficiency in detecting and identifying the correct organisms in diagnostic tests. In the case of zoonotic diseases these diagnostic tests need to work on both humans and animals. A wide variety of different methods are available, but modern methods are often based on the detection of specific DNA sequences.

The application of DNA technologies has improved our understanding and enabled the development of sciences like molecular epidemiology to describe the diversity and epidemiology of parasitic infections, such as those caused by *Toxoplasma gondii*, such techniques can be reliable methods to detect the parasite during host infection.

There are several different DNA sequences (or target genes) that can be used for the detection of *Toxoplasma*. Examples of these are the *Toxoplasma* SAG1 gene - the gene encoding surface antigen number 1; SAG2 and many others (Bajnok *et al.*, 2015a).Target genes such as these can be used to diagnose infection by *Toxoplasma* in warm-blooded hosts like humans and animals as they are specific to the parasite, and these genes are absent in the host. They are accurate as their function is to provide a defence against the host (Ideozu *et al.*, 2015; Haq *et al.*, 2016; Wen *et al.*, 2016). The use of specific target genes, such as these, can be used with the polymerase chain reaction to develop an accurate and sensitive diagnostic technique. The overall aims of this chapter are to test a collection of wood mice (*A. sylvaticus*) samples for *Toxoplasma* infection to establish which are infected. These can be used for later analysis of differences in DNA sequences of immune system genes (either polymorphisms or epigenetic marks such as methylation) between infected and uninfected mice. A collection of brains from 38 wood mice were available from a previous project, and these were used as a base population to investigate the prevalence of *Toxoplasma* infection and provide DNA for further downstream analyses.

3.2 **Objectives**

1. Extract DNA from Wood mice brain and heart samples.

2. Measuring the quantity and quality of the DNA obtained.

3. Conduct PCR reactions using generic mammalian tubulin primers to establish that each sample can be amplified.

4. Test for *Toxoplasma* using SAG1, SAG2 3end and SAG 2 5end PCR amplification using specific primers.

5. Use agarose gel electrophoresis to separate the DNA and identify PCR amplified DNA fragments.

6. Sequence, the PCR amplicons samples, to confirm that they are from *Toxoplasma*.

3.3 Material & Methods

DNA was extracted from brain and heart tissue from the wood mouse *A. sylvaticus* using a Phenol-chloroform DNA extraction method as described in Chapter 2. DNA concentrations were measured using a Nanodrop 2000 spectrophotometer. PCR amplification of the target genes (Tubulin, SAG1, SAG2) and agarose gel electrophoresis was carried out as described (Chapter 2, Section:2.2-2.3.1).

A collection of wood mouse (*A. sylvaticus*) samples was collected from the Malham Tarn area of the Yorkshire Dales as part of another project in 2014. Table 3.1 provides details of the mouse characteristics and other parasite infections. Further samples, obtained from an earlier study in 2013 were also used to supplement some aspects of this study – these are described earlier in the relevant section, (Chapter 2, Section: 2.1).

Table 3-1 *A. sylvaticus* collection from 2014

The table shows the year of collection, mouse identification number, sex, length (cm), weight (g) and infection intensity (numbers of parasites) for a range of gastrointestinal and other parasites (H, *Heligmosomoides*; P, *Plagiorchis*; S, *Syphacea*; C, *Capillaria*; Tr, *Trichostrongylus*; Ta, *Taenia,* Hy, *Hymenolepis*.)

Year	Mouse	Sex	L	Wt	H	P	S	C	Tr	Ta	Hy
2014	406	F	7.1	14	0	0	0	0	0	0	0
2014	408	F	8	15	12	0	0	0	0	0	0
2014	409	M	8	17	0	1	0	0	0	0	0
2014	410	M	8	19	0	0	0	0	0	0	0
2014	411	M	8	20	0	0	0	0	0	0	0
2014	412	M	6	13	0	0	0	0	0	0	0
2014	413	M	8.5	20	1	0	0	0	0	0	0
2014	414	M	9	21	3	0	3	0	0	0	0
2014	415	F	8.3	16	0	0	14	0	0	0	0
2014	416	M	8	18	1	0	0	1	0	0	0
2014	417	M	8	18	0	0	0	0	0	0	0
2014	419	F	8	22	1	0	0	0	0	0	3
2014	420	M	10.2	23	6	0	0	0	0	0	0
2014	421	F	7	13	7	0	0	0	0	0	0
2014	422	M	7.2	14	5	0	0	0	0	0	0
2014	423	M	7.2	14	28	0	0	0	0	0	0
2014	424	M	6.5	13	0	0	0	0	0	0	0
2014	425	M	8.5	16	4	0	0	0	0	0	0
2014	426	M	6.8	15	2	0	1	0	0	0	0
2014	427	F	6.6	16	0	2	0	0	0	0	0
2014	428	F	7.4	17	0	0	0	0	0	0	0
2014	429	M	7.5	18	0	0	0	1	0	0	0
2014	430	M	8.2	13	1	0	0	0	0	0	0
2014	431	F	7.7	15	10	0	0	0	0	0	0
2014	432	F	8.6	19	0	0	0	0	0	0	0
2014	433	M	8.1	16	6	1	2	0	0	0	0
2014	434	M	5	17	0	0	0	0	0	0	0
2014	435	M	7	16	0	0	0	0	0	0	0
2014	436	M	8	16	2	0	0	0	0	0	0
2014	437	M	7	16	0	0	0	0	0	0	0
2014	438	M	7.2	19	6	0	0	0	0	0	0
2014	439	M	6.5	18	0	0	0	0	0	0	0
2014	440	M	5	14	0	0	0	0	0	0	0
2014	441	M	72	13	0	0	0	0	0	0	0
2014	442	M	8	20	4	0	1	0	0	0	0
2014	443	M	9.2	25	4	2	0	0	0	0	0
2014	444	M	7.1	23	0	0	0	0	0	0	0
2014	445	M	9	19	0	1	0	0	0	0	0

3.4 **Results**

3.4.1 Extraction of DNA from *A. sylvaticus* samples.

Genomic DNA was extracted from the brain tissue from 38 *A. sylvaticus* (Table 3.1) by using phenol-chloroform, and then the concentration and purity were measured using a Nanodrop 2000 spectrophotometer. A ratio of absorbances at 260nm and 280nm (A260 over A280) gives a value of 1.8 for pure DNA. Results represented in Table 3.2. In all cases, there was DNA present at reasonable concentrations (ranging from 19.4 to 124.9 ng/µl). Samples were extracted with this method and had a high purity of 1.8 to 1.9. The extraction was successful and can be used to obtain DNA with high purity.

Table 3-2 Concentration and purity extracted of DNA from brain tissue from *Apodemus*

Information is provided on the tissue type (B = brain), the animal code and details of the concentration and purity of the DNA.

NO	Type	Code	Concentration A260, ng/μl	Purity 260/280
1	B	406	34	1.9
2	B	408	28	1.9
3	B	409	41	1.9
4	B	410	28	1.9
5	B	411	21	1.8
6	B	412	35	1.9
7	B	413	63	1.9
8	B	414	50	1.9
9	B	415	67	1.9
10	B	416	39	1.9
11	B	417	124	1.9
12	B	419	24	1.9
13	B	420	44	1.9
14	B	421	48	1.9
15	B	422	44	1.9
16	B	423	80	1.9
17	B	424	69	1.9
18	B	425	46	1.9
19	B	426	19	1.8
20	B	427	65	1.9
21	B	428	96	1.9
22	B	429	25	1.9
23	B	430	102	1.9
24	B	431	72	1.9
25	B	432	46	1.9
26	B	433	32	1.9
27	B	434	64	1.9
28	B	435	41	1.9
29	B	436	48	1.8
30	B	437	103	1.9
31	B	438	23	1.9
32	B	439	45	1.9
33	B	440	25	1.9
34	B	441	55	1.9
35	B	442	63	1.9
36	B	443	60	1.9
37	B	444	28	1.9
38	B	445	52	1.9

3.4.2 Analysis of DNA quality by Gel Electrophoresis:

To build up a resource of DNA to investigate infection with *Toxoplasma gondii* regarding host immune gene expression, DNA extraction was carried out, as described, on 38 samples. To evaluate the presence and purity of DNA, samples were examined by gel electrophoresis. In some gels DNA samples were visible as a smear (data not shown) with the smear representing a range of sizes of DNA from large to small and demonstrating that the DNA was good. Other samples showed no DNA and were extracted again. It was observed that there was some variability in the strength of the bands. This reflects differences in extraction efficiency or in amounts of starting material (45ng/µl compared with 25 ng/µl see Table 3.2 above). However, the gel electrophoresis demonstrated that a high proportion of smaller DNA fragments were present in all samples suggesting that some degradation may have occurred or that the samples contained a lot of RNA. The slightly higher ratios of the spectrophotometric analysis (A260nm/A280nm =1.9) also supports the possibility of an overabundance of RNA.

DNA quality, purity & concentration were measured using the Nanodrop spectrophotometer. Typical results are shown in figure 3.1.

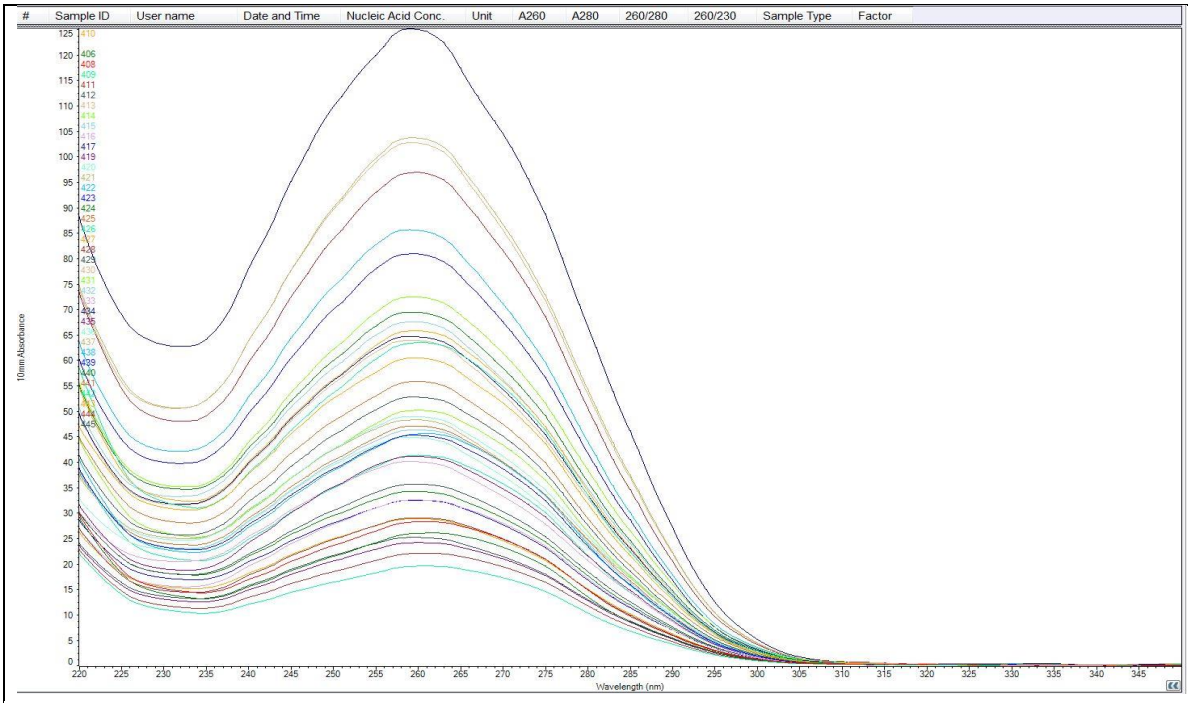

Figure 3-1 **Example Nanodrop chromatogram of *Apodemus* DNA samples.**

This figure is an example illustrating the output from the Nanodrop spectrophotometer showing the profile of absorbance across a range of wavelengths. DNA purity of mouse brain tissue extracted DNA was achieved in this way. The peak of this graph at 260nm represents the concentration of each sample. Each sample is indicated by a single line. The higher the peak and the sharper, the subsequent decline to 280nm means the highest amount and purity. For example, sample number 429 has the highest purity, followed by samples number 437.

Overall, this data shows that the extraction of the DNA has been successful, as has been confirmed by the quantitative measurements, purity measurements and by agarose gel electrophoresis. This method has obtained excellent purity of DNA for all the samples. However, the gel electrophoresis demonstrated that either a high proportion of smaller DNA fragments were present, or RNA contamination was present. To ensure that the DNA is suitable for use as a template for PCR, a control PCR amplification for host DNA is necessary. Generic mammalian primers for tubulin can be used for this purpose.

3.4.3 Use of Tubulin PCR to test for the quality of the Wood mouse DNA and the capability for PCR amplification.

To investigate the quality of the DNA extraction and suitability for use in PCR detection of the parasite, PCR amplification of the host tubulin gene was tested. PCR amplification using mouse tubulin primers is used routinely to amplify Mammalian DNA. The ability of tubulin primers to anneal to a wide variety of DNAs of many species of mammals including human DNA, makes this an excellent system to evaluate the quality of DNA. In our laboratory, these primers have been shown previously to amplify DNA from sheep (Terry *et al.*, 2001), foxes (Smith *et al.*, 2003), domestic mice (Marshall, 2004), wood mice (Hughes *et al.*, 2006; Thomasson, 2011; Bajnok *et al.*, 2015), rabbits, bats and humans (Murphy *et al.*, 2008; Dodd *et al.*, 2014; Haq *et al.*, 2016; Bajnok *et al.*, 2019b). The sizes of PCR amplicons vary between each of the other listed species.

Sequences of experiments carried out to develop a working protocol for the tubulin PCR reaction and to test the extracted DNA samples. In an initial analysis, an existing protocol was used. The results of the initial investigation using a control DNA sample and mouse 406 is shown in Figure 3.2. A band size of around 1200 base pairs was seen in the positive DNA control and mouse 406 while no bands were seen in the negative control (water). The band sizes of 1200bp are consistent with the sizes expected for the mouse tubulin gene in *Apodemus*. The bands seen in Figure 3.6 were very faint. This might be due to an error in loading, as loading small amounts of DNA is sometimes difficult, and it takes time to practice loading correctly. There are, however, several other interpretations, for instance, low concentration of the primer, or the presence of some inhibitors that inhibit the PCR, to work correctly, but it appears this result has worked successfully.

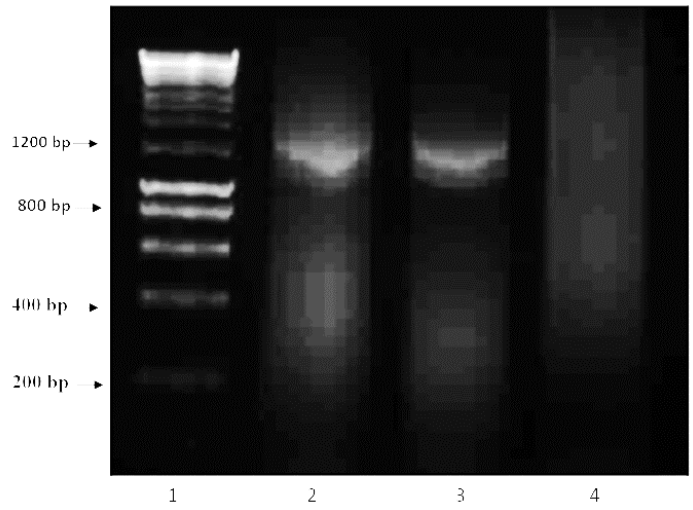

Figure 3-2 PCR amplification of Tubulin gene marker from *A. sylvaticus*.

Lane 1 is the 1Kb marker; lane 2 is a sample the genomic DNA of a mammal (mouse) used as a positive to indicate that the PCR has worked, lane 3 is *Apodemus* 406 DNA from Brain, 4 is the negative control (H_2O).

To test further samples and to try to improve the signal strength for the band, further PCR amplifications were carried out. An example is shown in figure 3.3. The results show that a faint band can be seen in some samples and that the PCR amplification has only partly worked. However, there was considerable background smearing which is obscuring the target band, and the band itself was faint. There are several possible reasons that have caused this PCR reaction to be poor. It could be because an increased amount of DNA was used (2µl instead of 1µl) and possibly due to too much primer. It also seen that primer dimers have produced a very strong smear in the positive samples:(414, 409, 410, 412) and also the negative control. This last result is supporting this notion that the primer concentration is too high.

To investigate whether the primer concentration was too high, some optimisation experiments were carried out. The PCR performed better once the primer concentration was reduced. to test amplification from the complete set of samples, a tubulin PCR amplification was carried out on wood mouse brain DNA samples from mice coded (406-445) with a reduced primer concentration (20 pM) to (10 pM). The results are shown in Figure 3.3. The results show that there is a band of 1200 bp in most samples and is negative in the negative control indicating that amplification using

the tubulin primers was specific. Only samples 415, 416 and 428 did not convincingly amplify. The negative results found for these samples suggest that they need to be tested again. It is possible that some pipetting errors occurred when setting up the tubes or the DNA was poor quality.

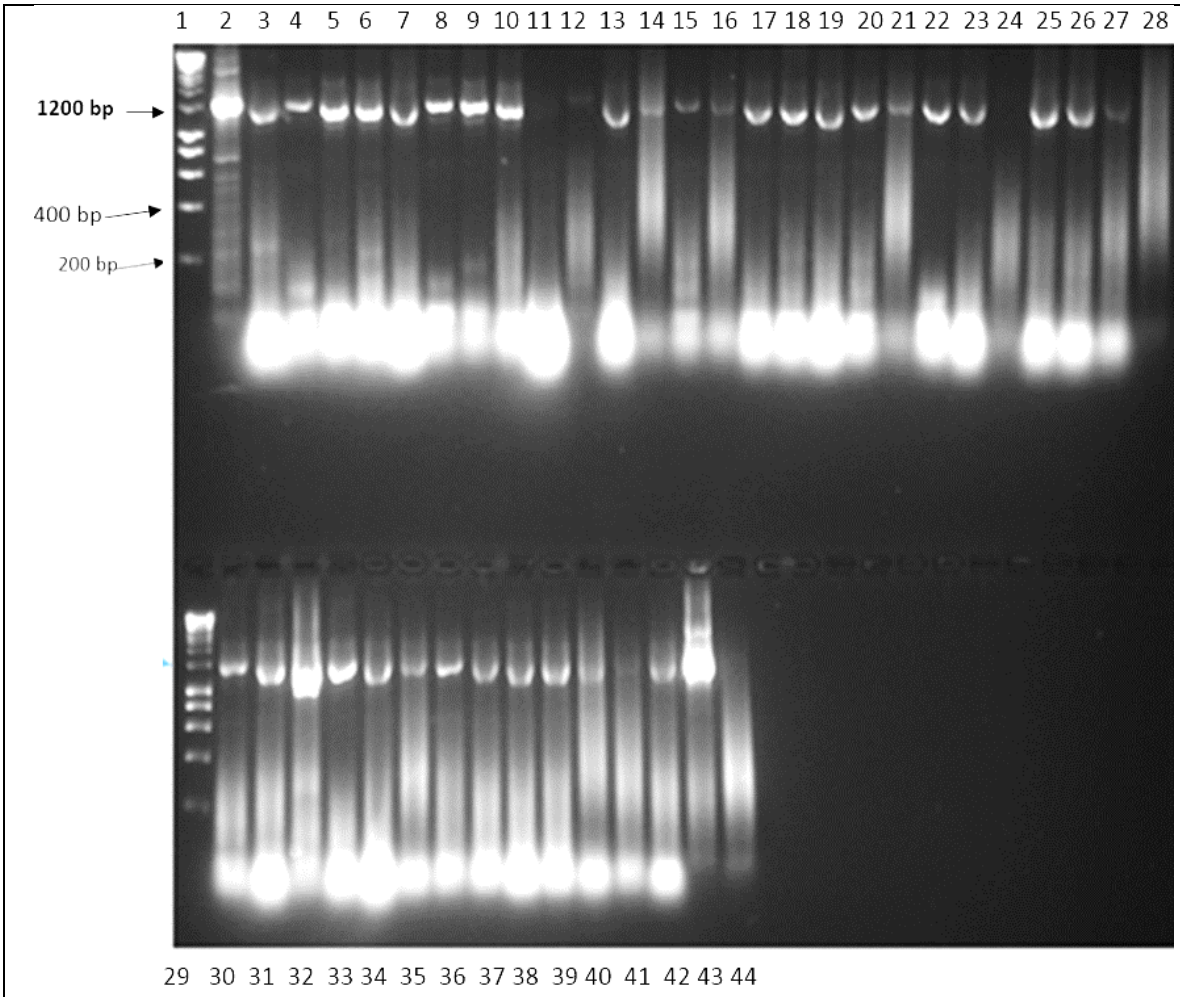

Figure 3-3 PCR amplification of the Tubulin gene marker from *A. sylvaticus* for samples 406 to 445.

Lanes were prepared as follows with the target DNA sample indicated. Lane 1= 1kb hyper ladder, lane 2 = positive control DNA, lane 3= 406, lane 4 = 408, lane 5 = 409, lane 6 = 410, lane 7 = 411, lane 8 = 412, lane 9 = 413, lane 10 = 414, lane 11 = 415, lane 12 = 416, lane 13 = 417, lane 14 = 419, lane 15 = 420, lane 16 = 421, lane 17 = 422, lane 18 = 423, lane 19 = 424, lane 20 = 425, lane 21 = 426, lane 22= 427, lane 23 = 428, lane 24 = 429, lane 25= 430, lane 26 = 431, lane 27 = 432, lane 28 = 433, lower panel: lane 29 = 1Kb hyper ladder, lane 31 = positive control of DNA, lane 32 = 434, lane 33 = 435, lane 34 = 436, lane 35 = 437, lane 36 = 438, lane 37 = 439, lane 38 = 440, lane 39 = 441, lane 40 = 442, lane 41 = 443, lane 42 = 444, lane 43 = 445, lane 44 = negative control contains just water.

The results presented show significant amplification in more than 90% of the samples, also, the negative control has not worked which means there is no contamination and the experiment worked well. In conclusion, 35 of the 38 wood mouse samples were tested, and the tubulin has been amplified successfully, and these samples could then

be used to test for the presence of *Toxoplasma* DNA. Further experiments demonstrated that the remaining three could be amplified if more template DNA was used.

3.4.4 Investigation of *Toxoplasma* infection in *Apodemus* samples using SAG1 PCR:

To detect whether these samples were infected, a specific nested PCR reaction was carried out using primers that recognised the SAG1 gene. The results from the second-round amplification are shown in figure 3.4. A band size of 522bp is expected in infected samples.

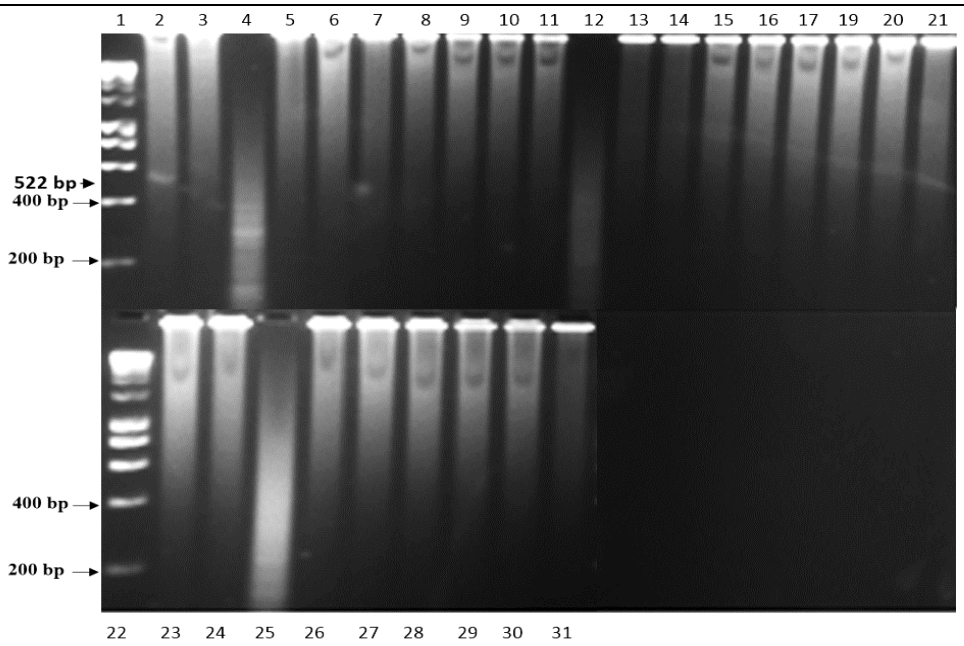

Figure 3-4 Second round PCR products from the specific nested PCR amplification the SAG1 gene of *Toxoplasma* in *A. sylvaticus* DNA samples.

Lane 1= 1kb hyper ladder, lane 2 = positive control of DNA, lane 3= 406, lane 4 = 408, lane 5 = 409, lane 6 = 410, lane 7 = 411, lane 8 = lane 412, lane 9 = 413, lane 10 = 414, lane 11 = 415, lane 12 = 416, lane 13 = 417, lane 14 = 419, lane 15 = 420, lane 16 = 421, lane 17 = 422, lane 18 = 423, lane 19 = 424, lane 20 = 425, lane 21 = 426, lower panel : lane 22= 1Kb hyper ladder, lane 23= 427, lane 24 = 428, lane 25 = 429, lane 26= 430, lane 27 = 431, lane 28 = 432, lane 29 = 433, lane 30 = 434, lane 31 = negative control containing just water.

The *A. sylvaticus* brain samples were tested using the SAG 1 nested PCR system to detect potential *Toxoplasma gondii* infections as described in Chapter 2. The results are shown in Figure 3.4. A very faint band in the positive control is seen, and the band size is approximately the correct size of 522bp as judged by a log size/mobility plot. There was no amplification for SAG1 in samples 406 - 434. There is a slight faint band in the sample no 408 it is about 180 bp, but this is below target. The negative control, containing water, shows no DNA amplified bands, and this confirms that the reaction was clear of any contaminants.

Using the SAG1 nested PCR, the positive control has worked and produced a band of the correct size, but there were no detectable bands in any of the samples. Due to the faint band in the positive control and the high background in the batches, it suggests that either the samples were uninfected or that the SAG 1 nested PCR was not performing optimally.

Furthermore, several different aspects might be contributing to conditions that might have been responsible for creating inhibitors which could be impeding the PCR to amplifying this target gene. For instance, it might be that the concentration of SAG1 is too low and SAG1 is sometimes challenging to expand in the experience of lab members. There is also, sometimes, an improvement with operator experience. To confirm the identity of the control band and any possible bands from the samples were purified and the amplicons sent for sequencing to Source Bioscience UK. They returned without a signal, and this was probably due to the low signal intensities. It would be necessary to try to work on the SAG1 PCR system to improve the performance.

To improve the SAG1 PCR, a new reaction mix, commercially supplied, was investigated. The MyTaq mix polymerase system from bio line was tested on just the positive control sample following the recommended protocol (see Chapter 2). Secondly, the objective was to investigate if there is any effect of the addition of β-Mercaptoethanol to the reaction mixture. The latter reagent is used in the previous experiments as part of the existing protocol.

Nested SAG1 PCR was carried out on the positive control using the MyTaq red mix with and without the β-Mercaptoethanol. The results are shown in figure 3.5.

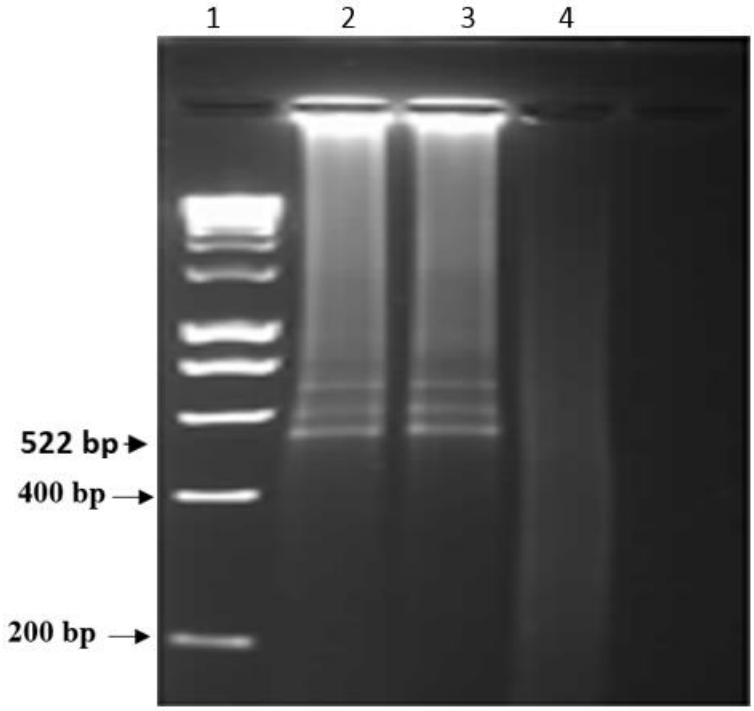

Figure 3-5 PCR amplification of the SAG1 PCR using the MyTaq buffer and polymerase system.

A 1.5 % agarose gel was used to resolve fragments of a smaller size for clarity. Lane 1= 1kb hyper ladder, lane 2 = positive control of infected brain from *A. sylvaticus* with β-Mercaptoethanol, Lane 3= positive control of infected brain from *A. sylvaticus* DNA without β-Mercaptoethanol, 4 = negative control containing just water.

Figure 3.5 demonstrates that the system appears to be working much better. Bands of the correct size were seen (522bp), but there were also other bands present which could confuse the diagnostic test. There appeared to be no difference between the presence and absence of β-Mercaptoethanol. To check that the 522bp bands were amplicons of the SAG1 gene, the PCR products were purified and sent to Source Bioscience for sequencing. The sequence that returned was viewed by the programme Finch TV, and this was followed by manual checking of the sequencing peaks and clarification of any ambiguous bases (removal of N's from the raw sequence. Figure (3.6), shows the sequence. This sequence was then used in a BLAST search using the programme Mega Blast. The results showed a somewhat similar sequence to the SAG1 gene and matched at 97%, and the probability that it was not SAG1 (E value

0.0) was zero and therefore confirmed that it was the correct product. The results show that it is the *Toxoplasma gondii* surface antigen one gene (SAG1). This demonstrates that the SAG1 PCR is amplifying the correct sequence. The sequence derived from the SAG1 amplification was compared with the SAG1 sequence, identified in the database (Accession No S85174 – the *T. gondii* SAG1 gene), by alignment using the programme CLUSTAL (Figure 3.7). The alignment was nearly perfect. The discrepancies could be due to a few errors in the sequence from the amplicon which could not be corrected. Al in all, the data support the conclusion that the 522bp band is the correct band.

TGGGCTAAAAAGGCTGCAAGAGACTCCCACTCTTGCGTACTCACCCAACAGGGA
ATCTGCCCAGCGGGTACTACAAGTAGCTGTACATCAAAGGCTGTAACATTGAGCT
CCTTGATTCCTGAAGCCAAAGATAGCTGGTGGACGGGGGATTCTGCTAGTCTCGA
CACGGCAGGCATCAAACTCACAGTTCCAATCCAGAAGTTCCCCGTGACAACGCA
GACGTTTGTGGTCGGTTGCATCAAGGGAGACGACGCACAGAGTTGTATGGTCAC
AGTGACAGTACAAGCCAGAGCCTCATCGGTCGTCAATAATGTCGCAAGGTGCTC
CTACGGTGCAAACAGCACTCTTGGTCCTGTCAAGTTGTCTGCGGAAGGACCCACT
ACAATGACCCTCGTGTGCGGGAAAGATGGAGTCAAAGTTCCTCAAGACAACAAT
CAGTACTGTTCCGGGACGACCCTGACTGGTTGCAAAC

Figure 3-6 DNA sequence of the 522bp band amplified by the SAG1 nested PCR (second round).

Figure 3-7 **Clustal alignment of the SAG1 forward sequence with the SAG1 gene (NCBI Accession No. S85174).**

Overall, the MyTaq buffer and polymerase system succeeded in amplifying the *Toxoplasma* SAG 1 gene while the adding β-Mercaptoethanol did not have any impact on the result.

SAG1 nested PCR was attempted on all of the *Apodemus* samples using the MyTaq system. Unfortunately, all were negative despite the positive control band appearing in all experiments. Variability in performance of the SAG1 PCR has been noted in our lab before. Further optimisation of the SAG1 PCR was abandoned as parallel studies on nested PCR using the SAG2 gene markers were providing better and more reliable results. The samples were not tested again with SAG1 in order not to waste samples on a PCR that was not fully optimised.

3.4.5 Investigation of *Toxoplasma* infection in wood mice using the SAG2 3' end *Toxoplasma* specific marker.

To further test the wood mice samples for the presence of *Toxoplasma*, PCR amplification of the 3' end of the SAG2 gene was carried out as described in Chapter 2. The resulting band is expected to be 221bp. The results are shown in figure 3.13. The positive control produced the target gene band size of 221 bp while the lack of a band in the negative control indicates the reaction was uncontaminated. Brain DNA samples from mouse numbers 406, 412, 416, 430, 434 and 443 also showed amplification of the target gene band size of 221bp. (See Figure 3.8) This demonstrated that these samples were positive for *Toxoplasma* infection and lack of amplification in other donors and the negative control suggested this was specific amplification. To confirm that the correct amplicons were being amplified, it is essential to carry out DNA sequencing on the SAG 2 amplicons following purification.

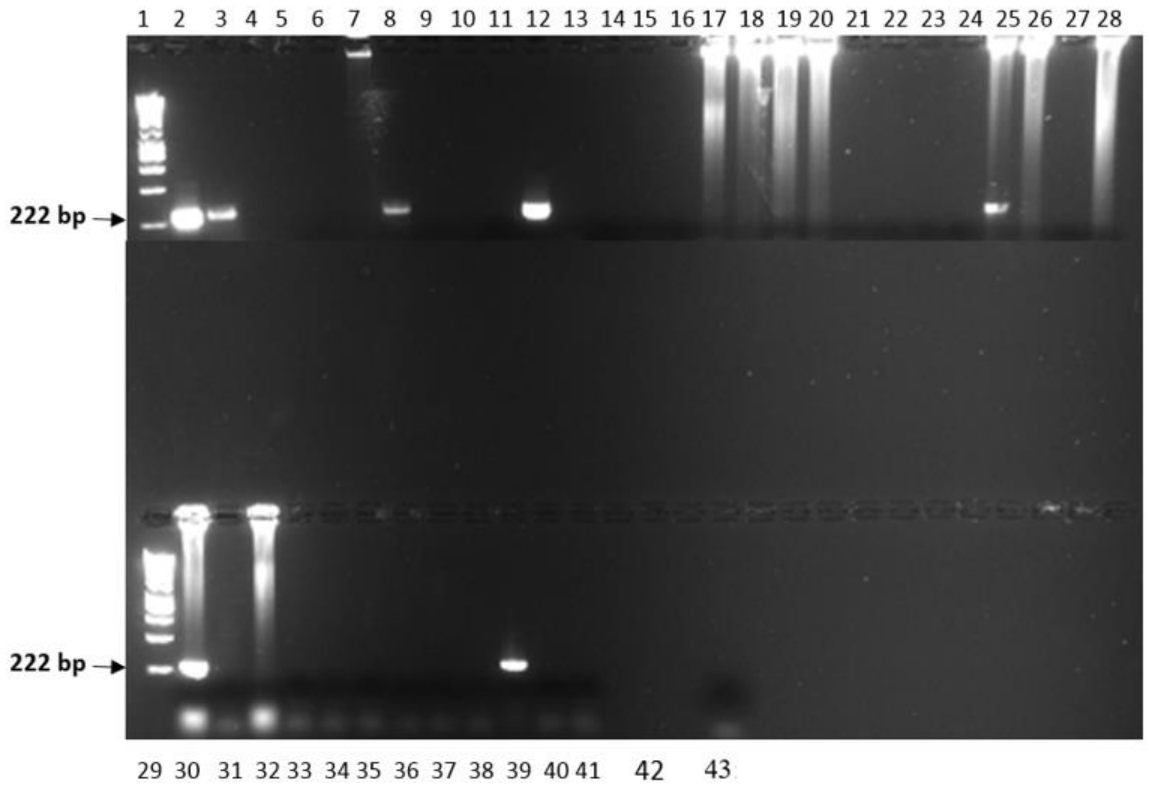

Figure 3-8 PCR amplification of the 3' end of the SAG2 gene by PCR.

A 1.5 % agarose gel was used to resolve fragments of a smaller size for clarity. Lane 1= 1kb hyper ladder, lane 2 = positive control DNA, lane 3= 406, lane 4 = 408, lane 5 = 409, lane 6 = 410, lane 7 = 411, lane 8 = 412, lane 9 = 413, lane 10 = 414, lane 11 = 415, lane 12 = 416, lane 13 = 417, lane 14 = 419, lane 15 = 420, lane 16 = 421, lane 17 = 422, lane 18 = 423, lane 19 = 424, lane 20 = 425, lane 21 = 426, lane 22= 427, lane 23 = 428, lane 24 = 429, lane 25= 430, lane 26 = 431, lane 27 = 432, lane 28 = 433, lower panel: lane 29 = 1kb hyper ladder, lane 30 = 434, lane 31 =435, lane 32 = 436, lane 33 = 437, lane 34 = 438, lane 35 = 439, lane 36 = 440, lane 37 = 441, lane 38 = 442, lane 39 = 443, lane 40 = 444, lane 41 = 445, lane 43 = negative control which contains just water.

3.4.6 Confirmation of the SAG2 3' END PCR amplification using DNA sequencing of amplicons.

To check that the bands were definitely amplicons of the SAG2 3' end of the gene, the PCR products from the positive control and mouse 430 (positive for *T. gondii*) were purified and was sent for sequencing. The sequence that returned was analysed using the programme Finch TV, and this was followed by manual checking of the sequencing peaks. Figure 3.9 shows the sequence. This sequence was then used in a search using the program BLAST to investigate the identity of the sequence.

A clustal alignment between the amplicon sequence and the identified sequence by BLAST.

TGGGTCTGGCGGAAGCGCAGTACTGCAGCAGTGTGTCGGCAAACAAGTTCCTCTGT
CACATAATCGCAGATCCGGAAATACATTTTCTCGCGTTCCTCCCAGGATCTACGCCA
AGAACAATCGCAATCCCACCCCTCAACAACGTTTTCTTTGCACGACAATTTCCAAGC
GGAGGCATGAGAATA.

Figure 3-9 DNA sequence of the amplified SAG2 3'end amplicon.

The BLAST result showed high homology to a range of sequences. Figure 3.10 shows the clustal alignment of that the sequence for the amplicon band, from the brain DNA of mouse 430, matched the SAG2 gene (Accession number: CB372842|CB372842.1) This shows that the amplicon from sample 430 is confirmed as the correct target being amplified for the SAG2 3' end sequence. Each of the DNA samples was amplified as three replicates, and a total of 8 mice from the collection were found to be infected. These were numbers 406, 410, 412, 416, 421, 430, 434, 443. It was now necessary to confirm these using the SAG2 5' PCR marker.

```
CLUSTAL O(1.2.4) multiple sequence alignment


SAG2                        TGGGTCTGGCGGAAGCGCAGTACTGCAGCAGTGTGTCGGCAAACAAGTTCCTCTGTCACA
ENA|CB372842|CB372842.1     TTTTTTTTTGAAAAGCGCAGTACTGCAGCAGTGTGTCGGCAAACAAGTTCCTCTGTCACA
                            *   * *   ..*********************************************

SAG2                        TAATCGCAGATCCGGAAATACATTTTCTCGCGTTCCTCCCAGGATCTACGCCAAGAACAA
ENA|CB372842|CB372842.1     TAATCGCAGATCCGGAAATACATTTTCTCGCGTTCCTCCCAGGATCTACGCCAAGAACAA
                            ************************************************************

SAG2                        TCGCAATCCCACCCCTCAACAACGTTTTCTTTGCACGACAATTTCCAAGCGGAGGCATGA
ENA|CB372842|CB372842.1     TCGCAATCCCACCCCTCAACAACGTTTTCTTTGCACGACAATTTCGAAGCGGAGGCATGA
                            ******************************************* **************

SAG2                        GAATA-------------------------------------------------------
ENA|CB372842|CB372842.1     AAATTGCAGGGTCGGACCGCTCTCACGAAAAAGACAAAAGCCGCACGGCCCATCTGGAGT
                            .***:
```

Figure 3-10 Clustal alignment of the SAG2 3' forward sequence with the SAG2 gene identified in the BLAST search.

3.4.7 Investigation of *Toxoplasma* infection in wood mice using the SAG2 5' end *Toxoplasma* specific marker.

To confirm the PCR results obtained for the SAG2 3' ends, PCR amplification was also carried out using primers to the 5' end of the SAG2 gene. The target band size was 242bp. Initially, four samples (410, 412, 421, 443) tested positive for *Toxoplasma* (data not shown). All of the samples were PCR tested at least three times. Of all of the samples, eight were positive, and they corresponded to the positive samples identified by the SAG2 3' end PCR (mice 406, 410, 412, 416, 421, 430, 434, 443). To ensure that the correct amplicons were being generated, bands were purified and sequenced. Use of the BLAST search and CLUSTAL alignment demonstrated that the sequences did indeed match the SAG 2 5' end.

3.4.8 Detection of *Toxoplasma gondii* in a new set of wood mouse samples using the SAG2, 5' end PCR.

To increase the sample size of wood mice, a further 15 mice collected the previous year (2013) were tested. In the case of these animals, the tissue available was mostly heart tissue and not a brain. Table 3.3 lists the details of these mice and the parasite profile of gastrointestinal parasites. These *Apodemus* samples were trapped and examined in 2013 from the same location in Malham Tarn, North Yorkshire, as were the previous batches. Extracted tissues were frozen until the DNA extraction was performed in 2017.

Table 3-3 New samples of *A. sylvaticus* with associated information.

The table shows the year of collection, mouse identification number, gender, length (cm), weight (g) and infection intensity (number of parasites) for a range of gastrointestinal and other parasites (H, *Heligmosomoides*; P, *Plagiorchis*; S, *Syphacea*; C, *Capillaria*; Tr, *Trichostrongylus*; Ta, *Taenia,* Hy, *Hymenolepis*.)

Year	Mouse	Sex	L	Wt	H	P	S	C	Tr	Ta	H
2013	368	M	8.5	18	5	5	0	0	0	0	0
2013	369	M	8.2	17	8	0	0	0	0	0	0
2013	370	F	5.7	9	0	0	0	0	0	0	0
2013	371	M	7	18	0	0	0	0	0	0	1
2013	373	M	8.5	18	7	0	0	0	0	0	0
2013	382	F	9	24	0	0	0	0	0	0	0
2013	386	F	7.3	14	0	0	0	0	0	0	0
2013	387	M	5	13	0	0	0	0	0	0	0
2013	388	M	9	19	0	0	0	0	0	0	0
2013	389	M	5.3	19	0	0	0	0	0	0	0
2013	391	F	8.4	20	0	0	0	0	0	0	0
2013	392	F	8	19	0	0	0	0	0	0	0
2013	393	M	8.4	21	12	9	0	0	0	0	0

DNA was extracted from these mice and tested with the Tubulin PCR as described for samples 406 - 445. The slight difference between these samples and those extracted previously (406 - 445) was that Qiagen kits were used for the extraction. These were found to be able to produce cleaner DNA and a more efficient yield. The new set of 15 samples of *Apodemus* were tested with the nested SAG2 5’ end PCR for the presence of *T. gondii*. In addition to these heart DNA extracts, a sample of brain tissue from mouse 387 was also tested. The results are shown in Figure 3.11.

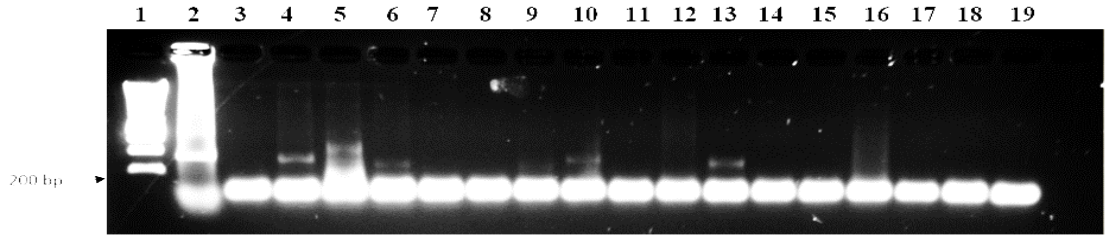

Figure 3-11 Detection of T. gondii DNA using the SAG2 5' end PCR.

Lane 1 = 1Kb hyper ladder, lane 2 = positive control, lane 3 = 368, lane 4 = 369, lane 5= 370, lane 6 = 371, lane 7= 372, lane 8 = 373, lane 9 = 382, lane 10 = 386, lane 11 = 387, lane 12 = 387 brain tissue, lane 13 = 388, lane 14 = 389, lane 15 = 390, lane 16 = 391, lane 17 = 392, lane 18 = 393, lane 19 = negative control consisting of water.

A positive control produced a band of the correct size, and the negative control was clear and positive bands were seen in samples 369, 370, 371, 386 and 388. Samples negative for *Toxoplasma* are 368, 372, 373, 382, 387, 389, 390, 391, 392 and393. The brain sample from mouse 387 was also negative. This suggests that 5 of these samples were infected.

To confirm these PCR results obtained using the SAG2, 5' end PCR, the above DNA from heart tissue from *Apodemus* were tested again to confirm these results by repeating the SAG2 5' end PCRs. Example results are shown in figure 3.12.

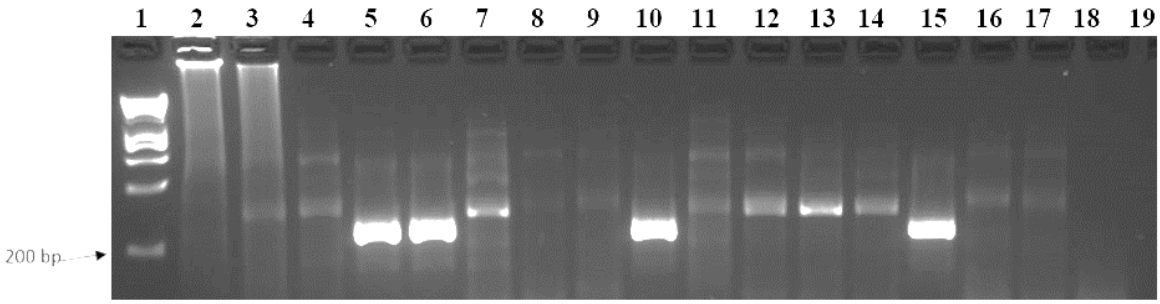

Figure 3-12 Detection of *T. gondii* DNA using the SAG2 5' end PCR.

Lane 1 = 1Kb hyper ladder, lane 2 = positive control, lane 3 = 368, lane 4 = 369, lane 5= 370, lane 6 = 371, lane 7= 372, lane 8 = 373, lane 9 = 382, lane 10 = 386, lane 11 = 387, lane 12 = 387 brain tissue, lane 13 = 388, lane 14 = 389, lane 15 = 390, lane 16 = 391, lane 17 = 392, lane 18 = 393, lane 19 = negative control consist of water.

A positive control produced a band of the correct size, and the negative control was clear and positive bands were seen in samples, 370, 371, 386 and 391. Samples negative for *Toxoplasma* are 368, 369, 372, 373, 382, 387, 388, 389, 390, 392 and 393. This suggests that 4 of these samples were infected.

In some experiments, occasional samples were found not to amplified when they have previously amplified. After replicating experiments, a total of 6 of the heart DNA samples were found to be infected (369, 370, 371, 386, 388 and 391). The overall infection status of all of the donors is presented in Tables 3.4 (infected samples) and Table 3.5 uninfected samples).

Table 3-4 Summary of *Apodemus samples* tested using the SAG PCRs for *T. gondii* detection (infected samples).

Sample No	Sex	SAG1 PCR	SAG2 3' ENDS	SAG 5' ENDS	Overview
406	F	-	+	+	+
410	F	-	+	+	+
412	M	-	+	+	+
416	M	-	+	+	+
421	F	-	+	+	+
430	M	-	+	+	+
434	M	-	+	+	+
443	M	-	+	+	+
369	M	Not tested	Not tested	+	+
370	F	Not tested	Not tested	+	+
371	M	Not tested	Not tested	+	+
386	F	Not tested	Not tested	+	+
388	M	Not tested	Not tested	+	+
391	F	Not tested	Not tested	+	+
TOTAL	14				

Table 3-5 Summary of *Apodemus* samples tested using the SAG PCRs for *T. gondii* detection (uninfected samples).

Sample No	Sex	SAG1 PCR	SAG2 3' ENDS	SAG 5' ENDS	Overview
408	F	-	Not tested	-	-
409	M	-	Not tested	-	-
411	M	-	Not tested	-	-
413	M	-	Not tested	-	-
414	M	-	Not tested	-	-
415	F	-	Not tested	-	-
417	M	-	Not tested	-	-
419	F	-	Not tested	-	-
420	M	-	Not tested	-	-
422	M	-	Not tested	-	-
423	M	-	Not tested	-	-
424	M	-	Not tested	-	-
425	M	-	Not tested	-	-
426	M	-	Not tested	-	-
427	F	-	Not tested	-	-
428	F	-	Not tested	-	-
429	M	-	Not tested	-	-
431	F	-	Not tested	-	-
432	F	-	Not tested	-	-
433	M	-	Not tested	-	-
435	M	-	Not tested	-	-
436	M	-	Not tested	-	-
437	M	-	Not tested	-	-
438	M	-	Not tested	-	-
439	M	-	Not tested	-	-
440	M	-	Not tested	-	-
441	M	-	Not tested	-	-
442	M	-	Not tested	-	-
444	M	-	Not tested	-	-
445	M	-	Not tested	-	-
H368	M	Not tested	Not tested	-	-
H387	M	Not tested	Not tested	-	-
H389	M	Not tested	Not tested	-	-
H390	NA	Not tested	Not tested	-	-
H392	F	Not tested	Not tested	-	-
Total 35					

In conclusion, a total of 49 *A. sylvaticus* were tested with a variety of *Toxoplasma* PCR diagnostic markers. Fourteen of those were positive for the parasite DNA. Thus prevalence of 28.6% (CI: 95% 17.8 – 42.5%) was observed.

3.4.9 Investigating the relationship between *Toxoplasma* infection and other parasitic infections in *A. sylvaticus*.

As the collections of mice available for this study had additional data on the presence of other parasites (gastrointestinal parasites). An opportunity exists to do a preliminary study to see if there might be a relationship between *Toxoplasma* infection and coinfection with the other parasites. *Taenia* and *Trichostrongylus* were not recorded in any of the mice in this study and were, therefore, not considered in the subsequent studies.

A total of 47 *Apodemus* were available that had infection data on both *Toxoplasma* and the other parasites. Possible co-infection was carried out by using 2 x 2 contingency table analysis of mice suing four categories: *Toxoplasma* infected; *Toxoplasma* uninfected and compared against infection status (positive or negative) for the other parasite.

Investigation of co-infection between *Toxoplasma* and *Capillaria* was investigated using the 2 x 2 contingency table analysis. The results are shown in Table 3.6

Table 3-6 Investigation into the association between *Toxoplasma* and Capillaria in *A. sylvaticus*.

Toxoplasma	infected	uninfected	Total
Capillaria+	1	1	2
Capillaria -	13	32	45
Total	14	33	47

Statistical analysis of the frequencies of infection presented in Table 3.6, using 2 x 2 contingency table analysing the result, showed that there was no significant association (P=0.5116).

Investigation of co-infection between *Toxoplasma* and *Syphacea* was investigated using the 2 x 2 contingency table analysis. The results are shown in Table 3.7

Table 3-7 Investigation into the association between *Toxoplasma* and Syphacea in *A. sylvaticus*.

Toxoplasma	infected	uninfected	Total
Syphacea+	0	5	5
Syphacea -	14	28	42
Total	14	33	47

Statistical analysis of the frequencies of infection presented in Table 3.7, using 2 x 2 contingency analysis, representing that there was no significant association (P=0.307) between *Toxoplasma* and *Syphacea*.

Investigation of co-infection between *Toxoplasma* and *Heligmosomoides* was investigated using the 2 x 2 contingency table analysis. The results are shown in Table 3.8

Table 3.8 Investigation into the association between *Toxoplasma* and *Heligmosomoides* in *A. sylvaticus*.

Toxoplasma	infected	uninfected	Total
Heligmosomoides+	5	16	21
Heligmosomoides-	9	17	26
Total	14	33	47

Statistical analysis of the frequencies of infection presented in Table 3.8, using 2 x 2 contingency analysis, illustrating there was no significant association (P=0.528) between *Toxoplasma* and *Heligmosomoides*.

Investigation of co-infection between *Toxoplasma* and *Hymenolepis* was investigated using the 2 x 2 contingency table analysis. The results are shown in Table 3.9

Table 3.9 Investigation into the association between *Toxoplasma* and *Hymenolepis* in *A. sylvaticus*.

Toxoplasma	infected	uninfected	Total
Hymenolepis +	1	1	2
Hymenolepis -	13	32	45
Total	14	33	47

Statistical analysis of the frequencies of infection presented in Table 3.9, using 2 x 2 contingency analysis, represented that there was no significant association (P= 0.5116) between *Toxoplasma* and *Hymenolepis*.

Investigation of co-infection between *Toxoplasma* and *Plagiorchis* was investigated using the 2 x 2 contingency table analysis. The results are shown in Table 3.10

Table 3.10 Investigation into the association between *Toxoplasma* and *Plagiorchis* in *A. sylvaticus*.

Toxoplasma	infected	uninfected	Total
Plagiorchis +	1	6	7
Plagiorchis -	13	27	40
Total	14	33	47

Statistical analysis of the frequencies of infection presented in Table 3.10, using 2 x 2 contingency table analysis, showed that there was no significant association (P= 0.6566) between *Toxoplasma* and *Plagiorchis*.

Polyparastism is known to occur in many species and this was investigated using the data obtained here. This was carried out by investigating whether there is a statistical association between *T. gondii* infection and infection with any other parasite (Table 3.11).

Table 3.11 Investigation into the association between *Toxoplasma* and any parasitic infection in *A. sylvaticus*.

Toxoplasma	infected	uninfected	Total
Any parasite +	6	20	26
Any parasite -	8	13	21
Total	14	33	47

Statistical analysis of the frequencies of infection presented in Table 3.11, showed that there was no significant association (P= 0.76) between *Toxoplasma* and any other parasitic infection.

In conclusion, there were no statistically significant relationships between infection with any of the gastrointestinal parasites and infection with *Toxoplasma*.

3.5 Discussion

This chapter aimed to look at a collection of wood mice, *A. sylvaticus* with the intention of determining the prevalence of infection and creating a sample set that could be used for later analysis of immunity specific genes. Overall, a prevalence of 28.6% (CI: 95% 17.8 – 42.5%) was detected in these wild mice. This also provided a sample size of 14 mice that could be used in later DNA investigations as examples of infected animals (see following chapters). As additional data was available on other parasitic infections in these mice, it was interesting to investigate whether there was evidence of co-infection with these parasites. Although there is no evidence from the literature that there would be any associations a preliminary analysis was easily conducted to address this question. In all cases, there was no significant association between *T. gondii* infection and co-infection with one of these gastrointestinal parasites.

In this latter analysis, a set of simple pairwise 2 x 2 contingency analyses were carried out to look for primary associations. This analysis showed no significant results which were supported by inspection of the data. Furthermore, an analysis was conducted to see if there was any relationship between *T. gondii* infection and the presence of any gastrointestinal parasites. No significant associations were found. However, there are some statistical limitations to these approaches. If there were a justification to look in more depth (e.g. a reason why an association might be present or results that showed one or more parasites having an association), a better approach would have been to utilise a statistical modelling approach that considered all parasites and information together. This would get around any confounding factors or problems of interpreting multiple statistical tests. If a P value of less than 0.05 is used as the criterion, then 1 in 20 parasite tests could be significant just by chance. This limitation would be overcome by a modelling approach that considered all tests together.

In this study, no association was found between *T. gondii* infection and other parasitic infections. However, studies in experimental mice have shown that *T. gondii* infection can increase fecundity of intestinal worms like *Heligmosomoides* (Ahmed *et al*., 2017). Other studies have shown that infection with *H. polygyrus* can enhance *T.*

gondii infection (Khan *et al*., 2008) or modulate neuroimmune responses to *T. gondii* infection (French *et al*., 2019). However, no evidence of these kinds of interactions were observed in our population of woodmice.There were several limitations encountered when developing the PCR diagnostic tools for the detection of the parasite. The SAG1 nested PCR is a robust test that has been used in many studies in our laboratory with a wide range of species (Duncanson *et al.*, 2001; Williams, 2005; Dodd *et al.*, 2014; Bajnok *et al.*, 2019), including *Apodemus* (Thomasson, 2011; Bajnok *et al.*, 2015). On this occasion, it was found to work sub-optimally for control samples but not at all in the *Apodemus* samples. Troubleshooting PCR protocols can be a lengthy process because it requires sequential elimination and testing to determine which reagents are working sub-optimally. As the SAG 2 diagnostic tests, being developed in parallel were working successfully attempts to develop the SAG further nested PCR were not continued. Ideally, each sample should be tested with all available markers to confirm infectivity (Bajnok *et al.*, 2015a, 2019), however, in this case, the results of the SAG2 nested PCRs were reliable. Several replicates of each PCR detection were carried out and, although occasional positives showed up as negative, the combination and broad consistency of the PCR identifications provided confidence of the individual infection status and prevalence in these mice.

A prevalence of 28.6% (CI: 95% 17.8 – 42.5%) (n=49) was measured in this collection of *Apodemus*. Comparison with other studies at this same site in years prior to 2011(Thomasson *et al.*, 2011), which showed a prevalence of 40.78 (CI: 95% 34.07 – 47.79%) (n=206), was of comparable magnitude as judged by the overlap of 95% confidence levels. Furthermore, the prevalence was comparable with a further collection of *Apodemus* from the same site (Bajnok *et al.*, 2015) where a prevalence of 34.92% (CI: 95% 27.14 – 43.59%) (n=126) was recorded. These high prevalence are high considering that this study site (Malham Tarn Field Centre) has a low estimated cat density (<2.5 cats/km^2) (Hughes et al. 2008) and that the cat is the definitive host. By comparison, other studies on an urban population of domestic mice, *Mus domestics*, found in an area of high cat density (>500 cats km^2) (Murphy *et al.*, 2008) had a higher prevalence of 59% (CI: 95% 50.13-67.87%) (n= 120) (Marshall, 2004). While the presence of cats is higher in the urban population, there is still a significant prevalence in the wild mice of Malham Tarn. This suggests that

the parasite could be utilising mechanisms of transmission that bypass the cat (Thomasson, 2011). The data provided here also support that notion. Vertical transmission, by means of congenital transmission, has been suggested as a possible mode of transmission that could explain this (Murphy *et al.*, 2008; Wen *et al.*, 2016) although the importance of vertical transmission remains controversial (Dubey *et al.*, 1995; Dubey, Lindsay et al., 2009; Innes *et al.*, 2009).

Dissection of the natural transmission cycles of *Toxoplasma* is complicated. The parasite is found at high prevalence's (approximately 30%) in several animal species (Tenter et al., 2001), and 30% globally in humans (Pappas et al. 2009). It has also been reported in all warm-blooded animals (birds and mammals) studied so far (Tenter et al., 2001; Dubey, Lindsay and Lappin, 2009), including marine mammals (Bigal et al. 2018) thus making it a highly successful parasite. An understanding of the transmission cycles could help us to understand how the parasite is so successful. Prevalence of infection is, of course, determined by the rate of transfer of parasite from host to host but is also related to the susceptibility and resistance of hosts to infection.

In laboratory mice, these mice are classically highly susceptible to infection with *Toxoplasma* and typically die within a week, It is, therefore, very surprising that wild mice, like the *Apodemus* studied here, harbour the parasite and are not killed. Evolution should select out those mice infected. Therefore, there must be a difference in resistance to the parasite in wild mice.

Studies in laboratory mice and rats have revealed interesting possible mechanisms of resistance. Laboratory rats are highly resistant, while lab mice are highly sensitive. Studies have shown that two enzymes, inducible nitric oxide synthase (iNOS) and Arginase act in opposition to determine resistance to *Toxoplasma* (Zhao, *et al.*, 2012). Rat peritoneal macrophages express high levels of iNOS and low levels of arginase and are highly resistant to infection, while mouse peritoneal macrophages express high levels of arginase and low levels of iNOS and are highly sensitive. This suggests that differences in expression of these two enzymes could affect resistance.

Furthermore, studies in rats have shown that different rat strains have different levels of resistance (Wang *et al.*, 2015) and that this resistance is correlated with the ratio

of iNOS expression to arginase expression (i.e. iNOS/Arg). In the more resistant strains, the rate is higher.

Further demonstration of the role of these enzymes can be found in a study by (Zhao *et al.*, 2013). They showed that there was a difference in resistance between peritoneal and alveolar macrophages from the same genetically inbred rat strain. Peritoneal macrophages are resistant and have high iNOS/Arg ratios while alveolar macrophages are not resistant and have low iNOS/Arg ratios. The other exciting thing that this study reveals, therefore, is that epigenetic control of these enzymes occurs. So resistance and sensitivity could be due to both genetic mechanisms (genetic polymorphisms that influence expression) or epigenetic polymorphism (for example changes in DNA methylation states).

These studies, therefore, suggest possible investigations in wild populations of mice to establish the mechanisms of resistance. Control of gene expression often involves the gene promoter region which interacts with protein complexes to switch the genes on and off. The *Apodemus* system studies in this chapter could potentially be used to investigate this further. for example, it would be possible to conduct DNA sequence analysis of the iNOS gene promotor and analysis of cytosine methylation patterns in *Toxoplasma* infected and uninfected mice to investigate any possible variants that could be linked to infection. These ideas form the basis of subsequent chapters.

Chapter 4: PCR Amplification of the iNOS & Arginase genes of *Apodemus sylvaticus*

4.1 **Introduction:**

Parasitic infection by *Toxoplasma gondii* is one of the most frequent infections. *T. gondii* can maintain an epidemic and spread amongst a broad spectrum of hosts and includes all warm-blooded animals (Tenter et al., 2001; Lüder *et al.*, 2003). Based on its distribution it is probably one of the most successful apicomplexan parasites. While it may have some pathology in its definitive host, the cat, the main impacts of it are on secondary hosts who are infected but not required to complete the life cycle. In humans, significant problems can occur in immunocompromised people such as those undergoing transplant therapy or have lower immunity due to AIDS/HIV infection. Significant pathology is associated with foetuses born from pregnant women who are infected during pregnancy when the parasite is transmitted to the foetus across the placenta (Coutinho *et al.*, 2012). The question as to what influences the susceptibility or resistance of a host to the parasite is a complex one.

In order to persist with an infection, the host might need to have a weakened immune system and this might either be due to an innate phenotype or immune-manipulation by the pathogen. One mechanism, that has been shown to be important in mice and rats, is the iNOS and Arginase expression systems. Typically, studies on inbred laboratory mice strains have shown these mice to be highly susceptible to infection and death caused by *T. gondii* (Zhao, *et al.*, 2012). In the case of most inbred laboratory rat strains, a higher degree of resistance to the parasite exists (Li et al., 2012). These differences in resistance/susceptibility are due to differing levels of iNOS and Arginase gene expression in cells such as macrophages (Zhao, *et al.*, 2012; Wang *et al.*, 2015). Both iNOS and Arginase use the same substrate (arginine) and generate, respectively, nitric oxide (NO) or urea as a product. As NO is a powerful effector against intracellular pathogens, macrophages expressing iNOS at a high level than Arginase are resistant to *T. gondii* infection. In the study by (Zhao, *et al.*, 2012), it was shown that lab strains of mice have a low iNOS to Arginase balance of expression and this is associated with a high level of infection.

Conversely, rat strains have high iNOS expression and low arginase expression, and this is correlated with a significantly higher degree of resistance. Furthermore, different rat inbred lines have different levels of resistance, and the degree of resistance is associated with the ratio of iNOS/Arginase expression (Wang *et al.*, 2015) This suggests that these two antagonistic processes play a significant role in resistance or sensitivity to *T. gondii* infection. Furthermore, additional studies comparing *T. gondii* infection in different rat tissues (peritoneal macrophages vs alveolar macrophages) showed differences in both resistance to infection and iNOS/Arginase expression profiles (Zhao, *et al.*, 2012; Cai *et al.*, 2013) Rat peritoneal macrophages are typically highly resistant to *T. gondii* and have a high iNOS/Arginase ratio of expression, however, in alveolar macrophages, from the same rat inbred line, a high degree of susceptibility to *T. gondii* infection and a low iNOS/Arginase ratio of expression was observed (Zhao *et al.*, 2013; Lun *et al.*, 2015). As the genetic background of peritoneal and alveolar macrophages are virtually identical in the same rat inbred line, then these tissue-specific differences may be due to epigenetic modifiers that alter the iNOS/Arginase balance. Such a process of epigenetic modification could be a lead into understanding the control of resistance/susceptibility to infection with *T. gondii*.

Susceptibility/resistance to *T. gondii* infection can be easily studied in laboratory animals, but these studies generally take place on a small number of inbred lines. This raises questions as to how the outcomes of these studies are reflected in natural populations of animals which have a much greater genetic diversity. Given that many studies demonstrate a high prevalence (around 30%) in many wild animal species, adaptations to resistance, or at least tolerance, must have evolved. Unfortunately, many of the tools and reagents needed for such studies are limited or non-existent for wild animal species. A fundamental necessity, therefore, is to develop the tools required for such analyses and to select suitable wild animal populations to study.

Some studies on *T. gondii* infection of wild rodents have been conducted at the Malham Tarn Field Centre in the Yorkshire Dales (Thomasson et al. 2011; Bajnok et al. 2015; Chapter 3, this thesis (Chapter 2, Table 2.1, Populations 2 and 3)) where a prevalence of *T. gondii* of 41%, 35% and 25%, respectively, have been reported. Collections of *A. sylvaticus* (wood mice), *Myodes glareolus* (bank voles) and *Microtus agrestis* (field voles) are available from this area and offer the opportunity to develop these tools. Very little is known about the iNOS/Arginase systems in these wild

species; however, their relationship with lab mice (*Mus musculus*) offers the possibility of developing these tools based on homology.

The laboratory studies conducted in mice and rats (Li et al., 2012; Zhao et al., 2013; Gao et al., 2015), show that rats resist infection because they have a high iNOS/Arginase gene expression ratio – that is, they have an imbalance in favour of iNOS expression over Arginase expression. In these studies, the laboratory mice had detectable deficient levels of iNOS activity, had an extremely low iNOS/Arginase expression ratio and consequently died relatively quickly from infection. If this situation were mirrored in natural populations of mice, then we would expect to see no infected mice at all – they would all be killed. To explain the parasite infection prevalence reported, of 25 – 41% in the Malham Tarn collection site (Thomasson et al. 2011; Bajnok et al 2015; Chapter 3, this thesis (Chapter 2, Table 2.1, Populations 2 and 3)) and other studies on natural populations, some mice, at least, must show a degree of resistance to infection. It also raises the question as to whether this degree of resistance might determine whether individual animals become infected or not. For example, animals with a high iNOS/Arginase ratio would be expected to be more resistant than those with a lower balance of these two enzymes. A very high iNOS/Arginase ratio might prevent infection completely (i.e. the animals would be uninfected) while those with a lower ration might be susceptible to disease but not die. If this were the case, then if we examined infected and uninfected mice, we might expect to see the infected mice had a lower iNOS/Arginase ratio (balance) than the uninfected mice. If we have tools to be able measure the expression of iNOS and Arginase from *A. sylvaticus*, then this is a hypothesis that can be tested.

This chapter aims to develop tools to investigate iNOS and arginase expression and to investigate the relationships with *Toxoplasma* infection in natural populations of wood mice and voles.

4.2 Objectives

1. Design and test PCR primers for Arginase to amplify the homologous gene from *A. sylvaticus*.

2. Sequence the amplified Arginase PCR products and confirm their identity.
3. Compare the *Apodemus* Arginase sequence with the arginase gene from *Mus musculus*
4. Design and test PCR primers for iNOS to amplify the homologous gene from *A. sylvaticus* and to design PCR primers that will be specific for amplification of iNOS mRNA. Sequence the amplified iNOS PCR products and confirm their identity. Compare the *Apodemus* iNOS sequence with the iNOS gene from *Mus musculus.*
5. Collect samples of *A. sylvaticus* and voles for use in DNA and RNA extraction and test for *T. gondii* infection using PCR based markers
6. Develop tools for investigating iNOS and arginase gene expression in *A. sylvaticus*.
7. Measure the expression of iNOS and Arginase levels in *T. gondii* infected *Apodemus*.

4.3 Methods:

A. sylvaticus were trapped as described in Chapter 2 from the Malham Tarn area and with ethical approval provided by the University of Salford (STR1718-32). The mice used for the studies in this chapter are populations 2,3 and 4 (Chapter 2, Table 2.1), where samples were specifically collected to enable analysis of both DNA and RNA. DNA and RNA were extracted from brain and heart tissue by phenol-chloroform methods or using bespoke kits as previously described. PCR primers were designed as described below or taken from existing publications (Zhao, *et al.*, 2012), to enable amplification of the *Apodemus* genes for iNOS and Arginase and to be able to amplify expressed iNOS mRNA from cDNA. Furthermore, information was used from a preliminary genome sequence for *A. sylvaticus*, which became available from Liverpool University during this work, to assist with this process (http://www.ebi.ac.uk/ena/data/view/GCA_001305905.1). PCR protocols, conversion of mRNA to cDNA and qPCR methods are described in Chapter 2 or part of the development section in this chapter. The strategy used to distinguish between mRNA derived cDNA, and genomic DNA was to design primers that spanned introns so that a smaller size band will be observed for mRNA compared to genomic DNA that included introns.

4.4 **Results:**

4.4.1 PCR Amplification of the Arginase gene from *Apodemus sylvaticus*

Published arginase gene primers were available for *Mus musculus* and used in several publications (Zhao, *et al.*, 2012; Zhao, *et al.*, 2012; Zhao *et al.*, 2013; Zhao *et al.*, 2013; Guo *et al.*, 2015; Qin *et al.*, 2017; Shen *et al.*, 2017) (Li at el 2012, Zhao et al 2013, Wang et al 2014, Gao et al 2015, Shen et al 2017, Qin et al 2017). These were initially tested to see if they could amplify the arginase gene from *Apodemus*. Primer sequences are shown in table 4.1.

Table 4-1 Summary of primers used for PCR amplification of the iNOS & ARG genes in *A. sylvaticus*.

Primer name	Forward	Reverse	Band Size	Reference
Arginase ARGF/ARGR:	5/ AAGAAAAGG CCGATTCACCT /3,	5/CACCTCCTCT GCTGTCTTCC/3 .	201bp in *Mus*	Z. Li et al 2012,
iNOSF / iNOS R	5’GCCTCGCTC TGGAAAGA 3’	5’TCCATGCAGA CA ACCTT 3’	499bp in *Mus*	Z. Li et al 2012
iNOS AF1,/AR1:	5/AATGTTCCAGA ATCCCTGGAC/3	5/GCCCCTCGC TGCATCGG/3	410bp in *Mus*	This study
iNOS B, F2/R2:	5/AGCTCATCTTT GCCAC/3	5/AAGTACGAG TGGTTCCAGG/ 3	468bp in *Mus*	This study
iNOS C, F3/R3:	5'AGAGGACAAC ATCCCAAGAAG-3'	5'-TCCCAGGAG GCTAGGATAAA -3'	604bp in *Mus*	This study
iNOS, cDNAF1/R1:	5'GAGAAGCTGA AGCCCAAGAA3'	5'GCTTGTCACC ACCAGAAGTAG 3'	620 bp DNA mRNA 263bp	This study
iNOS, cDNAF2/R2:	5’ CACATCTGGCA GGATGAGAAG 3’	5’ ACCTTGGTGTT GAAGGCATAG 3’	619bp DNA mRNA 200bp	This study

To investigate whether the Arginase primers (Li et al. 2012; Table 4.1) could amplify the gene from *A. sylvaticus,* the PCR was carried out on 24 *Apodemus* DNA samples extracted from brain tissue. The expected band size for these published primers was 201bp based on the sequence of the *Mus musculus* arginase gene. An example of the resulting gel electrophoresis is shown in figure 4.1. In some experiments, PCR results were not precise and had to be repeated to obtain definitive results (e.g. sample 417, figure 4.1). The majority of samples produced a single bright band. PCR amplicon sizes were calculated by using a standard curve of molecular log size plotted against mobility. After optimisation of PCRs and repeats a band size of 372 base pairs was observed in all samples. The negative control lane remained clear. Results for each *Apodemus* sample are shown in Table 4.2.

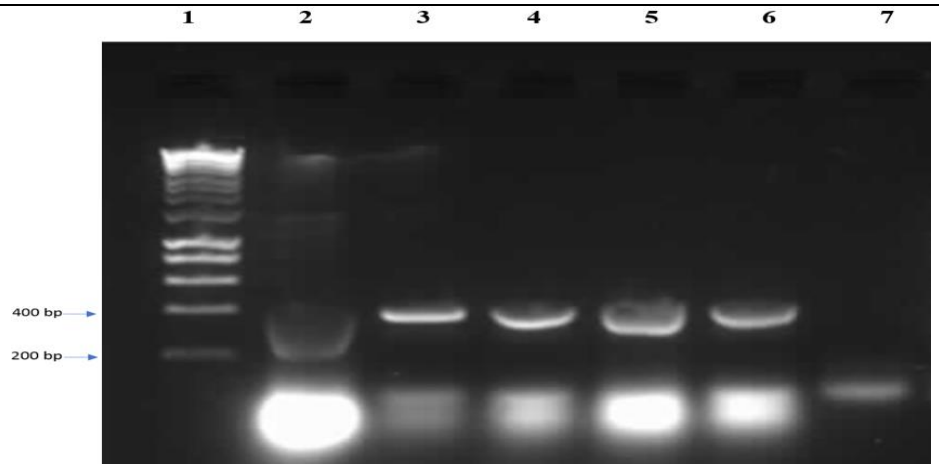

Figure 4-1 Gel electrophoresis of PCR amplification of the Arginase gene from *Apodemus* Brain.

Gel electrophoresis of PCR amplification of the Arginase gene from *Apodemus* Brain DNA. Lanes: 1= 1kb marker, 2= 417, 3= 419, 4= 420, 5= 437, 6= 438, 7= NC negative control (water)

Table 4-2 List of *Apodemus* samples and the band sizes of the PCR amplified Arginase gene fragment.

Year of capture	*Apodemus* Number	Sex	Length (cm)	Weight (g)	Arginase PCR (band size (bp))
2014	417	M	8	18	372
2014	419	F	8	22	372
2014	420	M	10.2	23	372
2014	422	M	7.2	14	372
2014	423	M	7.2	14	372
2014	424	M	6.5	13	372
2014	425	M	8.5	16	372
2014	426	M	6.8	15	372
2014	427	F	6.6	16	372
2014	428	F	7.4	17	372
2014	429	M	7.5	18	372
2014	430	M	8.2	13	372
2014	431	F	7.7	15	372
2014	432	F	8.6	19	372
2014	435	M	7	16	372
2014	436	M	8	16	372
2014	437	M	7	16	372
2014	438	M	7.2	19	372
2014	439	M	6.5	18	372
2014	440	M	5	14	372
2014	441	M	72	13	372
2014	442	M	8	20	372
2014	444	M	7.1	23	372
2014	445	M	9	19	372

This work demonstrates that the published primers (Li et al. 2012) are capable of amplifying a product from *A. sylvaticus* genomic DNA. However, a discrepancy exists between the size of this band (372bp) and the expected size based on the *Mus musculus* gene. Two possibilities therefore exist, either this is not the correct gene or that the scope of this fragment of the Arginase gene is larger than its homologue in *Mus musculus*. To investigate this question, it was necessary to sequence the PCR amplicon.

To confirm that the right gene has been amplified, DNA from sample numbers 417, 428 and 438 were selected randomly for sequencing The DNA was cleaned up by cleaning and purification of samples using Bioline kits (ISOLATE PCR and GEL KIT Bio-52060) as described in the Materials and Methods. Cleaned up amplicons were quantified, using a nanodrop spectrophotometer and sent for sequencing via a commercial company (Source Bioscience – as detailed in Chapter 2). Fragments were only sequenced using the forward primer. Sequence chromatograms were checked by eye and corrected as necessary to obtain reliable consensus sequences. These sequences were then analysed using the BLAST programme to determine the identity of the chains. The consensus sequence of sample 417 (population: 2, 2014 collection, see table 2.1), is shown in figure 4.2.

AGTGATTTGCCCTTTTCTTTATGTTGTGGGAGGCCCATCGTATAGAGAAGGCCT
CTATATCCCAGAACAAATCTACCAGAAGGTAGGTAAACCTCAGGCCATAAAGC
AGCAGCTGTGTGCGCCTGGCCAATGGGTTTGCCGGCCCCCCCGACTAGACTGC
CTGTCACATGGTGTGACAGCTCAATGTCACCACTAGATACACTTGGGAGTCAG
TTGTCCCAAACTTTGAAAGGTCAGTTATTTTGATCCGCTATGTCATTATCACTTT
TTTCGTTGTACGGCTCCTTTCAGGACTAGATATCATGGAAGTGAACCCCAACTC
TTGGGAAGACCGCAGATGAGGTGATC

Figure 4-2 Consensus sequence for the Arginase.

Consensus sequence for the Arginase gene fragment from sample 417, (population: 2, 2014 collection, see table 2.1).

The sequence obtained was 348 bp long – considerably longer than the predicted band size of 201 bp. The length of the fragment was shorter than the measured band size of 372 bp. The latter would include the forward primer which will not be seen in the sequence shown in figure 4.2 – so adding 20 bases for the forward primer raises the length of the sequence to 368 bp. A region towards the end of the sequence (shaded yellow) in Figure 4.2 is a strong (but not perfect) match with the reverse complement of the reverse primer (AAGACAGCAGAGGAGGTG). Two bases within the primer seem polymorphic when compared to the actual sequence derived from the *Apodemus* amplicon. This presumably depicts the end of the amplicon, three bases short of the total, making a fragment length of 365 base pairs. Given the experimental error associated with measuring the band size from the gel, this corresponds well with the estimated band size of 372 bp. It is assumed that the three bases beyond the reverse primer, in the sequence, are artefactual and derived from some contaminating sequence included within the sequencing chromatogram. At this end of the sequence chromatogram, the peaks were becoming indistinct and thus subject to interpretation error.

The sequence described above was used with the BLAST program to inspect the NCBI databases to check the identity of the sequence. The results confirmed the correct sequence (data not shown). This indicates that the right target sequence (*Mus*

domestics arginase) is being selected as the most likely match with 94 % identity. However, this is only over about 180 bp. The remaining half of the amplified sequence (when BLAST is carried out separately with that half) does not match with anything in the databases.

This suggests that the *Apodemus* gene is longer than the *Mus* homologue by around 180 base pairs. (This is consistent with the difference in the measured size of the PCR amplicon (372bp) and the predicted band size for *Mus* (201bp) and also the difference between the *Apodemus* sequence (365bp) and the matching sequence with *Mus* arginase (180bp)). To investigate this further, we needed to see if there was any existing detail on the Arginase gene sequence of *Apodemus*. At the time of writing, the main NCBI and other databases did not possess sequence information for this gene in *Apodemus*, however, in Liverpool, there was an ongoing unannotated and incomplete *Apodemus* sequencing project underway (https://www.ncbi.nlm.nih.gov/assembly/GCA_001305905.1/). The sequenced *Apodemus* amplicon was used to BLAST search the *Apodemus* genome project. This produced a match, as shown in figure 4.3.

The identity is 95% and confirms that this *A. sylvaticus* arginase fragment is longer than the equivalent in *Mus domestics*.

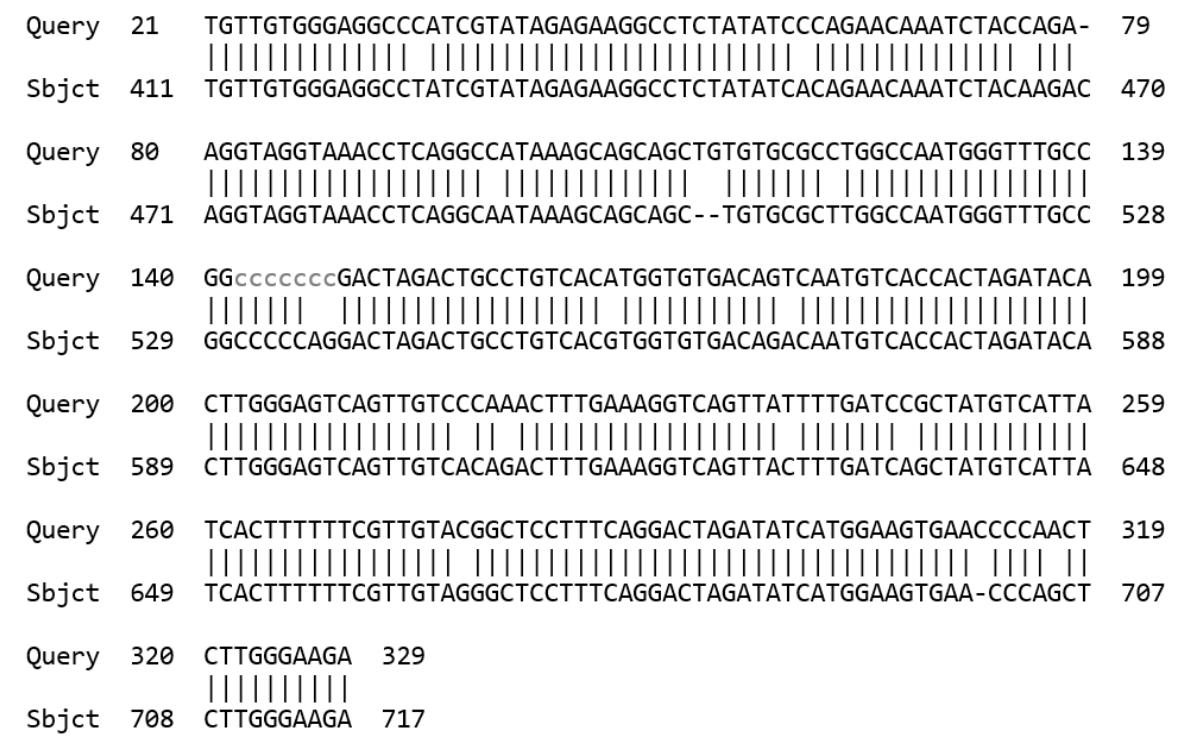

Figure 4-3 Alignment of the PCR amplicon from the brain tissue DNA of *Apodemus*.

Alignment of the PCR amplicon from the brain tissue DNA of *Apodemus* with a contig from the preliminary *Apodemus* genome project. The query sequence is the *Apodemus* Amplified DNA while the subject is the matched sequence from the *Apodemus* sequencing project. There is a 95% sequence match.

These experiments demonstrate that the *Mus musculus* primers can amplify a fragment of the Arginase gene from *A. sylvaticus.* However, the corresponding fragment of the gene is longer in *Apodemus* than in *Mus.*

4.4.2 PCR Amplification of the iNOS gene from *Apodemus sylvaticus*

To develop tools for the analysis of the iNOS gene in *A. sylvaticus*, it is necessary to develop PCR primer to amplify part of this gene. The gene in *Mus musculus* is a large gene of around 50kb in size and is split over 27 exons and therefore represents a complex challenge. The aim of this study is not to characterise the entire gene but to develop a PCR base system that can be used in qPCR to

quantify gene expression. What is ideally required are two sets of primers – one that can distinguish only genomic DNA and the other that detects cDNA. This can be achieved by designing PCR primers within intron sequences, that span an exon (detects genomic DNA (gDNA)) and primers within adjacent exons that span an intron (producing a truncated PCR product from correctly spliced cDNA copies of RNA).

Primers for qPCR detection of expression have already been published for *Mus* laboratory strains of mice (Li et al. 2012) (Forward 5' GCC TCG CTC TGG AAA GA 3' and reverse 5'TCC ATG CAG ACA ACC TT 3'). Initially, these primers were tried to achieve PCR amplification of a suitable fragment from *Apodemus*. Initial experiments were conducted similarly to those aimed at establishing PCR amplification of the arginase gene. Despite many PCR experiments and optimisation, the published primers did not amplify anything from *Apodemus* DNA. Thus, it would be necessary to design new PCR primers based on the annotated sequence of the iNOS gene from *Mus musculus* and the preliminary *Apodemus* genome sequence.

Several strategies were explored to design suitable primers. Typically, these involved selecting regions of the *Mus* iNOS gene, using the BLAST programme to identify the homologous region from the partial *Apodemus* genome sequence and to use primer design programmes to design appropriate PCR primers.

4.4.3 PCR Amplification of the iNOS gene from *Apodemus* using primers AF1 and AR1.

Based on the *Mus* sequence and corresponding preliminary *Apodemus* genome sequence, primers AF1 and AR1 were designed AF1: AATGTTCCAGAATCCCTGGAC, AR1: GCCCCTCGCTGCATCGG, (Table 4.1). This primer was designed to cover exon 13 and regions of exon 15 regions of the *Apodemus* sequence.

PCR amplification was carried out as described in chapter 2, and a range of annealing temperatures was used to determine the optimum: 52^0C – 63^0C. A band size of 499bp is predicted from the genomic sequence. The result is shown in Figure 4.6. This shows that there was no amplification at any of the annealing temperatures tried. Another experiment also failed to get this primer pair to anneal.

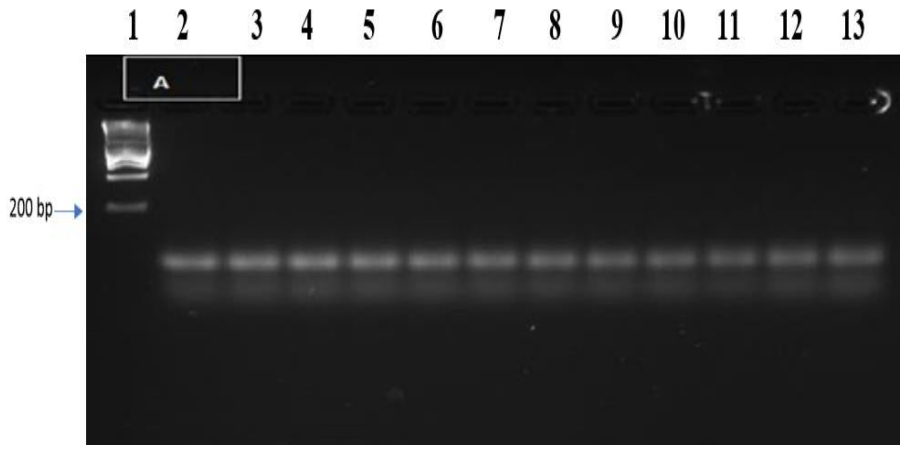

Figure 4-4 PCR amplification of the iNOS Primers AF1/AR1 using *Apodemus* genomic DNA.

A range of PCR annealing temperatures, across a gradient (52^0C – 63^0C), using gDNA from *Apodemus* heart tissue DNA as a test set. The sample came from mouse number 415. Lanes, 1= 1k ladder, 2= 520C, 3=530C, 4=540C, 5= 550C, 6= 560C, 6= 570C, 8= 580C, 9= 590C, 10= 600C, 11= 610C, 12= 620C, 13= 630C. Negative control was also run – not shown. This primer has failed to amplify the target gene sequence.

It appears there is no amplification at all, under any conditions, which means that this primer does not work with *Apodemus* DNA and therefore cannot amplify the iNOS gene.

4.4.4 PCR Amplification of the iNOS gene from *Apodemus* using primers iNOSBF2 and iNOSBR2.

Based on the failure of the AF1 and AR1 primers, the second set of iNOS primers were designed using the same approach (see Table 4.1). These primers were based on exon B: F2: AGCTCATCTTTGCCAC, R2: AAGTACGAGTGGTTCCAGG, expected band size: 468 was predicted. PCR amplification was carried out on genomic DNA from mouse 417 (heart tissue DNA), using a temperature gradient Figure 4.7 shows the results. No band of the expected size was found in any of the PCR conditions which spanned a generous range either side of the predicted annealing temperature. Further experiments failed to amplify from these primers

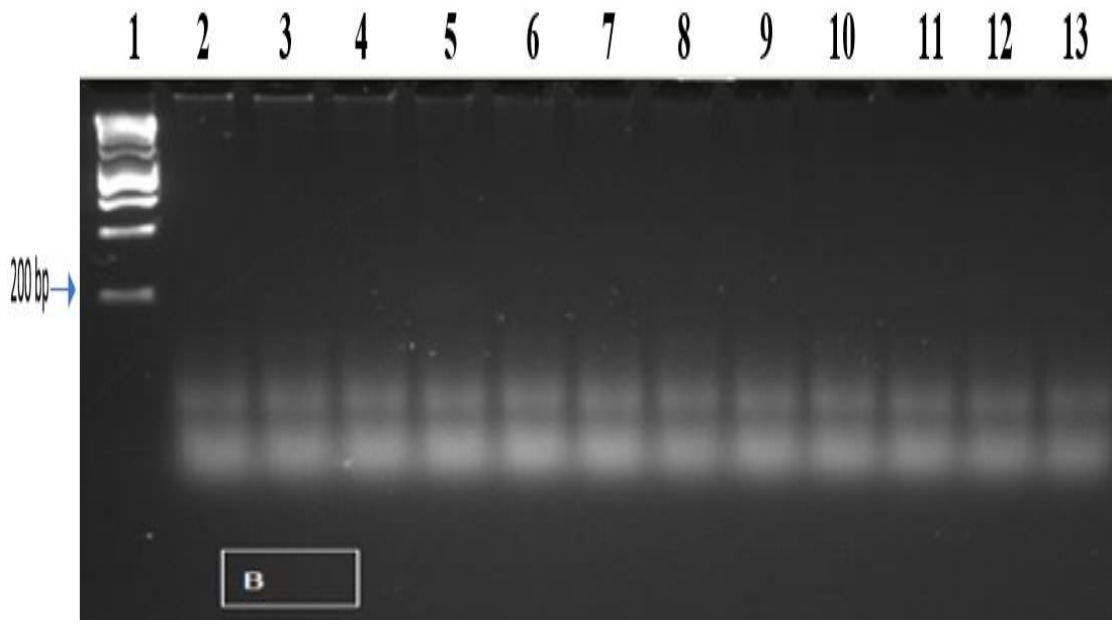

Figure 4-5 PCR amplification of the iNOS Primers BF2/BR2 using *Apodemus* genomic DNA.

A range of PCR annealing temperatures, across a gradient (52^0C – 63^0C), using gDNA from *Apodemus* heart tissue DNA as a test set. The sample came from mouse number 417. Lanes, 1= 1k ladder, 2= 52^0C, 3=53^0C, 4=54^0C, 5= 55^0C, 6= 56^0C, 6= 57^0C, 8= 58^0C, 9= 59^0C, 10= 60^0C, 11= 61^0C, 12= 62^0C, 13= 63^0C. Negative control was also run – not shown. This primer has failed to amplify the target gene sequence.

These results show that these primers are unsuitable for use with *Apodemus* DNA for amplification of the iNOS gene

4.4.5 Design of new PCR primers based on Exon 6 of the iNOS gene.

To improve the chances of finding appropriate PCR primers to use as tools for the amplification of the iNOS gene from gDNA, a strategy was developed to design primers around exon 6 of the gene. This region appeared to have suitable homology between the *Mus* gene sequences and those of *Apodemus*. Bioinformatic analysis of the locations of exon six was carried out by examining the *Mus* genome for the appropriate region (Figure 4.11). A pair of primers were chosen and compared with the *Apodemus* preliminary genome sequence to ensure that they matched exactly. The primers were then checked for hairpins and possible primer-dimer formation. Since the primers are within the introns flanking exon 6, they will only amplify genomic DNA and not cDNA. So in addition to acting as a PCR amplification method for the *Apodemus* iNOS gene, it can also be used to confirm the presence/absence of genomic DNA contamination of cDNA as a pure sample of cDNA derived from RNA should not contain these intron regions. The primers, iNOS CF3 and iNOS CR3 are shown in Table 4.1. Comparisons of the proposed amplicon from *Mus* and *Apodemus* are compared in Figure 4.8. Exon 6 is 163bp in *Apodemus* and longer (203bp) in *Mus* which means that the predicted amplicon sizes in both species are 566 and 604bp respectively.

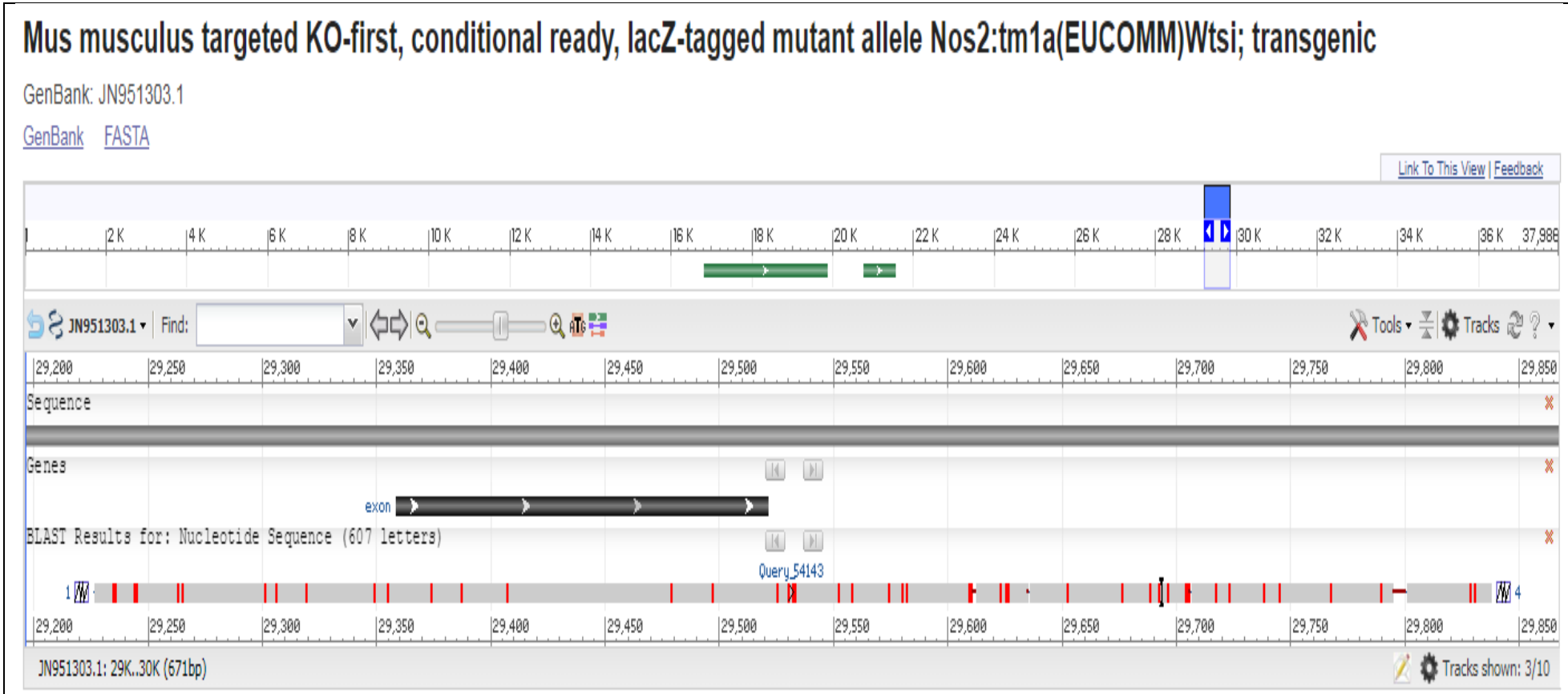

Figure 4-6 Graphic derived from the NCBI database showing exon 6 of the iNOS gene from *Mus musculus*.

The grey bar in the middle of the diagram shows the location of exon 6.

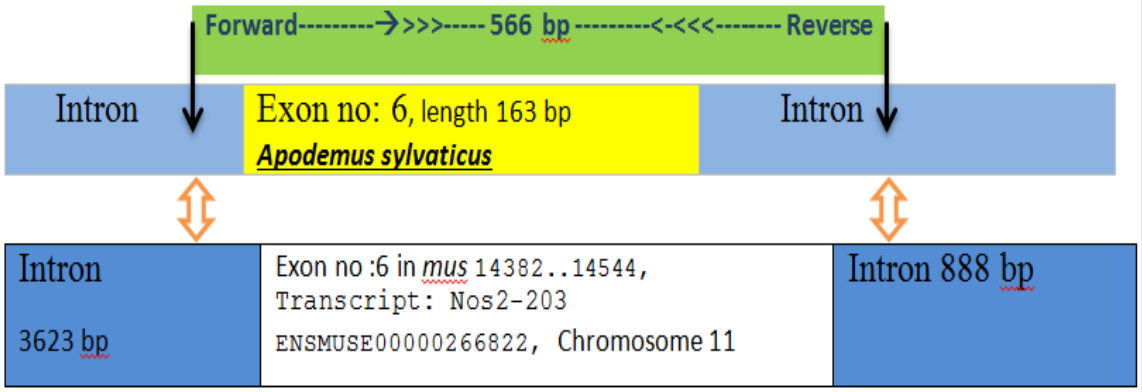

Figure 4-7 Schematic showing the proposed amplicons and primer design strategy for primers CF3 and CR3.

The upper diagram shows the *Apodemus* gene as derived from the bioinformatic analysis. Exon 6, the middle yellow section, is shorter than the equivalent exon in *Mus musculus* (lower diagram, white panel). The green bar indicates the proposed amplified fragment from both species.

4.4.6 PCR amplification of *Apodemus* DNA using the CF3/CR3 iNOS primers.

This pair of primers (see Table 4.1) was designed as described above and covered part of intron 6, exon 6, and part of intron 7. PCR amplification was carried out as before at a range of temperatures, and an optimum annealing temperature of 54^0 C was determined (data not shown). An expected band size of 604bp in *Mus* and 566bp in *Apodemus* were predicted. Figure 4.10 shows the resulting gel for a range of heart DNA samples taken from several different *Apodemus* animals (Population 2, table 2.1). A band size of 566 was seen in most of the samples. Some samples produced a smeared band that appeared a different size (e.g. lanes 5, 8,11) – it is thought that these were due to either overloading or sample preparation since they were not consistent in other experiments (where a band of 566 was seen for these samples).

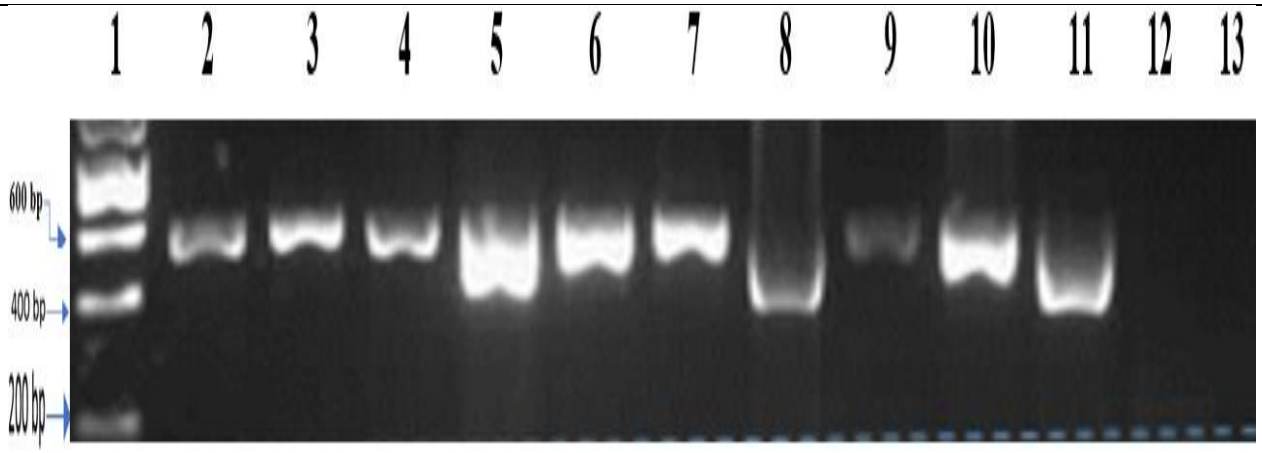

Figure 4-8 PCR amplification of the iNOS Primers CF3/CR3, the expected band size of this primer is around 566 bp, using *Apodemus* gDNA.

PCR amplification of gDNA from *Apodemus* heart tissue DNA from different animals. Numbers refer to the animals used. Lane 1= 1k ladder, 2= 440, 3= 413, 4= 414, 5= 415, 6= 416, 7= 417, 8= 419, 9= 420, 10= 421, 11= 422, 12= Negative control consisting of H_2O.

This shows that these set of primers work correctly and amplify a band of the correct size from *Apodemus*.

4.4.7 Design and evaluation of an iNOS gene cDNA specific primer

The iNOS gene expression has been shown to increase the resistance of rodent hosts to *Toxoplasma*. To develop tools for detecting iNOS mRNA, levels in *A. sylvaticus*, it is necessary to have a PCR methodology that can semi-quantitatively identify cDNA reverse transcribed from expressed mRNA. The strategy involves designing a primer that can amplify both the genomic DNA and cDNA created from mRNA. By developing a primer that spans two exons, PCR amplicons generated from cDNA will be shorter than those produced from genomic DNA because the intron will have been spliced out. To achieve this, two primers, iNOScDNAF1 and iNOScDNAR1 were designed (see Table 4.1: (5' GAGAAGCTGAAGCCCAAGAA 3'and 5' GCTTGTCACCACCAGAAGTAG 3') around exon 13 - 15 from the *Mus* genome sequence. The forward primer is located 31 bp from the beginning of exon 13, (Accession no: 23690.23884), while the reverse is located 49 bp from the start of the exon 15, (Accession no: 24899.25003). Thus spanning three exons and two introns. The expected size of the genomic fragment (gDNA) is 757 bp, while the cDNA generated from the spliced exon is expected to be 263bp. Figure 4.11 summarises this strategy.

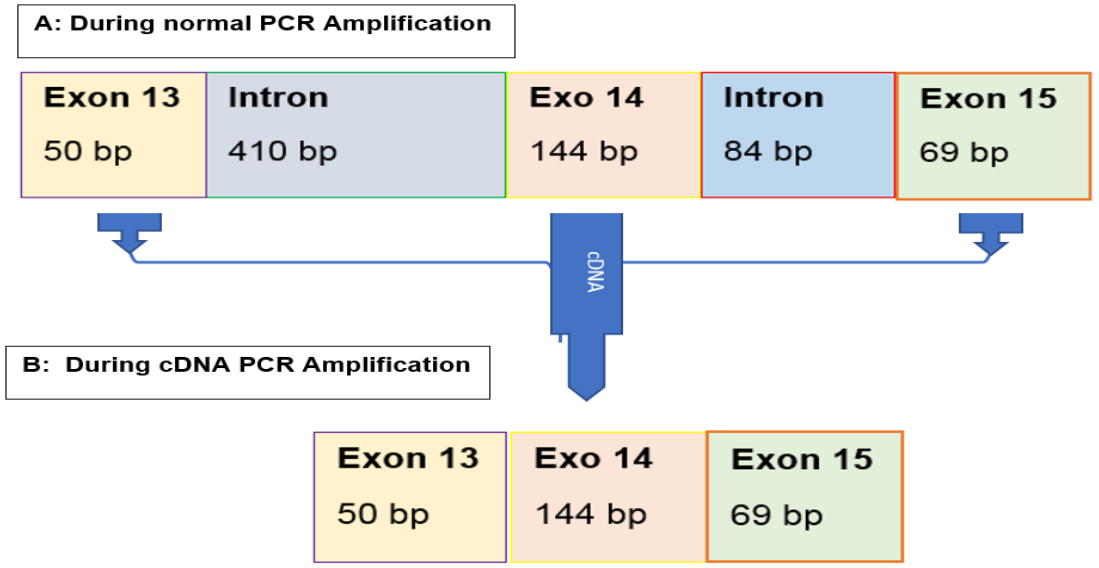

Figure 4-9 Procedure for the development of the iNOS cDNA specific primers. The top A bar shows the expected fragment generated from the genomic DNA (derived from accession number NCBI AF427516.1) which gives a total PCR fragment 757 bps. The middle B panel explains the arrangements of joined Exons 50 bp of exon 13, all the exon 14 about 144 bp, and 69 bp of 15 with the associated introns. In addition to that lower panel shows the joined exons when the mRNA has been spliced and converted to cDNA approximately 263 bp.

PCR amplification and optimisation were carried out using the primers, following protocols described in Chapter 2, with a range of annealing temperatures between 52-63^{0}C. Figure 4.12 shows the amplified PCR products detected on a 2% agarose gel.

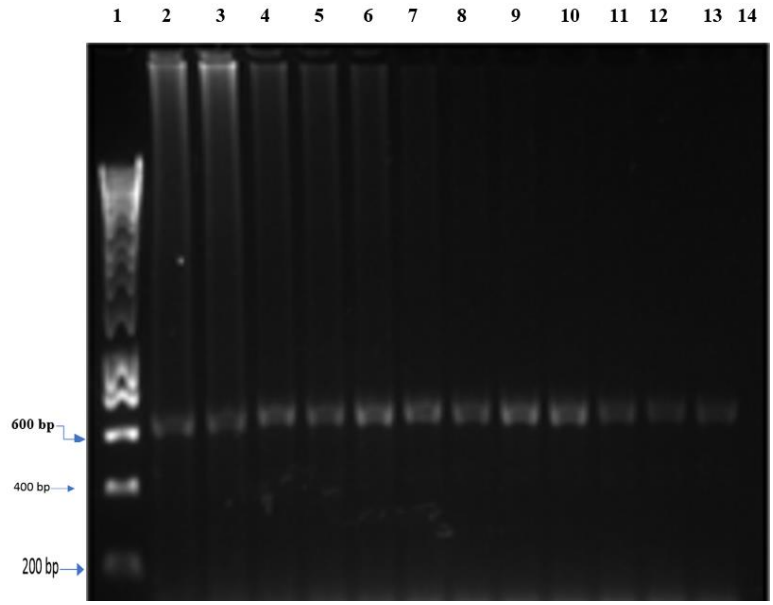

Figure 4-10 Agarose gel electrophoresis of products produced by primers iNOScDNAF1 and iNOScDNAR1.
A 2 % agarose gel showing PCR amplicons from genomic DNA from *Apodemus* 417 at different annealing temperatures. Lanes: 1= 1kb ladder, 2= 52^{0}C, 3=53^{0}C, 4=54^{0}C, 5= 55^{0}C, 6= 56^{0}C, 6= 57^{0}C, 8= 58^{0}C, 9= 59^{0}C, 10= 60^{0}C, 11= 61^{0}C, 12= 62^{0}C, 13= 63^{0}C C^0. 14= Negative control.

In this PCR, the iNOS primers successfully amplified from gDNA at all annealing temperatures and produced a band of the expected size of 757bp for genomic DNA. At the range of annealing temperatures used, indicates that 58-60^{0}C is probably the optimum annealing temperature. This shows that a set of primers have been developed that are capable of distinguishing genomic and cDNA and work in amplification of genomic DNA. The next stage is to evaluate their use for the detection of cDNA in the semi-quantification of mRNA expression.

4.4.8 Evaluation of the iNOS cDNAF1 and iNOScDNAR1 primers as for PCR tools to distinguish amplification of genomic and cDNA from *Apodemus* samples.

To test the iNOS cDNA F1 and iNOS cDNA R1, for the ability to distinguish amplification of genomic DNA and cDNA (i.e. from splice-edited mRNA), DNA and RNA were extracted from *Apodemus* heart tissue from mice samples H368 and H369. DNA was extracted using the DNeasy kit from Qiagen, as described in Chapter 2, and RNA extraction and conversion to cDNA was also carried out using Qiagen commercial kits as described in Chapter 2.PCR amplification of both prepared gDNA and cDNA, from *Apodemus* 2 and 3, was carried out using the iNOS cDNAF1 and iNOS cDNAR1 primers, with an annealing temperature of 54^0C, and run on a 2 % agarose gel. The results are shown in Figure 4.13.

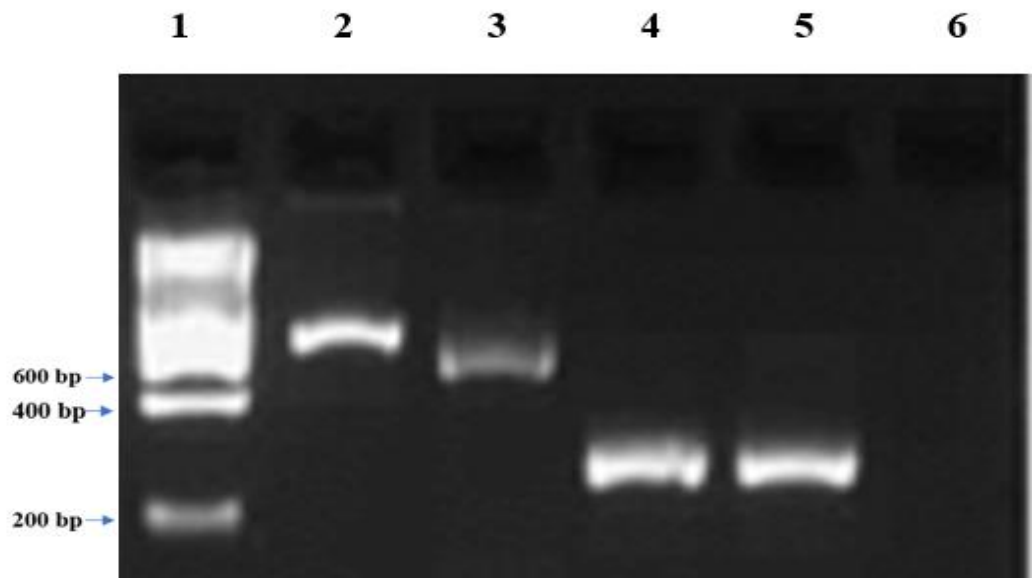

Figure 4-11 PCR amplification of gDNA and cDNA using primers iNOS cDNA F1 and iNOS cDNA R1.
Lanes: 1= 1kb hyper ladder, PCR products from gDNA which also contain intron, thus give a larger band size, from *Apodemus*: lane 2 = H368, lane 3= H369 *respectively;* while lanes 4 and 5 = PCR products from cDNA (derived from mRNA), which is lacking the exons, using *Apodemus* Heart tissues,(population 2, table 2.1) lane 4 = H368, lane 5 = H369, lane 6 = *negative control.*

The same primer pair has successfully amplified amplicons from both the gDNA, and RNA converted to cDNA. The cDNA amplification (lanes 4 and 5) produced a smaller band (shorter fragment) which comprises the spliced exons and is 260bp and corresponds to the expected size of 263bp. The gDNA amplified a band of 757bp which corresponds to the predicted size (757bp). The negative control produced no band as expected. This demonstrates the flexibility of this set of primers to be used for both DNA and cDNA PCR amplification. It also offers the opportunity to be able to check the purity of cDNA preparations because impure cDNA, when running on a gel following PCR amplification, will show up the contaminating band at 620bp.

To confirm that the cDNA has been correctly generated and amplified, the bands were purified and sent for sequencing. The sequence was returned, as a chromatogram, examined using the programme Finch TV and errors or unallocated bases were corrected to generate a consensus sequence (see Figure 4.12).

AGCTTCCGTGCTAATGCAAAAAGTCATGGCTTCCCGAGTCAGAGCCACAGTCCTC
TTTGTACTGAGACAGGGAAATCCGAGGCGCTAGACAGGGACCTGGCGGCCTTGT
TCAGCTATGCCTTCAACACCAAGGTTGTCTGCATGGACCAGTATAAGGCAAGCGC
CTTGGAAGAGGAGCAGCTACTTCTGGTGGTGACAAGCA

Figure 4-12 Figure 4.17 DNA Sequence.
Sequence result of the PCR products received from source Biosciences analysis of the PCR amplicons from the cDNA amplification using primers iNOScDNAF1 and iNOS cDNAR1, these are a more evident sequence about 200bp, while the rest of 63 bs were cut off from the beginning and at the ends, because there is an Ns which is a noise, that not chromatogram at the sequences, and not included for the alignments.

The consensus sequence was analysed using the program blast against the NCBI web site to confirm that this is the right gene and is the iNOS gene.

However, the iNOScDNAF1 and iNOScDNAR1 primer amplicon from cDNA was a match with *Mus caroli* nitric oxide synthase 2 (NOS2, synonymous with iNOS), transcript variantX3, mRNA (Accession number: XM_021176044.1). This confirms that the cDNA target has been successfully amplified. Furthermore, alignment of the amplified sequence (Figure 4.13) with the sequence in XM_021176044.1 shows a very high similarity with only a few SNPs. These are presumably differences between the *Mus* and *Apodemus* genes.

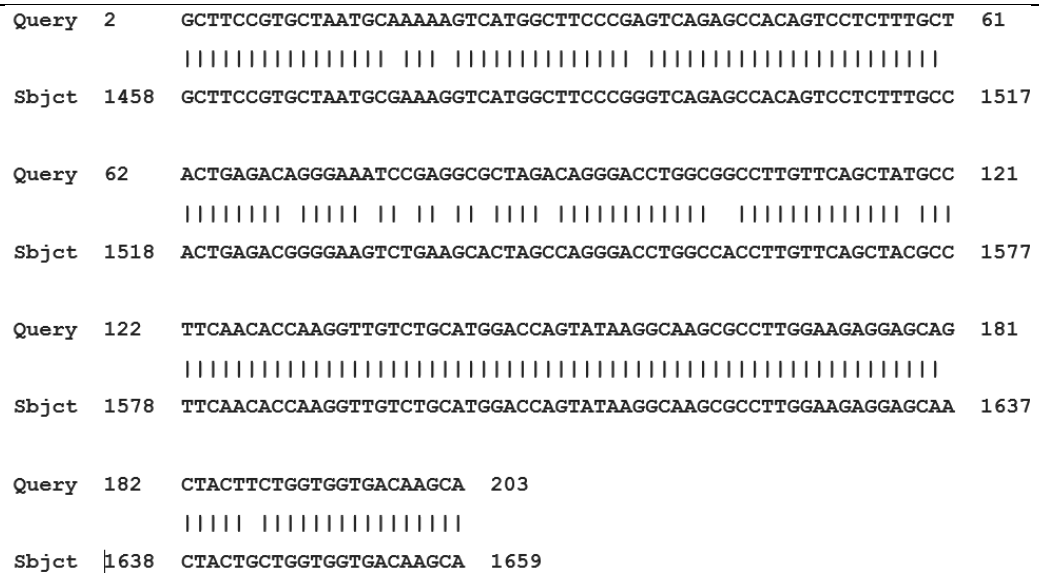

Figure 4-13 Alignments of *Apodemus* iNOScDNAF1 and iNOScDNAR1sequences from the BLAST search to the top match.

There is 93 % the identity between the sequences. The primers designed for detection of both of gDNA & cDNA have worked and can now be used for semi-quantitative PCR of cDNA derived from expressed messenger RNA. However, there is some mutation or called varied SNPs to the *Mus* where there is no presenting a vertical line.

4.4.9 Evaluation of the iNOS cDNA F2 and iNOS cDNA R2 primers as for PCR tools to distinguish amplification of genomic and cDNA from *Apodemus* samples.

As difficulties were experienced in designing primers for the iNOS gene in general, the second set of primers were developed in parallel with the iNOS cDNA F1/R1 primers to provide a backup methodology. These have been named iNOS cDNA F2/R2. These second primers have been designed in a similar way to the F1/R1 primers. The primers amplify 66 bp from exon 13 & 144 bp from exon 14 producing a total band size 210 bp, Figure 4.14 shows the final cDNA amplified consists of exon 13 & 14, when generated from cDNA., When generating amplicons from gDNA, by PCR, an expected band size 620 bp is produced.(*Apodemus* Heart tissues, (Population 2*,* Table 2.1)).The results of the PCR products shown in Figure 4.15.

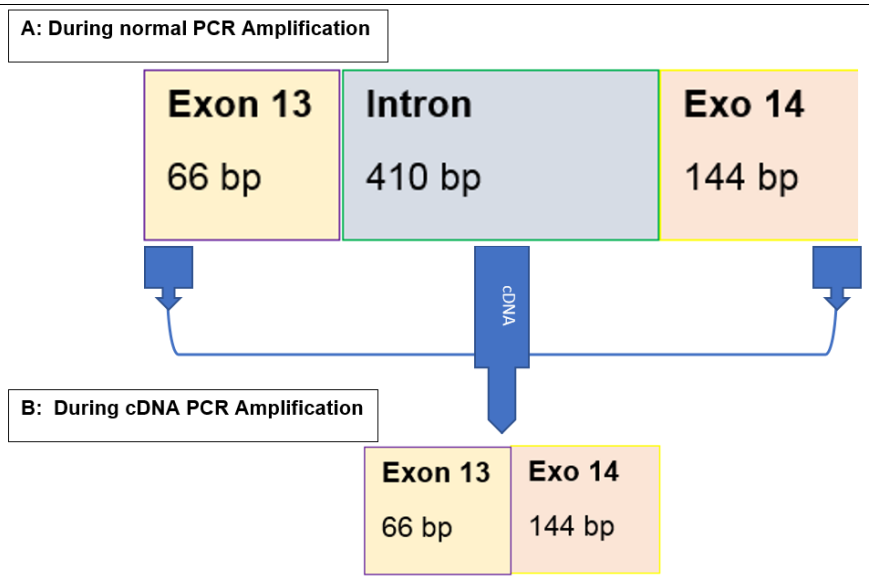

Figure 4-14 Strategy for the development of the iNOS cDNA specific primers.
The top A bar shows the expected fragment generated from the genomic DNA (derived from accession number NCBI AF427516.1) which gives a total PCR fragment 620 bps. The middle B panel explains the arrangements of joined exons 13 of 66 bp, and all of the exon 14 which is about 144 bp. in addition to that lower panel shows the joined exons when the mRNA has been spliced and converted to cDNA approximately 210 bp.

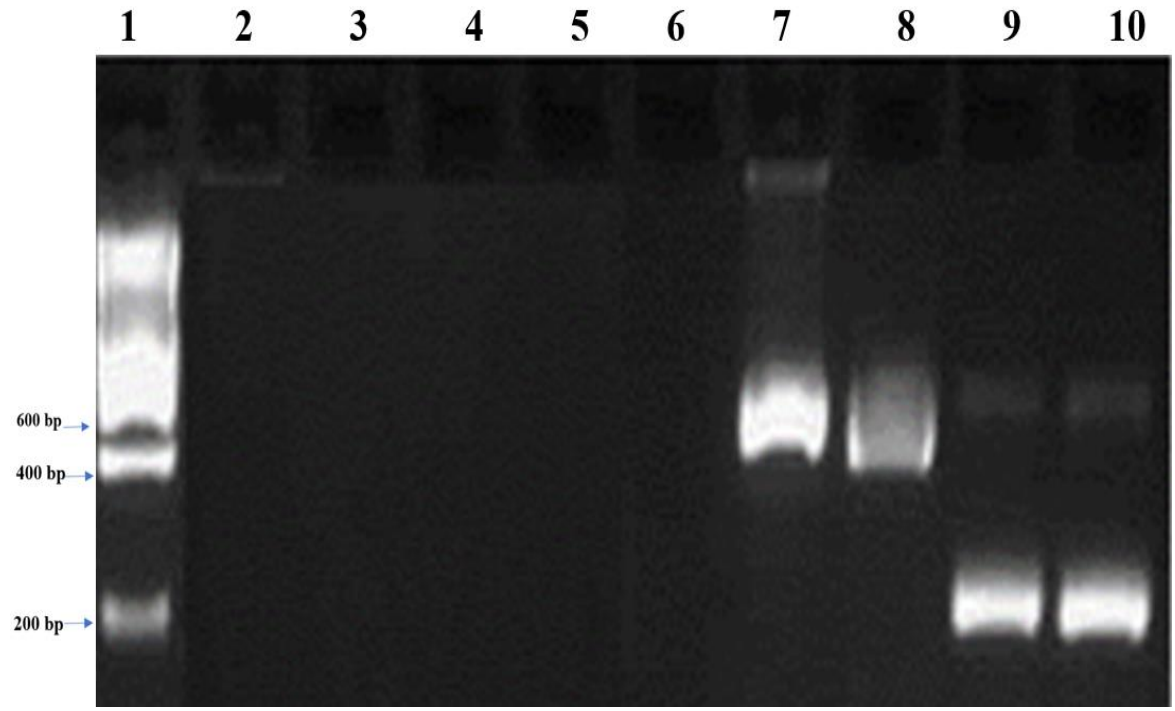

Figure 4-15 4.21 PCR amplification of gDNA and cDNA using primers iNOS cDNA F2 and iN-OS cDNAR2.
Lane 1= 1k hyper ladder, lane 2= H368, lane 3= H369, lane 4= H370, lane 5= H371, lane 6= negative control, these samples in the lanes 2,3,4,5, are RNA was treated by Turbo DNase, 6= negative control, lane 7= H368 and lane 8 = H369, these are gDNA achieved 620bp, of *Apodemus* Heart PCR, lane 9= H368 and lane 10= H369 of the mRNA TURBO DNA treated samples of *Apodemus* Heart converted to cDNA using Qiagen reverse transcriptase cDNA enzyme, expected band size of the Polymerase chain reaction approximately 210 bp from the cDNA.

Figure 4.15 shows PCR products of iNOS F2/R2, amplified from *Apodemus* RNA and DNA. Lanes 1,2,3,4,5, lanes contain RNA that was treated with Turbo DNase - this enzyme removes any contaminating DNA from RNA preparations. The lack of amplification demonstrates that RNA preparation is indeed DNA free. Lanes 7 and 8 contain gDNA to prove that the PCR can work and shows the larger band size of 620 bp representing the amplified exon and intron sequences. Lanes 9 and 10 show cDNA that was synthesised from the *A. sylvaticus* RNA. This demonstrates that cDNA synthesis has worked successfully. A band size 210 bp is produced by amplification of just the exons.

This demonstrates that both of the specific primers have worked and will detect the iNOS gene either is amplified from either gDNA or cDNA.

4.4.10 Preparation of RNA samples from infected and uninfected rodents.

To investigate the expression of the iNOS gene in relation to infection with *Toxoplasma gondii*, RNA is required from mouse brain tissue. As the previously characterised *Apodemus* were not collected and prepared with the aim of RNA extraction in mind, another collection of animals was made. This included 8 *A. sylvaticus* and four voles. DNA and RNA were extracted from the brain tissue of these animals. These were then tested for *T. gondii* infection using the DNA and examined for expression of iNOS and Arginase using the RNA.

For *Toxoplasma* detection, DNA was extracted from the twelve brain samples as described in Chapter 2. (Population 4, Table 2.1). RNA was extracted using the Qiagen RNase Fibrous Tissue Mini Kit for RNA extraction as described in Chapter 2. SAG2 PCR amplification was used on the DNA samples to test for the presence of *Toxoplasma*. Figure 4.16 below shows the results. This PCR was repeated twice more, and vole five and *Apodemus* 10 and 12 were infected.

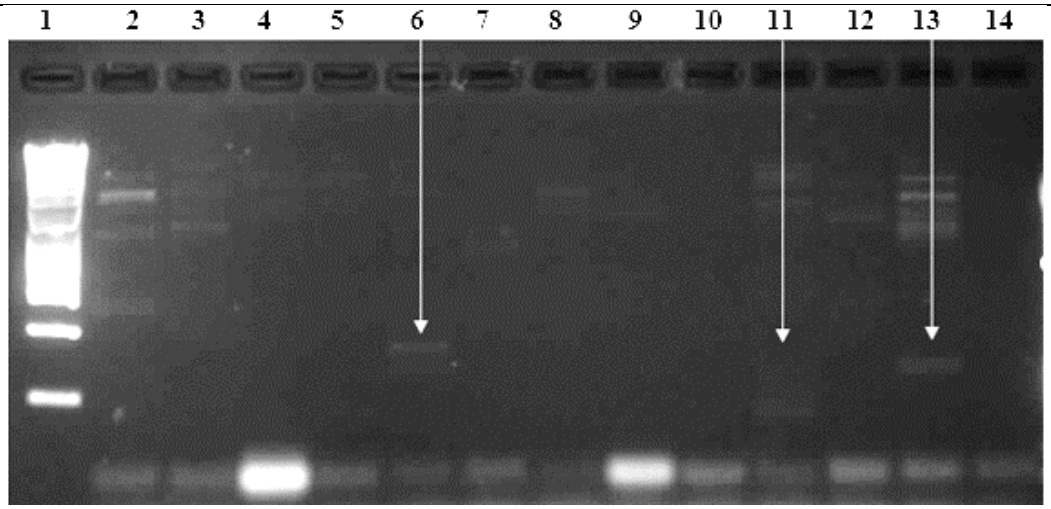

Figure 4-16 PCR Amplification using the SAG2 gene (2nd round) for *Toxoplasma* detection.
Lane 1, is1Kb ladder, extracted DNA from brain tissue, lane 2 = *Vole* 1, 3= *Vole* 2, 4 = *Apodemus* 3, 5 = *Apodemus* 4, 6 = *Vole* 5, 7 = *Vole* 6, 8 = *Apodemus* 7, 9 = *Apodemus* 8, 10= *Apodemus* 9, 11= *Apodemus* 10, 12= *Apodemus* 11, 13 = *Apodemus* 12, 14 = Negative control (H_2O), Bands can be seen in animals 5,10 and12 indicating that they are infected.

Table 4-3 Summary of SAG2 *Toxoplasma* Infection Status

Mouse no	Species	Diagnosis of *Toxoplasma*
1	*VOLE*	Not Infected
2	*VOLE*	Not Infected
3	*APODEMUS*	Not Infected
4	*APODEMUS*	Not Infected
5	*VOLE*	Infected
6	*VOLE*	Not Infected
7	*APODEMUS*	Not Infected
8	*APODEMUS*	Not Infected
9	*APODEMUS*	Not Infected
10	*APODEMUS*	Infected
11	*APODEMUS*	Not Infected
12	*APODEMUS*	Infected

RNA extraction was performed on the remaining pieces of the brain tissue samples. The concentration of RNA was measured using a nanodrop spectrophotometer (Table 4.4).

Table 4-4 Concentrations of Brain RNA.

Mouse no	RNA ConC ng/µl	A260	A280	260/280	260/203	Factor
1 *V*	941.9	23.548	11.185	2.11	3.22	40.00
2 *V*	952.6	23.815	11.191	2.13	2.81	40.00
3 *A*	360.3	9.007	4.240	2.12	1.48	40.00
4 *A*	361.4	9.035	4.264	2.12	1.45	40.00
5 *V*	517.3	12.932	6.257	2.07	2.98	40.00
6 *V*	970.3	24.258	11.442	2.12	2.81	40.00
7 *A*	274.5	6.861	3.373	2.03	2.86	40.00
8 *A*	742.1	18.552	9.005	2.06	2.02	40.00
9 *A*	543.2	13.581	6.429	2.11	3.94	40.00
10 *A*	94.1	2.353	1.088	2.16	13.80	40.00
11 *A*	483.0	12.074	5.757	2.10	2.59	40.00
12 *A*	503.8	12.595	6.000	2.10	2.34	40.00

Sufficient quantities of RNA were extracted from each brain sample. Furthermore, to confirm the concentrations as determined using the nanodrop spectrophotometer, 9µl of the RNA samples were examined by gel electrophoresis (Figure 4.17). RNA could be seen in all lanes as judged by bands representing the 28S and 18S RNA.

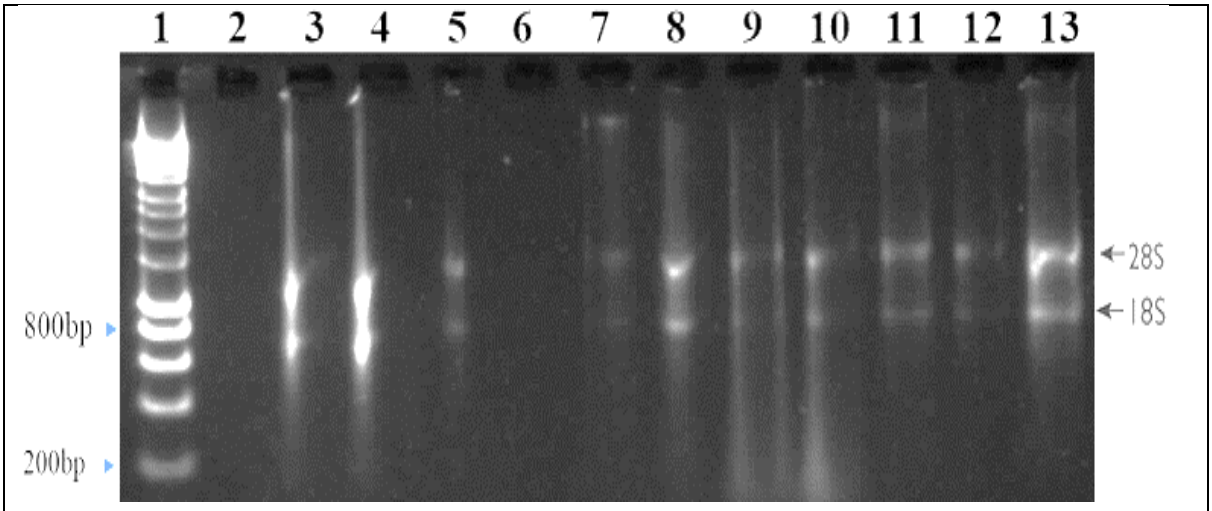

Figure 4-17 Agarose gel electrophoresis of RNA extraction.
Lane 1 is the 1Kb is a ladder, RNA extractions as follows: lane 2 = *Vole* 1, 3= *Vole* 2, 4 = *Apodemus* 3, 5 = *Apodemus* 4, 6 = *Vole* 5, 7 = *Vole* 6, 8 = *Apodemus* 7, 9 = *Apodemus* 8, 10= *Apodemus* 9, 11= *Apodemus* 10, 12= *Apodemus* 11, 13 = *Apodemus* 13. first band at 600 bp is the 18S RNA, while, the band at 800 bp is the 28S RNA.

Figure 4.17 confirms the presence of RNA and shows that it is of good quality. This RNA can be used for quantitative PCR (qPCR) measurement of gene expression.

4.4.11 Quantification of iNOS and Arginase RNA levels

Firstly, the RNA was converted to cDNA, which is a more stable and suitable template for RNA measurement by qPCR., cDNA was made using a Qiagen kit as described in Chapter 2. qPCR was carried out using a Retrogene qPCR machine from Qiagen. Each sample was measured in four replicates using fluorescent primers to the iNOS (iNOS cDNAF1/R1, table 4.1), Arginase (Z Li et al. 2012; Table 4.1) and tubulin (internal control) genes. Dilutions of each sample were used as follows: 1/10, 2/10, 3/10, The tubulin gene primers were included as internal controls and water were included as a negative control in all experiments.

The results for the q-PCR amplification were collected, and all three genes (iNOS, Arginase and tubulin) had a good best fit with R^2 values as follows: 0.905, 0.931 and 0.993, respectively. The results of the amplification and measurements are shown in Table 4.5.

Table 4.5 indicates the animal number and the species (Vole or *Apodemus*) and the infection status with *Toxoplasma*. In columns 3-5, the CT values (mean of 4 replicates) of the three genes (iNOS, Arginase and tubulin) are shown. Using the internal tubulin control, these have all been corrected so that they represent expression levels relative to each other (Column 6, Arginase; Column 7, iNOS; Column 9, tubulin control). It has been shown (Gao et al., 2015) that the sensitivity and resistance of rodent hosts to *Toxoplasma* is related to the ratio of the expression of iNOS/Arginase. Column 8 shows the iNOS/Arginase ratios for each animal. These latter values have been calculated from the corrected relative expression levels.

Table 4-5 Summary of the Expression Level s of ARGINASE and iNOS.

No	T. gondii	Arg/Ct Mean	iNOS/Ct Mean	Control Ct	Corrected Ct Arg	Corrected Ct iNOS	Ratio iNOS/Arg	Corrected Control
1 V	-	15.596	18.413	11.92	15.60	18.41	1.18	11.92
2 V	-	15.123	18.06	13.12	16.65	19.88	1.19	11.92
3 A	-	15.816	15.776	12.46	16.53	16.49	1.00	11.92
4 A	-	15.063	14.823	12.67	16.01	15.76	0.98	11.92
5 V	+	13.903	13.956	13.05	15.22	15.28	1.00	11.92
6 V	-	14.563	19.68	11.38	13.90	18.79	1.35	11.92
7 A	-	15.25	17.95	15.95	20.41	24.02	1.18	11.92
8 A	-	14.936	14.566	11.25	14.10	13.75	0.98	11.92
9 A	-	15.143	18.75	13.08	16.62	20.57	1.24	11.92
10 A	+	13.823	12.7	12.89	14.95	13.73	0.92	11.92
11 A	-	14.36	20.673	9.9	11.93	17.17	1.44	11.92
12 A	+	15.323	12.7	8.83	11.35	9.41	0.83	11.92

From Table 4.5, it can be seen that the iNOS/Arginase ratios range from 0.83 to 1.44 and that the infected animals have a broadly lower rate of iNOS to arginase than the uninfected animals. Analysis of the distributions of the infected compared to the uninfected animals were compared. The data did not conform to a normal distribution (tested using a Shapiro-Wilks Test) and therefore a Mann-Whitney U-Test was conducted. This showed that there was a significant difference between infected and uninfected animals (P=0.05). The infected animals had a higher iNOS to Arginase ratio (Figure 4.18).

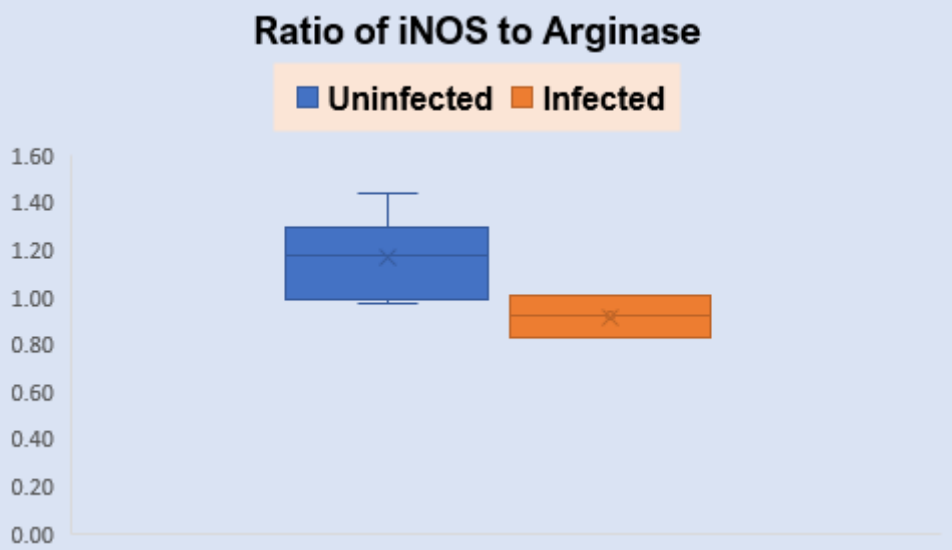

Figure 4-18 Box and whisker plot.

Box and whisker plot of the mean iNOS/Arginase ratios. The orange box represents infected animals, while the blue box is uninfected. There is a standard error of the means of 0.054 for the non-infected iNOS/Arg ratios and a standard error of 0.05 for the infected mice. There is a significant difference between the distribution of the iNOS/Arginase ratios (P= 0.05), of the infected and uninfected animals (Mann-Whitney U-Test).

Figure 4.19 shows the distribution of the Arginase and iNOS levels in both infected and uninfected animals. It can be seen that in the infected animals, the Arginase expression is higher than the iNOS expression, while in the uninfected animals the Arginase expression is lower than the iNOS expression.

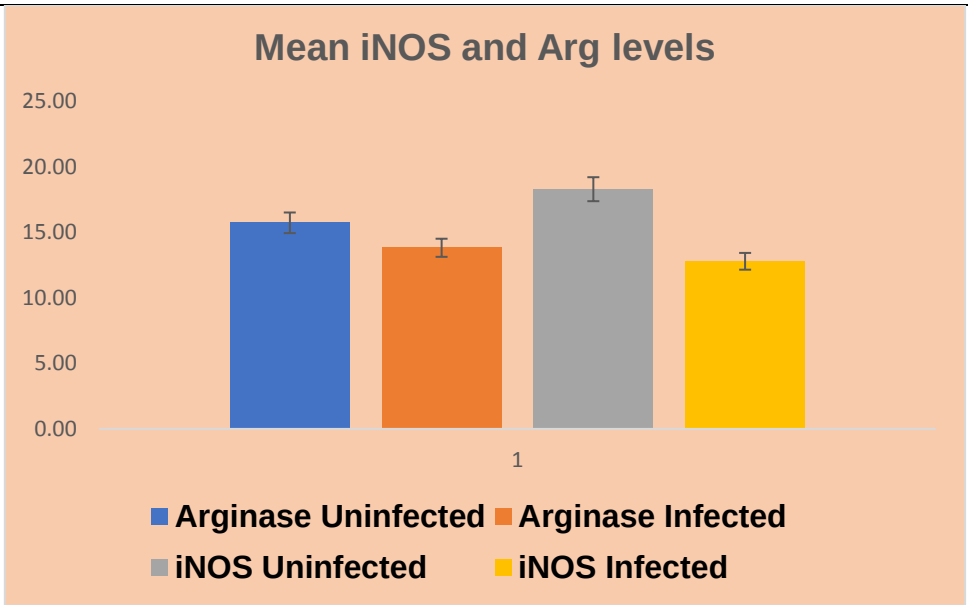

Figure 4-19 Bar chart showing the mean, corrected iNOS and Arginase expression levels.

The yellow and orange bars show the mean iNOS and Arginase expression levels in infected animals, respectively, while the blue and light blue bars show the Arginase and iNOS expression levels in the uninfected animals.

Since the 12 animals used in this study were from different species (*Apodemus* and voles), these results may be confounded by mixing the species. To eliminate the effect of that, the iNOS/Arginase ratios were considered only on the 8 *A. sylvaticus* brain samples. Figure 4.20 shows a box and whisker plot of the iNOS/Arginase ratios for the 8 *Apodemus* samples (2 infected and six uninfected). Again, there is an observable difference between the distribution of iNOS/Arginase ratios of infected and uninfected *Apodemus* however this was a very small sample size and only approached significance (P = 0.065). This provides evidence that iNOS/Arginase ratios are different between the infected and uninfected animals.

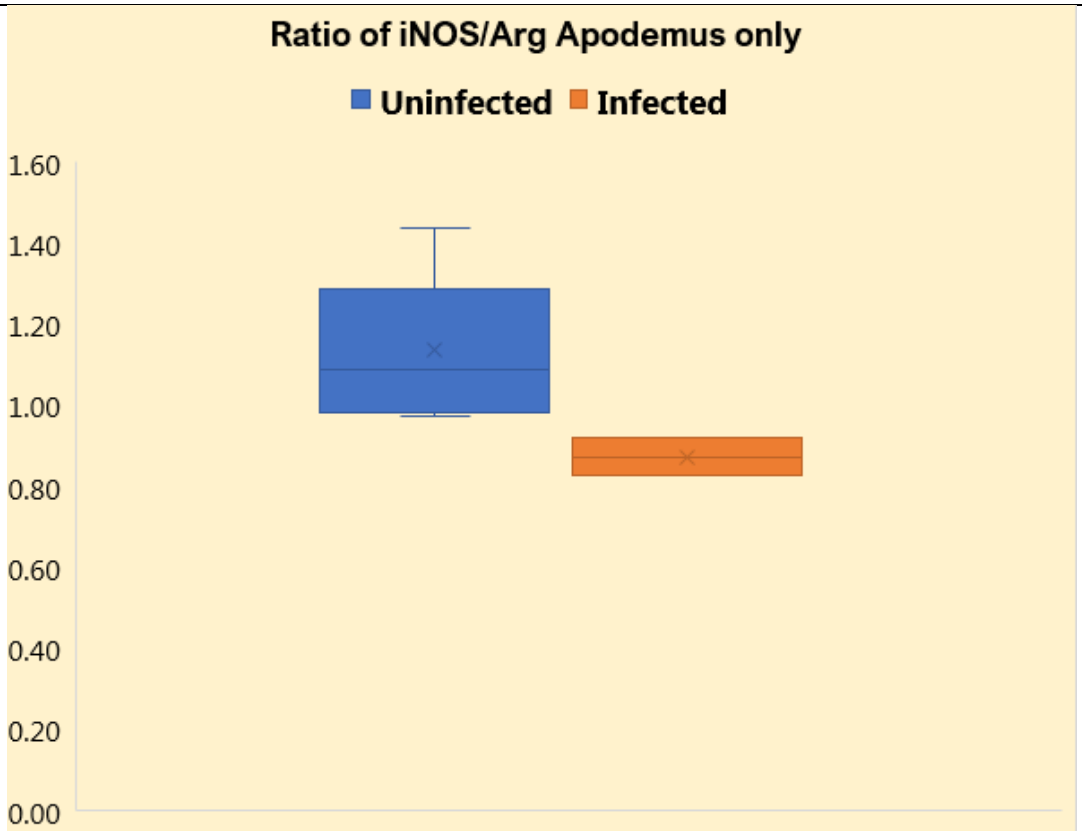

Figure 4-20 Box and whisker plot of the mean iNOS/Arginase ratios.

Box and whisker plot of the mean iNOS/Arginase ratios. The orange box represents infected animals, while the blue box shows uninfected animals. There is a standard error of the means of 0.054 in non-infected iNOS/Arg ratios and a standard error of 0.05 for the infected mice. There is not a significant difference between the distribution of the iNOS/Arginase ratios (P= 0.065), although this approaches significance, of the infected and uninfected animals.

4.5 Discussion

This chapter aimed to measure the gene expression of iNOS and Arginase, with regards to diagnosing and investigating *Toxoplasma* infection of the *Apodemus* samples. DNA and RNA were extracted from brain tissues, from *Apodemus* and voles from the Malham Tarn area, and high yields were obtained for both nucleic acids. Use of the SAG2 PCR marker to test for *Toxoplasma* presence shows a prevalence of 25% of the animals infected (2/8 *Apodemus*; 1/4 voles). Gel electrophoresis was used to confirm that the RNA was of good quality as judged by the bright 18S and 26S bands. Primers were chosen for the Arginase gene to amplify the homologous gene from *A. sylvaticus,* based on the *Mus musculus* primers used in a previous study (Z. Li, Z. J. Zhao, *et al.*, 2012), The PCR product was sequenced and confirmed the identity with 95% similarity to the arginase gene from *Mus musculus*.

Previously designed PCR primers from the iNOS gene of *M. musculus* (Z.Li et al., 2012) failed to amplify the homologous gene from *A. sylvaticus*. Several combinations of primers were tried before a set of successful primers were designed which could distinguish between *A. sylvaticus* genomic DNA and cDNA generated from reverse transcriptase conversion of RNA. Sequencing of the amplified iNOS PCR products from the DNA and cDNA, outcomes confirmed their identity and showed that the portion of the *Apodemus* iNOS gene was 94% similar to the iNOS gene from *Mus musculus*. Thus, these tools could be used for investigating iNOS and arginase gene expression in *A. sylvaticus*.

The results confirm that the uninfected animals had a higher expression level of the iNOS relative to the lower level of arginase. In the case of the infected animals, the expression level of the Arginase gene was higher than the iNOS gene when measured using qPCR. Previous studies have shown that a determinant of sensitivity and resistance to *T. gondii* infection is the ratio of iNOS/Arginase expression – a high ratio appears to confer resistance while a lower rate, sensitivity. In this study, the infected animals had a significantly lower iNOS/Arginase ratio than uninfected animals (P=0.05). As these experiments were conducted on 12 animals of mixed species (*A. sylvaticus* and voles), there is the possibility that the mixture of species was responsible for confounding this analysis. To address this, the 8 *Apodemus* mice were examined separately. Of these, two were infected while six were not. When the

iNOS/Arginase ratios were calculated, there was, again, an observable difference between the uninfected (higher rate) than the infected but due to the small sample size this only approached significance (P=0.065).

In previous studies in mice and rats (Li et al., 2012; Zhao et al., 2013; Gao et al., 2015) expression at high levels of inducible nitric oxide synthase (iNOS) prevented infection in rats but did not in mice. The laboratory mice inbred lines had low iNOS activity, were very sensitive to infection with *Toxoplasma* and died quickly. The balance of iNOS and Arginase expression, two enzymes that share the same substrate Arginine, determine whether a cell or tissue produces either nitric oxide (NO) (high iNOS expression) or urea (high Arginase expression). The former is known to kill intracellular pathogens including *Toxoplasma*. Differences in resistance, to *Toxoplasma*, in different inbred rat lines, has been correlated with the ratio of iNOS to Arginase gene expression. These studies in laboratory rodents highlight the importance of these enzymes in infection, but very little is known about the role of these infections in natural populations of rodents.

There have been a wide range of studies on *Toxoplasma* infection in rodents where often high prevalence have been reported (e.g. (Marshall, 2004)) with a number of studies based, primarily on *A. sylvaticus* around the Malham Tarn Field Centre in Yorkshire, UK (Thomasson et al. 2011; Bajnok et al. 2015; this study, Chapter 3, 4). In these latter studies, prevalence of between 25 – 41% have been reported: 40.78% (CI: 95% 34.07 – 47.79%; n=206) (Thomasson et al. 2011), 34.92% (CI: 95% 27.14 – 43.59%; n=126) (Bajnok et al. 2015), 28.6% (CI: 95% 17.8 – 42.5%; n=49) (this study, Chapter 3), 25 % (CI: 95% 8.2 - 53.8%; n=12) (this study, this chapter).

If these wild *Apodemus* behaved in the same way as the laboratory mice and had shallow iNOS levels, they would become infected and die quickly. So there clearly must be some inherent resistance which at least allows them to survive. Furthermore, the uninfected mice could either be uninfected because that have not been exposed to the parasite or because they have a higher degree of innate resistance to the parasite. As the iNOS/Arginase gene expression balance determines resistance and sensitivity in laboratory model systems, this question could be investigated in the wild *Apodemus* and voles used in this study. As described above a significant difference was observed in the iNOS/Arginase ratios thereby supporting the hypothesis that uninfected mice are associated with higher iNOS/Arginase ratios while infected mice have lower rates. In the study of (Zhao, *et al.*, 2012; Zhao *et al.*, 2013), iNOS RNA

expression was undetectable in 4 laboratory strains of mice (Swiss, BALB/C, C57BL/6 and NIH) giving iNOS/Arginase ratios of, respectively, 0/2.6; 0/2.5; 0/2.4 and 0/2.6 – giving proportions effectively of zero. In these mice, death occurred in, respectively, 6, 5, 7- and 6-days post-infection. In the case of the wild infected mice the ratio was much higher, at 0.92, while the wild infected mice were (significantly) higher still at 1.17. While the age of the wild mice could not be determined, they were adult mice suggesting that they were not under the same survival pressure as the laboratory mice. This indicates that there is a gradient of severity of infection, zero to low iNOS ratio results in rapid death, a ratio of below one is associated with infection but survival while mice with a ratio above 1 remain uninfected (Li et al. 2012; Gao et al. 2015.) The ratio of 1 refers to the concentrations of iNOS/Arginase – since these enzymes draw from the same substrate (arginine) a balance of above 1 will draw substrate away from Arginase while below 1 it will draw it away from iNOS. Thus the outcomes of iNOS and Arginase expression are finely balanced. It is appreciated that it is not possible to draw direct comparisons between the wild and laboratory mice since different infection routes and doses may apply. It is also recognised that the collection of wild mice is small. While more extensive collections were available for some studies, these were not collected in such a way or at a time to enable RNA extraction. However, these results are indicative of a fascinating phenomenon that deserves further study.

These studies suggest that there is a genetic component to host resistance - the ability to control iNOS and Arginase levels. As far as we know, there are no studies that investigate this question. One possibility would be looking at the DNA sequence of the promoter region of the iNOS gene to identify any polymorphisms that might correlate with infection or the lack of it. This question is addressed in the next chapter.

In the case of one study, (Zhao *et al.*, 2013; Shen *et al.*, 2017)it was shown that control of the iNOS gene might be under epigenetic control. In this study, the authors looked at iNOS expression and infection with *T. gondii* in rat peritoneal macrophages and compared with alveolar macrophages from the same inbred rat lines. In the case of the peritoneal macrophages, resistance to infection was evidence and correlated with high iNOS levels compared to Arginase. This confirmed the results of (Zhao, *et al.*, 2012; Zhao *et al.*, 2013; Shen *et al.*, 2017). However, alveolar macrophages from the same genetic background (same inbred line) showed a high degree of susceptibility to *Toxoplasma* infection and also showed a low level of iNOS expression compared to Arginase expression. They were thereby suggesting that an epigenetic difference

between the two types of macrophage was occurring which decreased the iNOS levels (in alveolar macrophages) and consequently increased susceptibility to infection. Many mechanisms of epigenetic control exist, but one of these involves the DNA methylation of cytosine residues which can act to either shut down or switch on a gene. This often occurs in locations called CpG islands (Bird et al. 1985; Bird, 1986) where CG residues become methylated and control the expression of the gene (Antequera and Bird, 1988; Bird, 2002). If such methylation sites existed in the iNOS 5' UTR (untranslated region), the 5' promoter and exon 1, they might be responsible for transient control of iNOS expression and thereby influence infection with *Toxoplasma*. In the following chapter, in addition to looking for Single Nucleotide Polymorphisms (SNPs) that might be associated with infection, bisulphite treatment of DNA from the 5' promoter regions was also examined for the presence of epigenetic polymorphisms that might be related to infection or the lack of it.

Chapter 5: Investigation of genetic and epigenetic variation in the Inducible Nitric Oxide Synthase (iNOS) gene from *Apodemus sylvaticus*.

5.1 **Introduction:**

The Inducible Nitric Oxide Synthase (iNOS) gene plays an essential role in the immune response to parasitic diseases and to intracellular parasites like *Toxoplasma gondii*. The gene product (protein) it produces is responsible for generating nitric oxide, an important molecule that acts against pathogens and elicits other immune responses. DNA methylation can play a role in the epigenetic control of gene expression of genes such as iNOS and this gene is differentially expressed in a range of physiological inflammatory circumstances. The iNOS protein utilises the amino acid arginine as a substrate and competes with the enzyme L-Arginase which can draw on this to generate urea (Spink and Evans, 1997; Li, Z., *et al.*, 2012; Zhao *et al.*, 2013). There are three forms of the enzyme, NOS1 which is also known as neuronal or nNOS, NOS3 also known as endothelial or eNOS and NOS2 also known as iNOS (Vannini, Kashfi and Nath, 2015). High levels of iNOS expression are associated with resistance to many parasites, for example *Schistosoma japoncium* (Liu *et al.*, 2017; Shen *et al.*, 2017). In the latter study, it was shown that iNOS knock out rats are more sensitive to infection by *S. japonicum*. In the case of *T. gondii*, there is an exciting story. Laboratory strains of mice are known to be highly susceptible to *T. gondii* infection and die quickly while laboratory strains of rats are relatively resistant. Studies have shown that mouse peritoneal macrophages express high L-arginase levels and low iNOS levels; rat peritoneal macrophages, on the other hand, express high iNOS expression (Li et al., 2012). As these correlates with a sensitivity of the peritoneal macrophages to infection (mice) or resistance to infection (rats), it is proposed that this high iNOS/ low Arginase balance is what confers resistance and vice-versa for sensitivity (Li et al., 2012). This is supported by other studies that show that different strains of laboratory rats have differing levels of resistance to *T. gondii* infection and that this also correlates with the iNOS/Arginase expression balance in these strains (Gao et al., 2015). Furthermore, these differences in resistance in different rat inbred lines suggest that there is variability in resistance (Gao *et al.*, 2014). Since that study uses only six inbred rat

lines (which are equivalent to picking six rats from the wild), it raises the question as to how much variability in resistance levels are found in wild natural populations of animals like rats or mice. In addition to host genetic differences in iNOS expression some drugs such as glucorticoids, commonly used in the clinic as drugs to reduce inflammation caused by autoimmune diseases, have the effect of suppressing nitric oxide production by macrophages.(Wang, 2014), showed that peritoneal macrophages from rats showed depressed iNOS expression, depressed NO production and increased sensitivity to infection with *T. gondii* in response to glucocorticoid treatment. They suggest that this may explain the resultant acute *Toxoplasmosis* that can be associated with this treatment. Interestingly, alveolar macrophages from rats, unlike peritoneal macrophages are sensitive to infection by *T. gondii* and they are also associated with a reversed expression balance and have a high Arginase to low iNOS expression balance (Zhao *et al.*, 2013). This further supports the notion that expression of iNOS is associated with resistance and low expression (or at least a small imbalance compared with Arginase expression) is associated with sensitivity. As the rat lines used in these laboratory studies are inbred lines (i.e. genetically identical), this suggests that there is a difference in regulation of expression of iNOS and Arginase in alveolar compared to peritoneal macrophages. As these are derived from genetically inbred rats, these differences cannot be due to DNA sequence differences but must be due to epigenetic changes. This suggests that epigenetic control of the iNOS gene is a factor involved in regulation of expression of this gene.

One of the critical methods of epigenetic control of gene expression is the methylation of tracts of DNA, especially the so-called CpG Islands (Antequera and Bird, 1988). These are tracts (or single motifs) of CG residues where the cytosine residue can become methylated causing regulation of expression of the gene (this can act to either switch the gene on or off or to modulate expression). This enables the gene to be controlled with more permanency for more extended control as might be required in a differentiated tissue type. It is possible that methylation differences account for the differences in expression of the iNOS gene in alveolar and peritoneal macrophages although this has not been determined.

The iNOS gene is located at position 17q11.2-12 (chromosome 17, the q arm, position 11.2 to 12) in humans (Qidwai and Jamal, 2010), while for the mouse (*Mus musculus*)

it is located on chromosome 11(Mcdonald et al., 1995). The *Mus musculus* iNOS gene is a large gene that has 27 exons spread over about 45-50kB of genomic sequence on chromosome 11 and produces an mRNA of approximately 3700bp depending on the mouse strain (Guo *et al.*, 2007) The promoter region and the 5' untranslated region (5'UTR) has also been characterised (Lowenstein *et al.*, 1993). Similarly, the human iNOS gene (referred to as NOS2) has also been described and is located on chromosome 17, has a length of approximately 4200bp and occupies about 45-50kB of genomic DNA (Charles *et al.*, 1993; Mehrabian *et al.*, 1994). Like the mouse gene, the sequence spans over 27 exons (Chartrain *et al 1994*; Marsden *et al.*, 1994; Spink and Evans, 1997). Again the promoter and 5'UTR have been characterised (e.g. (Yamashita *et al.*, 1998)). A summary of the gene structure of the promoter, 5'UTR and Exon in *Mus musculus* is shown in figure 5.1

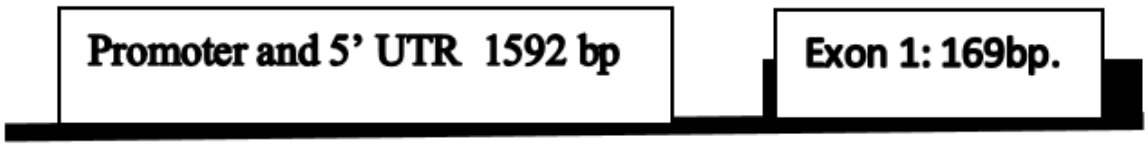

Figure 5-1 Schematic Diagram of the iNOS gene of *Mus musculus*.

There are no published data on the iNOS gene of *A. sylvaticus*. However, a partially completed and, as yet, unannotated genome is available (https://www.ncbi.nlm.nih.gov/assembly/GCA_001305905.1/).

It has been established that DNA methylation can reduce iNOS gene activity (Hmadcha *et al.*, 1999; Chan, Henderson and Jacobsen, 2005) the higher methylation, the lower the expression and vice-versa (Kuriakose & Miller, 2010). Methylation of the iNOS gene promoter has been shown to be modified by exposure to particulate matter in humans (Tarantini *et al.*, 2009), with suppressed methylation and an associated increase in expression of iNOS. Furthermore, there is evidence for methylation acting as an epigenetic method of silencing the human NOS2 gene (Gross *et al.*, 2014).

If expression of iNOS, and specifically methylation of the iNOS promoter, is associated with resistance to infection with *T. gondii* in animals, it should be possible to detect a difference in the frequency of methylation in infected versus uninfected animals. A broad hypothesis is that infected (sensitive) animals would have methylated cytosines within the promoter region of the iNOS gene causing the gene to be switched off and

allow parasite growth. Conversely, uninfected animals (resistant animals or those not exposed to the parasite) would be expected to have a lower frequency of methylated cytosines within the iNOS promoter region (i.e. those animals that have been exposed to the parasite but are resistant would have an unmethylated iNOS promoter). This chapter aims to test this hypothesis. In this study, DNA from the brains of *A. sylvaticus* were available from a previous study (Bajnok et al. 2015) and comprisesr 116 samples, 44 of which were *Toxoplasma* infected., A further set of 38 samples were collected 2014, tested for *T. gondii* and 8 of them found to be infected and 30 of them were not infected (see Chapter 3). Additionally, a third group of 12 samples were collected in 2017, tested for *Toxoplasma* and three of them were found to be positive with nine of them negative. The screening methods and results for the 2014 and 2017 samples are described in Chapter 3.

In order to investigate the above hypothesis, tools have been developed to analyse the iNOS gene from *A. sylvaticus* (see Chapter 4) to enable a detailed investigation of the variation in this gene.

The broad methodology for this chapter is to sequence the promoter and exon 1 region of the *Apodemus* iNOS gene to search for CpG islands and to investigate if there are any single nucleotide polymorphisms (SNPs) across the population of mice which might have a association with infection. Furthermore, these samples will undergo bisulphate treatment. This is a method which modifies unmethylated cytosines and can distinguish between unmethylated and methylated cytosines once the bisulphite treated DNA has been sequenced. Thus, it will be possible to investigate differences in the methylation patterns, in the iNOS promoter region and exon one, between *T. gondii* infected and uninfected *A. sylvaticus*.

5.2 Objectives

1. Obtain the sequence of the *Mus musculus* iNOS gene promoter and exon one from databases
2. Align the *Mus musculus* iNOS gene promoter with matching sequences from the partial *A. sylvaticus* genome to determine the exact sequence of the homologous region in *Apodemus*.
3. Identify potential methylation sites (CpG islands) within the *Apodemus* iNOS gene.
4. Design primers for amplifying the iNOS promoter and exon one region from *A. sylvaticus* to enable sequencing of this region.
5. Design primers for the amplification of bisulphite treated regions of the *Apodemus* iNOS gene promoter and exon 1.
6. Test the efficacy of the designed primers to amplify the correct regions
7. Develop protocols for bisulphite treatment of *Apodemus* DNA to investigate methylation patterns.
8. Amplify, sequence, bisulphite treat, and bisulphite sequence the iNOS gene promoter and exon one from an extensive collection of *A. sylvaticus* that have been tested for *T. gondii* infection.
9. Analyse Single Nucleotide Polymorphisms (SNPs) and differences in methylated bases between *T. gondii* infected and uninfected *A. sylvaticus*.

5.3 Methods:

5.3.1 *Apodemus* Samples

This study was submitted for ethical approval at the University of Salford, No: STR1718-32 and involves collections of wood mice, *A. sylvaticus*, made from the Field Studies Council Centre at Malham Tarn in North Yorkshire England (see Chapter 2; Figure 2.1). Permissions and collection methods have been described previously (Morger *et al.*, 2014). The study makes use of DNA extracted from the brains of 116 wood mice, *A. sylvaticus*, that were collected between 2012 and 2014 (Chapter 2,

Table 2.1, Population 1) (Morger *et al.*, 2014; Bajnok *et al.*, 2015a). A further 38 and 12 wood mice brains collected in 2014 and 2017, respectively, were also used (see Chapter 2; figure 2.1, populations 3 and 4). Animals were collected and killed using the 'Code of Practice for the Humane Killing of Animals under Schedule one of the Animals (Scientific Procedures) Act 1986 as previously described (Rogan *et al.*, 2007). The 116 wood mice DNA samples have been previously tested for *Toxoplasma* infection (Bajnok et al., 2015) and the remaining 50 were extracted and tested for *T. gondii* infection by the author of this thesis, using the SAG 2 gene method as described in Chapter 2.1.

5.4 **Results**

5.4.1 The sequence of the *Mus musculus* iNOS gene promoter and exon 1.

To work with the *A. sylvaticus* iNOS gene promoter and exon 1, it was necessary to identify a homologous sequence from the related species *Mus musculus* to be able to identify the region in *A. sylvaticus*. The PubMed database was searched to obtain a possible sequence. An appropriate sequence from *Mus musculus* was identified that represented the relevant region (GenBank: accession number L23806.1).

5.4.2 Alignment of the *Mus musculus* iNOS gene promoter with matching sequences from the partial *Apodemus sylvaticus* genome

The Mus musculus Inducible nitric oxide synthase (Nos2) gene, promoter and 5' UTR was obtained from GenBank: accession number L23806.1. Approximately 1000 bp was located that covered the whole of Exon 1 (169 bp) and 831 bp of the promoter region upstream from exon 1. Figure 5.2 shows the sequence of the *Mus musculus* iNOS gene and indicates the Promoter region, the TATA box (in red) and Exon 1 (in yellow).

TGATTTGTAATTCATTTATTCAATCAACAATTTATTTGTTCTCCCAACTATTGAGG
CCACACACTTTTTGGGTGACTTAGTCTGTGTACCTCAGACAAGGGCAAAACACG
AGGCTGAGCTGACTTTGGGGACCATGCGAAGATGAGTGGACCCTGGCAGGAT
GTGCTAGGGGGATTTTCCCTCTCTCTGTTTGTTCCTTTTCCCCTAACACTGTCAA
TATTTCACTTTCATAATGGAAAATTCCATGCCATGTGTGAATGCTTTATTGGAAG
CATTGTAAGAAATTATAATTTATTCGTTTTTGTTTGTTTCTCAGAACAGGGTTTTT
CTGTGTAGTGTTCCTGGCTTATCCTAGAACTTACTCTGTAGACCAGGCTAGCCC
AAACTCAGGGATCAGCCTTTCTCTGTCTCCTGAATCCCGGGATTAAAGGCTTAT
GCCACCACACCCAGGTAGGACATTATAATCCTATATATAAGAAGTCACCCACAC
ATACAAACACACACACACCACACACACACACACACACACACACACACACACAGA
GAGAGAGAGAGAGAGAGAGAGGGAGAGAGAGAGAGAGAGAGAATGCCACT
GAGAAAAAAAATAAAAAGGCTTCACTCAGCACAGCCCATCCACTATTCTGCCCA
AGCTGACTTACTACTAGTGGGGAAATGCTGGTCAGACGGCATCTGTGCCCACA
GCTTGCCTTCCATCCTTTCTAGAAAACCTCCTGATGAATGTGTCCTGGGCGTGT
TGGAATATTGGCACCATCTAACCTCACTGAGAGAACAGACAGAAAGCCAGAGA
GCTCCGTGCCCAGAACAAAATCCCTCAGCAGCTGCAAGCCAGGGTATGTGGTT
TAGCTAAGAAAAGCCAGCCTCCCTCCCTAGTGAGTCCCAGTTTTGAAGTGACTA
CGTGCTGCCTAGGGGCCACTGCCTTGGACGGGCGACCAGGAAGAGATGGCCT
TGCATGAGGATACACCACAGAGTGATGTAATCAAGCACACAGACTAGGAGTGT
CCATCATGAATGAGCTAACTTGCACACCCAACTGGGGACTCTCCCTTTGGGAAC
AGTTATGCAAAATAGCTCTGCAGAGCCTGGAGGGGTATAAAATACCTGATGGCTG
CTGCCAGGGTCACAACTTTACAGGGAGTTGAAGACTGAGACTCTGGCCCCACG
GGACACAGTGTCACTGGTTTGAAACTTCTCAGCCACCTTGGTGAAGGGACTGA
GCTGTTAGAGACACTTCTGAGGCTCCTCACGCTTGGGTCTTGTTCACTCCACGG
AGTAGCCTAGTCAACTGCAAGAGAACGGAGAACG

Figure 5-2 The Mus musculus inducible nitric oxide synthase (Nos2) gene, promoter region and 5' UTR.

This is obtained from Sequence ID: L23806.1. The sequence not highlighted is the promoter region, the TATA box is highlighted in red and Exon 1 is highlighted in yellow.

There is likely to be sequence divergence between the iNOS gene promoter (+ exon 1) between the homologous genomic regions of *Mus musculus* and *A.sylvaticus*. To understand and identify these differences, the promotor region from *M. musculus* (GenBank: L23806.1)was compared to the partial *A. sylvaticus* genome (https://www.ncbi.nlm.nih.gov/assembly/GCA_001305905.1/) using the programme BLAST. This genome, as yet, is unannotated and so the *Apodemus* iNOS sequence would need to be inferred by homology. The iNOS gene from *Mus* Figure 5.3 shows the degree of homology when aligned.

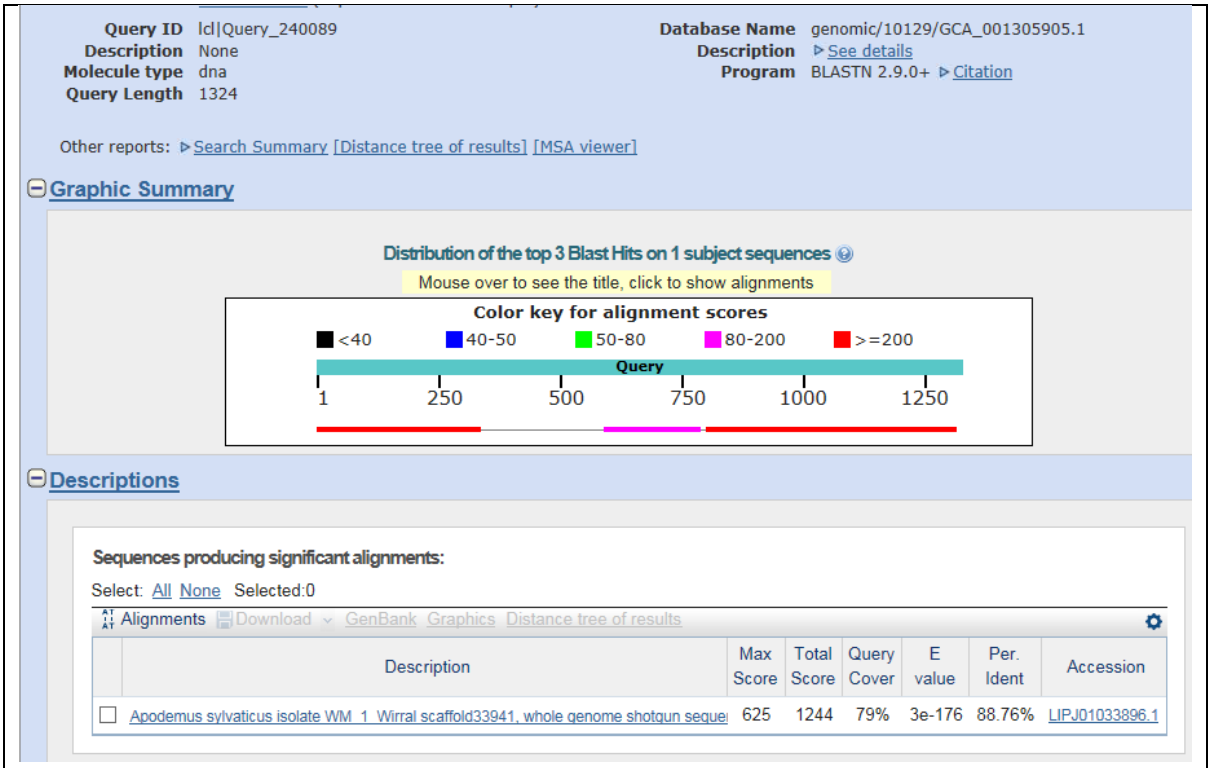

Figure 5-3 results of the BLAST using the iNOS gene promoter and Exon 1 from Mus *Musculus* against the partial *A. sylvaticus*

The results of the BLAST programme alignment using the iNOS gene promoter and Exon 1 from *Mus musculus* against the partial *A. sylvaticus* whole genome sequence ID: LIPJ01033896.1. The *Apodemus* sequence shows 88.76% identity to the sequence of *Mus musculus*. Red and purple bars indicate a high degree of homology. The grey bar represents novel sequence that is present in the *Apodemus* sequence but absent in the *Mus musculus* sequence.

The alignment of the *Apodemus* and *Mus* sequences show 88.76% identity. Overall the homology is high, but there is a region of the promotor that is present in the *Apodemus sequence* but not in the *Mus musculus* sequence. This sequence may be an artefact of the partial assembly of the *Apodemus* genome sequence. This needs to be explored further by direct sequencing of this region from *A. sylvaticus* DNA. Figure 5.4 shows examples of sections of the alignments between the *Apodemus* and *Mus* iNOS promoter and exon one sequences. It can be seen that there are both single nucleotide polymorphisms (SNPs) and insertions in the *Apodemus* sequence that distinguish it from the gene homologue in *Mus*.

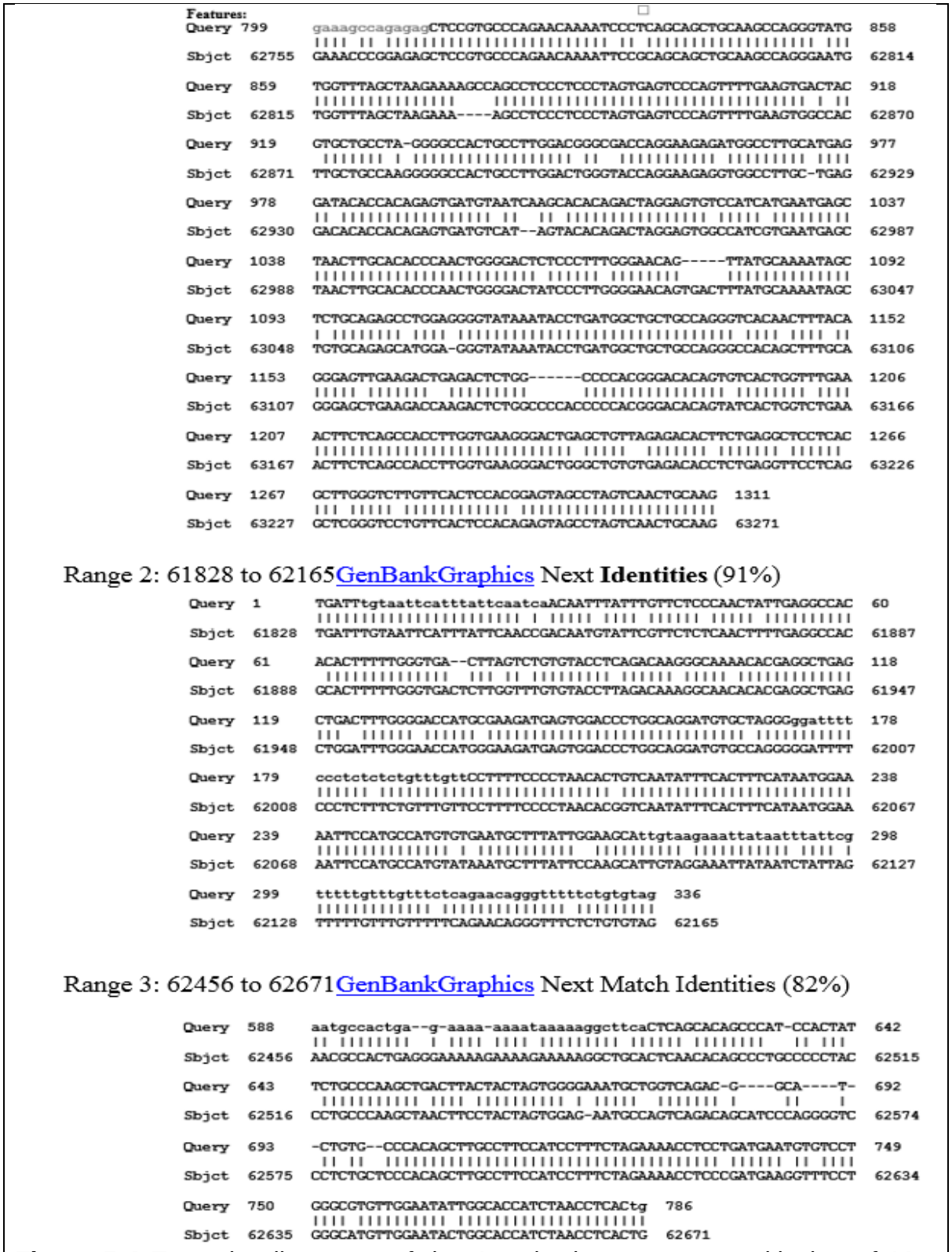

Figure 5-4 Example alignments of the *A. sylvaticus* sequence with that of *Mus musculus*.

The alignments show that there is variation between the *Mus*, sequence and the *Apodemus* sequence. These different alignments each represent different sections of the sequence that have been aligned by the Blast programme.

5.4.3 Design of PCR primers for amplification of the iNOS gene promotor, 5'UTR and Exon 1 from *A. sylvaticus*.

Having established the equivalent homologous gene sequence from *A. sylvaticus*, it was possible to design PCR primers that would amplify regions of the iNOS gene promotor, 5'UTR and Exon 1. The program PRIMER3 was used to design primers for PCR amplification. These are shown in Table 5.1, and their locations in the iNOS gene and promotor are shown in figure 5.5. Three sets of primers were designed which covered either the entire promotor and Exon 1 (Primers A) or parts of the sequence (Primers B and C).

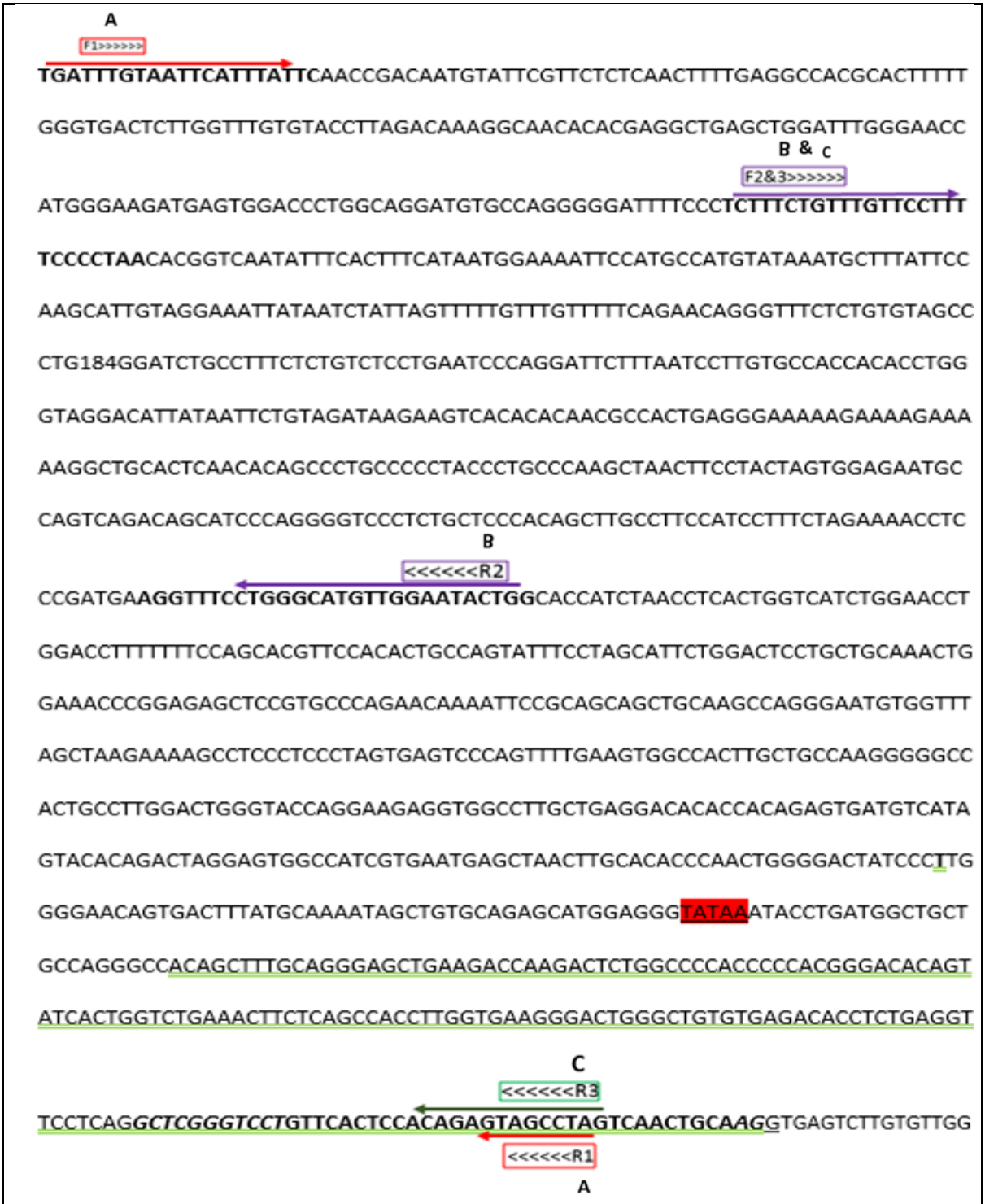

Figure 5-5 The sequence of the *Apodemus* iNOS promoter, 5'UTR and Exon 1.

This sequence was derived from the partial *Apodemus* genome sequence by using homology with the *Mus musculus* sequence. Primer pairs (A, B and C) are indicated and the locations shown in bold. Detailed primer sequences are available in Table 5.1. The green underline section shows the region spanning Exon 1 and the red box indicates the proposed TATA box based on homology with the *Mus* sequence.

Of the three primer pairs, the A primers were expected to amplify a fragment of 1253 bp, while the primer pairs B and C should amplify fragments of 458bp and 1075bp respectively.

Table 5-1 Designed iNOS primers which covered the promoter, 5' UTR and exon one from *A. sylvaticus*. The final column indicates whether the PCR amplification was successful or not.

Forward Sequence	Reverse Sequence	Expected Band Size	PCR success
A F1: 5' TGATTTGTAATTCATT TATTC 3'	A R1: 5'ACTAGGCTACTCCGT GGAGTGA3'	1253 bp	No
B F2: 5'TCTTTCTGTTTGTT CCTTTTCCCCTAA3'	B R2: 5'AGTATTCCAACATGC CCAGGAAACCT3'	458 bp	Yes
C F3: 5'TCTTTCTGTTTGTT CCTTTTCCCCTAA3'	C R3: 5'CTA GGC TAC TCT GTG GAG TGA AC3'	1075 bp	Yes

PCR amplification was performed on *Apodemus* DNA samples using the primers described in Table 5.1. The results are shown in figure 5.6. Primer pairs A, B and C successfully amplified a PCR product, but pair A did not.

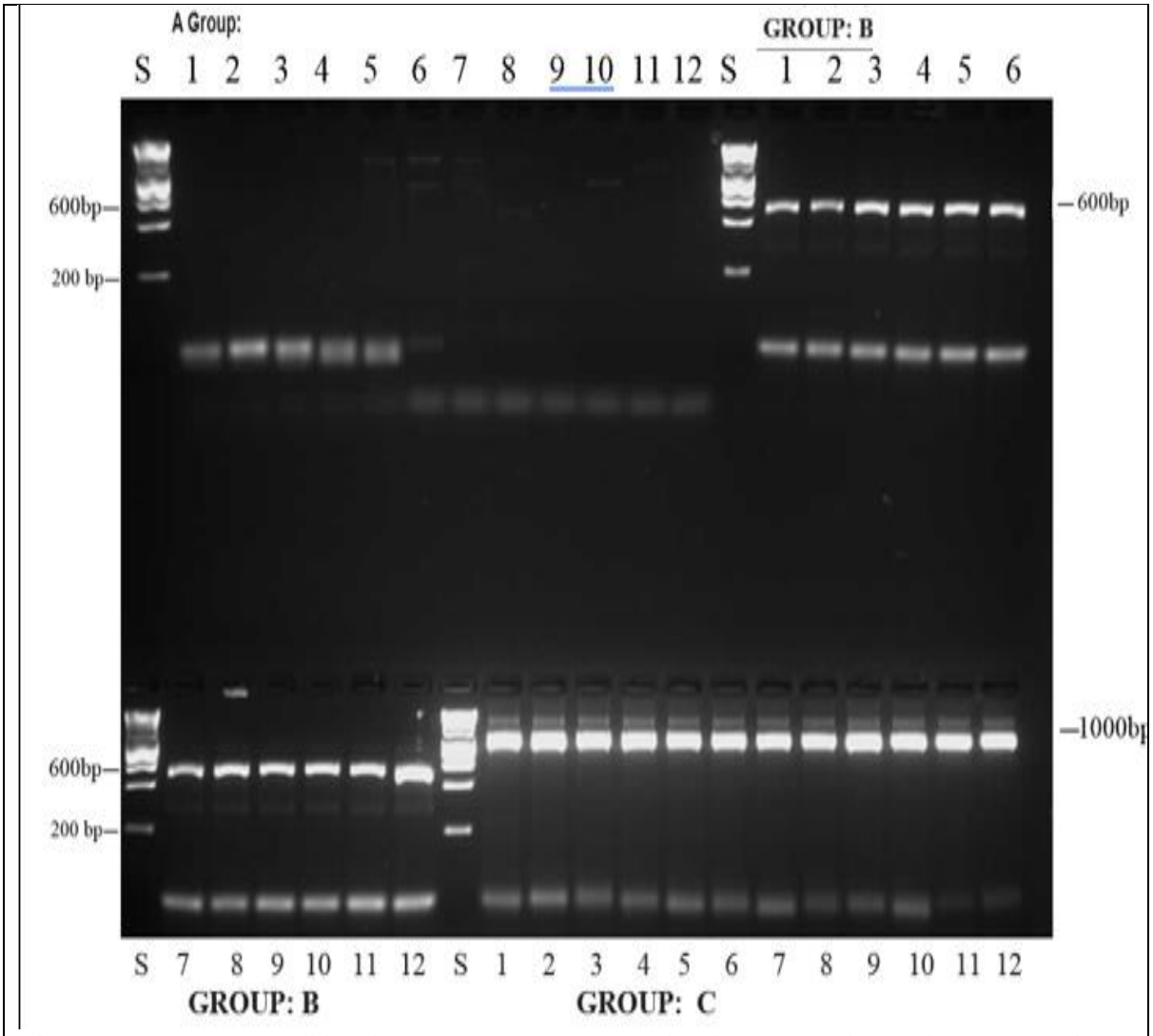

Figure 5-6 PCR amplification of DNA from *A. sylvaticus* samples using PCR primer pairs A, B and C (see Table 5.1).

The PCR products have been amplified with an annealing temperature 60^0c for all samples. Lanes 1-12 (Group A) show the results of the amplification by primer pair A. The expected band size is 1253bp. Group B lanes 1 -12 show the amplification results from the B primer pair. The expected band size is 458. The Group C lanes 1-12 show the results using the C pair of primers. The expected band size is 1075 bp. The lanes labelled S show the 1Kb ladder. The *Apodemus* sample codes are as follows: Lane 1 is 68h, 2 is 69h, 3 is 70h, 4 is 71h, 4 is 72h, 5 is 73h, 6 is 82h, 7 is 86h, 8 is 87 h, 9 is 87b, 10 is 88h, 11 is 89h. 12 is 90h. These are DNA samples extracted from heart tissue DNA from *Apodemu*s. (Heart tissue DNA was used for primer optimisation experiments to conserve brain DNA for later studies). The results show that primer combination B amplified the target band size of 458bp, and the C primer has amplified the target expected band size 1075 bp. However, the primer A combination failed to amplify any product.

Agarose gel electrophoresis of PCR amplified products from primer pair combinations demonstrated that bands of the correct size, respectively 458bp and 1075bp, could be amplified by primer pairs B and C when using an annealing temperature of 60^{o}C on a template of heart DNA extracted from several *A. sylvaticus*. Primer pair A failed to amplify under these conditions.

5.4.4 Testing the efficacy of the designed primers to amplify the correct regions of the iNOS gene promoter and exon 1.

Having designed primers that should amplify the iNOS promoter and exon1 from *A. sylvaticus*, these primers need to be tested to see if they amplify the correct products. As the primer pair A failed to amplify a product, only amplicons from Primers B and C were used. The B primer pair is illustrated in Figure 5.7 and amplifies part of the promoter and 5'UTR. This primer covers approximately 458 bp region of the genome.

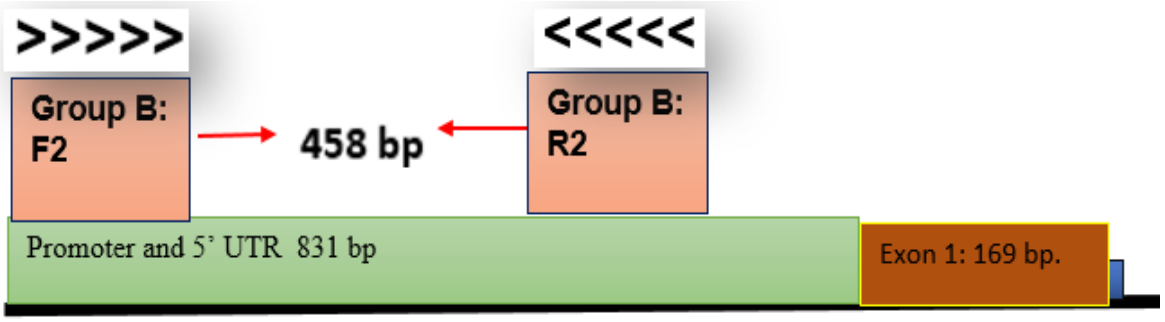

Figure 5-7 Schematic diagram of the iNOS B primer pair.
The F2-R2 primers cover 458 bp of the promoter 5' UTR region which is upstream of the exon.

One of the samples from group B primer PCR products was chosen randomly, then purified and sent to Source Bioscience for sequencing. The sequence was analysed using the program Finch TV to enable manual inspection of sequencing peaks and the program Chromaspro was used to analyse the sequences. The final consensus sequence is presented in Figure 5.8.

87B, R:

GTAAGCCGAAGGCACTACAGATAGAAGCTAGGCATTCTGTGGGAGCAAGGGACC
CCTGGGATGCTGTCTGACTGGCATTCTCCACTAGTAGGAAGTTAGCTTGGGCAGG
GTAGGGGGCAGGGCTGTGTTGAGTGCATCCTTTTTTCTTTTCTTTTCTTTTTCCCTC
GGTGGCATTGTGTGTGACTTCTTATCTATAGAATTATAATGTCCTACCCAGGTGTG
GTGGCACAAGTCTTTAATCCTGGGATTCAGGAGACAGAGAAAGGCAGATCCCTG
AGTTTGGGCCAGCCTGGTCTACAAAGTGAGTTCTAGGACAAGCCAGGGCTACAC
AGAGAAACCCTGTTCTGAAAAACAAACAAAAACTAATAGATTATAATTTCCTAC
AATGCTTGGAATAAAGCATTTATACATGGCATGGAATTTTCCATTATGAAAGTGA
AATATTGACCGTGTTAGGGGAAAAGGAAAAAAAAAAAAAAA

Figure 5-8 Consensus sequence of the iNOS Promoter sequence generated using the B pair of primers.
DNA sequence obtained from *Apodemus* sample number 87 generated by the B primer pair following visual inspection of the chromatogram and analysis to ensure the quality of the sequence.

The consensus sequence from the amplified B primer pair (Figure 5.8) was analysed by the program BLAST to search for related sequences in the NCBI database and to confirm that the correct sequence has been amplified. the results of BLAST and figure 5.9 shows the detail of the best alignments and confirms that the correct sequence has been amplified.

```
Query  175   TGTGTGTGACTTCTTATCTATAGAATTATAATGTCCTACCCAGGTGTGGTGGCACAAGTC  234
             ||||  ||||||||||||  |||||  ||||||||||||||||  ||||||||||| ||| |
Sbjct  1039  TGTGGGTGACTTCTTATATATAGGATTATAATGTCCTACCTGGGTGTGGTGGCATAAGCC  980

Query  235   TTTAATCCTGGGATTCAGGAGACAGAGAAAGGCAGATCCCTGAGTTTGGGCCAGCCTGGT  294
             ||||||||  ||||||||||||||||||||||||  ||||||||||||||||||  ||||||||
Sbjct  979   TTTAATCCCGGGATTCAGGAGACAGAGAAAGGCTGATCCCTGAGTTTGGGCTAGCCTGGT  920

Query  295   CTACAAAGTGAGTTCTAGGACAAGCCAGG---GCTACACAGAGAAACCCTGTTCTGAAAA  351
             |||||  |||  ||||||||||  ||||||||    |||||||||  ||||||||||||||  ||
Sbjct  919   CTACAGAGTAAGTTCTAGGATAAGCCAGGAACACTACACAGAAAAACCCTGTTCTGAGAA  860

Query  352   ACAAACAAAAACTAATAGATTATAATTTCCTACAATGCTTGGAATAAAGCATTTATACAT  411
             ||||||||||||  ||||  ||||||||||  ||||||||||  ||||||||||| | ||||
Sbjct  859   ACAAACAAAAACGAATAAATTATAATTTCTTACAATGCTTCCAATAAAGCATTCACACAT  800

Query  412   GGCATGGAATTTTCCATTATGAAAGTGAAATATTGACCGTGTTAGGGGAAAAGGaaaaaa  471
             ||||||||||||||||||||||||||||||||||||  ||||||||||||||||||  |||
Sbjct  799   GGCATGGAATTTTCCATTATGAAAGTGAAATATTGACAGTGTTAGGGGAAAAGGAACAAA  740
```

Figure 5-9 Example alignments of the *A. sylvaticus* sequence with that *of Mus musculus*. The alignments show that there is minor variation between the *Mus*, sequence and the *Apodemus* sequence but that the correct sequence has been amplified.

The arrangement of the C group of primer pairs (F3-R3) is illustrated in Figure 5.10 and covers both the promoter region and the whole of exon 1. A product of 1075bp is predicted.

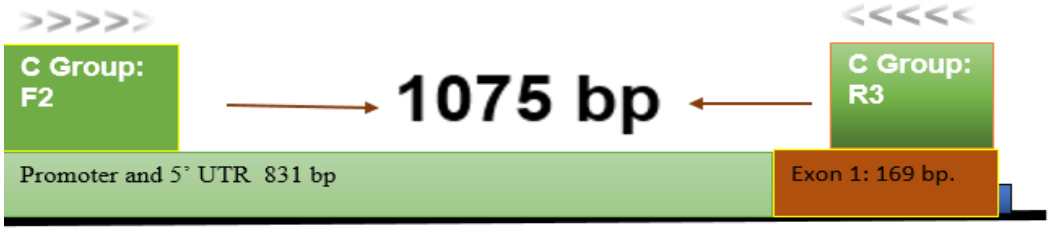

Figure 5-10 A schematic diagram of the C group of primers (F3-R3) in the *Apodemus* iNOS gene. These primers cover the 5' UTR, promoter & exon1 and should amplify a predicted fragment size of 1075bp.

The PCR products were sequenced and demonstrated to be the correct sequence. Figure 5.11 shows the consensus sequence and Figure 5.12 shows a BLAST program

alignment that demonstrates a high degree of homology with the *Mus musculus* iNOS gene. Figure 5.13 shows detailed alignments between the PCR amplified *Apodemus* sequence and the *Mus musculus* sequence in GenBank. It contained a broad overall homology with occasional SNPs or insertions/deletions when compared. This demonstrated that the correct gene had been amplified.

>L5 not BIOS

TCttGtTTGTTCctTTTTcCCCCTAACCACGGGTCAAAtaTTTCaaATTTCATAAATGGAAAAATTCCCaTGc
CCAgGTAtaAAATGCtTTTaTTCCAAGCATTGTTAGGAAAATTATAATCtATTAGGtTTTGTTTGTTtTCAG
AACAgGGGTTCTCTGTGTAGCCCTGGCTTGTCCTAGAACTCACTCTGTAGACCAGGCTgGCCCAAACT
CAGGGATCTGCCTTTCTCTGTCTCCTGAATCCCAGGATTAAAGACTTGTGCCACCACACCTGGGTAGG
ACATTATAATTCTATAGATAAGAAGTCACACACAATGCCACTGAGGGAAAAAGAAAAGAAAAGAAAA
AAGGCTGCACTCAACACAGCCCTGCCCCCTACCCTGCCCAAGCTAACTTCCTACTAGTGGAGAATGCC
AGTCAGACAGCATCCCAGGGGTCCCTCTGCTCCCACAGCTTGCCTTCCATCCTTTCTAGAAAACCTCCC
GATGAAGGTTTCCTGGGCATGTTGGAATACTGGCACCATCTAACCTCACTGGTCGTCTAGAACCTGGA
CCTTTTTTCCCAGCACGTTCCACACTGCCAGTATTTCCTAGCATTCTGGACTCCTGCTGCAAACTGGAA
ACCCGGAGAGCTCCATGCCCAGAACAAAATCCCGCAGCAGCTGCAAGCCAGGGAATGTGGTTTAGCT
AAGAAAAGCCTCCCTCCTTAGTGAGTCCCAGTTTTGAAGTGGCCACTTGCTGCCAAGGGGGCCACTG
CCTTGGACTGGGTACCAGGAAGAGGTGGCCTTGCTGAGGACACACCACAGAGTGATGTCATAGTAC
ACAGACTAGGAGTGGCCATCGTGAATGAGCTAACTTGCACACCCAACTGGGGACTATCCCTTGGGGA
ACAGTGACTTTATGCAAAATAGCTGTGCAGAGCATGGAGGGTATAAATACCTGATGGCTGCTGCCAG
GGCCACAGCTTTGCAGGGAGCTGAAGACCAAGACTCTGGCCCCACCCCCACGGGACACAGTATCACT
GGTCTGAAACTTCTCAGCCACCTTGGTGAAGGGACTGGGCTGTGTGAGACA

Figure 5-11 *The consensus sequence from amplified* Apodemus *DNA using primers F3 and R3.*

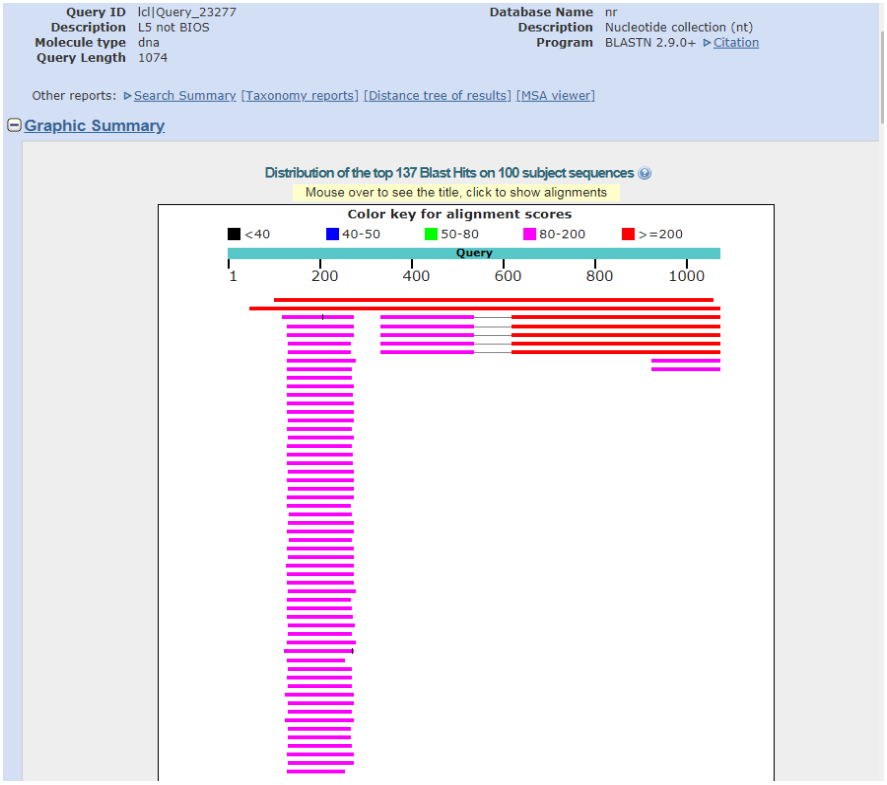

Figure 5-12 BLAST alignment of the *Apodemus* sequence from the amplified iNOS C group primers (F3, R3).

The BLAST program confirmed a strong homology and alignment with the iNOS promoter of *Mus musculus,* the red lines indicates an excellent alignment. The gene map at the top of the figure, illustrated with a red line, shows that 975 bp of the sequence of sample no. L5 has a 97% identity to the *Apodemus* sequence. The lower panel shows the BLAST sequence alignment with the database sequence.

Figure 5-13 Comparison of the sequence of iNOS promoter and exon 1 amplified, using primers F3 and R3 from *Apodemus* DNA with the *Mus musculus* equivalent sequence.

5.4.5 Identification of potential methylation sites (CpG islands) within the *Apodemus* iNOS gene.

DNA methylation is a fundamental process involved in the regulation of gene expression, and characterisation of methylation patterns in the iNOS gene could potentially open an opportunity to investigate the role of iNOS gene expression in wild mice populations. In practical terms, DNA methylation is usually detected by bisulfited treatment of DNA which chemically modifies unmethylated cytosines such that they are replaced by thymine residues which are identified during DNA sequencing. Methylated cytosines remain intact. To understand whether methylation is involved in iNOS gene expression and linked to *Toxoplasma* infection, there is the opportunity to develop approaches to compare methylation patterns in infected and uninfected wood mice. To do this, there is a need to develop tools to enable this.

Having used similarity with the *Mus musculus* genome to identify the region of the *Apodemus* genome that represents the iNOS gene promoter and exon1, this sequence was used to look for potential CpG islands. To do this, bioinformatics tools to simulate bisulphite treatment, while leaving CG residues intact, were used to identify potential CpG motifs. The results are shown in Figure 5.14.

>The bisulfited converted sequence:

TTTATTTTAAGTATTGTAGGAAATTATAATTTATTAGTTTTTGTTTGTTTTTTAGAATAGGGTTTTTTTG
TGTAGTTTTGGGATTTGTTTTTTTTTGTTTTTTGAATTTTAGGATTTTTTAATTTTTGTGTTATTATATTT
GGGTAGGATATTATAATTTTGTAGATAAGAAGTTATATATAACGTTATTGAGGGAAAAAGAAAAGA
AAAAGGTTGTATTTAATATAGTTTTGTTTTTTATTTTGTTTAAGTTAATTTTTTATTAGTGGAGAATGTT
AGTTAGATAGTATTTTAGGGGTTTTTTTGTTTTTATAGTTTGTTTTTTATTTTTTTTAGAAAATTTTTCG
ATGAAGGTTTTTTGGGTATGTTGGAATATTGGTATTATTTAATTTTATTGGTTATTTGGAATTTGGATT
TTTTTTTTTAGTACGTTTTATATTGTTAGTATTTTTTAGTATTTTGGATTTTTGTTGTAAATTGGAAATTC
GGAGAGTTTCGTGTTTAGAATAAAATTTCGTAGTAGTTGTAAGTTAGGGAATGTGGTTTAGTTAAGA
AAAGTTTTTTTTTTTAGTGAGTTTTAGTTTTGAAGTGGTTATTTGTTGTTAAGGGGGTTATTGTTTTGG
ATTGGGTATTAGGAAGAGGTGGTTTTGTTGAGGATATATTATAGAGTGATGTTATAGTATATAGATT
AGGAGTGGTTATCGTGAATGAGTTAATTTGTATATTTAATTGGGGATTATTTTTTGGGGAATAGTGA
TTTTATGTAAAATAGTTGTGTAGAGTATGGAGGGTATAAATATTTGATGGTTGTTGTTAGGGTTATA
GTTTTGTAGGGAGTTGAAGATTAAGATTTTGGTTTTATTTTTACGGGATATAGTATTATTGGTTTG
AAATTTTTTAGTTATTTTGGTGAAGGGATTGGGTTGTGTGAGATATTTTTGAGGTTTTTTAGGTTCGG
GTTTTGTTTATTTTATAGAGTAGTTTAGTTAATTGTAAG

Figure 5-14 CpG islands in the *Apodemus* iNOS gene promoter & exon1 sequence. The iNOS gene sequence from *A. sylvaticus* was obtained using the homologous region from the Mus musculus iNOS gene. By utilising a bioinformatics program on http://www.zymoresearch.com/tools/bisulfite, nine CpGs Islands were identified (highlighted in green). The proposed TATA box is highlighted in red The sequence contains a high proportion of “T” s, this is because all “C”s have been converted to “T”s (as would happen in bisulphite treatment) except those adjacent to “G”s.

Figure 5.14 shows nine potential CpG islands. Experimental analysis will be required to determine if these are indeed methylated. Details of the methylation process are explained in more detail in Figure 5.15.

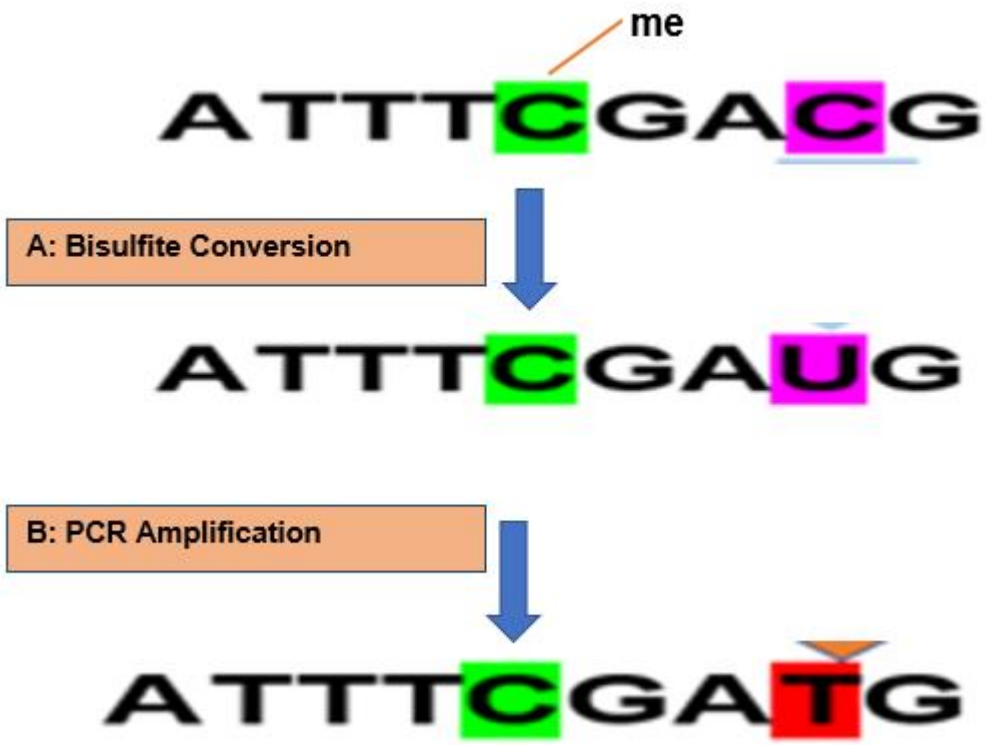

Figure 5-15 Schematic diagram of the process of bisulphite treatment.

A Bisulphate treatment adding a methyl group into unmethylated cytosine C in , is highlighted in purple residues, thus converted it to uracil, and then to amplified in the PCR as a A. B, the last stage is when it is read by sequencing, it will be read as a T. While, the methylated cytosine in green stays the same (Han *et al.*, 2017).

5.4.6 Designing primers for the amplification of bisulphite treated regions of the *Apodemus* iNOS gene promoter and exon 1.

To conduct the bisulphite sequencing reaction, it is necessary to PCR amplify the iNOS gene regions from the bisulphite treated DNA. Primers will need to be able to recognise cytosine residues that could have been converted in thymine residues –

so an entirely new set of PCR primers is required. These were designed using bioinformatic tools available online (as described in Chapter 2) found at http://www.zymoresearch.com/tools/bisulfite.

Table 5.2 shows the sequences of the primers designed to amplify regions of the iNOS gene promoter, Exon 1 and the 5' UTR. However, this software can also predict possible mutations that will cause unmethylated cytosines to convert to Thymine when bisulphite treated. Figure 5.15 shows the potential changes that could occur to unmethylated cytosines and the conservation of methyl cytosines in the *Apodemus* iNOS gene promoter and exon 1. The nine possible CpG islands are identified in green and potentially unmethylated cytosines as converted to Ts, are indicated in red. The locations of the designed primers (Table 5.2) are indicated schematically in Figure 5.16. Figure 5.17 illustrates the positions of the nine putative CpG islands and shows their locations along the sequence.

Table 5-2 Designed iNOS primers for use on bisulphite treated DNA to PCR amplify different regions covering the promoter and exon 1 of the *Apodemus* iNOS gene.

Forward Sequence	Reverse Sequence	Expected Band Size
BIOS F1: 5'TATTGGTTATTTGGAATTTGGATTTTTTTTTTTAG3'	BIOS R1: 5'ATAATCCCCAATTAAATATACAAATTAACTCATTCAC3'	348 bp
BIOS F2: 5' TATTGGTTATTTGGAATTTGGATTTTTTTTTTTAG3'	BIOS R2: 5'CAATATTCCAACATACCCAAAAAACCTTCA3'	71 bp
BIOS F3: 5'TGAAGGTTTTTTGGGTATGTTGGAATATTG3'	BIOS R3: 5'TTTTACATAAAATCACTATTCCCCAAAAAATAATCCCC3'	421 bp
BIOS F4: 5'GTTATTGAGGGAAAAAGAAAAGAAAAAGGTTG3'	BIOS R4: CCACTCCTAATCTATATACTATAACATCACTC	514 bp
BIOS F5: 5'AGATAGTATTTTAGGGGTTTTTTTGTTTTTATAGTTTG3'	BIOS R5: 5' CAAAACCCRAACCTAAAAAACCTC3'	683 bp

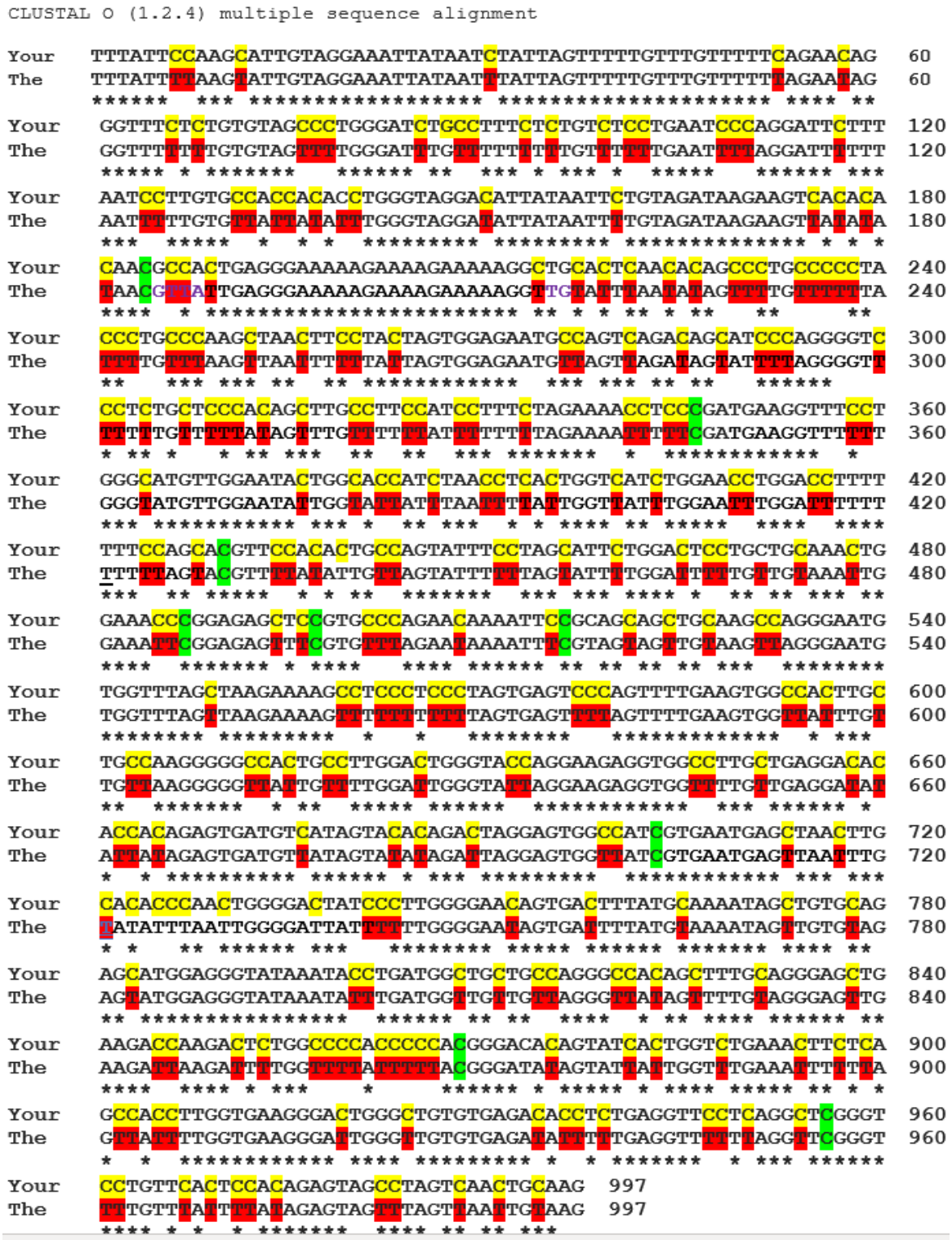

Figure 5-16 Clustal alignments of the predicted bisulphite treated sequence (The), and the *Apodemus* iNOS sequence (Your).

The highlighted cytosine residues in yellow which are linked to the red Thymine residues are the unmethylated cytosine residues while the highlighted cytosine residues in green represent methylated bases which remain the same after bisulphite treatment.

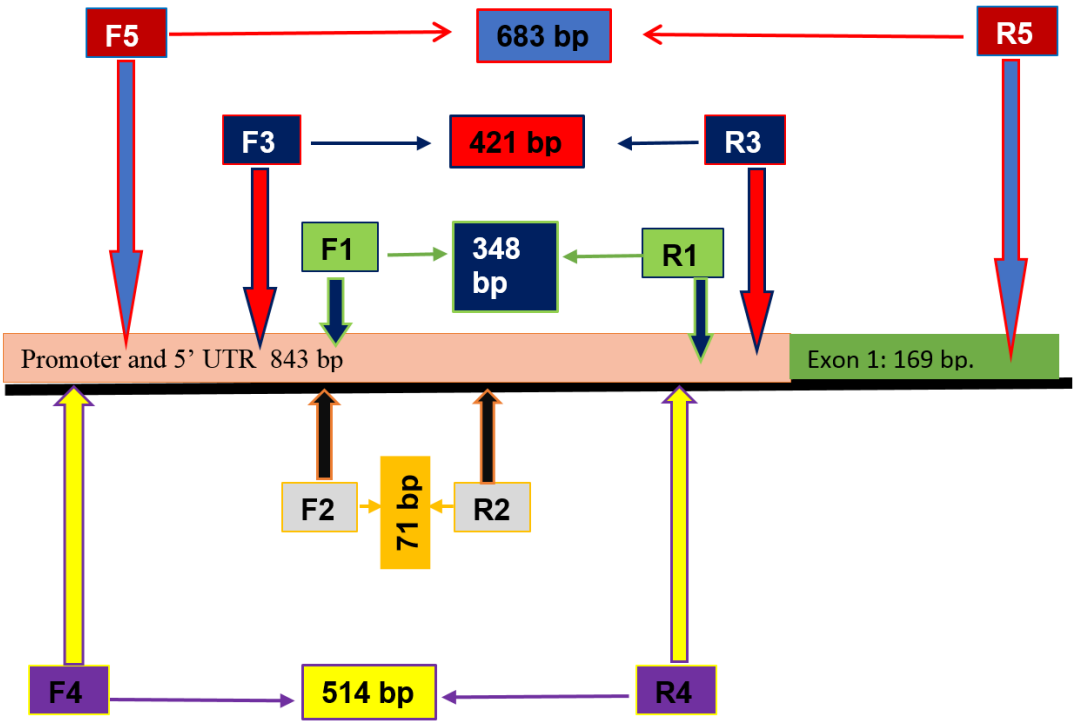

Figure 5-17 Locations of the bisulphate treatment primers on the map of the iNOS Promoter & Exon 1.

F= Forward primer, R= reverse primer. Predicted amplified fragments are presented in base pairs for each primer combination. BIOSF1/R1 = 348 bp, BIOSF2/2 = 71 bp, BIOSF3/R3= 421 bp, BIOSF4/R4= 515 bp. These primers are in the promoter region. However, BIOSF5/R5= 683 bp potentially amplifies both 514 bp of the promoter and 136 bp of exon 1.

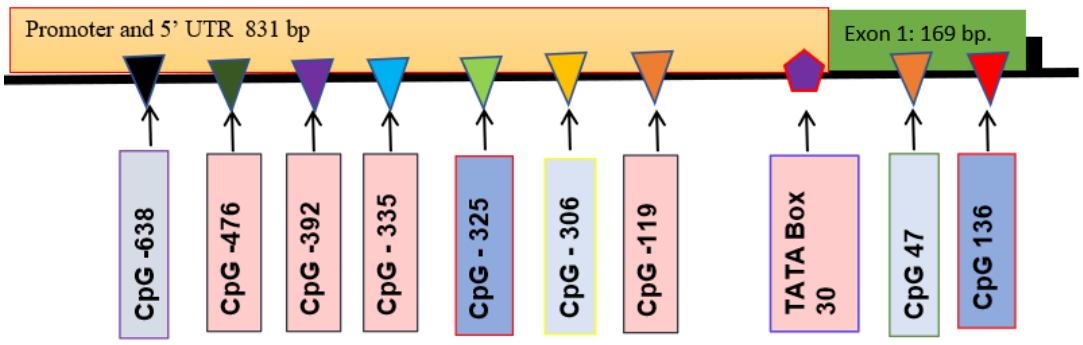

Figure 5-18 The locations of the putative CpG islands.

CpG islands were predicted using the Zymo Research online software on the *Apodemus* iNOS promoter and Exon 1. The numbers indicate the location relative to the start of Exon 1. So, for example, CpG 47 (a positive number) lies 47bp downstream of the beginning of Exon 1 while CpG – 119 (a negative number) is located 119bp upstream of the start of Exon 1.

Having used bioinformatic analyses, mainly from the Zymo Research website http://www.zymoresearch.com/tools/bisulfite, primers have been successfully designed that could amplify portions of the *Apodemus* iNOS gene promoter and Exon 1. Furthermore, potential CpG islands exist and have been identified and located. The next stage is to bisulphite treat the DNA, PCR amplify the products and sequence them to determine whether any of the CpG islands are methylated and could act as epigenetic marks.

5.4.7 PCR amplification of bisulphite treated DNA from the iNOS gene promoter and Exon 1

To investigate methylation of the iNOS gene, PCR reactions using the designed bisulphite primers need to be carried out on bisulphite treated DNA. Treatment of DNA was carried out using a kit supplied by Zymo Research. PCR amplifications were

carried out using the bisulphite treated primers (Table 5.2). Expected band sizes for primers BIOS F1-F5 and BIOS R1-R5 are summarised in figure 5.19.

Bisulphite treated DNA was PCR amplified using BIOS F1 and NIOS R1 primers (expected band size 348 bp) using DNA extracted from *Apodemus* brain tissue. These primers were expected to amplify part of the promoter region upstream of Exon1. The results are shown in figure 5.19.

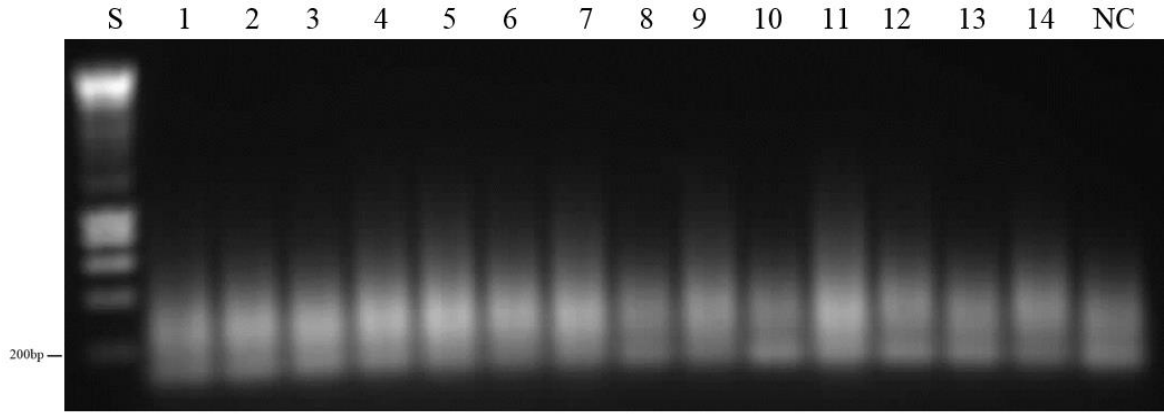

Figure 5-19 PCR amplification of bisulphite treated *Apodemus* brain DNA using Primers BIOS F1/R1.
Apodemus samples 1-14 are loaded on lanes 1-14. While lane S is the 1Kb is ladder DNA biomarker. Lane NC is the negative control (water). Amplification of the 348bp band failed to work.

No amplification was seen when using primers F1/R1. Optimisation of the annealing temperatures was carried out between 52^0C and 63^0C, and no amplification was achieved under any of the conditions. PCR amplification using all four other primer sets, BIOSF2/BIOS R2, BIOS F3/BIOSR3, BIOS F4/BIOS R4, BIOSF5/BIOS R5 was also carried out in combination with optimisation of annealing temperatures as conducted for primers BIOSF1/R1. No amplification was observed for any of the primers under any of the optimisation conditions (data not shown).

As all PCRs were failing, further investigation of the best PCR conditions was carried out. On advice from the company Bioline about PCR amplification of methylated DNA, a new specific polymerase and reaction mixture was tried. The Bioline Taq HOT

START (HS) red mix is a high fidelity Taq polymerase and buffer system which can be more productive with difficult amplifications. These reagents were used to PCR amplify *Apodemus* brain bisulphite treated DNA utilising the set of five primer groups (Bios F1/R1- Bios F5/R5) (Data not shown).

Again, the amplification was still not working. Again, optimisation was carried out using annealing temperatures of 55^0C and 63^0C. Additionally, higher concentrations of starting DNA were used in the PCR reactions by adding more bisulphite treated DNA. Several experiments were conducted, and all of the bisulphate primers pairs were assessed. None of the primers pairs produced amplification products (data not shown) except the BIOSF5/ BIOSR5 pairing which provided the correct band size when amplified with an annealing temperature of 60^0c. Figure 5.20 shows an example set of results for the primers BIOSF5/BIOSR5 when 3µl of methylation treated Brain DNA was used.

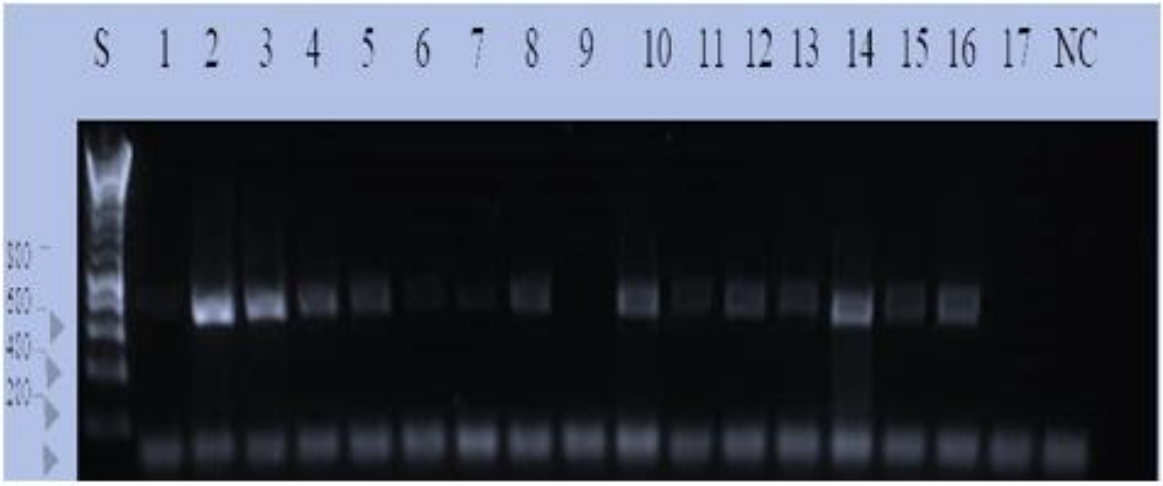

Figure 5-20 PCR amplification of bisulphate treated *Apodemus* brain DNA using Primer pair F5/R5.

Lane S on the left is the 1Kb DNA Hyper ladder. lane 1, B5, lane 2, B9, lane 3, B11, lane 4, B12, lane 5, B13, lane 6, B16, lane 7, B18, lane 8, B19, lane 9, B20, lane 10, B21, lane 11, B25, lane 12, B26, lane 13, B33, lane 14, B38, lane 15, B46, lane 16, B56, lane 17, B57. NC is the negative control (PCR water). The majority of the samples amplified a band of 683bp, to a greater or lesser degree, except samples B5, B20, B57.

By increasing the amount of the treated bisulphate DNA up to 3 µl per amplification, reducing the amount of water and using an annealing temperature of 60^0c, PCR amplification using primer pair F5/R5 was successful. As these primers amplified the whole of the exon one and a good-sized section of the adjacent upstream promoter, these were used for an large scale amplification to investigate the methylation patterns in a collection of *Toxoplasma* infected and uninfected mice.

A collection of 116 *A. sylvaticus* brain DNA samples (Bajnok et al., 2015), table 2.1 (population 1), and a further 50 samples, collected and tested for *T. gondii* infection by the author (Chapter 4), were bisulphite treated and PCR amplified using the bisulphite primers BIOS F5/R5. Samples were purified from the gels and sent to a third-party company for DNA sequencing. Additionally, the same region was amplified and sequenced from non-bisulphite treated DNA. Bisulphite sequencing was broadly successful, although in some cases, some samples were unable to be amplified. In other cases, sequences obtained were of lower quality and some of these sequences could not be used.

Once the sequencing results had been received, the sequence was checked using Chromas software and visual inspection of chromatograms, unidentified bases (Ns) were checked and verified to build a consensus sequence for each of the samples. In some instances, when an anonymous basis could not be verified, that part of the sequence had to be removed from the analysis. A blast search was conducted on the NCBI database to confirm that the correct gene sequence had been amplified in each case. The sequences showed a 97% match with the *Mus musculus* Nos2 promoter region and Exon 1 (LOC111365144) on chromosome 11 and confirmed that the correct sequence of the iNOS promoter and exon1 had been amplified from *Apodemus*. Clustal Omega alignments were carried out to align bisulphite treated samples with their untreated counterparts. An example of the bisulphite treated and untreated sequences (mouse 92) are shown in Figure 5.21. Methylated C residues remain unchanged by bisulphite treatment, but all non-methylated C residues are changed to T. In the example shown in Figure 5.21, the majority of cytosines are unmethylated, but a single methylated cytosine can be seen at position 665 in the bisulphite sequence.

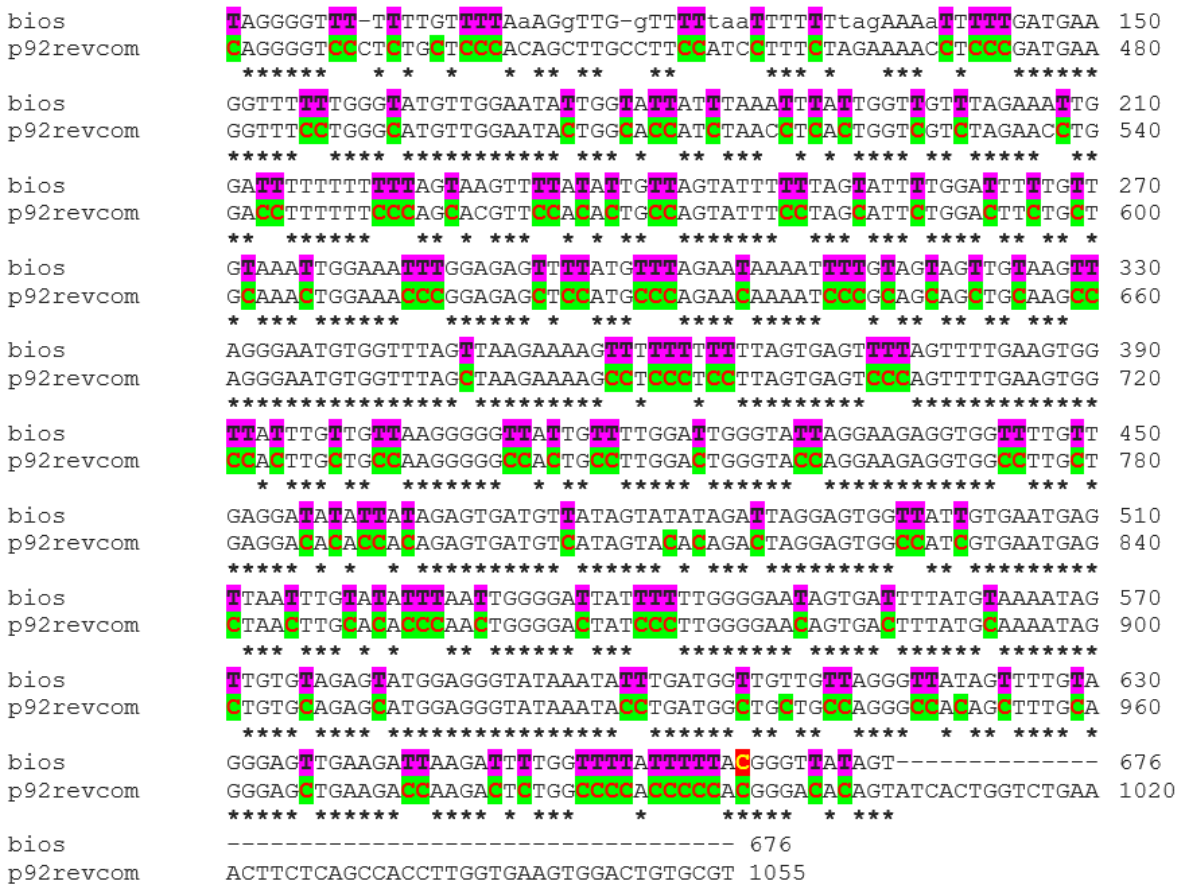

Figure 5-21 Clustal alignment, of the DNA sequences of the bisulphate, treated DNA and non-treated DNA from Heart from mouse P92, table 2.1 population 2.

The upper sequence shows the bisulphite treated sequence and the lower is the untreated one. Bases highlighted in purple and green show unmethylated cytosines (green) converted the thymine (purple) by bisulphite treatment. In this example, one base towards the end of the sequence (highlighted red) at position 665 is methylated as it remains a cytosine in the bisulphite treated DNA. Occasional sequencing inconsistencies were detected such as in the first line of this alignment (incorrect pairing and gaps) – such sections of section were removed from any further analysis.

Figure 5.22 shows the locations of possible CpG islands in the iNOS promoter and exon 1, that could be methylated in the *Apodemus* DNA samples. These have been annotated and described in relation to the start of Exon 1 (shown in purple in Figure 5.24). The CpG islands are highlighted in red, and those with a negative number are found within the promoter (CpG-59, CpG-119, CpG-175, CpG-392, CpG-394, CpG-

476) and those with positive numbers are located within Exon 1. The numbers refer to the number of bases upstream (negative) or downstream (positive) of the start of Exon 1. One CpG island (CpG47) is located within Exon1.

Figure 5-22 Predicted CpG islands within the *Apodemus* sequence amplified by primers BIOS F5/R5.

CpG islands are highlighted in red. One CpG island (CpG47) is located in the Exon 1, at nucleotide 47 in Exon 1 (last line in the diagram). The highlighted sequence in purple is the start of Exon 1. The highlighted nucleotides TATAAA in red are the putative TATA box, based on the *Mus musculus* homologue, which is -30 bp from the start of the exon. The remaining CpG islands highlighted in red are CpG-59, CpG-119, CpG-175, CpG-392, CpG-394, CpG-476 which are all found in the upstream promoter region.

Figure 5.23 shows an example of alignment for mouse J10, indicating the CpG islands and the effect of bisulphite treatment on the sequence. The difference between Figures 5.22 and 5.23 are that the first one shows predicted CpG sites while the second one shows actual sites.

```
CLUSTAL O(1.2.4) multiple sequence alignment
M4BIO           ------------------------------------------------------------      0
L4non           TTCTGtCTCTaaaTgtcaggatatAAGAgaagTGTgtcaTCAcTggGGTAgGACActtta      60
M4BIO           ------------------------------------------------------------      0
L4non           GtTcgacAgTaAgAtGTgTCGCtCAGTAgtcCccGCgCGACAACGAAGAGgGAAGAAgAG      120
M4BIO           ------------------------------------------------------------      0
L4non           AAGAAAgAGtGTaCTCtacACAGACCTGTGCCCtATCctGTGCACGAtatstTCtTATTa      180
M4BIO           ---------------------AGTTTTTGGGGGtgTTTTTgTTTTTAAAggggGtTTTTT      39
L4non           GTGGAGAGaaTCactcTGAgAGCgtATCacAGGTCTCTCTGTTCTCACAGAgttcgctTt      240
                                        * *    *** * * **** * * ** *     ***

M4BIO           TTTTTTTTTAAAAAATTTTTTggAaaaggTTTTTGGGGtatTgGGGaAAaggGGTtTTtT      99
L4non           atCtCTTTTagAGaaAAtCTCGataagagtTTCtTggGCAcaTGTgAgTATAgGcACCat      300
                 * * ***** * **  * * *  **  **** * *** *   * **  *  **     *

M4BIO           TaAATTTTTTggGGtTTTgaaaATTGGatTTTTTTTTTTaataTgTTTTAtagtgagaa      159
L4non           ATatcatCTCaggtgttATagaGcAcggacactTTTTTTTagcgCatttTaCACtgtCac      360
                  *   * *  **  **   * *    ***   *********     ***** * **  *

M4BIO           taTTTTTTaataTTTGgGAtTTTTTTTaAAAA--tggaAaATTggGAgagTTTTGtgttT      217
L4non           tgTaTcTTaGcgcttTggagtCTcgtgGcgcAAtggagaAcCcgaGAGatCtaTGtgCag      420
                * * * ***    ** *** * *  *     *   *  **   * ****  * ****

M4BIO           aaaAAAAAATTTTGgtggaggTaaaAttggaGgAATggggttTataaaaaAAAAgTTTTT      277
L4non           AgaAcAAtattGCagcacagGcacaacacaGagaaTGtggtTgatatgAgaAAcgtCTCT      480
                * ** ** ***   *   *** * **      ***** **** ***  * *** ** * *

M4BIO           TTTTataGaGaGTTagagTTgagaagtggaTaTgTggTgataaGGGGGaTagTgTTTgag      337
L4non           CTctAgaGaGtgtCacagTTgagctgtgcaCacgtggtcacaacGGGcaCtgcgcttgag      540
                 * ** **** ** * *******  *** * * ***** * ** *** *  * * *****

M4BIO           aggGtgTtttgtgaAGagGtggTTgTggaGaggATATaaTAgAGAGagaTgaTAtagTAT      397
L4non           aggGtgtcacgagaAGatGtcgccgtggaGaacACACCaCAcAGaGagaTgttAgagcAC      600
                *******   * ***** ** *  *******  * *  * * ********* ** ** *

M4BIO           ATAGATTAGGAGTGGTTATTGTGAATGAGTTAATTTGTATATTTAATTGGGGATTATTTT      457
L4non           ACAGACTAGGAGTGGCCATCGTGAATGAGCTAACTTGCACACCCAACTGGGGACTATCCC      660
                * *** *********  ** ********* *** *** * *   ** ****** ***

M4BIO           TTGGGGAATAGTGATTTTATGTAAAATAGTTGTGTAGAGTATGGAGGGTATAAATATTTG      517
L4non           TTGGGGAACAGTGACTTTATGCAAAATAGCTGTGCAGAGCATGGAGGGTATAAATACCTG      720
                ******** ***** ****** ******* **** **** ****************  **

M4BIO           ATGGTTGTTGTTAGGGTTATAGTTTTGTAGGGAGTTGAAGATTAAGATTTTGGTTTTATT      577
L4non           ATGGCTGCTGCCAGGGCCACAGCTTTGCAGGGAGCTGAAGACCAAGACTCTGGCCCCACC      780
                **** ** **  ****  * ** **** ****** ******  **** * ***    *

M4BIO           TTtaTGGGATATAGTATTATTGGTTTGAAATTTTTTAGTTATTTtGGgGAA---------      628
L4non           CCCACGGGACACAGTATCACTGGTCTGAAACTTCTCAGCCACCTTGGTGAAGGGACTGGG      840
                   * **** * ***** * **** ***** ** * **  *  **** ***

M4BIO           ---------------------   628
L4non           CTGTGTGAGACACtTCtGAGT   861
```

Figure 5-23 An example clustal alignment of the DNA sequences of the bisulphate treated DNA and non-treated DNA showing actual CpG sites.

These sequences were taken from the Braine DNA of mouse J10. This was an example alignment, using DNA from brain tissue, and is used here to illustrate how alignments were carried out. The upper sequence (M4BIO) shows the bisulphite treated sequence and the lower sequence (L4non) is the untreated one. Bases highlighted in red and green represent the sites of the CpG islands. Unmethylated cytosines (green) are converted to thymines (red) by bisulphite treatment. In this example, all the bases in the CpG islands are unmethylated as all of the bisulphite treated Cs are converted to Ts. In this sample, CpG -394 is actually heterozygous although it is recorded as unmethylated in this alignment. Clustal alignments are not ideal methods for displaying heterozygotes.

In addition to identifying methylated and unmethylated bases, there is also the possibility, since *Apodemus* is diploid that there will be heterozygous bases which could either be single nucleotide polymorphisms or could be heterozygous for methylation status. Figure 5.24 shows an example of the appearance of a heterozygote on the chromatogram.

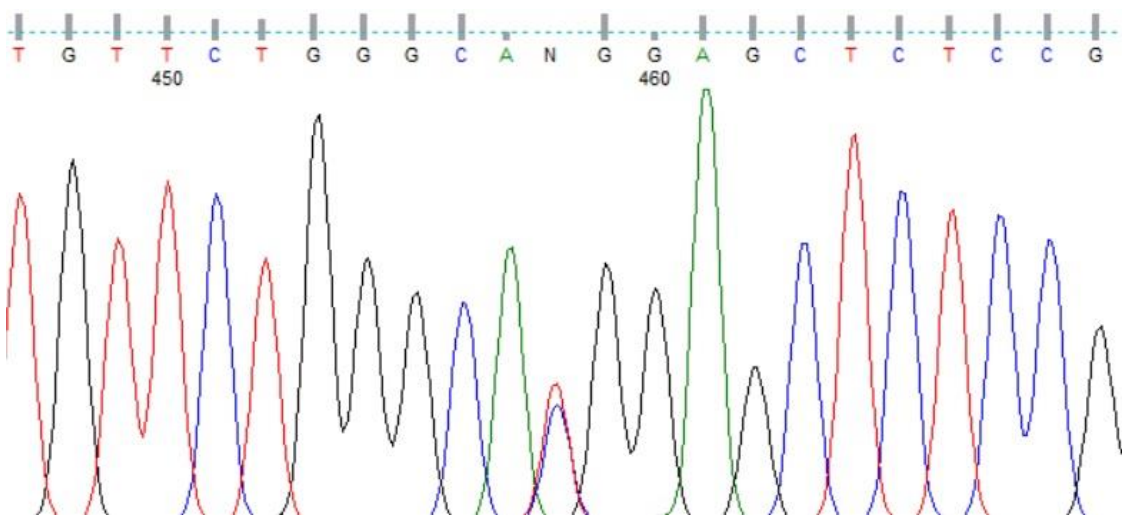

Figure 5-24 Chromatograph of a DNA sequence showing a heterozygous base. The overlapping peaks (red and blue) at position 458 indicate a heterozygote with C and T representing the two alleles.

DNA sequences were obtained from 116 *A. sylvaticus* brain samples which had been amplified using primers BIOSF5/R5 and their corresponding primers for non-bisulphite treated DNA. The sequences were analysed for single nucleotide polymorphisms (SNPs), DNA methylation events and inspected for heterozygotes at sites where both the SNPs and the methylation/unmethylation events occurred. Figure 5.25 summarises the region of the iNOS gene and promoter that are covered by this amplified region.

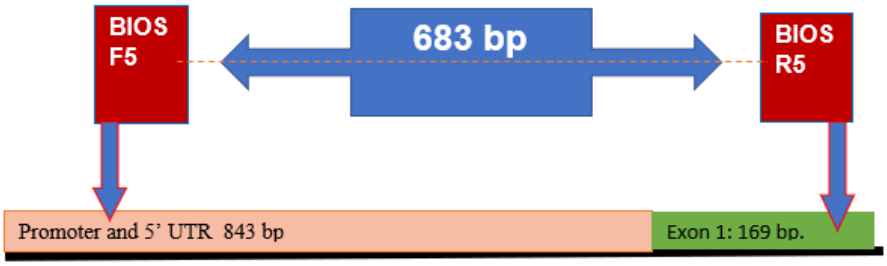

Figure 5-25 Summary of the PCR amplified region covered by the BIOSF5/R5 primers.

Analysis of the sequences shows that the *Apodemus* promoter, 5' UTR and Exon 1, consists of seven putative CpG islands. The number of CpGs islands in the *Apodemus* sequence is more significant than the corresponding sequence in *Mus musculus* which has three less. A comparison between the identical sequences in *A. sylvaticus* and *Mus musculus* is shown in Figure 5.26. (A more extended sequence of the *Mus musculus* promoter is shown, and one CpG island exists outside of the corresponding region in the *Apodemus* sequence).

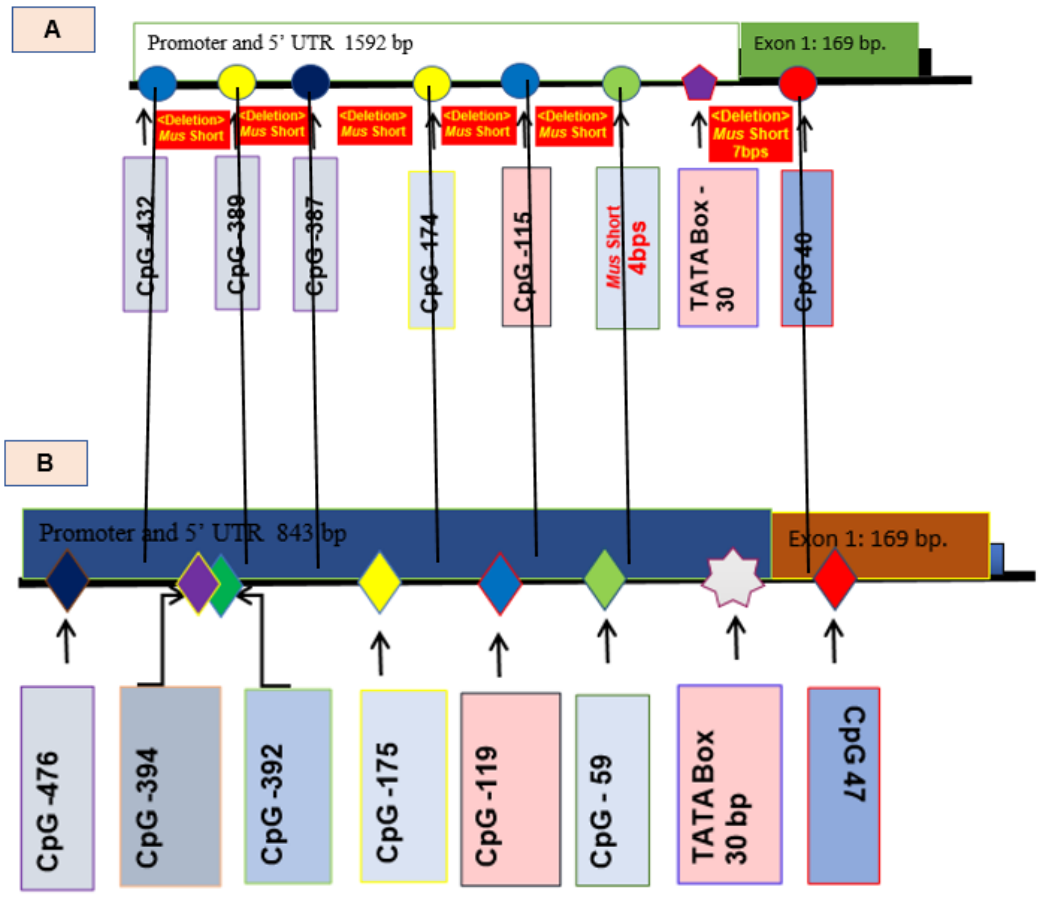

Figure 5-26 Comparison of the CpG islands.

in the promoter regions of the iNOS gene of *A. sylvaticus* and *Mus musculus*. A. The upper panel shows a diagram of the *Mus musculus* nos2 gene for inducible nitric oxide synthase, promoter region and 5'UTR (GenBank: L23806.1). B. The lower panel shows a diagram of the *Apodemus* iNOS promoter and Exon 1. There are sevenCpGs islands: CpG island 47 is in Exon1 while CpG-59, CpG-119, CpG-175, CpG-392, CpG-394, CpG-476 map to the Promoter and 5' UTR. In the *Mus* sequence there is an equivalent CpG island at the same location in Exon 1 and corresponding CpG islands in the *Mus* gene promoter.

Multiple sequence alignments were carried out, using Clustal Omega, to identify differences in methylation pattern across all of the 683 base pair sequences obtained from the *Apodemus* brain DNA samples. An example alignment of bisulphite treated sequences at CpG island CpG47 is shown in figure 5.27. The presence of a C residue in each of these samples indicates that this was a methylated cytosine.

Figure 5-27 Example lustal alignment of the consensus sequences of several *Apodemus* samples in the CpG island at exonic region 47.

(This is positioned at 47 base pairs into Exon 1). The highlighted green C is the methylated cytosine. Sequence identities refer to the codes in column 3 of Table 5.3.

Another example (Figure 5.28), shows another *Apodemus* CpG island found in the promoter region and is located at position -59 (59 base pairs ahead of the start of the gene). In most of the samples, this CpG island is unmethylated (converted to a T by bisulphite treatment).

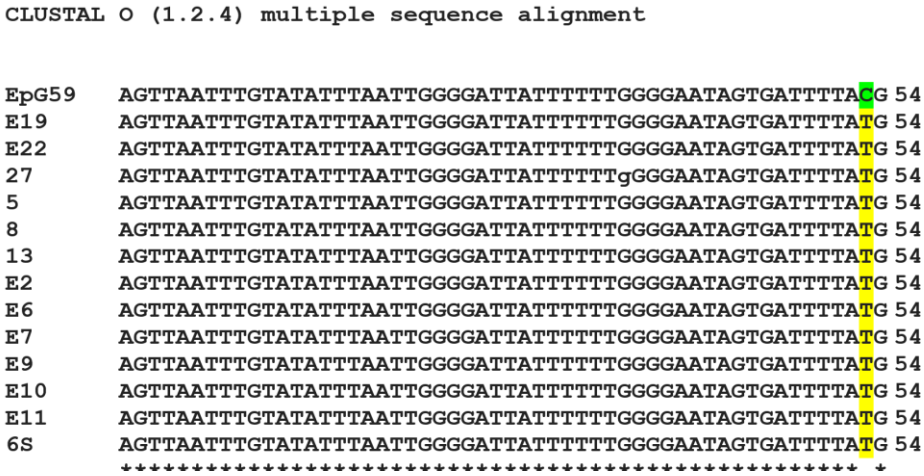

Figure 5-28 Example Clustal alignment of the consensus sequences of a number of *Apodemus* samples in the CpG -59 island in the promoter region.

This one is CpG -59 which indicates that it is 59 base pairs upstream of the start of the gene. The highlighted green C is a methylated cytosine while the yellow highlighted T residues indicate those that have been modified by bisulphite treatment. Sequence identities refer to the codes in column 3 of Table 5.3.

Figure 5.29 shows another example, using the CpG island at position -119 (119 base pairs upstream of the start of Exon 1). Again, in this example, residues that remain as C residues, post-bisulphite treatment, are methylated while those that are converted to T are unmethylated.

Similarly, figures 5.30, 5.31 and 5.32 show example alignments of, respectively, the following CpG islands within the upstream promoter region: CpG -175, CpG -392 (and CpG -394) and CpG -476.

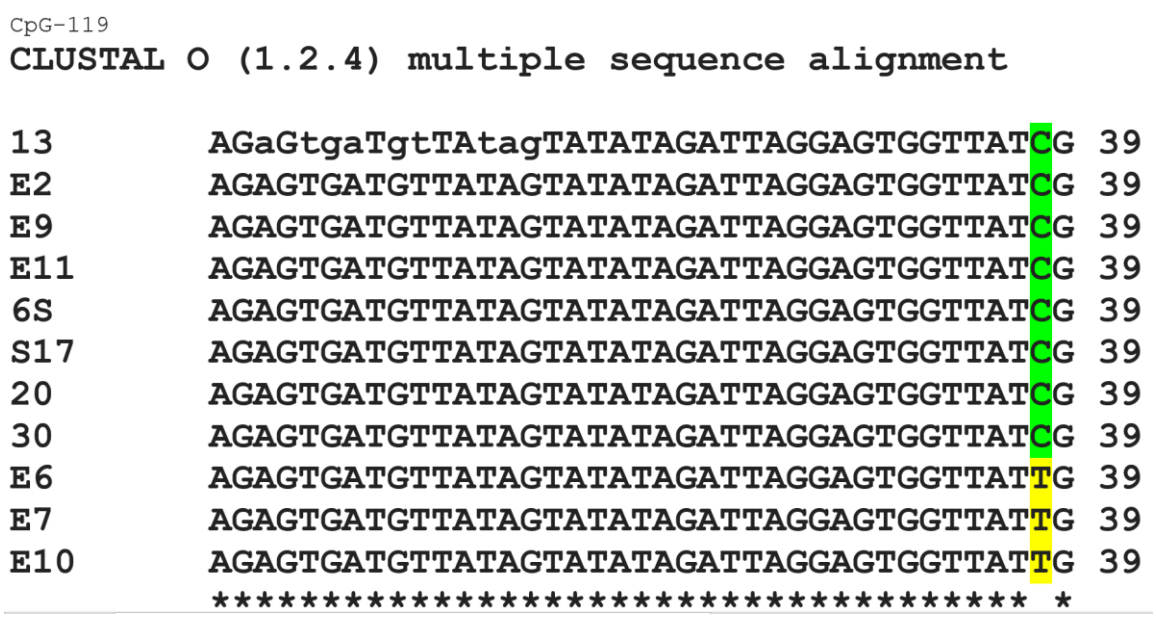

Figure 5-29 Example Clustal alignment of the consensus sequences of a number of *Apodemus* samples in the CpG island in the promoter region.

This one is CpG -119 which indicates that it is 119 base pairs upstream of the start of the gene. The highlighted green Cs are methylated cytosines while the yellow highlighted T residues indicate those that have been modified by bisulphite treatment. Sequence identities refer to the codes in column 3 of Table 5.3.

Figure 5-30 Clustal alignment of the consensus sequences of a number of *Apodemus* samples in the CpG island in the promoter region.

This one is CpG -175 which indicates that it is 175 base pairs upstream of the start of the gene. The highlighted green Cs are methylated cytosines while the yellow highlighted T residues indicate those that have been modified by bisulphite treatment. Sequence identities refer to the codes in column 3 of Table 5.3.

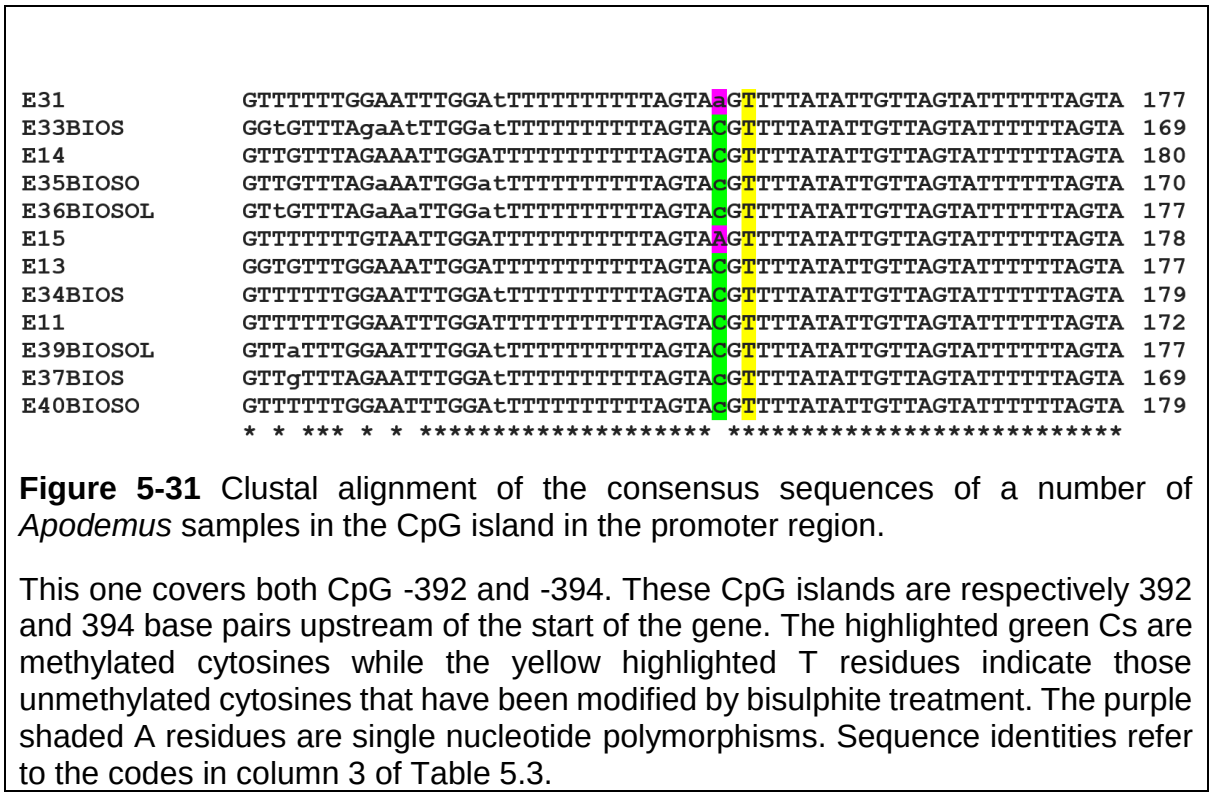

Figure 5-31 Clustal alignment of the consensus sequences of a number of *Apodemus* samples in the CpG island in the promoter region.

This one covers both CpG -392 and -394. These CpG islands are respectively 392 and 394 base pairs upstream of the start of the gene. The highlighted green Cs are methylated cytosines while the yellow highlighted T residues indicate those unmethylated cytosines that have been modified by bisulphite treatment. The purple shaded A residues are single nucleotide polymorphisms. Sequence identities refer to the codes in column 3 of Table 5.3.

Figure 5-32 Clustal alignment of the consensus sequences of a number of *Apodemus* samples in the CpG island in the promoter region.

This one is CpG -476 which indicates that it is 476 base pairs upstream of the start of the gene. Sequence identities refer to the codes in column 4 of Table 5.3.

A summary of the sequences at each of the CpG island sites is listed in Table 5.3. Included for each site, SNPs and methylation status is included. As each site is expected to have a CG duo of residues, any deviation from this is listed as an SNP and indicated with the relevant base. In the case of cytosine residues, the methylation status of the CpG island is indicated. Since the wood mice are diploid, the two alleles of the iNOS gene are shown as C^m/C^m, C^m/C or C/C for, respectively, homozygous methylated, heterozygous and homozygous unmethylated cytosines.

An additional collection of wild rodents was carried out to enable simultaneous extraction of RNA from the same animals to allow for correlation of data on infection, iNOS genotype and iNOS/Arginase expression. The genotype data from these 12 animals are presented in Table 5.4. Due to the unpredictability of collecting wild animals, the catch of *Apodemus* on this occasion was low, and some voles were additionally caught. Both species were included, and similarities between the iNOS promoter and Exon 1 regions enabled both species to be included in specific analyses.

Table 5.3 Variation in methylation patterns in the CpG islands of the iNOS gene promoter and Exon 1. Column 1, mouse identity code; column 2, *Toxoplasma* infection status; column 3, additional code for DNA sequences; columns 4 – 10, nucleotide identity at each numbered CpG island, A, C, G, T refer to the four standard bases, C^m refers to methylated cytosines. NS, no sequence available. As these mice are diploid C/C, for example, refers to both alleles where C/C^m, for example, represents a heterozygote. In the case of a single base entry, this refers to being homozygous for that base.

Table 5-3 Variation in methylation patterns in the CpG islands of the iNOS gene promoter and Exon 1

Mouse code	Diagno-sis of *Toxopl-asma*	DNA Code	CpG^{-476}	CpG^{-394}	CpG^{-392}	CpG^{-175}	CpG^{-119}	CpG^{-59}	CpG^{47}
J23	+	E2	G	A	C/C	C/C	C^m/C^m	C/C	C^m/C^m
J43	+	E6	G	C^m/C^m	C/C	C/C	C/C	C/C	C^m/C^m
J44	+	E7	C/C	C/C	C/C	C/C	C/C	C/C	C^m/C^m
J52	+	E8	C^m/C^m	C^m/C^m	C/C	C/C	C/C	C/C	C^m/C^m
J53	+	E9	G	C/C	C/C	C/C	C^m/C^m	C/C	C^m/C^m
J54	+	E10	G	C^m/C^m	C/C	C/C	C/C	C/C	C/C
J60	+	E11	G	C^m/C^m	C/C	C/C	C^m/C^m	C/C	C^m/C^m
J71	+	E12	C^m/C^m	A	C^m/C^m	C/C	C/C	C/C	C^m/C^m
J72	+	E13	G	C^m/C^m	C/C	C/C	C/C	C/C	C^m/C^m
J75	+	M34	G	A	C/C	C/C	C/C	C/C	C/C
J78	+	E14	G	G	C/C	C/C	C/C	C/C	C^m/C^m
J84	+	E15	G	A	C/C	C/C	C/C	C/C	C^m/C^m
J85	+	E16	NS	NS	NS	C/C	C^m/C^m	A	C^m/C^m
J86	+	E17	NS	NS	NS	C/C	C/C	C/C	C^m/C^m
J87	+	E18	NS	NS	NS	C/C	C^m/C^m	C/C	C^m/C^m

Table 5.4. Variation in methylation patterns in the CpG islands of the iNOS promoter and Exon 1. in a new collection of wild rodents. This collection was specifically made to enable collection of RNA for gene expression studies to facilitate correlation with infection and iNOS sequence data. Column 1, mouse identity code; column 2, *Toxoplasma* infection status; column 3, species (A, *Apodemus* or V, voles); columns 4 – 10, nucleotide identity at each numbered CpG island, A, C, G, T refer to the four standard bases, C^m refers to methylated cytosines. NS, no sequence available. As these mice are diploid C/C, for example, refers to both alleles where C/C^m, for example, represents a heterozygote. In the case of a single base entry this refers to being homozygous for that base.

Table 5-4 Variation in methylation patterns in the CpG islands of the iNOS promoter and Exon 1. in a new collection of wild rodents.

Mouse code	Diagnosis of *Toxoplasma*	Species	CpG^{-476}	CpG^{-394}	CpG^{-392}	CpG^{-175}	CpG^{-119}	CpG^{-59}	CpG^{47}
A1	-	V	NS	NS	NS	NS	C^m/C^m	C^m/C	C/C
A2	-	V	A	NS	NS	C/C	A	A	NS
A3	-	A	C/C	C^m/C	C^m/C^m	C/C	C^m/C^m	C/C	C/C
A4	-	A	G	A	C/C	C/C	C/C	C/C	C^m/C^m
A6	-	A	C/C	C^m/C	C^m/C	C/C	C/C	C/C	C^m/C^m
A7	-	A	G	C/C	C/C	C/C	C/C	C/C	C^m/C
A8	-	A	G	C^m/C^m	C/C	C/C	C/C	C/C	C^m/C^m
A9	-	A	G	C^m/C^m	C/C	C/C	C/C	C/C	C^m/C^m
A11	-	A	C/C	C^m/C	C/C	C/C	C^m/C^m	C/C	C^m/C
A5	+	V	G	C/C	C/C	NS	C^m/C^m	C/C	C^m/C^m
A10	+	V	NS	NS	NS	NS	NS	NS	C^m/C^m
A12	+	V	NS	C^m/C	C/C	NS	NS	NS	NS

Due to the low catch of *Apodemus* and the supplementation of these new catches with voles, the promoter region and exon one from voles was investigated for sequence similarity. There were differences in the sequences between the *Apodemus* and vole brain DNA which resulted in length differences in the promoter region. However, the homologous CpG islands could be identified.

Analysis was carried out on the associations between *Toxoplasma* infection and sequence status at each CpG island (2x 2 contingency table, Fishers Exact Test). Table 5.5 and Figure 5.33 show the results for CpG island 47. This CpG island resides within Exon 1. In the infected animals, a high proportion (86.66%) had homozygous methylated cytosines at this position with very much lower proportions of unmethylated cytosines or heterozygotes or other any SNPs have been found. This was in contrast to the uninfected animals that had a much lower frequency of methylated cytosine residues (61.17%). There was a significant association between infection and methylation status (P = 0.0001). In the case of CpG island -59, which resides in the promoter region, there was no significant association with infection status (P = 0.598), At this site, the majority of cytosine residues were unmethylated whether the animals were infected or not (Table 5.6 and Figure 5.34). CpG island -119, in the upstream promoter region, had a high frequency of homozygous genotypes and there was no association with infection (P = 0.479) (Table 5.7 and Figure 5.35). In the case of CpG island -175, the majority of cytosines were unmethylated and there was no association with infection (P = 0.252) (Table 5.8 and Figure 5.36).

Table 5-5 CpG island 47 in *Apodemus* Exon 1.

CpG47	Infected	% Infected	Not infected	% Not infected	Total
Methylated Homozygote	39	86.66	52	61.17	91
Any SNPs	6	13.33	33	38.82	39
TOTAL	45	100	85	100	130

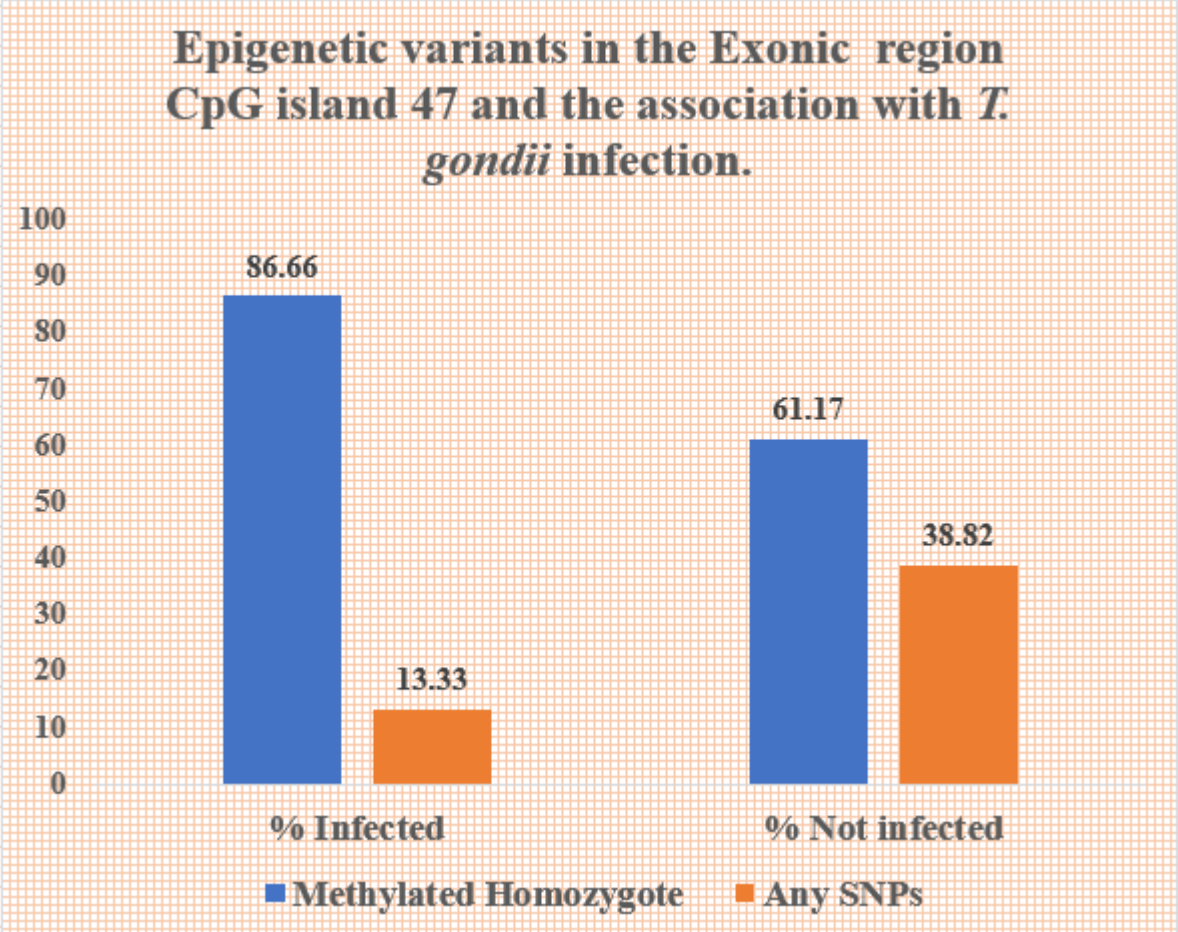

Figure 5-33 Epigenetic variants in CpG island 47 and the association with *T. gondii* infection.

The blue columns indicate the percentage of infected *Apodemus* and the orange columns indicate the percentage of uninfected *Apodemus* with a particular sequence variant. CM/CM, homozygote methylated cytosine, and the any other SNPs. Two tailed Fishers Exact Test , shows a significant association between infection status and cytosine methylation status P = 0.0001.

Table 5-6 CpG island -59 in the *Apodemus* promotor.

CpG-59	Infected	% Infected	Not infected	% Not infected	Total
Methylated Homozygote	2	4	1	1.13	3
Any Other SNPs	47	96	87	98.86	134
TOTAL	49	100	88	100	137

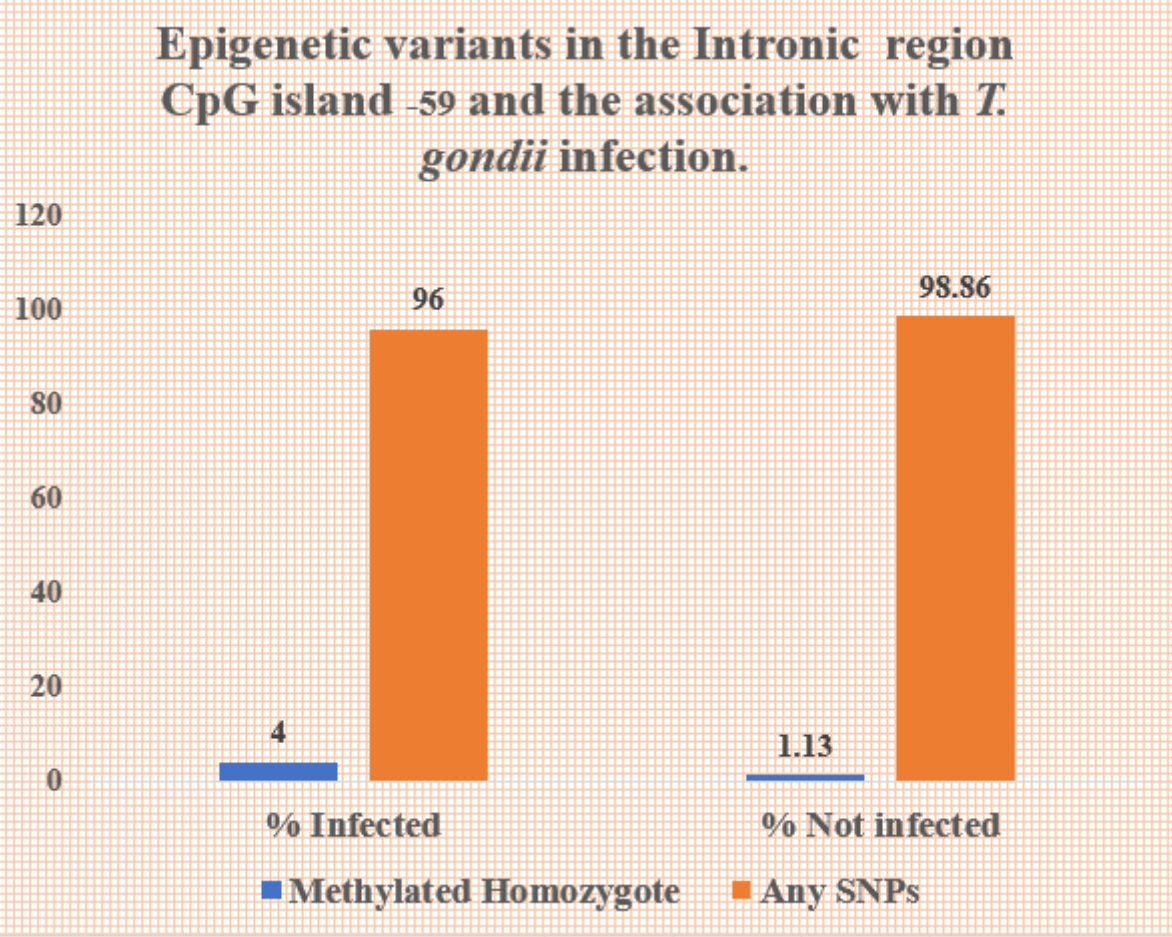

Figure 5-34 Epigenetic variants in CpG island -59 and the association with *T. gondii* infection.

The blue columns indicate the percentage of infected *Apodemus* and the orange columns indicate the percentage of uninfected *Apodemus* with a particular sequence variant. CM/CM, homozygote methylated cytosine and the any other SNPs. Two tailed Fishers Exact Test , shows no significant association between infection status and cytosine methylation status. (P = 0.598).

Table 5-7 CpG island -119 in the *Apodemus* promotor.

CpG-119	Infected	% Infected	Not infected	% Not infected	Total
Methylated Homozygote	22	51.16	41	45.5	63
Any Other SNPs	21	48.23	49	54.44	70
TOTAL	43	100	90	100	133

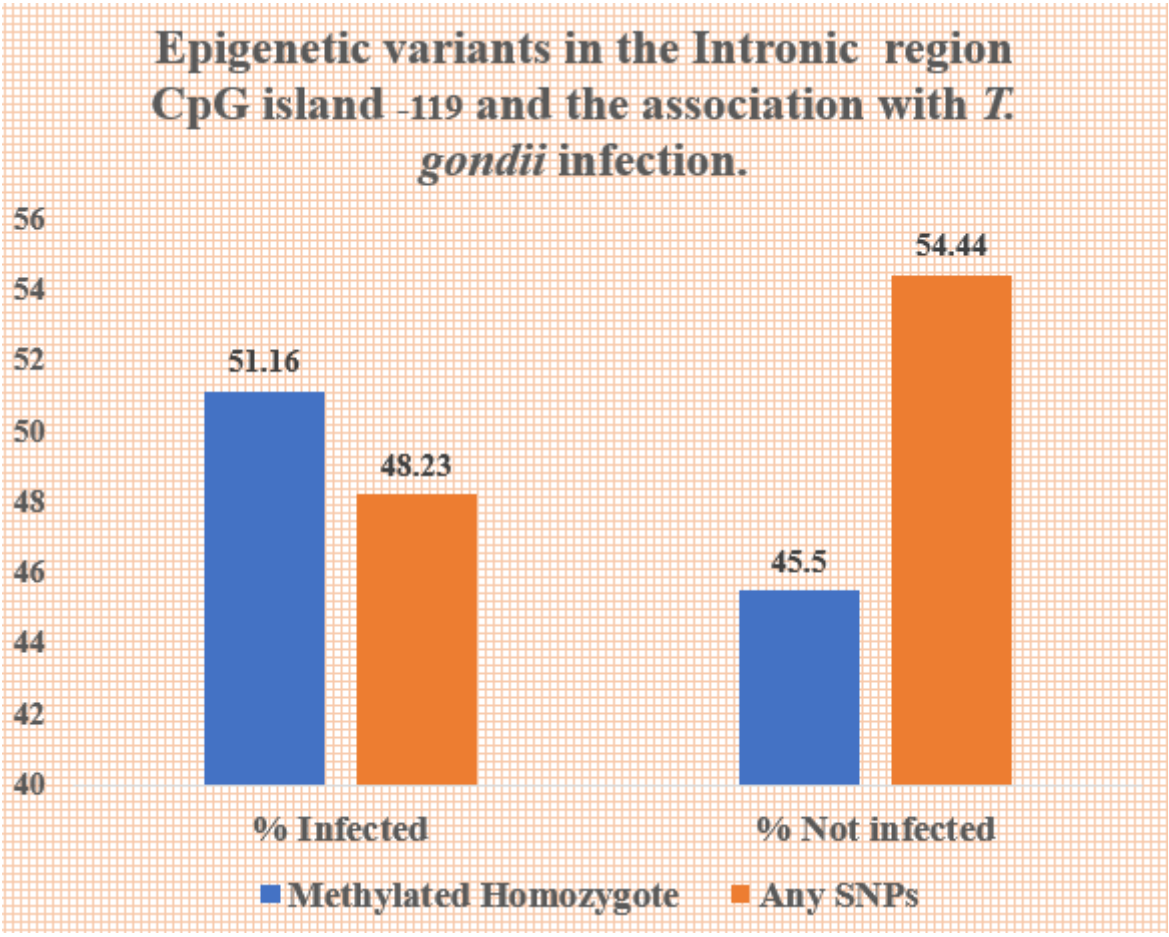

Figure 5-35 Epigenetic variants in CpG island -119 and the association with *T. gondii* infection.

The blue columns indicate the percentage of infected *Apodemus* and the orange columns indicate the percentage of uninfected *Apodemus* with a particular sequence variant. CM/CM and the any other SNPs. Two tailed Fishers Exact Test , shows no significant association between infection status and cytosine methylation status. (P = 0.479).

Table 5-8 CpG island -175 in the *Apodemus* promotor.

CpG-175	Infected	% Infected	Not infected	% Not infected	Total
Methylated Homozygote	1	2.5	1	1.20	2
Any other SNPs	39	97.5	82	98.79	121
TOTAL	40	100	83	100	123

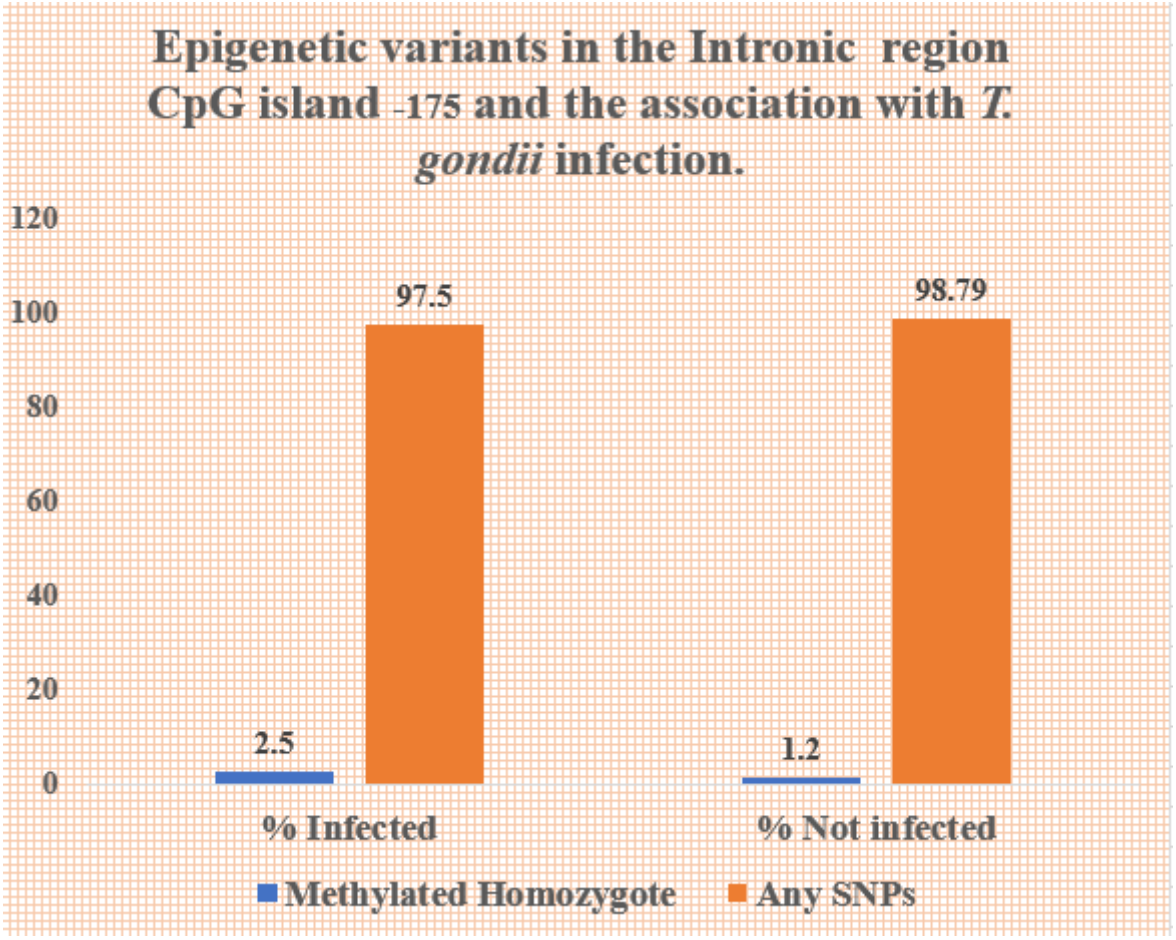

Figure 5-36 Epigenetic variants in CpG island -175 and the association with *T. gondii infection.*

The blue columns indicate the percentage of infected *Apodemus* and the orange columns indicate the percentage of uninfected *Apodemus* with a particular sequence variant. CM/CM, homozygote methylated cytosine, and the any other SNPs. Two tailed Fishers Exact Test , shows no significant association between infection status and cytosine methylation status. (P = 0.252).

Table 5-9 CpG island -392 in the *Apodemus* promotor.

CpG-392	Infected	% Infected	Not infected	% Not infected	Total
Methylated Homozygote	2	6.6	3	4.5	5
Any other SNPs	28	93.3	63	95.5	91
TOTAL	30	100	66	100	96

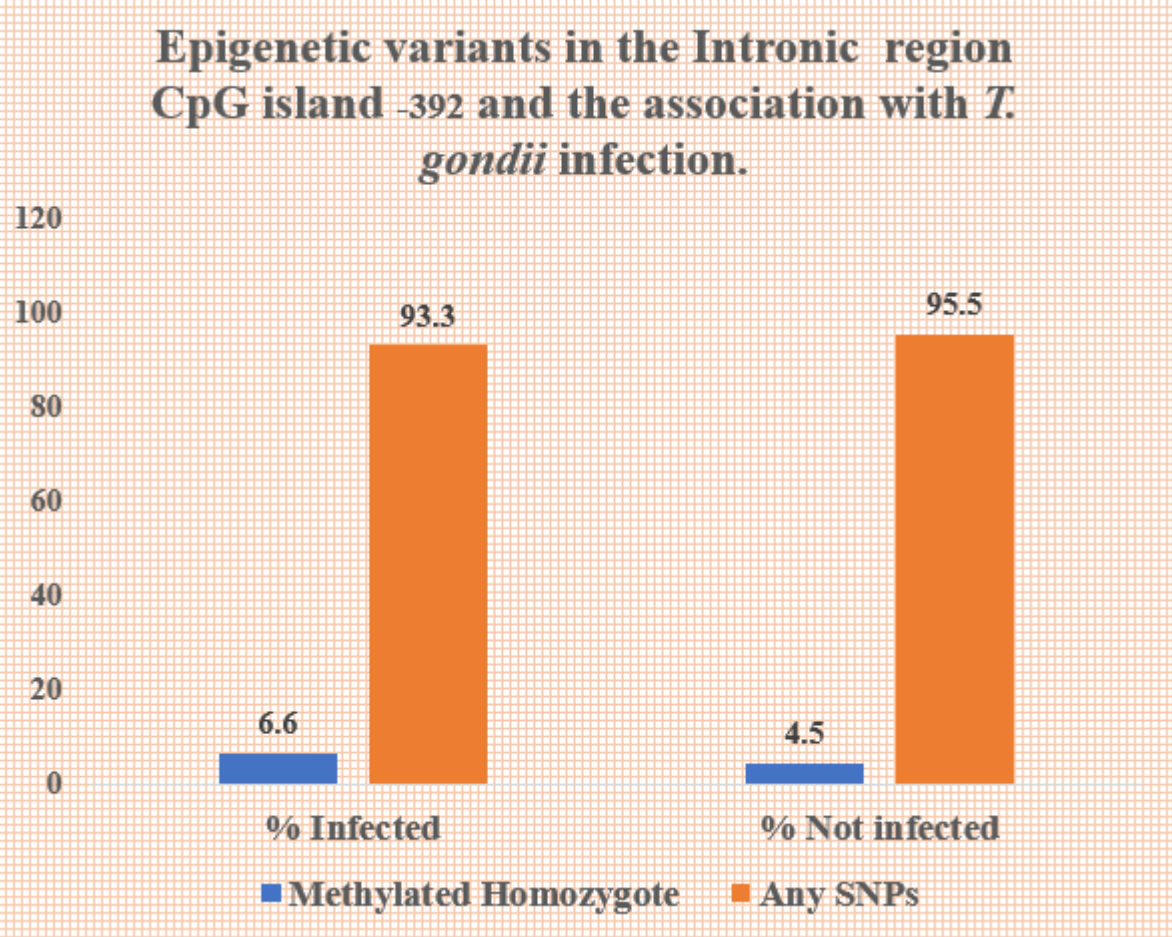

Figure 5-37 Epigenetic variants in CpG island -392 and the association with *T. gondii* infection.

The blue columns indicate the percentage of infected *Apodemus* and the orange columns indicate the percentage of uninfected *Apodemus* with a particular sequence variant. CM/CM, and the any other SNPs. Two tailed Fishers Exact Test , shows no significant association between infection status and cytosine methylation status. (P = 0.537).

Table 5-10 CpG island -394 in the *Apodemus* promotor.

CpG-394	Infected	% Infected	Not infected	% Not infected	Total
Methylated Homozygote	10	33	25	37	35
Any other SNPs	20	67	42	63	62
TOTAL	30	100	67	100	97

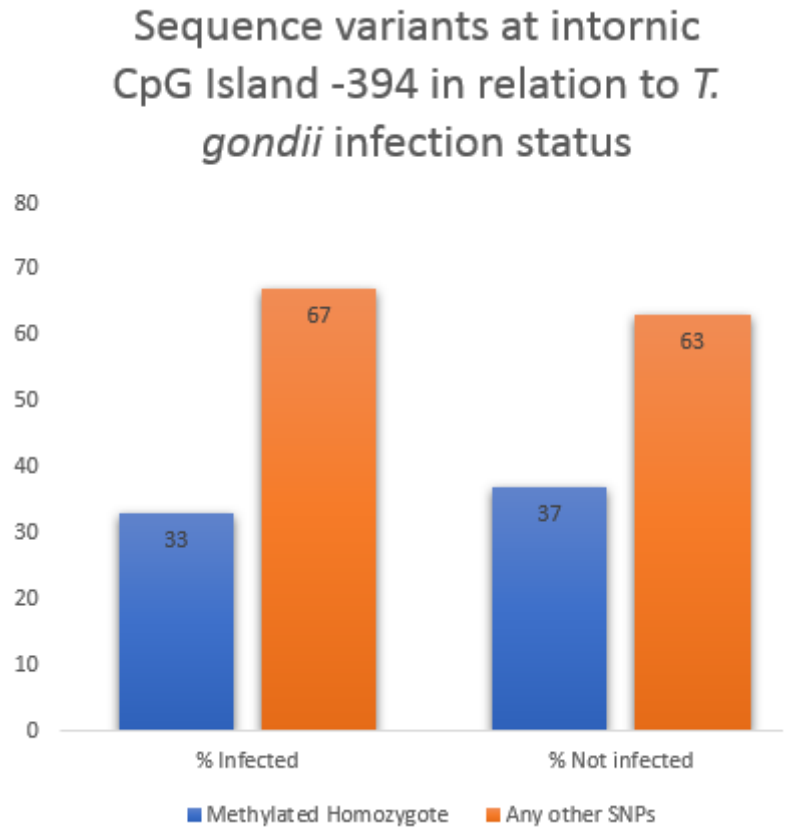

Figure 5-38 Epigenetic variants in CpG island -394 and the association with *T. gondii* infection

The blue columns indicate the percentage of infected *Apodemus* and the orange columns indicate the percentage of uninfected *Apodemus* with a particular sequence variant. CM/CM, and the any other SNPs. Two tailed Fishers Exact Test , shows no significant association between infection status and cytosine methylation status. (P = 0.656).

Table 5-11 CpG island -476 in the *Apodemus* promotor.

CpG-476	Infected	% Infected	Not infected	% Not infected	Total
Methylated Homozygote	3	11	2	3	5
Any other SNPs	25	89	62	97	87
TOTAL	28	100	64	100	92

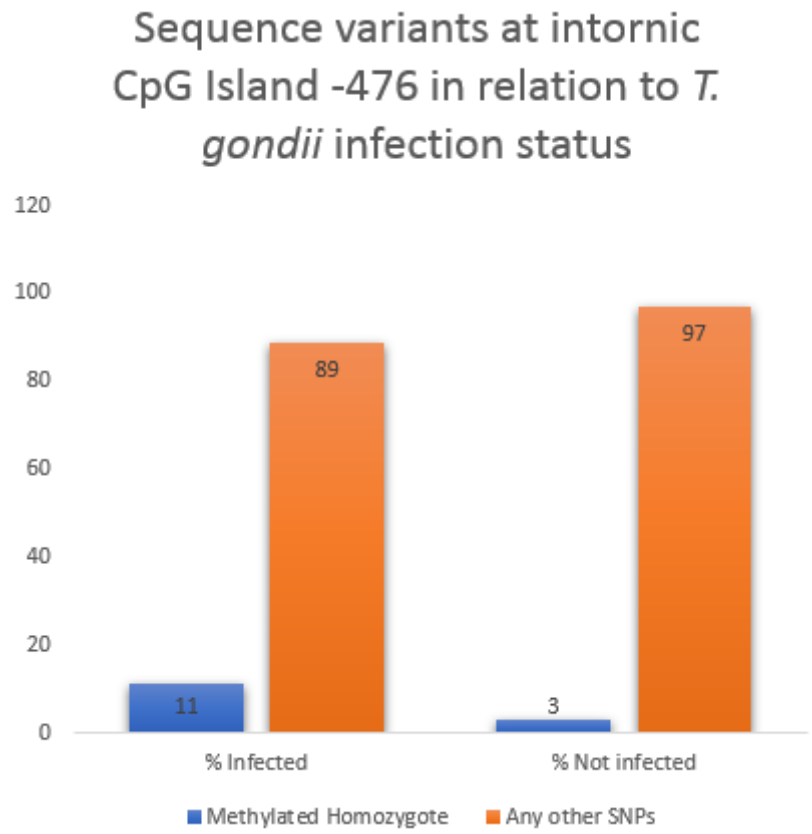

Figure 5-39 Epigenetic variants in CpG island -476 and the association with *T. gondii* infection.

The blue columns indicate the percentage of infected *Apodemus* and the orange columns indicate the percentage of uninfected *Apodemus* with a particular sequence variant. CM/CM, homozygote methylated cytosine and the any other SNPs. Two tailed Fishers Exact Test , shows a significant association between infection status and cytosine methylation status. (P = 0.049).

CpG island -392, in the upstream promoter region, had a high frequency of unmethylated cytosines and there was no association with infection (P = 0.537) (Table 5.9 and Figure 5.37). In the case of the adjacent CpG island -394, there was a wide range of genotypes, including SNPs, and there was no association with infection (P = 0.656) (Table 5.10 and Figure 5.38). In the final CpG island – 476, there was a high frequency of SNPs but no association with infection (P = 0.049) (Table 5.11 and Figure 5.39).

A key aspect of the hypothesis that the iNOS/Arginase balance affects the outcome of infection, is that genetic or epigenetic changes would influence iNOS expression. DNA methylation is generally reported to be associated with inhibition of gene expression and therefore down regulates the production of the associated protein. Methylation of the iNOS gene would therefore be expected to be associated with down regulation of the iNOS protein. In the case of CpG island -47, where a significant association was found between methylation status and *T. gondii* infection status, this relationship can be further analysed with respect to iNOS expression. Data presented in Table 5.5 can be simplified to address this. In the situation where CpG -47 is fully methylated (i.e. the C^mC^m genotype) or mutated due to a SNP, the iNOS gene would be switched off resulting in a lack of production of iNOS. This accounts for 86.66% (39/45) of infected mice compared with 61.17 % (52/85) of uninfected mice. In the case of the other genotypes, homozygous unmethylated and the heterozygous state, iNOS would be expected to be produced. This is the case in 13.33% (6/45) of infected mice and 38.82% (33/85) of uninfected mice. Infected mice have a greater frequency of possessing non-iNOS producing genotypes than uninfected mice (Fisher exact test, *P* = 0.0001).

5.5 Discussion

The aim of this chapter was to investigate whether structural differences in the iNOS gene might relate to differences in iNOS expression and influence infection with *T. gondii.* In Chapter 4, it was demonstrated that differences in the relative expression of iNOS and Arginase were related to infection with *T. gondii*. The availability of DNA samples from a large collection of characterised wood mice offered the opportunity to compare structural differences in these genes between infected and uninfected animals. In infected mice, a low iNOS/Arginase expression ratio was found while a high iNOS to arginase ratio of expression was found in uninfected animals. The structural differences between these two states could be, for example, single nucleotide polymorphisms (SNPs) that associate with infection status. Evidence from the control of infection in rat peritoneal macrophages (resistant) compared with alveolar macrophages (sensitive) suggested the control of resistance might be epigenetic (Z.-J. Zhao *et al.*, 2013). The DNA taken from the brain tissue of this collection of wood mice also offered the opportunity to investigate epigenetic mechanisms, such as DNA methylation, in relation to infection. In order to investigate possible structural differences between the DNA of infected and uninfected animals, the upstream promoter region and first exon were chosen for the focus of this investigation. This is because these regions are often the parts of a gene that are responsible for control of gene expression.

Little is known about the iNOS gene in *A. sylvaticus*, so a key activity was to make use of genome information from *Mus musculus* to design tools to search for genetic and epigenetic marks that might be of interest. The availability of detailed resources for *Mus* and the opportunity to utilise partial genome sequence information for *Apodemus* generated in Liverpool, meant that PCR primers and other tools could be developed.

A collection of 144 *A. sylvaticus* was available from other studies (Bajnok et al., 2015) and collected as part of this study. These wood mice had been characterised for infection with *T. gondii*, other parasites and host phenotypes (weight and length as indicators of age, sex, adult/juvenile status). In this study, DNA sequences were obtained from the iNOS gene promotor and Exon 1 from these mice. Additionally, the methylation status of 7 identified CpG islands was determined. Analysis of SNPs within

this region showed that several SNPs existed but none were associated with infection. However, analysis of DNA methylation status of these genes demonstrated a significant association between methylation differences and infection status at the exonic CpG 47, and the intronic CpG -476 a CPG island that is located within Exon 1 and 47 base pairs after the transcription start site (P=0.0001), while the intronic -476 bp before the starting the exon 1 (p=0.049).

These data showed that 87% of the infected mice possessed the homozygous methylated cytosine (C^mC^m) genotype at CpG island 47 while only 61.17% of the uninfected mice possessed this genotype. Additionally, in the uninfected mice there was a higher frequency of non-methylated genotypes, with regards to other SNPs (C^mC/CC and SNPs) than the infected mice with 38.82% instead of 13.33% respectively, A SNP, at this position, was observed in one mouse that presumably removes this site as a CpG island.

This raises an important question as to the role of this polymorphic CpG island in relation to infection. There are many studies that link methylation of CpG islands with expression of the iNOS gene (for example, Chan et al. 2005; Hmadcha et al., 1999) the higher methylation, the lower the expression and vice-versa (Kuriakose & Miller, 2010). This suggests that there might be a link between iNOS gene regulation and *T. gondii* infection within this wood mouse population. In experimental studies in rats, it has been shown that there is an epigenetic effect that influences differences in the susceptibility of peritoneal and alveolar macrophages to infection with *T.gondii*, Within the same inbred line of rats, peritoneal macrophages are resistant to infection with *T. gondii* while alveolar macrophages are highly susceptible (Zhao *et al.*, 2013). Furthermore, these cell types differ in iNOS and Arginase expression levels with peritoneal macrophages expressing high iNOS and low Arginase levels while alveolar macrophages show the opposite expression levels. Nothing seems to be known about the differences in iNOS gene regulation in these cell types but, since the differences are epigenetic, it is possible that differences in methylation patterns in CpG islands could account for this.

Since epigenetic modifications can affect iNOS gene expression and iNOS gene expression can influence *T. gondii* infection, it is possible that methylation polymorphism could be linked to infection status in natural populations of *A. sylvaticus*.

Given that methylation of cytosine residues acts to suppress iNOS expression, it would be expected that non-methylated genotypes would be associated with iNOS gene expression. In this study, two genotypes (the heterozygous C^mC and homozygous CC, C^M, SNPs genotypes) would express iNOS while the homozygous C^mC^m genotype and any SNPs that destroy the CpG island would not. When the frequency of iNOS expressing genotypes (C^mC, SNPs and CC) in the wood mouse population is considered, only 13.33% of infected mice had these genotypes compared to 38.82% of uninfected mice. Similarly, the putative iNOS non-expressing genotypes (C^mC^m and CpG island destroying SNPs were found in 86.66% of infected mice and only 61.17% of uninfected mice. This significantly (P=0.0001) association between expressing and non-expressing genotype with infection suggests that this genotype is integrally associated with resistance and susceptibility to *T. gondii* infection. As well the intronic CpG -476, with regads to sicnificancy of (P=0.049).

Although a significant association has been discovered between methylation patterns and *T. gondii* infection, it raises the question as to what is happening in those wood mice whose genotypes do not conform to the associations described above. In the case of the uninfected mice, there is unlikely to be an absolute correlation since this group of mice include two groups of mice: those that have been challenged by infection but are resistant and those that have never been exposed to the parasite. In a natural population of wood mice, it is not possible to distinguish individual mice in these two populations although the 38.82% of uninfected mice possessing iNOS non-expressing genotypes could contribute to the former group. In the case of the infected mice, 13.33% of the mice possess the resistant iNOS expression related genotypes. One explanation for these mice could be due, not to the expression of the iNOS gene but instead, to the expression of the Arginase gene. If the expression of Arginase was higher in these mice, it might out compete the iNOS gene expression and result in lower NO levels and higher susceptibility to infection. Previous studies in rats (Wang *et al.*, 2015) showed that susceptibility or resistance to infection was related not to the absolute expression of iNOS but to the iNOS/Arginase expression ratio. Data reported in chapter 4, that shows differences in iNOS/Arginase expression ratios between infected and uninfected mice, is consistent with the possibility that both enzymes contribute to this. Further work is necessary to address this question in more detail.

In conclusion, this study has demonstrated that methylation status of a two CpG islands in Exon 1 and the intrinsic -476, of the iNOS gene is associated with infection status in a natural population of wood mice. Extensive searches of the literature suggest that this is the first time that this phenomenon has been reported in natural populations of mice and furthermore, this phenomenon does not seem to have been described in laboratory mice either. A hypothesis was proposed at the outset of this chapter: that there could be a relationship between the methylation status of the iNOS gene promoter and infection status in natural populations. The data represented in this chapter demonstrates that this is indeed the case and raises important questions about the role of iNOS gene expression in resistance to *T. gondii* in natural populations of wood mice. It also raises important questions as to whether iNOS gene expression might be a key regulator of resistance in a wider range of hosts of *T. gondii* or perhaps even a wider range of host-pathogen interactions involving intracellular pathogens.

Chapter 6: General discussion

Discussion

The aims of this thesis were to investigate genetic and epigenetic mechanisms of iNOS gene expression in relation to infection of natural populations of *A. sylvaticus* with the parasite *Toxoplasma gondii*. This ubiquitous parasite can probably be considered one of the most successful protozoon parasites based on its ability to infect most warm-blooded animals. Despite the cat being the only definitive host where the parasite can complete a full lifecycle, high prevalence of the parasite is found in a wide range of animal species. For example, in our laboratory, using PCR based technologies, we have found prevalence's of 10% in bats (Dodd *et al.*, 2014), up to 70% in new born lambs (Duncanson *et al.*, 2001; MARSHALL *et al.*, 2004) and 100% in human cancer patients (Bajnok *et al.*, 2019b). Broader studies have demonstrated the parasite in dolphins (Costa-Silva *et al.*, 2019), in high prevalence in a wide range of animal species (Blackston *et al.*, 2001; Tenter *et al.*, 2001) (Tenter et al. 2000; Dubey 2010) and prevalence's ranging from 10 – 80% in humans (Pappas., 2009). The success of this parasite raises interesting epidemiological questions as to how the parasite spreads and becomes so ubiquitous (Wen *et al.*, 2016). However, if it can spread so readily through intermediate hosts from bats to marine mammals and generate such high prevalence, this raises interesting questions as to why the parasite does not go on to achieve 100% prevalence in all species. Most animal populations show a range of degrees of susceptibility to pathogen infections. Host resistance probably plays a significant part in protecting subsets of populations of individuals from infection. In laboratory studies, the enzymes iNOS and L-Arginase have been shown to play key roles in defining laboratory mice as susceptible to *Toxoplasma gondii* infection (low iNOS expression/high Arginase expression) and in defining rats as resistant (high iNOS expression/low Arginase expression). In chapter 1, the hypothesis was proposed that iNOS and Arginase expression might be responsible for regulating infection by *T. gondii* in wild animals. Three broad objectives were set, and the outcomes showed that *T. gondii* could be detected in *A. sylvaticus* from the

sample site at Malham, in the Yorkshire Dales, and that there was a significant difference in the balance of iNOS to Arginase (the iNOS/Arginase ratio) between infected and uninfected animals. Infected animals had a lower iNOS/Arginase ratio, suggesting that iNOS higher might be preventing infection. Furthermore, a study of the promoter region and 1st Exon of the iNOS and the intronic -476 gene showed an epigenetic mutation at a CpG islands that was significantly associated with prevention of infection. Using a nested PCR with the *T. gondii* specific biomarker, SAG2, a 28% (CI: 95% 17.8-42.5%) prevalence was found in collections of *Apodemus* made for use within this thesis. , This was compatible with previous studies conducted in the same area where prevalence's of infection of 41% (Thomasson et al. 2011) and 35% (Bajnok et al. 2015) were reported. Samples of brain tissue collected for this study were used for the extraction of DNA and RNA which could be used for expression studies while a large collection of brain tissue DNA samples were available from a previous study (Bajnok et al. 2015) which could be used for epigenetic studies…..

In laboratory, laboratory strains of mice are found to be highly sensitive to infection with *T. gondii* and may survive less than a week. Measurement of RNA expression levels by qPCR, protein expression by western blotting and production of substrates has shown that this sensitivity is associated with a low iNOS/Arginase expression ratio (Li *et al.*, 2012). however, laboratory rats are much more resistant and can survive much longer. Measurement of iNOS and Arginase expression levels have shown that these rats have a much higher iNOS/Arginase expression ratio than mice (Zhao, *et al.*, 2012). Furthermore, different rat strains have a greater or lesser degree of resistance and these degrees of resistance are related to the iNOS/Arginase ratio, with a high ratio being associated with resistance due to the toxicity of nitric oxide to *T. gondii* (Gao et al. 2015). As these data are derived from a small number of genetically inbred lines, each of these lines essentially represents a single individual rat. so put into the context of wild rats, these inbred lines would be equivalent of selecting individual rats from the wild. This suggests that in the wild there is probably a large variation in the ability of individual animals to be resistant to *T. gondii* infection (and possibly therefore a variation in the ability to resist infection in general). This raises important questions therefore about the nature of resistance to *T. gondii* in wild animals. Such resistance would be hard to measure in wild animals since populations of individual animals cannot be tracked through the infection process and survivability

easily tracked. Furthermore, it raises questions as to possible mechanisms of resistance in wild animals. For example, are the same mechanisms involving the balance of iNOS/Arginase responsible for resistance/sensitivity to *T. gondii* infections in wild animals as in laboratory animals.

Wild populations of *A. sylvaticus* offer the possibility of investigating these questions for wild animals. Since prevalence's of up to 40% *T. gondii* infection are found in the wild *Apodemus* from Malham Tarn in the Yorkshire Dales, these mice cannot be as susceptible to infection as laboratory mice because they would die quickly, fail to reach reproductive age, fail to reproduce and would therefore be selected against. The very demonstration of infected wood mice suggests that they must indeed be much more resistant than laboratory mouse strains. These mice therefore offer a good model system for investigating mechanisms of resistance.

In the case of the *Apodemus* studied in this thesis, their infection status was measured by PCR. Infected mice are clearly mice that must have a degree of sensitivity in that the innate immune system has not prevented infection from occurring. In the case of uninfected mice, these mice could be the product of two possible outcomes. Firstly, they might not have been exposed to the parasite and are therefore uninfected. Secondly, they could have been exposed to the parasite, but their innate immune system has rendered them resistant and therefore the parasitic infection has not taken hold. Unfortunately, in uninfected mice it is not possible to make this distinction for individual mice. Collectively, however, it may be possible to draw some conclusions about mechanisms of resistance and specifically investigate the role of iNOS and Arginase in resistance/sensitivity in these wild animals. In this study, it was hypothesised that infected mice would be sensitive to infection (i.e. their innate immune system had allowed an infection to take hold) and therefore, they would have a low iNOS/Arginase balance. On the other hand, the proportion of uninfected mice that had been exposed to the parasite, but resisted infection would be deemed to have a high iNOS/Arginase balance. Unfortunately, the non-exposed group of mice in this cohort would contribute noise to the analysis. Despite this, when iNOS and Arginase expression levels were measured in infected and uninfected *Apodemus* (Chapter 4) the uninfected mice did have a significantly higher iNOS/Arginase balance when measured by qPCR. These differences in the mRNA production of the iNOS gene and the Arginase mRNA show that there are differences in expression between the two

groups. Unfortunately, differences in expression at the RNA level do not always indicate differences in the protein expression level. Quantitative Western blotting would need to be carried out to measure protein levels for each enzyme in uninfected and infected mice. This was not able to be carried out in the time frame of this PhD and would be considered important future work. Another PhD student, A.Alshammmari, was however able to do western blotting on a different set of *Apodemus* brain tissues, collected from Malham, and he was able to show that there was a significant increase in the iNOS/Arginase ratio in uninfected mice (Alshammmari, Personal Communication). These data support the qPCR data from this study and show that iNOS expression is higher and Arginase expression is lower in uninfected than infected mice. These data, taken together, support the laboratory studies and show that arginase and iNOS are indeed involved the process of resistance/sensitivity to *T. gondii* infection in wild *A. sylvaticus*.

There are, of course, limitations to the interpretation of these data. For example, it is not clear whether iNOS and Arginase are the causative agents of resistance/sensitivity. These data only show an association between enzyme expression levels and infection. In the laboratory, it is possible to generate transgenic mice that lack either iNOS or Arginase and investigate the causal relationship between infection and iNOS/Arginase expression. In wild animals, such experiments cannot be done. Furthermore, the unknown status of the uninfected mice (i.e. whether they are resistant or simply have not been exposed to the parasite) makes it difficult to be sure about the actual status of resistance of these animals. If it were possible to identify which animals had not been exposed, then this would give a much clearer picture. These data also do not tell us whether the iNOS and Arginase expression systems are the controlling factor or whether they are simply components in the pathway of resistance with some other process determining resistance. To ascertain this, it would be necessary to look for genetic mutations associated with resistance and see if they mapped to either or both of these genes.

Another set of laboratory studies suggested that there might be epigenetic control of the iNOS/Arginase system operating. (Zhao *et al.*, 2013) showed, in rats, that peritoneal macrophages were highly resistant to *T. gondii* infection while alveolar macrophages from the same inbred lines were sensitive. They also demonstrated a correlation between the iNOS/Arginase balance and sensitivity (peritoneal

macrophages had high INOS and low Arginase; alveolar macrophages had low iNOS and high Arginase). As these two cell types were from the same genetically identical inbred lines of rats, their primary DNA sequences was identical and therefore changes to expression levels in both cell types must be epigenetic. This led to another hypothesis, tested in Chapter 5, that it might be possible to locate epigenetic marks that differed between the infected and uninfected *Apodemus*. The iNOS gene was selected for this study. Since gene expression is often controlled by the promoter regions of a gene and the iNOS gene is a large gene occupying some 50kb of genome, the promoter and exon 1 was selected. Furthermore, DNA methylation has been shown to be an important epigenetic mechanism that is involved in gene regulation (Bird et al 1985; Bird 1986). Specifically, gene regions known as CpG islands can be methylated or demethylated to enable long term control of gene regulation. It was hypothesised that there would be a different pattern of methylation in the promoter region of the iNOS gene when comparing *T. gondii* infected and uninfected *Apodemus*.

Analysis of single nucleotide polymorphisms and epigenetic polymorphisms (methylated and not methylated cytosines), were carried out on 144 animals within the iNOS gene promoter and exon 1. Interesting differences between infected uninfected animals were observed that could potentially be linked to expression differences in iNOS gene expression. Several CpG islands and SNPs were examined in the promoter and Exon 1 for differences in methylation or sequence when comparing infected and uninfected mice. Only two of these CpG islands in Exon 1 CpG47 (47 bp downstream of the transcription start site) and the second located CpG^{-}476 bp from the begging the Exon1. were found to have different methylation patterns which were significantly different in the infected and uninfected population of wood mice. In the infected mouse population, 86.66% of mice were methylated at this site with 13.33% being heterozygous for methylation and SNPs. Only 2% of these mice did not have methylated residues at this location. On the other hand, only 61.17% of the uninfected mice had methylation at this location. This CpG island seems therefore to be associated with infection status. As methylation is usually associated with genes being switched off, this suggests that the iNOS gene is switched off in the homozygous methylated CpG 47 (86.66% of infected mice) and half of the gene copies switched off in the heterozygous individuals (11%). Thus, in the infected mice, 98% of the mice had the gene switched off or partially switched off. In gene expression terms this would

mean that the iNOS/Arginase balance would be low in these mice and therefore they could be considered to be non-resistant to infection and hence their positive infection status. The situation in the uninfected mice is less clear cut. In this group, 70% of mice had methylated CpG47 or were heterozygous. The remaining 29% were non-methylated (with 1% with a SNP that could not be methylated). In this case these animals would be expected to have high iNOS expression levels and therefore it would fit with their uninfected status. Of the 70% of that had a methylated/partially methylated CpG47, these animals could simply be animals that have not been exposed to the parasite or possibly have some other mode of resistance. The latter could, for example, be caused by low levels of Arginase expression, thus causing the iNOS/Arginase balance to be high despite low iNOS expression. To establish this, it would be necessary to investigate the Arginase gene and its expression, Unfortunately, it was not possible to do this in the timeframe of this PhD thesis.

The role of Arginase may indeed be important. A recent study in humans was carried out on the role of iNOS and Arginase in airway inflammation in miners (Breton and Marutani, 2014; Zhang *et al.*, 2019). They demonstrated that the Arginase gene was epigenetically controlled by methylation. In this case, the Arginase gene was shut down by methylation and this resulted in high iNOS activity which was associated with inflammation in the airway. ,

The remaining six CpG islands found in the wood mouse promoter region, (CpG-59,, CpG-119, CpG-175, CpG-392, CpG-394), showed no association with infection and in 3 of the cases the majority showed no methylation patterns. This suggests that it is only two the CpG 47 & CpG-476 islands that are important with respect to infection with *T. gondii*. As these locations are within exon 1, intronic -476 it might suggest that the mechanism of silencing is that the methylation interferes with the functioning of the RNA polymerase that transcribes the iNOS gene. To our knowledge, this is the first report of a gene location that might control resistance/sensitivity to infection with *T. gondii*.

In humans there are seven CpG island within the human NOS2 (iNOS) exons that can be methylated and result in silencing of the iNOS gene expression (Barter, Bui and Young, 2012; De Andrés *et al.*, 2013). In studies on CpG island methylation in humans in relation to cancer cells, suggest that methylation commonly occurs within

gene exons to switch off genes and that it less commonly occurs in the promoter region (Greenberg and Bourc'his, 2019).

DNA methylation of the iNOS gene is of general interest in human medicine as it has been associated with a number of aspects. Firstly, it has been shown that the iNOS gene is differentially methylated in the M1 and M2 types of macrophages (Bakshi et al., 2019) and therefore controls the levels of nitric oxide produced from each type. Alzheimer's disease has been associated with high levels of iNOS gene expression and that drugs affecting the methylation of the iNOS gene could be a potential source of treatments (Abdolmaleky *et al.*, 2004).

Hypomethylation effects iNOS synthesis levels, and can be associated with Leishmania infection, lack of sufficiency of wound healing in injured vascular tissues and in pollution related diseases like asthma (Xu *et al.*, 1996; Chartraid *et al.*, 2000; Torrone *et al.*, 2012; Bandara *et al.*, 2019). However, hypermethylation of CpGs in the promoter region of the iNOS gene can cause a number of conditions such as fragile chromosome X and diabetes type 2 (Hmadcha *et al.*, 1999; Hoeijmakers, 2009; Methylation *et al.*, 2009; Blundell and Blundell, 2010; Feinberg, 2018; Schuster *et al.*, 2019)

In this study, the identification of a specific methylation locus associated with expression of the iNOS gene and potential resistance to *T. gondi*i infection could open up new avenues to investigate the role of iNOS in other infectious diseases and other disease systems. Future studies should be aimed at determining the complete patterns of DNA methylations across different parts of the iNOS gene and its promoter. Confirmation of the role of specific CpG islands in the control of iNOS gene expression could be determined by using Crispr-Cas9 editing systems to specifically mutate CpG islands such that methylation cannot occur. In the case of CpG-47, and intronic CpG-476, the equivalent location could be identified in laboratory strains of Mus musculus and editing experiments conducted to see if resistance can be generated in these highly sensitive hosts of *T. gondii* infection.

References:

Abdolmaleky, H. M., Smith, C. L., Faraone, S. V., Shafa, R., Stone, W., Glatt, S. J., & Tsuang, M. T. (2004). Methylomics in psychiatry: modulation of gene–environment interactions may be through DNA methylation. *American Journal of Medical Genetics Part B: Neuropsychiatric Genetics*, *127*(1), 51-59.

Ahmadi, M., Gharibi, T., Dolati, S., Rostamzadeh, D., Aslani, S., Baradaran, B., ... & Yousefi, M. (2017). Epigenetic modifications and epigenetic based medication implementations of autoimmune diseases. *Biomedicine & Pharmacotherapy*, *87*, 596-608.

Ahmed N, French T, Rausch S, Kühl A, Hemminger K, Dunay IR, Steinfelder S, Hartmann S. (2017). *Toxoplasma* Co-infection Prevents Th2 Differentiation and Leads to a Helminth-Specific Th1 Response. *Front Cell Infect Microbiol*. *7*, 341-353..

Ahmadipour, B., Sharifi, M., & Khajali, F. (2018). Pulmonary hypertensive response of broiler chickens to arginine and guanidinoacetic acid under high-altitude hypoxia. *Acta Veterinaria Hungarica*, *66*(1), 116-124.

Akira, S., Uematsu, S., & Takeuchi, O. (2006). Pathogen recognition and innate immunity. *Cell*, *124*(4), 783-801.

Al Khaled, Y., Tierling, S., Laqqan, M., Lo Porto, C., & Hammadeh, M. E. (2018). Cigarette smoking induces only marginal changes in sperm DNA methylation levels of patients undergoing intracytoplasmic sperm injection treatment. *Andrologia*, *50*(1), e12818.

Alivand, M. R., Sabouni, F., & Soheili, Z. S. (2016). Probable chemical hypoxia effects on progress of CNV through induction of promoter CpG demethylation and overexpression of IL17RC in human RPE cells. *Current eye research*, *41*(9), 1245-1254.

Alkhaled, Y., Laqqan, M., & Tierling, S. Lo Porto C, Amor H, Hammadeh ME. 2018. Impact of cigarette-smoking on sperm DNA methylation and its effect on sperm parameters. *Andrologia*, *50*(4), e12950.

Alvarado-Cruz, I., Sánchez-Guerra, M., Hernández-Cadena, L., De Vizcaya-Ruiz, A., Mugica, V., Pelallo-Martínez, N. A., ... & Quintanilla-Vega, B. (2017). Increased methylation of repetitive elements and DNA repair genes is associated with higher DNA oxidation in children in an urbanized, industrial environment. *Mutation Research/Genetic Toxicology and Environmental Mutagenesis*, *813*, 27-36.

Anakwue, R. C., & Anakwue, A. C. (2014). Cardiovascular disease risk profiling in Africa: Environmental pollutants are not on the agenda. *Cardiovascular toxicology*, *14*(3), 193-207.

Antequera, F., & Bird, A. P. (1988). Unmethylated CpG islands associated with genes in higher plant DNA. *The EMBO journal*, *7*(8), 2295-2299.

Araujo, F. G., & Remington, J. S. (1974). Protection against *Toxoplasma gondi*i in mice immunized with *Toxoplasma* cell fractions, RNA and synthetic polyribonucleotides. *Immunology*, *27*(4), 711.

Asumda, F. Z., Hatzistergos, K. E., Dykxhoorn, D. M., Jakubski, S., Edwards, J., Thomas, E., & Schiff, E. R. (2018). Differentiation of hepatocyte-like cells from human pluripotent stem cells using small molecules. *Differentiation*, *101*, 16-24.

Azam, F., & Malfatti, F. (2007). Microbial structuring of marine ecosystems. *Nature Reviews Microbiology*, *5*(10), 782-791.

Baccarelli, A., Zanobetti, A., Martinelli, I., Grillo, P., Hou, L., Lanzani, G., ... & Schwartz, J. (2007). Air pollution, smoking, and plasma homocysteine. *Environmental health perspectives*, *115*(2), 176-181.

Bahl, A., Brunk, B., Crabtree, J., Fraunholz, M. J., Gajria, B., Grant, G. R., ... & Li, L. (2003). PlasmoDB: the Plasmodium genome resource. A database integrating experimental and computational data. *Nucleic acids research*, *31*(1), 212-215.

Bajnok, J. (2017). *Development of approaches for investigating the distribution of Toxoplasma gondii infection in natural populations of animals and humans* (Doctoral dissertation, University of Salford).

Bajnok, J., Boyce, K., Rogan, M. T., Craig, P. S., Lun, Z. R., & Hide, G. (2015). Prevalence of *Toxoplasma gondi*i in localized populations of *Apodemus sylvaticus* is linked to population genotype not to population location. *Parasitology*, *142*(5), 680-690.

Bajnok, J., Tarabulsi, M., Carlin, H., Bown, K., Southworth, T., Dungwa, J., ... & Hide, G. (2019). High frequency of infection of lung cancer patients with the parasite *Toxoplasma gondi*i. *ERJ open research*, *5*(2).

Bakshi, C., Vijayvergiya, R., & Dhawan, V. (2019). Aberrant DNA methylation of M1-macrophage genes in coronary artery disease. *Scientific reports*, *9*(1), 1-22.

Bakulski, K. M., & Fallin, M. D. (2014). Epigenetic epidemiology: promises for public health research. *Environmental and molecular mutagenesis*, *55*(3), 171-183.

Bandara, N., Gurusinghe, S., Kong, A., Mitchell, G., Wang, L. X., Lim, S. Y., & Strappe, P. (2019). Generation of a nitric oxide signaling pathway in mesenchymal stem cells promotes endothelial lineage commitment. *Journal of cellular physiology*, *234*(11), 20392-20407.

Barrow, T. M., & Michels, K. B. (2014). Epigenetic epidemiology of cancer. *Biochemical and biophysical research communications*, *455*(1-2), 70-83.

Barter, M. J., Bui, C., & Young, D. A. (2012). Epigenetic mechanisms in cartilage and osteoarthritis: DNA methylation, histone modifications and microRNAs. *Osteoarthritis and cartilage*, *20*(5), 339-349.

Bégin, P., & Nadeau, K. C. (2014). Epigenetic regulation of asthma and allergic disease. *Allergy, Asthma & Clinical Immunology*, *10*(1), 27.

Béji-Hamza, A., Hassine-Zaafrane, M., Khélifi-Gharbi, H., Della Libera, S., Iaconelli, M., Muscillo, M., ... & Aouni, M. (2015). Hepatitis E virus genotypes 1 and 3 in wastewater samples in Tunisia. *Archives of virology*, *160*(1), 183-189.

Bergamaschi, E., Canu, I. G., Prina-Mello, A., & Magrini, A. (2017). Biomonitoring. In *Adverse effects of engineered nanomaterials* (pp. 125-158). Academic Press.

Berrens, R. V., Andrews, S., Spensberger, D., Santos, F., Dean, W., Gould, P., ... & von Meyenn, F. (2017). An endosiRNA-based repression mechanism counteracts transposon activation during global DNA demethylation in embryonic stem cells. *Cell Stem Cell*, *21*(5), 694-703.

Bind, M. A. C., Coull, B. A., Peters, A., Baccarelli, A. A., Tarantini, L., Cantone, L., ... & Schwartz, J. D. (2015). Beyond the mean: quantile regression to explore the association of air pollution with gene-specific methylation in the normative aging study. *Environmental health perspectives*, *123*(8), 759-765.

Bind, M. A., Lepeule, J., Zanobetti, A., Gasparrini, A., Baccarelli, A. A., Coull, B. A., ... & Schwartz, J. (2014). Air pollution and gene-specific methylation in the Normative Aging Study: association, effect modification, and mediation analysis. *Epigenetics*, *9*(3), 448-458.

Bird, A. (2002). DNA methylation patterns and epigenetic memory. *Genes & development*, *16*(1), 6-21.

Black, M. W., & Boothroyd, J. C. (2000). Lytic cycle of *Toxoplasma gondi*i. *Microbiol. Mol. Biol. Rev.*, *64*(3), 607-623.

Black, M. W., & Boothroyd, J. C. (2000). Lytic cycle of *Toxoplasma gondi*i. *Microbiol. Mol. Biol. Rev.*, *64*(3), 607-623.

Blackston, C. R., Dubey, J. P., Dotson, E., Su, C., Thulliez, P., Sibley, D., & Lehmann, T. (2001). High-resolution typing of *Toxoplasma gondi*i using microsatellite loci. *The Journal of parasitology*, 1472-1475.

Blundell, R. J. (2010). Investigation into genome-scale ordered RNA structure (GORS) in murine norovirus and other positive-stranded RNA viruses.

Bolhassani, A., & Zahedifard, F. (2012). Therapeutic live vaccines as a potential anticancer strategy. *International journal of cancer*, *131*(8), 1733-1743.

Bollati, V., Angelici, L., Rizzo, G., Pergoli, L., Rota, F., Hoxha, M., ... & Pesatori, A. C. (2015). Microvesicle-associated microRNA expression is altered upon particulate matter exposure in healthy workers and in A549 cells. *Journal of Applied Toxicology*, *35*(1), 59-67.

Bollati, V., Motta, V., Iodice, S., & Carugno, M. (2016). Epigenomic Studies in Epidemiology. In *Epigenomics in Health and Disease* (pp. 163-182). Academic Press.

Boyce, K., Hide, G., Craig, P. S., Harris, P. D., Reynolds, C., Pickles, A., & Rogan, M. T. (2012). Identification of a new species of digenean Notocotylus malhamensis n. sp.(Digenea: Notocotylidae) from the bank vole (Myodes glareolus) and the field vole (Microtus agrestis). *Parasitology*, *139*(12), 1630-1639.

Boyce, K., Hide, G., Craig, P. S., Reynolds, C., Hussain, M., Bodell, A. J., ... & Rogan, M. T. (2014). A molecular and ecological analysis of the trematode Plagiorchis elegans in the wood mouse *Apodemus sylvaticus* from a periaquatic ecosystem in the UK. *Journal of helminthology*, *88*(3), 310-320.

Breton, C. V., & Marutani, A. N. (2014). Air pollution and epigenetics: recent findings. *Current environmental health reports*, *1*(1), 35-45.

Brown, T. A., Lee, J. W., Holian, A., Porter, V., Fredriksen, H., Kim, M., & Cho, Y. H. (2016). Alterations in DNA methylation corresponding with lung inflammation and as a biomarker for disease development after MWCNT exposure. *Nanotoxicology*, *10*(4), 453-461.

Brunst, K. J., & Wright, R. J. (2016). Social disparities in lung growth and respiratory health. In *Health disparities in respiratory medicine* (pp. 147-171). Humana Press, Cham.

Bryant, C. E., & Monie, T. P. (2012). Mice, men and the relatives: cross-species studies underpin innate immunity. *Open biology*, *2*(4), 120015.

Cai, Y., Chen, H., Jin, L., You, Y., & Shen, J. (2013). STAT3-dependent transactivation of miRNA genes following *Toxoplasma gondi*i infection in macrophage. *Parasites & vectors*, *6*(1), 356.

Calderaro, A., Peruzzi, S., Piccolo, G., Gorrini, C., Montecchini, S., Rossi, S., ... & Dettori, G. (2009). Laboratory diagnosis of *Toxoplasma gondi*i infection. *International journal of medical sciences*, *6*(3), 135.

Cantone, L., Angelici, L., Bollati, V., Bonzini, M., Apostoli, P., Tripodi, A., ... & Baccarelli, A. A. (2014). Extracellular histones mediate the effects of metal-rich air particles on blood coagulation. *Environmental research*, *132*, 76-82.

Cao, Y. (2015). Environmental pollution and DNA methylation: carcinogenesis, clinical significance, and practical applications. *Frontiers of medicine*, *9*(3), 261-274.

Chance, B., Saronio, C., & Leigh, J. S. (1975). Functional intermediates in reaction of cytochrome oxidase with oxygen. *Proceedings of the National Academy of Sciences*, *72*(4), 1635-1640.

Charles, I. G., Palmer, R. M., Hickery, M. S., Bayliss, M. T., Chubb, A. P., Hall, V. S., ... & Moncada, S. (1993). Cloning, characterization, and expression of a cDNA encoding an inducible nitric oxide synthase from the human chondrocyte. *Proceedings of the National Academy of Sciences*, *90*(23), 11419-11423.

Chartrain, N. A., Geller, D. A., Koty, P. P., Sitrin, N. F., Nussler, A. K., Hoffman, E. P., ... & Mudgett, J. S. (1994). Molecular cloning, structure, and chromosomal localization of the human inducible nitric oxide synthase gene. *Journal of biological chemistry*, *269*(9), 6765-6772.

Chen, G., Wang, C., Wang, J., Yin, S., Gao, H., Xiang, L. U., ... & Yang, L. I. (2016). Antiosteoporotic effect of icariin in ovariectomized rats is mediated via the Wnt/β-catenin pathway. *Experimental and therapeutic medicine*, *12*(1), 279-287.

Chen, R., Meng, X., Zhao, A., Wang, C., Yang, C., Li, H., ... & Kan, H. (2016). DNA hypomethylation and its mediation in the effects of fine particulate air pollution on cardiovascular biomarkers: a randomized crossover trial. *Environment international*, *94*, 614-619.

Chen, R., Qiao, L., Li, H., Zhao, Y., Zhang, Y., Xu, W., ... & Hu, H. (2015). Fine particulate matter constituents, nitric oxide synthase DNA methylation and exhaled nitric oxide. *Environmental science & technology*, *49*(19), 11859-11865.

Chi, G. C., Liu, Y., MacDonald, J. W., Barr, R. G., Donohue, K. M., Hensley, M. D., ... & Kaufman, J. D. (2016). Long-term outdoor air pollution and DNA methylation in

circulating monocytes: results from the Multi-Ethnic Study of Atherosclerosis (MESA). *Environmental Health*, *15*(1), 119.

Cho, D. I., Kim, M. R., Jeong, H. Y., Jeong, H. C., Jeong, M. H., Yoon, S. H., ... & Ahn, Y. (2014). Mesenchymal stem cells reciprocally regulate the M1/M2 balance in mouse bone marrow-derived macrophages. *Experimental & molecular medicine*, *46*(1), e70-e70.

Chogtu, B., Bhattacharjee, D., & Magazine, R. (2016). Epigenetics: The new frontier in the landscape of asthma. *Scientifica*, *2016*.

Chong, C. K., Jeong, W., Kim, H. Y., An, D. J., Jeoung, H. Y., Ryu, J. E., ... & Nam, H. W. (2011). Development and clinical evaluation of a rapid serodiagnostic test for toxoplasmosis of cats using recombinant SAG1 antigen. *The Korean journal of parasitology*, *49*(3), 207.

Ciani, L., & Salinas, P. C. (2005). WNTs in the vertebrate nervous system: from patterning to neuronal connectivity. *Nature Reviews Neuroscience*, *6*(5), 351-362.

Clifford, R. L., Jones, M. J., MacIsaac, J. L., McEwen, L. M., Goodman, S. J., Mostafavi, S., ... & Carlsten, C. (2017). Inhalation of diesel exhaust and allergen alters human bronchial epithelium DNA methylation. *Journal of Allergy and Clinical Immunology*, *139*(1), 112-121.

Cliquet, F., Gurbuxani, J. P., Pradhan, H. K., Pattnaik, B., Patil, S. S., Regnault, A., ... & Singh, R. (2007). The safety and efficacy of the oral rabies vaccine SAG2 in Indian stray dogs. *Vaccine*, *25*(17), 3409-3418.

Collins, M., Fouser, L., Wynn, T. A., Yarovinsky, A. W. C., Sher, A., & Grigg, M. (2010). Redundant and Pathogenic Roles for IL-22 in.

Consales, C., Toft, G., Leter, G., Bonde, J. P. E., Uccelli, R., Pacchierotti, F., ... & Struciński, P. (2016). Exposure to persistent organic pollutants and sperm DNA methylation changes in Arctic and European populations. *Environmental and molecular mutagenesis*, *57*(3), 200-209.

Costa-Silva, S., Sacristán, C., Gonzales-Viera, O., Díaz-Delgado, J., Sánchez-Sarmiento, A. M., Marigo, J., ... & Marcondes, M. C. C. (2019). *Toxoplasma gondi*i em cetáceos do Brasil: estudo histopatológico e imuno-histoquímico. *Revista Brasileira de Parasitologia Veterinária*, *28*(3), 395-402.

Coutinho, L. B., Gomes, A. O., Araújo, E. C., Barenco, P. V. C., Santos, J. L., Caixeta, D. R., ... & Silva, N. M. (2012). The impaired pregnancy outcome in murine congenital toxoplasmosis is associated with a pro-inflammatory immune response, but not correlated with decidual inducible nitric oxide synthase expression. *International journal for parasitology*, *42*(4), 341-352.

Crary-Dooley, F. K., Tam, M. E., Dunaway, K. W., Hertz-Picciotto, I., Schmidt, R. J., & LaSalle, J. M. (2017). A comparison of existing global DNA methylation assays to low-coverage whole-genome bisulfite sequencing for epidemiological studies. *Epigenetics*, *12*(3), 206-214.

Czaja, A. J. (2017). next-generation transformative advances in the pathogenesis and management of autoimmune hepatitis. *Alimentary pharmacology & therapeutics*, *46*(10), 920-937.

Czaja, A. J. (2018). Epigenetic changes and their implications in autoimmune hepatitis. *European journal of clinical investigation*, *48*(4), e12899.

Dai, L., Bind, M. A., Koutrakis, P., Coull, B. A., Sparrow, D., Vokonas, P. S., & Schwartz, J. D. (2016). Fine particles, genetic pathways, and markers of inflammation and endothelial dysfunction: analysis on particulate species and sources. *Journal of exposure science & environmental epidemiology*, *26*(4), 415-421.

Das, D. N., Panda, P. K., Naik, P. P., Mukhopadhyay, S., Sinha, N., & Bhutia, S. K. (2017). Phytotherapeutic approach: a new hope for polycyclic aromatic hydrocarbons induced cellular disorders, autophagic and apoptotic cell death. *Toxicology mechanisms and methods*, *27*(1), 1-17.

de Andrés, M. C., Imagawa, K., Hashimoto, K., Gonzalez, A., Roach, H. I., Goldring, M. B., & Oreffo, R. O. (2013). Loss of methylation in cpg sites in the NF-κB enhancer elements of inducible nitric oxide synthase is responsible for gene induction in human articular chondrocytes. *Arthritis & Rheumatism*, *65*(3), 732-742.

de Planell-Saguer, M., Lovinsky-Desir, S., & Miller, R. L. (2014). Epigenetic regulation: The interface between prenatal and early-life exposure and asthma susceptibility. *Environmental and molecular mutagenesis*, *55*(3), 231-243.

De Vleeschouwer, K., Van der Plancken, I., Van Loey, A., & Hendrickx, M. E. (2008). The kinetics of acrylamide formation/elimination in asparagine–glucose systems at different initial reactant concentrations and ratios. *Food chemistry*, *111*(3), 719-729.

Denkers, E. Y., Gazzinelli, R. T., Martin, D., & Sher, A. (1993). Emergence of NK1. 1+ cells as effectors of IFN-gamma dependent immunity to *Toxoplasma gondi*i in MHC class I-deficient mice. *The Journal of experimental medicine*, *178*(5), 1465-1472.

Dlugonska, H. (2008). *Toxoplasma* rhoptries: unique secretory organelles and source of promising vaccine proteins for immunoprevention of toxoplasmosis. *BioMed Research International*, *2008*.

Dodd, N. S., Lord, J. S., Jehle, R., Parker, S., Parker, F., Brooks, D. R., & Hide, G. (2014). *Toxoplasma gondi*i: prevalence in species and genotypes of British bats (Pipistrellus pipistrellus and P. pygmaeus). *Experimental parasitology*, *139*, 6-11.

Dubey, J. P. (2014). The history and life cycle of *Toxoplasma gondi*i. In *Toxoplasma gondii* (pp. 1-17). Academic Press.

Dubey, J. P., Lindsay, D. S., & Lappin, M. R. (2009). Toxoplasmosis and other intestinal coccidial infections in cats and dogs. *Veterinary Clinics: Small Animal Practice*, *39*(6), 1009-1034.

Dubey, J. P., Miller, N. L., & Frenkel, J. K. (1970). Characterization of the new fecal form of *Toxoplasma gondi*i. *The Journal of parasitology*, 447-456.

Dubey, J. P., Weigel, R. M., Siegel, A. M., Thulliez, P., Kitron, U. D., Mitchell, M. A., ... & Todd, K. S. (1995). Sources and reservoirs of *Toxoplasma gondi*i infection on 47 swine farms in Illinois. *The Journal of parasitology*, 723-729.

Duncanson, P., Terry, R. S., Smith, J. E., & Hide, G. (2001). High levels of congenital transmission of *Toxoplasma gondi*i in a commercial sheep flock. *International journal for parasitology*, *31*(14), 1699-1703.

Dupont, C. D., Christian, D. A., & Hunter, C. A. (2012, November). Immune response and immunopathology during toxoplasmosis. In *Seminars in immunopathology* (Vol. 34, No. 6, pp. 793-813). Springer-Verlag.

Elsheikha, H. M. (2008). Congenital toxoplasmosis: priorities for further health promotion action. *Public health*, *122*(4), 335-353.

Ettinger, A., & Wittmann, T. (2014). Fluorescence live cell imaging. In *Methods in cell biology* (Vol. 123, pp. 77-94). Academic Press.

Fan, T., Fang, S. C., Cavallari, J. M., Barnett, I. J., Wang, Z., Su, L., ... & Christiani, D. C. (2014). Heart rate variability and DNA methylation levels are altered after short-term metal fume exposure among occupational welders: a repeated-measures panel study. *BMC Public Health*, *14*(1), 1279.

Feinberg, A. P. (2018). The key role of epigenetics in human disease prevention and mitigation. *New England Journal of Medicine*, *378*(14), 1323-1334.

Ferguson, D. J. P. (2004). Use of molecular and ultrastructural markers to evaluate stage conversion of *Toxoplasma gondi*i in both the intermediate and definitive host. *International journal for parasitology*, *34*(3), 347-360.

Ferreira, I. M. R., Vidal, J. E., de Mattos, C. D. C. B., de Mattos, L. C., Qu, D., Su, C., & Pereira-Chioccola, V. L. (2011). *Toxoplasma gondi*i isolates: Multilocus RFLP–PCR genotyping from human patients in Sao Paulo State, Brazil identified distinct genotypes. *Experimental parasitology*, *129*(2), 190-195.

Figueroa-Lopez, A. M., Leyva-Madrigal, K. Y., Cervantes-Gamez, R. G., BELTRÁN-ARREDONDO, L. A. U. R. A., & MALDONADO-MENDOZA, I. E. (2017). Induction of Bacillus cereus chitinases as a response to lysates of Fusarium verticillioides. *Romanian Biotechnological Letters*, *22*(4), 12722.

Finch, T. V. (1956). Spontaneous rupture of a uterus varix at 28 weeks' pregnancy. *American journal of obstetrics and gynecology*, *72*(6), 1189.

Follmann, E. H., Ritter, D. G., & Baer, G. M. (1996). Evaluation of the safety of two attenuated oral rabies vaccines, SAG1 and SAG2, in six Arctic mammals. *Vaccine*, *14*(4), 270-273.

Frank, T. S., Svoboda-Newman, S. M., & Hsi, E. D. (1996). Comparison of methods for extracting DNA from formalin-fixed paraffin sections for nonisotopic PCR. *Diagnostic molecular pathology: the American journal of surgical pathology, part B*, *5*(3), 220-224.

Franti, C. E., Riemann, H. P., Behymer, D. E., Suther, D., Howarth, J. A., & Ruppanner, R. (1976). Prevalence of *Toxoplasma gondi*i antibodies in wild and domestic animals in northern California. *Journal of the American Veterinary Medical Association*, *169*(9), 901-906.

French T, Düsedau HP, Steffen J, Biswas A, Ahmed N, Hartmann S, Schüler T, Schott BH, Dunay IR. (2019). Neuronal impairment following chronic *Toxoplasma gondii* infection is aggravated by intestinal nematode challenge in an IFN-γ-dependent manner. *J Neuroinflammation*. *16*, 159 – 177.

Furuta, T., Kikuchi, T., Akira, S., Watanabe, N., & Yoshikawa, Y. (2006). Roles of the small intestine for induction of toll-like receptor 4-mediated innate resistance in

naturally acquired murine toxoplasmosis. *International immunology*, *18*(12), 1655-1662.

Gajria, B., Bahl, A., Brestelli, J., Dommer, J., Fischer, S., Gao, X., ... & Pinney, D. F. (2007). ToxoDB: an integrated *Toxoplasma gondi*i database resource. *Nucleic acids research*, *36*(suppl_1), D553-D556.

Ganley, A. R., & Kobayashi, T. (2007). Phylogenetic footprinting to find functional DNA elements. In *Comparative Genomics* (pp. 367-379). Humana Press.

Gao, J. M., Yi, S. Q., Wu, M. S., Geng, G. Q., Shen, J. L., Lu, F. L., ... & Lun, Z. R. (2015). Investigation of infectivity of neonates and adults from different rat strains to *Toxoplasma gondi*i Prugniaud shows both variation which correlates with iNOS and Arginase-1 activity and increased susceptibility of neonates to infection. *Experimental parasitology*, *149*, 47-53.

Gao, T., Zhao, M. M., Zhang, L., Li, J. L., Yu, L. L., Lv, P. A., ... & Zhou, G. H. (2017). Effects of in ovo feeding of l-arginine on the development of lymphoid organs and small intestinal immune barrier function in posthatch broilers. *Animal Feed Science and Technology*, *225*, 8-19.

Gavrieli, Y., Sherman, Y., & Ben-Sasson, S. A. (1992). Identification of programmed cell death in situ via specific labeling of nuclear DNA fragmentation. *The Journal of cell biology*, *119*(3), 493-501.

Gayral, P., Weinert, L., Chiari, Y., Tsagkogeorga, G., Ballenghien, M., & Galtier, N. (2011). Next-generation sequencing of transcriptomes: a guide to RNA isolation in nonmodel animals. *Molecular Ecology Resources*, *11*(4), 650-661.

Ghosh, M., Öner, D., Poels, K., Tabish, A. M., Vlaanderen, J., Pronk, A., ... & Hoet, P. H. (2017). Changes in DNA methylation induced by multi-walled carbon nanotube exposure in the workplace. *Nanotoxicology*, *11*(9-10), 1195-1210.

Goldstein, E. J., Montoya, J. G., & Remington, J. S. (2008). Management of *Toxoplasma gondi*i infection during pregnancy. *Clinical Infectious Diseases*, *47*(4), 554-566.

Goodrich, J. M., Sánchez, B. N., Dolinoy, D. C., Zhang, Z., Hernández-Ávila, M., Hu, H., ... & Téllez-Rojo, M. M. (2015). Quality control and statistical modeling for environmental epigenetics: a study on in utero lead exposure and DNA methylation at birth. *Epigenetics*, *10*(1), 19-30.

Goodson, J. M., Weldy, C. S., MacDonald, J. W., Liu, Y., Bammler, T. K., Chien, W. M., & Chin, M. T. (2017). In utero exposure to diesel exhaust particulates is associated with an altered cardiac transcriptional response to transverse aortic constriction and altered DNA methylation. *The FASEB Journal*, *31*(11), 4935-4945.

Graindorge, A., Frenal, K., Jacot, D., Salamun, J., Marq, J. B., & Soldati-Favre, D. (2016). The conoid associated motor MyoH is indispensable for *Toxoplasma gondi*i entry and exit from host cells. *PLoS pathogens*, *12*(1).

Grbić, V. (2003). SAG2 and SAG12 protein expression in senescing Arabidopsis plants. *Physiologia Plantarum*, *119*(2), 263-269.

Greenberg, M. V., & Bourc'his, D. (2019). The diverse roles of DNA methylation in mammalian development and disease. *Nature reviews Molecular cell biology*, 1-18.

Gross, T. J., Kremens, K., Powers, L. S., Brink, B., Knutson, T., Domann, F. E., ... & Monick, M. M. (2014). Epigenetic silencing of the human NOS2 gene: rethinking the role of nitric oxide in human macrophage inflammatory responses. *The Journal of Immunology*, *192*(5), 2326-2338.

Gruntman, E., Qi, Y., Slotkin, R. K., Roeder, T., Martienssen, R. A., & Sachidanandam, R. (2008). Kismeth: analyzer of plant methylation states through bisulfite sequencing. *BMC bioinformatics*, *9*(1), 371.

Guo, H. M., Gao, J. M., Luo, Y. L., Wen, Y. Z., Zhang, Y. L., Hide, G., ... & Lun, Z. R. (2015). Infection by *Toxoplasma gondi*i, a severe parasite in neonates and AIDS patients, causes impaired anion secretion in airway epithelia. *Proceedings of the National Academy of Sciences*, *112*(14), 4435-4440.

Guo, L., Byun, H. M., Zhong, J., Motta, V., Barupal, J., Zheng, Y., ... & Marco, S. G. (2014). Effects of short-term exposure to inhalable particulate matter on DNA methylation of tandem repeats. *Environmental and molecular mutagenesis*, *55*(4), 322-335.

Guo, Z., Shao, L., Du, Q., Park, K. S., & Geller, D. A. (2007). Identification of a classic cytokine-induced enhancer upstream in the human iNOS promoter. *The FASEB Journal*, *21*(2), 535-542.

Hai-Rong, C., & Ning, J. (2006). Extremely Rapid Extraction of DNA from Bacteria and Yeast. *Biotechnol. Lett*, *28*(1), 55-59.

Han, Y., Ren, J., Lee, E., Xu, X., Yu, W., & Muegge, K. (2017). Lsh/HELLS regulates self-renewal/proliferation of neural stem/progenitor cells. *Scientific reports*, *7*(1), 1-14.

Haq, S. Z., Abushahama, M. S., Gerwash, O., Hughes, J. M., Wright, E. A., Elmahaishi, M. S., ... & Hide, G. (2016). High frequency detection of *Toxoplasma gondi*i DNA in human neonatal tissue from Libya. *Transactions of the Royal Society of Tropical Medicine and Hygiene*, *110*(9), 551-557.

Hargrave, K. E., Woods, S., Millington, O. R., Chalmers, S., Westrop, G. D., & Roberts, C. W. (2019). Multi-omics studies demonstrate *Toxoplasma gondi*i-induced metabolic reprogramming of murine dendritic cells. *Frontiers in cellular and infection microbiology*, *9*, 309.

He, P., Zhang, H. X., Sun, C. Y., Chen, C. Y., & Jiang, H. Q. (2016). Overexpression of SASH1 inhibits the proliferation, invasion, and EMT in hepatocarcinoma cells. *Oncology Research Featuring Preclinical and Clinical Cancer Therapeutics*, *24*(1), 25-32.

Hejlíček, K., Literák, I., & Nezval, J. (1997). Toxoplasmosis in wild mammals from the Czech Republic. *Journal of Wildlife Diseases*, *33*(3), 480-485.

Hew, K. M., Walker, A. I., Kohli, A., Garcia, M., Syed, A., McDonald-Hyman, C., ... & Hammond, S. K. (2015). Childhood exposure to ambient polycyclic aromatic hydrocarbons is linked to epigenetic modifications and impaired systemic immunity in T cells. *Clinical & Experimental Allergy*, *45*(1), 238-248.

Hickey, M. J., Granger, D. N., & Kubes, P. (2001). Inducible nitric oxide synthase (iNOS) and regulation of leucocyte/endothelial cell interactions: studies in iNOS-deficient mice. *Acta physiologica scandinavica*, *173*(1), 119-126.

Hide, G., & Tait, A. (2009). Molecular epidemiology of African sleeping sickness. *Parasitology*, *136*(12), 1491-1500.

Hmadcha, A., Bedoya, F. J., Sobrino, F., & Pintado, E. (1999). Methylation-dependent gene silencing induced by interleukin 1β via nitric oxide production. *The Journal of experimental medicine*, *190*(11), 1595-1604.

Hodjat, M., Rahmani, S., Khan, F., Niaz, K., Navaei–Nigjeh, M., Nejad, S. M., & Abdollahi, M. (2017). Environmental toxicants, incidence of degenerative diseases, and therapies from the epigenetic point of view. *Archives of toxicology*, *91*(7), 2577-2597.

Hoeijmakers, J. H. (2009). DNA damage, aging, and cancer. *New England Journal of Medicine*, *361*(15), 1475-1485.

Holland, N., Bolognesi, C., Kirsch-Volders, M., Bonassi, S., Zeiger, E., Knasmueller, S., & Fenech, M. (2008). The micronucleus assay in human buccal cells as a tool for biomonitoring DNA damage: the HUMN project perspective on current status and knowledge gaps. *Mutation Research/Reviews in Mutation Research*, *659*(1-2), 93-108.

Hou, L., Zhang, X., Zheng, Y., Wang, S., Dou, C., Guo, L., ... & Kang, C. M. (2014). Altered methylation in tandem repeat element and elemental component levels in inhalable air particles. *Environmental and molecular mutagenesis*, *55*(3), 256-265.

Howe, D. K., Honoré, S., Derouin, F., & Sibley, L. D. (1997). Determination of genotypes of *Toxoplasma gondi*i strains isolated from patients with toxoplasmosis. *Journal of clinical microbiology*, *35*(6), 1411-1414.

Hu, M. J., Wu, S. W., Wei, M. L., Xi, J., Wang, L., Han, Y. Z., ... & Xu, L. (2016). Cloning identification and functional analysis of human IL-17A promoter. *Asian Pacific journal of tropical medicine*, *9*(8), 777-780.

Huang, Q., Zhang, J., Peng, S., Tian, M., Chen, J., & Shen, H. (2014). Effects of water soluble PM2. 5 extracts exposure on human lung epithelial cells (A549): a proteomic study. *Journal of Applied Toxicology*, *34*(6), 675-687.

Huang, X., Xuan, X., Hirata, H., Yokoyama, N., Xu, L., Suzuki, N., & Igarashi, I. (2004). Rapid immunochromatographic test using recombinant SAG2 for detection of antibodies against *Toxoplasma gondi*i in cats. *Journal of clinical microbiology*, *42*(1), 351-353.

Huen, K., Calafat, A. M., Bradman, A., Yousefi, P., Eskenazi, B., & Holland, N. (2016). Maternal phthalate exposure during pregnancy is associated with DNA methylation of LINE-1 and Alu repetitive elements in Mexican-American children. *Environmental research*, *148*, 55-62.

Huen, K., Yousefi, P., Bradman, A., Yan, L., Harley, K. G., Kogut, K., ... & Holland, N. (2014). Effects of age, sex, and persistent organic pollutants on DNA methylation in children. *Environmental and molecular mutagenesis*, *55*(3), 209-222.

Hughes, J. M., Thomasson, D., Craig, P. S., Georgin, S., Pickles, A., & Hide, G. (2008). Neospora caninum: detection in wild rabbits and investigation of co-infection with *Toxoplasma gondi*i by PCR analysis. *Experimental parasitology*, *120*(3), 255-260.

Hughes, J. M., Williams, R. H., Morley, E. K., Cook, D. A. N., Terry, R. S., Murphy, R. G., ... & Hide, G. (2006). The prevalence of Neospora caninum and co-infection with *Toxoplasma gondi*i by PCR analysis in naturally occurring mammal populations. *Parasitology*, *132*(1), 29-36.

Hunter, C. A., & Sibley, L. D. (2012). Modulation of innate immunity by *Toxoplasma gondi*i virulence effectors. *Nature Reviews Microbiology*, *10*(11), 766-778.

Hwang, J., Mitz, A. R., & Murray, E. A. (2019). NIMH MonkeyLogic: Behavioral control and data acquisition in MATLAB. *Journal of neuroscience methods*, *323*, 13-21.

Iaconelli, M., Muscillo, M., Della Libera, S., Fratini, M., Meucci, L., De Ceglia, M., ... & La Rosa, G. (2017). One-year surveillance of human enteric viruses in raw and treated wastewaters, downstream river waters, and drinking waters. *Food and environmental virology*, *9*(1), 79-88.

Ideozu, E. J., Whiteoak, A. M., Tomlinson, A. J., Robertson, A., Delahay, R. J., & Hide, G. (2015). High prevalence of trypanosomes in European badgers detected using ITS-PCR. *Parasites & vectors*, *8*(1), 480.

Igarashi, J., Muroi, S., Kawashima, H., Wang, X., Shinojima, Y., Kitamura, E., ... & Held, W. A. (2008). Quantitative analysis of human tissue-specific differences in methylation. *Biochemical and biophysical research communications*, *376*(4), 658-664.

Innes, E. A. (2010). A brief history and overview of *Toxoplasma gondi*i. *Zoonoses and public health*, *57*(1), 1-7.

Innes, E. A., Bartley, P. M., Buxton, D., & Katzer, F. (2009). Ovine toxoplasmosis. *Parasitology*, *136*(14), 1887-1894.

Iwasaki, A., & Medzhitov, R. (2010). Regulation of adaptive immunity by the innate immune system. *science*, *327*(5963), 291-295.

Jackson1, M. H., Hutchison, W. M., & Siim2, J. C. (1986). Toxoplasmosis in a wild rodent population of central Scotland and a possible explanation of the mode of transmission. *Journal of Zoology*, *209*(4), 549-557.

Jakubek, E. B., Bröjer, C., Regnersen, C., Uggla, A., Schares, G., & Björkman, C. (2001). Seroprevalences of *Toxoplasma gondi*i and Neospora caninum in Swedish red foxes (Vulpes vulpes). *Veterinary parasitology*, *102*(1-2), 167-172.

Ji, H., Myers, J. M. B., Brandt, E. B., Brokamp, C., Ryan, P. H., & Hershey, G. K. K. (2016). Air pollution, epigenetics, and asthma. *Allergy, Asthma & Clinical Immunology*, *12*(1), 51.

Jiménez, K. M., & Forero, D. A. (2018). Effect of master mixes on the measurement of telomere length by qPCR. *Molecular biology reports*, *45*(4), 633-638.

Jitender, P. D. (2008). The history of *Toxoplasma gondi*i—the first 100 years. *J. Eukaryot. Microbiol*, *55*(6), 467-475.

JOHNSON, J. D., HOLLIMAN, R. E., & SAVVA, D. (1990). Detection of *Toxoplasma gondi*i using the polymerase chain reaction.

Joiner, K. A., & Roos, D. S. (2002). Secretory traffic in the eukaryotic parasite *Toxoplasma gondi*i: less is more. *The Journal of cell biology*, *157*(4), 557-563.

Jorge, Y. C., Duarte, M. C., & Silva, A. E. (2010). Gastric cancer is associated with NOS2-954G/C polymorphism and environmental factors in a Brazilian population. *BMC gastroenterology*, *10*(1), 64.

Jung, K. H., Torrone, D., Lovinsky-Desir, S., Perzanowski, M., Bautista, J., Jezioro, J. R., ... & Miller, R. L. (2017). Short-term exposure to PM 2.5 and vanadium and changes in asthma gene DNA methylation and lung function decrements among urban children. *Respiratory research*, *18*(1), 63.

Kallianpur, G. (2004). Indian Statistical Institute. *Encyclopedia of Statistical Sciences*, *5*.

Khan, A., Taylor, S., Ajioka, J. W., Rosenthal, B. M., & Sibley, L. D. (2009). Selection at a single locus leads to widespread expansion of *Toxoplasma gondi*i lineages that are virulent in mice. *PLoS Genetics*, *5*(3).

Khan, A., Taylor, S., Su, C., Sibley, L. D., Paulsen, I., & Ajioka, J. W. (2007). Genetics and genome organization of *Toxoplasma gondi*i. In *Toxoplasma: molecular and cellular biology* (pp. 193-207). Horizon Bioscience.

Khan IA, Hakak R, Eberle K, Sayles P, Weiss LM, Urban JF Jr. (2008). Coinfection with *Heligmosomoides polygyrus* fails to establish CD8+ T-cell immunity against *Toxoplasma gondii*. *Infect Immun*.;*76,*1305 -1313

Khan, I. A., Schwartzman, J. D., Matsuura, T., & Kasper, L. H. (1997). A dichotomous role for nitric oxide during acute *Toxoplasma gondi*i infection in mice. *Proceedings of the National Academy of Sciences*, *94*(25), 13955-13960.

Khanaliha, K., Motazedian, M. H., Kazemi, B., Shahriari, B., Bandehpour, M., & Sharifniya, Z. (2014). Evaluation of recombinant SAG1, SAG2, and SAG3 antigens for serodiagnosis of toxoplasmosis. *The Korean journal of parasitology*, *52*(2), 137.

Kijlstra, A., Meerburg, B., Cornelissen, J., De Craeye, S., Vereijken, P., & Jongert, E. (2008). The role of rodents and shrews in the transmission of *Toxoplasma gondi*i to pigs. *Veterinary parasitology*, *156*(3-4), 183-190.

Kim, A. Y., Lee, E. M., Lee, E. J., Kim, J. H., Suk, K., Lee, E., ... & Jeong, K. S. (2018). SIRT2 is required for efficient reprogramming of mouse embryonic fibroblasts toward pluripotency. *Cell death & disease*, *9*(9), 1-15.

Kim, B. J., Lee, S. Y., Kim, H. B., Lee, E., & Hong, S. J. (2014). Environmental changes, microbiota, and allergic diseases. *Allergy, asthma & immunology research*, *6*(5), 389-400.

Kingsley, S. L., Eliot, M. N., Whitsel, E. A., Huang, Y. T., Kelsey, K. T., Marsit, C. J., & Wellenius, G. A. (2016). Maternal residential proximity to major roadways, birth weight, and placental DNA methylation. *Environment international*, *92*, 43-49.

Kissinger, J. C., Gajria, B., Li, L., Paulsen, I. T., & Roos, D. S. (2003). ToxoDB: accessing the *Toxoplasma gondi*i genome. *Nucleic acids research*, *31*(1), 234-236.

Kluess, J. W., Kahlert, S., Kröber, A., Diesing, A. K., Rothkötter, H. J., Wimmers, K., & Dänicke, S. (2015). Deoxynivalenol, but not E. coli lipopolysaccharide, changes the response pattern of intestinal porcine epithelial cells (IPEC-J2) according to its route of application. *Toxicology letters*, *239*(3), 161-171.

Koblansky, A. A., Jankovic, D., Oh, H., Hieny, S., Sungnak, W., Mathur, R., ... & Ghosh, S. (2013). Recognition of profilin by Toll-like receptor 12 is critical for host resistance to *Toxoplasma gondi*i. *Immunity*, *38*(1), 119-130.

Kucera, K., Koblansky, A. A., Saunders, L. P., Frederick, K. B., Enrique, M., Ghosh, S., & Modis, Y. (2010). Structure-based analysis of *Toxoplasma gondi*i profilin: a parasite-specific motif is required for recognition by Toll-like receptor 11. *Journal of molecular biology*, *403*(4), 616-629.

Kunisawa, J., Takahashi, I., & Kiyono, H. (2007). Intraepithelial lymphocytes: their shared and divergent immunological behaviors in the small and large intestine. *Immunological reviews*, *215*(1), 136-153.

Kuriakose, J. S., & Miller, R. L. (2010). Environmental epigenetics and allergic diseases: recent advances. *Clinical & Experimental Allergy*, *40*(11), 1602-1610.

La Rosa, G., Della Libera, S., Brambilla, M., Bisaglia, C., Pisani, G., Ciccaglione, A. R., ... & Iaconelli, M. (2017). Hepatitis E virus (genotype 3) in slurry samples from swine farming activities in Italy. *Food and environmental virology*, *9*(2), 219-229.

Lafay, F., Bénéjean, J., Tuffereau, C., Flamand, A., & Coulon, P. (1994). Vaccination against rabies: construction and characterization of SAG2, a double avirulent derivative of SADBern. *Vaccine*, *12*(4), 317-320.

Lahvis, G. P. (2016). Rodent models of autism, epigenetics, and the inescapable problem of animal constraint. In *Animal models of behavior genetics* (pp. 265-301). Springer, New York, NY.

Laqqan, M., Tierling, S., Alkhaled, Y., Lo Porto, C., Solomayer, E. F., & Hammadeh, M. (2017). Spermatozoa from males with reduced fecundity exhibit differential DNA methylation patterns. *Andrology*, *5*(5), 971-978.

Lary, D. J., Lary, T., & Sattler, B. (2015). Using machine learning to estimate global PM2. 5 for environmental health studies. *Environmental health insights*, *9*, EHI-S15664.

Lau, Y. L., & Fong, M. Y. (2008). *Toxoplasma gondi*i: serological characterization and immunogenicity of recombinant surface antigen 2 (SAG2) expressed in the yeast Pichia pastoris. *Experimental parasitology*, *119*(3), 373-378.

Leclercq, B., Happillon, M., Antherieu, S., Hardy, E. M., Alleman, L. Y., Grova, N., ... & Garçon, G. (2016). Differential responses of healthy and chronic obstructive pulmonary diseased human bronchial epithelial cells repeatedly exposed to air pollution-derived PM4. *Environmental Pollution*, *218*, 1074-1088.

Leclercq, B., Platel, A., Antherieu, S., Alleman, L. Y., Hardy, E. M., Perdrix, E., ... & Nesslany, F. (2017). Genetic and epigenetic alterations in normal and sensitive

COPD-diseased human bronchial epithelial cells repeatedly exposed to air pollution-derived PM2. 5. *Environmental Pollution*, *230*, 163-177.

Lekutis, C., Ferguson, D. J., & Boothroyd, J. C. (2000). *Toxoplasma gondi*i: identification of a developmentally regulated family of genes related to SAG2. *Experimental parasitology*, *96*(2), 89-96.

Leter, G., Consales, C., Eleuteri, P., Uccelli, R., Specht, I. O., Toft, G., ... & Giwercman, A. (2014). Exposure to perfluoroalkyl substances and sperm DNA global methylation in Arctic and European populations. *Environmental and molecular mutagenesis*, *55*(7), 591-600.

Letten, A. D., Ke, P. J., & Fukami, T. (2017). Linking modern coexistence theory and contemporary niche theory. *Ecological Monographs*, *87*(2), 161-177.

Li, J., Wang, L., & Zhao, F. (2017). Epigenetics-based individual interventions against the health risks of PM 2.5. *Science Bulletin*, *62*(11), 743-744.

Li, R., Yang, L., Lindholm, K., Konishi, Y., Yue, X., Hampel, H., ... & Shen, Y. (2004). Tumor necrosis factor death receptor signaling cascade is required for amyloid-β protein-induced neuron death. *Journal of Neuroscience*, *24*(7), 1760-1771.

Li, W., Ren, G., Huang, Y., Su, J., Han, Y., Li, J., ... & Zhang, L. (2012). Mesenchymal stem cells: a double-edged sword in regulating immune responses. *Cell Death & Differentiation*, *19*(9), 1505-1513.

Li, Z., Zhao, Z. J., Zhu, X. Q., Ren, Q. S., Nie, F. F., Gao, J. M., ... & Wang, Y. (2012). Differences in iNOS and arginase expression and activity in the macrophages of rats are responsible for the resistance against T. *gondi*i infection. *PloS one*, *7*(4).

Lillycrop, K. A., & Burdge, G. C. (2014). Environmental challenge, epigenetic plasticity and the induction of altered phenotypes in mammals. *Epigenomics*, *6*(6), 623-636.

Lillycrop, K. A., & Burdge, G. C. (2015). Maternal diet as a modifier of offspring epigenetics. *Journal of developmental origins of health and disease*, *6*(2), 88-95.

Liu, J., Xie, K., Chen, W., Zhu, M., Shen, W., Yuan, J., ... & Zhang, J. (2017). Genetic variants, PM2. 5 exposure level and global DNA methylation level: A multi-center population-based study in Chinese. *Toxicology letters*, *269*, 77-82.

Louwies, T., Panis, L. I., Provost, E., Jacobs, G., Nawrot, T. S., & De Boever, P. (2018). DNA hypomethylation in association with internal and external markers of traffic exposure in a panel of healthy adults. *Air Quality, Atmosphere & Health*, *11*(6), 673-681.

Lovik, M. (2015). Particulate Matter-Induced Immune Activation. *Edited by Emanuela Corsini and Henk van Loveren*.

Lowenstein, C. J., Alley, E. W., Raval, P., Snowman, A. M., Snyder, S. H., Russell, S. W., & Murphy, W. J. (1993). Macrophage nitric oxide synthase gene: two upstream regions mediate induction by interferon gamma and lipopolysaccharide. *Proceedings of the National Academy of Sciences*, *90*(20), 9730-9734.

Lüder, C. G., Algner, M., Lang, C., Bleicher, N., & Groβ, U. (2003). Reduced expression of the inducible nitric oxide synthase after infection with *Toxoplasma gondi*i facilitates parasite replication in activated murine macrophages. *International journal for parasitology*, *33*(8), 833-844.

Lun, Z. R., Lai, D. H., Wen, Y. Z., Zheng, L. L., Shen, J. L., Yang, T. B., ... & Ayala, F. J. (2015). Cancer in the parasitic protozoans Trypanosoma brucei and *Toxoplasma gondi*i. *Proceedings of the National Academy of Sciences*, *112*(29), 8835-8842.

Madden, T. (2013). The BLAST sequence analysis tool. In *The NCBI Handbook [Internet]. 2nd edition*. National Center for Biotechnology Information (US).

Mähl, P., Cliquet, F., Guiot, A. L., Niin, E., Fournials, E., Saint-Jean, N., ... & Gueguen, S. (2014). Twenty year experience of the oral rabies vaccine SAG2 in wildlife: a global review. *Veterinary research*, *45*(1), 77.

Manstead, A. S., & McCulloch, C. (1981). Sex-role stereotyping in British television advertisements. *British Journal of Social Psychology*, *20*(3), 171-180.

Marsden, P. A., Hall, A. V., Heng, H. Q., Duff, C. L., Shi, X. M., & Tsui, L. C. (1994). Localization of the human gene for inducible nitric oxide synthase (NOS2) to chromosome 17q11. 2-q12. *Genomics;(United States)*, *19*(1).

Marshall, P. A., Hughes, J. M., Williams, R. H., Smith, J. E., Murphy, R. G., & Hide, G. (2004). Detection of high levels of congenital transmission of *Toxoplasma gondi*i in natural urban populations of Mus domesticus. *Parasitology*, *128*(1), 39-42.

Matchima, K., Vongprasert, J., & Chutiman, N. (2018). The Development of a Correction Method for Ensuring a Continuity Value of The Chi-square Test with a Small Expected Cell Frequency. *Naresuan University Journal: Science and Technology (NUJST)*, *26*(1), 98-105.

Matsushita, M., & Fujita, T. (2002). The role of ficolins in innate immunity. *Immunobiology*, *205*(4-5), 490-497.

McCullough, S. D., Dhingra, R., Fortin, M. C., & Diaz-Sanchez, D. (2017). Air pollution and the epigenome: a model relationship for the exploration of toxicoepigenetics. *Current Opinion in Toxicology*, *6*, 18-25.

Mehrabian, M., Xia, Y. R., Wen, P. Z., Warden, C. H., Herschman, H. R., & Lusis, A. J. (1994). Localization of murine macrophage inducible nitric oxide synthase to mouse chromosome 11. *Genomics*, *22*(3), 646-647.

Mehta, B., Daniel, R., & McNevin, D. (2013). High resolution melting (HRM) of forensically informative SNPs. *Forensic Science International: Genetics Supplement Series*, *4*(1), e376-e377.

Mercorio, R., Bonzini, M., Angelici, L., Iodice, S., Delbue, S., Mariani, J., ... & Bollati, V. (2017). Effects of metal-rich particulate matter exposure on exogenous and endogenous viral sequence methylation in healthy steel-workers. *Environmental research*, *159*, 452-457.

Methyltransferase, M. S., hMLH1 Primer, I., & hMLH1 Primer, I. I. Universal Methylated Human DNA Standard & Control Primers.

Miousse, I. R., Chalbot, M. C. G., Aykin-Burns, N., Wang, X., Basnakian, A., Kavouras, I. G., & Koturbash, I. (2014). Epigenetic alterations induced by ambient particulate matter in mouse macrophages. *Environmental and molecular Mutagenesis*, *55*(5), 428-435.

MISHIMA, M., XUAN, X., SHIODA, A., OMATA, Y., FUJISAKI, K., NAGASAWA, H., & MIKAMI, T. (2001). Modified protection against *Toxoplasma gondi*i lethal infection and brain cyst formation by vaccination with SAG2 and SRS1. *Journal of Veterinary Medical Science*, *63*(4), 433-438.

Montrose, L., Goodrich, J. M., & Dolinoy, D. C. (2017). Toxicoepigenetics and Effects on Life Course Disease Susceptibility. *Translational Toxicology and Therapeutics: Windows of Developmental Susceptibility in Reproduction and Cancer*, 439-472.

Montrose, L., Noonan, C. W., Cho, Y. H., Lee, J., Harley, J., O'Hara, T., ... & Ward, T. J. (2015). Evaluating the effect of ambient particulate pollution on DNA methylation in Alaskan sled dogs: potential applications for a sentinel model of human health. *Science of the Total Environment*, *512*, 489-494.

Mordukhovich, I., Kloog, I., Coull, B., Koutrakis, P., Vokonas, P., & Schwartz, J. (2016). Association between particulate air pollution and QT interval duration in an elderly cohort. *Epidemiology (Cambridge, Mass.)*, *27*(2), 284.

Morger, J., Bajnok, J., Boyce, K., Craig, P. S., Rogan, M. T., Lun, Z. R., ... & Tschirren, B. (2014). Naturally occurring Toll-like receptor 11 (TLR11) and Toll-like receptor 12 (TLR12) polymorphisms are not associated with *Toxoplasma gondi*i infection in wild wood mice. *Infection, Genetics and Evolution*, *26*, 180-184.

Morley, E. K., Williams, R. H., Hughes, J. M., Terry, R. S., Duncanson, P., Smith, J. E., & Hide, G. (2005). Significant familial differences in the frequency of abortion and *Toxoplasma gondi*i infection within a flock of Charollais sheep. *Parasitology*, *131*(2), 181-185.

Mun, H. S., Aosai, F., Norose, K., Chen, M., Piao, L. X., Takeuchi, O., ... & Yano, A. (2003). TLR2 as an essential molecule for protective immunity against *Toxoplasma gondi*i infection. *International immunology*, *15*(9), 1081-1087.

Murad, F. (2006). Shattuck lecture. *Nitric oxide and cyclic GMP in cell signaling and drug development. N Engl J Med*, *355*(19), 2003-2011.
Murad, F. (2006). Shattuck lecture. *Nitric oxide and cyclic GMP in cell signaling and drug development. N Engl J Med*, *355*(19), 2003-2011.

Muramatsu, T., Mizutani, Y., Ohmori, Y., & Okumura, J. I. (1997). Comparison of three nonviral transfection methods for foreign gene expression in early chicken embryosin ovo. *Biochemical and biophysical research communications*, *230*(2), 376-380.
Murphy, R. G., Williams, R. H., Hughes, J. M., Hide, G., Ford, N. J., & Oldbury, D. J. (2008). The urban house mouse (Mus domesticus) as a reservoir of infection for the human parasite *Toxoplasma gondii*: an unrecognised public health issue?. *International journal of environmental health research*, *18*(3), 177-185.

Murphy, R. G., Williams, R. H., Hughes, J. M., Hide, G., Ford, N. J., & Oldbury, D. J. (2008). The urban house mouse (Mus domesticus) as a reservoir of infection for the

human parasite *Toxoplasma gondii*: an unrecognised public health issue?. *International journal of environmental health research*, *18*(3), 177-185.

Muthukumaran, K. (2016). Studying the effects of Ubisol-Q10 in animal models of Alzheimer's and Parkinson's disease.

Negara, L. A. (2015). Nasionalisme. *Modul Pendidikan dan Pelatihan Prajabatan Golongan III. LAN. https://doi. org/10.1017/CBO9781107415324*, *4*.

Nielsen, S. S., Checkoway, H., Criswell, S. R., Farin, F. M., Stapleton, P. L., Sheppard, L., & Racette, B. A. (2015). Inducible nitric oxide synthase gene methylation and parkinsonism in manganese-exposed welders. *Parkinsonism & related disorders*, *21*(4), 355-360.

Noël, A., Xiao, R., Perveen, Z., Zaman, H., Le Donne, V., & Penn, A. (2017). Sex-specific lung functional changes in adult mice exposed only to second-hand smoke in utero. *Respiratory research*, *18*(1), 104.

Nowakowska, D., Colón, I., Remington, J. S., Grigg, M., Golab, E., Wilczynski, J., & Sibley, L. D. (2006). Genotyping of *Toxoplasma gondii* by multiplex PCR and peptide-based serological testing of samples from infants in Poland diagnosed with congenital toxoplasmosis. *Journal of Clinical Microbiology*, *44*(4), 1382-1389.

Nunez, R., Spiro, B., Pentecost, A., Kim, A., & Coletta, P. (2002). Organo-geochemical and stable isotope indicators ofenvironmental change in a marl lake, Malham Tarn, North Yorkshire, UK. *Journal of Paleolimnology*, *28*(4), 403-417.

Orciari, L. A., Niezgoda, M., Hanlon, C. A., Shaddock, J. H., Sanderlin, D. W., Yager, P. A., & Rupprecht, C. E. (2001). Rapid clearance of SAG-2 rabies virus from dogs after oral vaccination. *Vaccine*, *19*(31), 4511-4518.

Osterholzer, J. J., Olszewski, M. A., Murdock, B. J., Chen, G. H., Erb-Downward, J. R., Subbotina, N., ... & Horowitz, J. C. (2013). Implicating exudate macrophages and Ly-6Chigh monocytes in CCR2-dependent lung fibrosis following gene-targeted alveolar injury. *The Journal of Immunology*, *190*(7), 3447-3457.

Pak, T. R., Lynch, G. R., & Tsai, P. S. (2002). Estrogen accelerates gonadal recrudescence in photo-regressed male Siberian hamsters. *Endocrinology*, *143*(10), 4131-4134.

Panni, T., Mehta, A. J., Schwartz, J. D., Baccarelli, A. A., Just, A. C., Wolf, K., ... & Waldenberger, M. (2016). Genome-wide analysis of DNA methylation and fine particulate matter air pollution in three study populations: KORA F3, KORA F4, and the Normative Aging Study. *Environmental health perspectives*, *124*(7), 983-990.

Pappas, G., Roussos, N., & Falagas, M. E. (2009). Toxoplasmosis snapshots: global status of *Toxoplasma gondii* seroprevalence and implications for pregnancy and congenital toxoplasmosis. *International journal for parasitology*, *39*(12), 1385-1394.

Pavanello, S., Bonzini, M., Angelici, L., Motta, V., Pergoli, L., Hoxha, M., ... & Baccarelli, A. (2016). Extracellular vesicle-driven information mediates the long-term

effects of particulate matter exposure on coagulation and inflammation pathways. *Toxicology letters*, *259*, 143-150.

Peng, C., Bind, M. A. C., Colicino, E., Kloog, I., Byun, H. M., Cantone, L., ... & Vokonas, P. S. (2016). Particulate air pollution and fasting blood glucose in nondiabetic individuals: associations and epigenetic mediation in the normative aging study, 2000–2011. *Environmental health perspectives*, *124*(11), 1715-1721.

Peng, C., Luttmann-Gibson, H., Zanobetti, A., Cohen, A., De Souza, C., Coull, B. A., ... & Gold, D. R. (2016). Air pollution influences on exhaled nitric oxide among people with type II diabetes. *Air Quality, Atmosphere & Health*, *9*(3), 265-273.

Peng, C., Sanchez-Guerra, M., Wilson, A., Mehta, A. J., Zhong, J., Zanobetti, A., ... & Schwartz, J. (2017). Short-term effects of air temperature and mitochondrial DNA lesions within an older population. *Environment international*, *103*, 23-29.

Pérez, I., Varona, A., Blanco, L., Gil, J., Santaolalla, F., Zabala, A., ... & Larrinaga, G. (2009). Increased APN/CD13 and acid aminopeptidase activities in head and neck squamous cell carcinoma. *Head & Neck: Journal for the Sciences and Specialties of the Head and Neck*, *31*(10), 1335-1340.

Pifer, R., & Yarovinsky, F. (2011). Innate responses to *Toxoplasma gondii* in mice and humans. *Trends in parasitology*, *27*(9), 388-393.

Prandovszky, E., Gaskell, E., Martin, H., Dubey, J. P., Webster, J. P., & McConkey, G. A. (2011). The neurotropic parasite *Toxoplasma gondii* increases dopamine metabolism. *PloS one*, *6*(9).

Prendergast, G. C., & Jaffee, E. M. (Eds.). (2013). *Cancer immunotherapy: immune suppression and tumor growth*. Academic Press.

Proctor, M. C. F. (1994). Seasonal and shorter-term changes in surface-water chemistry on four English ombrogenous bogs. *Journal of Ecology*, 597-610.

Proctor, M. C. F. (1994). Seasonal and shorter-term changes in surface-water chemistry on four English ombrogenous bogs. *Journal of Ecology*, 597-610.

QIAGEN (2018) ‘RNeasy Fibrous Tissue Mini Handbook’, (January).

Qidwai, T., & Jamal, F. (2010). Inducible nitric oxide synthase (iNOS) gene polymorphism and disease prevalence. *Scandinavian journal of immunology*, *72*(5), 375-387

Qin, A., Lai, D. H., Liu, Q., Huang, W., Wu, Y. P., Chen, X., ... & Ayala, F. J. (2017). Guanylate-binding protein 1 (GBP1) contributes to the immunity of human mesenchymal stromal cells against *Toxoplasma gondii*. *Proceedings of the National Academy of Sciences*, *114*(6), 1365-1370.

Rai, P. K. (2016). Impacts of particulate matter pollution on plants: Implications for environmental biomonitoring. *Ecotoxicology and environmental safety*, *129*, 120-136.

Resch, G., Held, A., Faber, T., Panzer, C., Toro, F., & Haas, R. (2008). Potentials and prospects for renewable energies at global scale. *Energy policy*, *36*(11), 4048-4056.

Roach, H. I., & Aigner, T. (2007). DNA methylation in osteoarthritic chondrocytes: a new molecular target. *Osteoarthritis and cartilage*, *15*(2), 128-137.

Robertson, S., & Miller, M. R. (2018). Ambient air pollution and thrombosis. *Particle and fibre toxicology*, *15*(1), 1.

Rogan, M. T., Craig, P. S., Hide, G., Heath, S., Pickles, A., & Storey, D. M. (2007). The occurrence of the trematode Plagiorchis muris in the wood mouse *Apodemus sylvaticus* in North Yorkshire, UK. *Journal of helminthology*, *81*(1), 57-62.

Rouatbi, M., Amdouni, Y., Amairia, S., Rjeibi, M. R., Sammoudi, S., Rekik, M., & Gharbi, M. (2017). Molecular detection and phylogenetic analyses of *Toxoplasma gondii* from naturally infected sheep in Northern and Central Tunisia. *Veterinary medicine and science*, *3*(1), 22-31.

Ruan, W. K., & Zheng, S. J. (2011). Polymorphisms of chicken toll-like receptor 1 type 1 and type 2 in different breeds. *Poultry science*, *90*(9), 1941-1947.
Ruan, W. K., Wu, Y. H., An, J., Cui, D. F., Li, H. R., & Zheng, S. J. (2012). Toll-like receptor 2 type 1 and type 2 polymorphisms in different chicken breeds. *Poultry science*, *91*(1), 101-106.

Rummel, J. D., Beaty, D. W., Jones, M. A., Bakermans, C., Barlow, N. G., Boston, P. J., ... & Hallsworth, J. E. (2014). A new analysis of Mars “special regions”: findings of the second MEPAG Special Regions Science Analysis Group (SR-SAG2).

Ruzicka, W. B. (2015). Epigenetic mechanisms in the pathophysiology of psychotic disorders. *Harvard review of psychiatry*, *23*(3), 212.

Sabounchi, S., Bollyky, J., & Nadeau, K. (2015). Review of environmental impact on the epigenetic regulation of atopic diseases. *Current allergy and asthma reports*, *15*(6), 33.

Sanchez-Guerra, M., Zheng, Y., Osorio-Yanez, C., Zhong, J., Chervona, Y., Wang, S., ... & Koutrakis, P. (2015). Effects of particulate matter exposure on blood 5-hydroxymethylation: results from the Beijing truck driver air pollution study. *Epigenetics*, *10*(7), 633-642.

Sando, D., Appert, F., Burns, S. R., Zhang, Q., Gallais, Y., Sacuto, A., ... & Le Breton, J. M. (2019). Influence of flexoelectricity on the spin cycloid in (110)-oriented BiFe O 3 films. *Physical Review Materials*, *3*(10), 104404.

Santibáñez-Andrade, M., Quezada-Maldonado, E. M., Osornio-Vargas, Á., Sánchez-Pérez, Y., & García-Cuellar, C. M. (2017). Air pollution and genomic instability: the role of particulate matter in lung carcinogenesis. *Environmental Pollution*, *229*, 412-422.

Schubert, D. W. (1997). Spin coating as a method for polymer molecular weight determination. *Polymer Bulletin*, *38*(2), 177-184.

Schumacher, C. L., Coulon, P., Lafay, F., Benejean, J., Aubert, M. F. A., Barrat, J., ... & Flamand, A. (1993). SAG-2 oral rabies vaccine.

Schuster, J., Uzun, A., Stablia, J., Schorl, C., Mori, M., & Padbury, J. F. (2019). Effect of prematurity on genome wide methylation in the placenta. *BMC medical genetics*, *20*(1), 116.

Shen, H., Martin, F. L., & Su, Y. (2014). Environmental chemical stressors as epigenome modifiers: a new horizon in assessment of toxicological effects. *Chinese science bulletin*, *59*(4), 349-355.

Shen, J., Lai, D. H., Wilson, R. A., Chen, Y. F., Wang, L. F., Yu, Z. L., ... & Yang, T. B. (2017). Nitric oxide blocks the development of the human parasite Schistosoma japonicum. *Proceedings of the National Academy of Sciences*, *114*(38), 10214-10219.

Shiue, S. M., Huang, L. J., Tsai, W. H., & Chen, Y. L. (2018, October). On Four Metaheuristic Applications to Speech Enhancement—Implementing Optimization Algorithms with MATLAB R2018a. In *Proceedings of the 30th Conference on Computational Linguistics and Speech Processing (ROCLING 2018)* (pp. 266-275).

Shu, K., Kuang, N., Zhang, Z., Hu, Z., Zhang, Y., Fu, Y., & Min, W. (2014). Therapeutic effect of daphnetin on the autoimmune arthritis through demethylation of proapoptotic genes in synovial cells. *Journal of translational medicine*, *12*(1), 287.

Shyamasundar, S., Ng, C. T., Lanry Yung, L. Y., Dheen, S. T., & Bay, B. H. (2015). Epigenetic mechanisms in nanomaterial-induced toxicity. *Epigenomics*, *7*(3), 395-411.
Sibley, L. D., & Boothroyd, J. C. (1992). Virulent strains of *Toxoplasma gondii* comprise a single clonal lineage. *Nature*, *359*(6390), 82-85.

Sibley, L. D., & Boothroyd, J. C. (1992). Virulent strains of *Toxoplasma gondii* comprise a single clonal lineage. *Nature*, *359*(6390), 82-85.

Smith, G. C., Gangadharan, B., Taylor, Z., Laurenson, M. K., Bradshaw, H., Hide, G., ... & Craig, P. S. (2003). Prevalence of zoonotic important parasites in the red fox (Vulpes vulpes) in Great Britain. *Veterinary parasitology*, *118*(1-2), 133-142.

Somineni, H. K., Zhang, X., Myers, J. M. B., Kovacic, M. B., Ulm, A., Jurcak, N., ... & Ji, H. (2016). Ten-eleven translocation 1 (TET1) methylation is associated with childhood asthma and traffic-related air pollution. *Journal of Allergy and Clinical Immunology*, *137*(3), 797-805.

Soo, R., Putti, T., Tao, Q., Goh, B. C., Lee, K. H., Kwok-Seng, L., ... & Hsieh, W. S. (2005). Overexpression of cyclooxygenase-2 in nasopharyngeal carcinoma and association with epidermal growth factor receptor expression. *Archives of Otolaryngology–Head & Neck Surgery*, *131*(2), 147-152.

Spanò, M., & Pacchierotti, F. (2015). Environmental Impact on DNA Methylation in the Germline: State of the Art and Gaps of Knowledge.

Spink, J., & Evans, T. (1997). Binding of the transcription factor interferon regulatory factor-1 to the inducible nitric-oxide synthase promoter. *Journal of Biological Chemistry*, *272*(39), 24417-24425.

Stevens, R. C., Steele, J. L., Glover, W. R., Sanchez-Garcia, J. F., Simpson, S. D., O'Rourke, D., ... & Shuber, A. P. (2019). A novel CRISPR/Cas9 associated technology for sequence-specific nucleic acid enrichment. *PloS one*, *14*(4).

Stovall, M., Smith, S. A., Langholz, B. M., Boice Jr, J. D., Shore, R. E., Andersson, M., ... & Malone, K. E. (2008). Dose to the contralateral breast from radiotherapy and risk of second primary breast cancer in the WECARE study. *International Journal of Radiation Oncology* Biology* Physics*, *72*(4), 1021-1030.

Sturge, C. R., & Yarovinsky, F. (2014). Complex immune cell interplay in the gamma interferon response during *Toxoplasma gondii* infection. *Infection and immunity*, *82*(8), 3090-3097.

Su, C., Khan, A., Zhou, P., Majumdar, D., Ajzenberg, D., Dardé, M. L., ... & Sibley, L. D. (2012). Globally diverse *Toxoplasma gondii* isolates comprise six major clades originating from a small number of distinct ancestral lineages. *Proceedings of the National Academy of Sciences*, *109*(15), 5844-5849.

Sun, B., Shi, Y., Yang, X., Zhao, T., Duan, J., & Sun, Z. (2018). DNA methylation: A critical epigenetic mechanism underlying the detrimental effects of airborne particulate matter. *Ecotoxicology and environmental safety*, *161*, 173-183.

Swiderski, K., Caldow, M. K., Naim, T., Trieu, J., Chee, A., Koopman, R., & Lynch, G. S. (2019). Deletion of suppressor of cytokine signaling 3 (SOCS3) in muscle stem cells does not alter muscle regeneration in mice after injury. *PloS one*, *14*(2).

Swiderski, K., Caldow, M. K., Naim, T., Trieu, J., Chee, A., Koopman, R., & Lynch, G. S. (2019). Deletion of suppressor of cytokine signaling 3 (SOCS3) in muscle stem cells does not alter muscle regeneration in mice after injury. *PloS one*, *14*(2).

Swift, M. L. (1997). GraphPad prism, data analysis, and scientific graphing. *Journal of chemical information and computer sciences*, *37*(2), 411-412.

Takeuchi, O., & Akira, S. (2010). Pattern recognition receptors and inflammation. *Cell*, *140*(6), 805-820.

Tallei, T. E., & Pelealu, J. J. (2019). The data on metagenomic profile of bacterial diversity changes in the different concentration of fermented romaine lettuce brine. *Data in brief*, *25*, 104190.

Tao, M. H., Zhou, J., Rialdi, A. P., Martinez, R., Dabek, J., Scelo, G., ... & Boffetta, P. (2014). Indoor air pollution from solid fuels and peripheral blood DNA methylation: findings from a population study in Warsaw, Poland. *Environmental research*, *134*, 325-330.

Tarantini, L., Bonzini, M., Apostoli, P., Pegoraro, V., Bollati, V., Marinelli, B., ... & Bertazzi, P. A. (2009). Effects of particulate matter on genomic DNA methylation content and iNOS promoter methylation. *Environmental health perspectives*, *117*(2), 217-222.

Tenter, A. M., Heckeroth, A. R., & Weiss, L. M. (2000). *Toxoplasma gondii*: from animals to humans. *International journal for parasitology*, *30*(12-13), 1217-1258.

Tenter, A. M., Heckeroth, A. R., & Weiss, L. M. (2001). Erratum-*Toxoplasma gondii*: From animals to humans (International Journal for Parasitology (2000) 30 (1217-1258) PII: S0020751900001247). *International Journal for Parasitology*, *31*(2), 217-220

Terry, R. S., Smith, J. E., Duncanson, P., & Hide, G. (2001). MGE-PCR: a novel approach to the analysis of *Toxoplasma gondii* strain differentiation using mobile genetic elements. *International journal for parasitology*, *31*(2), 155-161.

Thomasson, D., Wright, E. A., Hughes, J. M., Dodd, N. S., Cox, A. P., Boyce, K., ... & Rogan, M. T. (2011). Prevalence and co-infection of *Toxoplasma gondii* and Neospora caninum in *Apodemus sylvaticus* in an area relatively free of cats. *Parasitology*, *138*(9), 1117-1123.

Tobie, E. J., von Brand, T., & Mehlman, B. (2001). Cultural and physiological observations on Trypanosoma rhodesiense and Trypanosoma gambiense. *Journal of Parasitology*, *87*(4), 714-717.

Toraño, E. G., García, M. G., Fernández-Morera, J. L., Niño-García, P., & Fernández, A. F. (2016). The impact of external factors on the epigenome: in utero and over lifetime. *BioMed research international*, *2016*.

Torrone, D. Z., Kuriakose, J. S., Moors, K., Jiang, H., Niedzwiecki, M. M., Perera, F. F., & Miller, R. L. (2012). Reproducibility and intraindividual variation over days in buccal cell DNA methylation of two asthma genes, interferon γ (IFNγ) and inducible nitric oxide synthase (iNOS). *Clinical epigenetics*, *4*(1), 3.

Tretyakova, N., & Wang, Y. (2018). Epigenetics in Toxicology.

Vaiserman, A. (2016). Epidemiological Epigenetics in Medicine. In *Medical Epigenetics* (pp. 67-86). Academic Press.

Vaitkienė, P., Skiriutė, D., Skauminas, K., & Tamašauskas, A. (2013). GATA4 and DcR1 methylation in glioblastomas. *Diagnostic pathology*, *8*(1), 7.

Vannier, E., & Krause, P. J. (2012). Human babesiosis. *New England Journal of Medicine*, *366*(25), 2397-2407.

Vannini, F., Kashfi, K., & Nath, N. (2015). The dual role of iNOS in cancer. *Redox biology*, *6*, 334-343.

Wang, H., Tanihata, T., Fukumoto, S., & Hirai, K. (1997). Excretory/secretory products of plerocercoids of Spirometra erinaceieuropaei induce the expression of inducible nitric oxide synthase mRNA in murine hepatocytes. *International journal for parasitology*, *27*(4), 367-375.

Wang, S., Gao, M., An, T., Liu, Y., Jin, J., Wang, G., ... & Wang, J. (2015). Genetic diversity and virulence of novel sequence types of Streptococcus suis from diseased and healthy pigs in China. *Frontiers in microbiology*, *6*, 173.

Wang, T., Gao, J. M., Yi, S. Q., Geng, G. Q., Gao, X. J., Shen, J. L., ... & Lun, Z. R. (2014). *Toxoplasma gondii* infection in the peritoneal macrophages of rats treated with glucocorticoids. *Parasitology research*, *113*(1), 351-358.

Wang, Z., Neuburg, D., Li, C., Su, L., Kim, J. Y., Chen, J. C., & Christiani, D. C. (2005). Global gene expression profiling in whole-blood samples from individuals exposed to metal fumes. *Environmental health perspectives*, *113*(2), 233-241.

Wei, X. Q., Charles, I. G., Smith, A., Ure, J., Feng, G. J., Huang, F. P., ... & Liew, F. Y. (1995). Altered immune responses in mice lacking inducible nitric oxide synthase. *Nature*, *375*(6530), 408-411.

Weinberg, J. B., Granger, D. L., Pisetsky, D. S., Seldin, M. F., Misukonis, M. A., Mason, S. N., ... & Gilkeson, G. S. (1994). The role of nitric oxide in the pathogenesis of spontaneous murine autoimmune disease: increased nitric oxide production and nitric oxide synthase expression in MRL-lpr/lpr mice, and reduction of spontaneous glomerulonephritis and arthritis by orally administered NG-monomethyl-L-arginine. *The Journal of experimental medicine*, *179*(2), 651-660.

Weinberg, J. B., Misukonis, M. A., Shami, P. J., Mason, S. N., Sauls, D. L., Dittman, W. A., ... & Bachus, K. E. (1995). Human mononuclear phagocyte inducible nitric oxide synthase (iNOS): analysis of iNOS mRNA, iNOS protein, biopterin, and nitric oxide production by blood monocytes and peritoneal macrophages.

Weiner, L. (2008). Cancer Immunotherapy: Immune Suppression and Tumor Growth. *The New England Journal of Medicine*, *358*(16), 1764-1765.

Weiss, L. M., & Dubey, J. P. (2009). Toxoplasmosis: a history of clinical observations. *International journal for parasitology*, *39*(8), 895-901.

Wen, Y. Z., Lun, Z. R., Zhu, X. Q., Hide, G., & Lai, D. H. (2016). Further evidence from SSCP and ITS DNA sequencing support Trypanosoma evansi and Trypanosoma equiperdum as subspecies or even strains of Trypanosoma brucei. *Infection, Genetics and Evolution*, *41*, 56-62.

Wheeler, D., & Bhagwat, M. (2007). BLAST quickstart. In *Comparative Genomics* (pp. 149-175). Humana Press.

Wheeler, D., & Bhagwat, M. (2007). BLAST quickstart. In *Comparative Genomics* (pp. 149-175). Humana Press.

Wiley, K. E., Zuo, Y., Macartney, K. K., & McIntyre, P. B. (2013). Sources of pertussis infection in young infants: a review of key evidence informing targeting of the cocoon strategy. *Vaccine*, *31*(4), 618-625.

Williams, R. H., Morley, E. K., Hughes, J. M., Duncanson, P., Terry, R. S., Smith, J. E., & Hide, G. (2005). High levels of congenital transmission of *Toxoplasma gondii* in longitudinal and cross-sectional studies on sheep farms provides evidence of vertical transmission in ovine hosts. *Parasitology*, *130*(3), 301-307.

Wilson, M. S., Feng, C. G., Barber, D. L., Yarovinsky, F., Cheever, A. W., Sher, A., ... & Wynn, T. A. (2010). Redundant and pathogenic roles for IL-22 in mycobacterial, protozoan, and helminth infections. *The Journal of Immunology*, *184*(8), 4378-4390.

Xu, W., Charles, I. G., Liu, L., Moncada, S., & Emson, P. (1996). Molecular cloning and structural organization of the human inducible nitric oxide synthase gene (NOS2). *Biochemical and biophysical research communications*, *219*(3), 784-788.

Yamashita, T., Agulnick, A. D., Copeland, N. G., Gilbert, D. J., Jenkins, N. A., & Westphal, H. (1998). Genomic structure and chromosomal localization of the mouse LIM domain-binding protein 1 gene, Ldb1. *Genomics*, *48*(1), 87-92.

Yan, C., Liang, L. J., Zhang, B. B., Lou, Z. L., Zhang, H. F., Shen, X., ... & Zheng, K. Y. (2014). Prevalence and genotyping of *Toxoplasma gondii* in naturally-infected synanthropic rats (Rattus norvegicus) and mice (Mus musculus) in eastern China. *Parasites & vectors*, *7*(1), 591.

Yang, D. Y., Eng, B., Waye, J. S., Dudar, J. C., & Saunders, S. R. (1998). Improved DNA extraction from ancient bones using silica-based spin columns. *American Journal of Physical Anthropology: The Official Publication of the American Association of Physical Anthropologists*, *105*(4), 539-543.

Yang, L., Hou, X. Y., Wei, Y., Thai, P., & Chai, F. (2017). Biomarkers of the health outcomes associated with ambient particulate matter exposure. *Science of the Total Environment*, *579*, 1446-1459.

Yang, P., Zhou, B., Cao, W. C., Wang, Y. X., Huang, Z., Li, J., ... & Zeng, Q. (2017). Prenatal exposure to drinking water disinfection by-products and DNA methylation in cord blood. *Science of the Total Environment*, *586*, 313-318.

Yarovinsky, F. (2014). Innate immunity to *Toxoplasma gondii* infection. *Nature Reviews Immunology*, *14*(2), 109-121.

Yin, C. C., He, Y., Zhou, D. H., Yan, C., He, X. H., Wu, S. M., ... & Zhu, X. Q. (2010). Seroprevalence of *Toxoplasma gondii* in rats in southern China. *Journal of Parasitology*, *96*(6), 1233-1234.

Yu, L., Faustina Pappoe, F., & Shen, J. (2019). Strategies Developed by *Toxoplasma* to Survive in Host. *Frontiers in microbiology*, *10*, 899.

Zhang, Q., Wang, W., Niu, Y., Xia, Y., Lei, X., Huo, J., ... & Ying, Z. (2019). The effects of fine particulate matter constituents on exhaled nitric oxide and DNA methylation in the arginase–nitric oxide synthase pathway. *Environment international*, *131*, 105019.

Zhao, Z. J., Zhang, J., Wei, J., Li, Z., Wang, T., Yi, S. Q., ... & Lun, Z. R. (2013). Lower expression of inducible nitric oxide synthase and higher expression of arginase in rat alveolar macrophages are linked to their susceptibility to *Toxoplasma gondii* infection. *Plos one*, *8*(5).

http://www.ebi.ac.uk/ena/data/view/GCA_001305905.1

http://www.physics.csbsju.edu/stats/contingency_NROW_NCOLUMN_form.html

http://www.zymoresearch.com/tools/bisulfite

https://blast.ncbi.nlm.nih.gov/Blast.cg

https://blast.ncbi.nlm.nih.gov/Blast.cgi?PAGE_TYPE=BlastSearch&PROG_DEF=blastn&BLAST_SPEC=Assembly&ASSEMBLY_NAME=GCA_001305905.1

https://en.freedownloadmanager.org/Windows-PC/FinchTV-FREE.html

https://nt.global.ssl.fastly.net/images/mapeasystrollmalhamwatersinkstomalhamtarn.jpg

https://www.bioinformatics.org/sms/rev_comp.html

https://www.ebi.ac.uk/Tools/msa/clustalo/

https://www.graphpad.com/demos

https://www.idtdna.com

https://www.idtdna.com/pages/tools/oligoanalyzer

https://www.ncbi.nlm.nih.gov/assembly/GCA_001305905.1/

https://www.sourcebioscience.com

https://www.thermofisher.com/uk/en/home/brands/thermo-scientific/molecular-biology/molecular-biology-learning-center/molecular-biology-resource-library/thermo-scientific-web-tools/multiple-primer-analyzer.html

https://www.zymoresearch.com/pages/bisulfite-primer-seeker

www.scienceprimer.com/copy-number-calculator-for-realtime-pcr.

https://web.stanford.edu/group/parasites/ParaSites2006/Toxoplasmosis/references.html

Appendix:

Table 5-5 Variation in methylation patterns in the CpG islands of the iNOS gene promoter and Exon 1.

Mouse code	Diagnosis of *Toxoplasma*	DNA Code	CpG^{-476}	CpG^{-394}	CpG^{-392}	CpG^{-175}	CpG^{-119}	CpG^{-59}	CpG^{47}
J88	+	E19	NS	NS	NS	C/C	C^m/C^m	C/C	C^m/C^m
J89	+	E20	NS	NS	NS	C/C	C^m/C^m	C/C	C^m/C^m
J97	+	E21	NS	NS	NS	C/C	C/C	C/C	C^m/C^m
J99	+	E22	NS	NS	NS	C/C	C/C	C/C	C^m/C^m
J102	+	E23	NS	NS	NS	C/C	C^m/C^m	C/C	C^m/C^m
J103	+	E24	NS	NS	NS	C/C	C^m/C^m	C/C	C^m/C^m
J106	+	E25	NS	NS	NS	C^m/C	C^m/C^m	A	C^m/C^m
J108	+	E26	NS	NS	NS	C^m/C	C^m/C	C/C	C^m/C^m
J110	+	E27	NS	NS	NS	C/C	C^m/C^m	C/C	C^m/C^m
J111	+	E28	NS	NS	NS	C/C	C/C	C/C	C^m/C^m
J112	+	E29	NS	NS	NS	C/C	C^m/C	C/C	C^m/C^m
J113	+	E30	NS	NS	NS	NS	C^m/C^m	C/C	C^m/C^m
J114	+	E31	G	A	C/C	C/C	C/C	C/C	C^m/C^m
J115	+	E32	C/C	C^m/C	C^m/C	C/C	C/C	C/C	C^m/C
J116	+	E33	G	C^m/C^m	C/C	C/C	C^m/C^m	C/C	C^m/C^m
J117	+	E34	G	C^m/C^m	C/C	C/C	C^m/C^m	C/C	C^m/C
J118	+	E35	G	C^m/C	C/C	C/C	C^m/C^m	C/C	C^m/C^m
J119	+	E36	C/C	C^m/C	C/C	C/C	C/C	C/C	C^m/C^m
J121	+	E37	G	C^m/C	C/C	C/C	C^m/C^m	C/C	C^m/C^m
J123	+	E38	C/C	C^m/C	C^m/C	C/C	C^m/C^m	C/C	C^m/C
J124	+	E39	G	C^m/C^m	C/C	C/C	C/C	C/C	C^m/C^m
J125	+	E40	C/C	C^m/C	C/C	C/C	C^m/C^m	C/C	C^m/C
J6	+	B6	G	A	C/C	C/C	C^m/C	C/C	C^m/C^m
J59	+	B22	G	C^m/C	C/C	C/C	C/C	C/C	C^m/C^m

J32	+	B23	G	A	C/C	C/C	C^m/C^m	C/C	C^m/C^m
J120	+	B24	C^m/C^m	C^m/C^m	C/C	C/C	C/C	C/C	C^m/C
J1	-	M1	g	C^m/C	C/C	C/C	C^m/C^m	C/C	C/C
J2	-	M2	G	C^m/C	C^m/C	C/C	C^m/C^m	C/C	C^m/C^m
J3	-	M3	C/C	A	C^m/C	C/C	C/C	C/C	C^m/C^m
J10	-	M4	C/C	C^m/C	C/C	C/C	C/C	C/C	C/C
J11	-	M5	G	C^m/C^m	C/C	C/C	C/C	C/C	C^m/C
J14	-	M6	G	A	C/C	C/C	C/C	C/C	C^m/C
J15	-	M7	G	A	C/C	C/C	C/C	C/C	C/C
J22	-	M8	G	C/C	C/C	C/C	C/C	C/C	C^m/C
J24	-	M9	G	C^m/C^m	C/C	C/C	C^m/C^m	C/C	C^m/C^m
J27	-	M10	G	A	C/C	C/C	C^m/C	C/C	C/C
J29	-	M11	G	A	C/C	C/C	C/C	C/C	C^m/C
J30	-	M12	G	A	C^m/C	C/C	C^m/C^m	A	C^m/C^m
J34	-	M14	G	C^m/C^m	C/C	C/C	C/C	C/C	C/C
J35	-	M15	G	A	C/C	C/C	C/C	C/C	C^m/C^m
J36	-	M16	C^m/C	C^m/C^m	C/C	C/C	C/C	C/C	C^m/C
J37	-	M17	G	C^m/C	C^m/C	C/C	C/C	C/C	C^m/C^m
J39	-	M18	C/C	C^m/C	C^m/C	C/C	C^m/C^m	C/C	C^m/C
J40	-	1NB	C/C	C/C	G	C/C	C/C	C/C	C^m/C^m
J41	-	2NB	C/C	A	C/C	C/C	C/C	C/C	C^m/C^m
J42	-	M19	G	A	C/C	C/C	C/C	C/C	C^m/C^m
J45	-	3NB	NS	NS	NS	C/C	C/C	C/C	C/C
J47	-	M20	G	C/C	C/C	C/C	C^m/C^m	C/C	C^m/C
J48	-	M21	C/C	C^m/C	C^m/C	C/C	C^m/C^m	C/C	C^m/C^m
J49	-	M22	G	A	C/C	C/C	C^m/C^m	C/C	C^m/C
J50	-	M23	G	C/C	C/C	C/C	C/C	C/C	C^m/C^m
J55	-	M24	G	C^m/C^m	C/C	C/C	C^m/C^m	C/C	C^m/C
J63	-	M25	G	C^m/C^m	C/C	C/C	C/C	C/C	C^m/C^m
J65	-	M26	G	C^m/C	C^m/C^m	C/C	C^m/C^m	C/C	C^m/C^m

J66	-	M27	G	A	C/C	C/C	C^m/C^m	C/C	C^m/C^m
J 67	-	M28	G	A	C/C	C/C	C/C	C/C	C^m/C^m
J68	-	M29	G	C^m/C^m	C/C	C/C	C/C	C/C	C^m/C^m
J69	-	M30	G	C^m/C^m	C/C	C/C	C/C	C/C	C^m/C^m
J70	-	M31	C^m/C^m	C^m/C^m	C^m/C	C/C	C^m/C^m	C/C	C^m/C
J73	-	M32	A	C^m/C^m	C/C	C/C	C/C	C/C	C^m/C^m
J74	-	M33	C/C	C/C	C/C	C/C	C/C	C/C	C^m/C^m
J76	-	M35	G	C^m/C^m	C/C	C/C	C^m/C^m	C/C	C^m/C
J77	-	4NB	NS	NS	NS	C/C	C/C	C/C	C^m/C^m
J80	-	M36	G	C^m/C^m	C/C	C/C	C^m/C^m	C/C	C^m/C
J81	-	M37	C^m/C	C^m/C^m	C^m/C	C/C	C^m/C^m	C/C	C^m/C^m
J82	-	M38	NS	NS	NS	C/C	C^m/C^m	C/C	C^m/C^m
J90	-	7NB	NS	NS	NS	C/C	C^m/C^m	NS	NS
J91	-	8NB	NS	NS	NS	NS	A	NS	C^m/C^m
J93	-	9NB	NS	NS	NS	NS	NS	C^m/C^m	NS
J94	-	M39	NS	NS	NS	C/C	C^m/C^m	C/C	C^m/C
J95	-	10 NB	NS	NS	NS	C/C	C/C	C/C	C^m/C^m
J96	-	M40	NS	NS	NS	C/C	C^m/C^m	C/C	C^m/C
J100	-	M41	NS	NS	NS	C^m/C	C^m/C	C/C	C^m/C
J101	-	M43	NS	NS	NS	NS	C^m/C^m	C/C	C^m/C^m
J104	-	M44	NS	NS	NS	C/C	C^m/C^m	C/C	C^m/C
J105	-	M45	NS	NS	NS	C/C	C^m/C^m	C/C	C^m/C^m
J46	-	M46	NS	NS	NS	C/C	C^m/C^m	C/C	C^m/C
J4	-		C^m/C	C^m/C	C/C	C/C	C^m/C^m	C/C	C^m/C
J5	-	B1	C/C	A	C/C	C/C	C^m/C	C/C	C^m/C^m
J9	-	B2	C/C	A	C/C	C/C	C/C	C/C	C^m/C
11	-	B3	C^m/C	C^m/C^m	C/C	C/C	C^m/C^m	C/C	C^m/C^m
J12	-	B4	C^m/C	A	C/C	C/C	C^m/C^m	C/C	C^m/C
J13	-	B5	G	A	C/C	C/C	C/C	C/C	C^m/C^m

J16	-	B6	C^m/C^m	C^m/C^m	C/C	C/C	C/C	C/C	C^m/C
J18	-	B7	G	C^m/C^m	C/C	C/C	C^m/C^m	C/C	C^m/C^m
J20	-	B9	A	C^m/C^m	C/C	C/C	C/C	C/C	C/C
J21	-	B10	G	C^m/C^m	C/C	C/C	C/C	C/C	C^m/C^m
J25	-	B11	A	C^m/C^m	C/C	C/C	C^m/C^m	C/C	C^m/C
J26	-	B12	NS	NS	NS	C/C	C^m/C^m	C/C	C^m/C^m
J33	-	B13	NS	C^m/C	C/C	C/C	C^m/C^m	C/C	C^m/C^m
J38	-	B14	C/C	C^m/C^m	C/C	C/C	C/C	C/C	C^m/C^m
J46	-	B15	G	A	C/C	C/C	C/C	C/C	C^m/C^m
J51	-	NS	G	C/C	C/C	C/C	C/C	C/C	NS
J56	-	B16	C/C	C/C	C/C	C/C	C^m/C^m	C/C	C/C
J57	-	B17	NS	NS	NS	C/C	C^m/C^m	C/C	C^m/C^m
J58	-	B18	C^m/C	C^m/C^m	C/C	C/C	C^m/C^m	C/C	C^m/C^m
J61	-	B20	C/C	C/C	C/C	C/C	C^m/C^m	C/C	C^m/C^m
J64	-	B21	A	C^m/C^m	C/C	C/C	C/C	C/C	C^m/C^m
83	-		G	C^m/C^m	C/C	C/C	C/C	C/C	C^m/C^m
98	-		G	A	C/C	C/C	C/C	C/C	C^m/C^m
406	+	6S	NS	NS	NS	C^m/C^m	C^m/C^m	C/C	C^m/C^m
411	-	11S	NS	NS	NS	NS	C^m/C^m	C/C	C^m/C^m
412	+	12S	NS	NS	NS	NS	NS	C^m/C^m	C^m/C
414	-	14S	NS	NS	NS	NS	NS	C^m/C^m	C^m/C^m
415	-	15S	NS	NS	NS	C/C	C/C	C/C	C^m/C^m
417	-	17S	C^m/C	C/C	C^m/C^m	C/C	C^m/C^m	C/C	C^m/C^m
419	-	19S	NS	NS	NS	NS	C^m/C	C/C	C^m/C^m
421	+	21S	NS	NS	NS	NS	NS	C^m/C^m	C^m/C^m
422	-	22S	NS	NS	NS	C/C	C^m/C^m	C/C	C^m/C^m
423	-	23S	NS	NS	NS	NS	C^m/C	C/C	C^m/C^m
424	-	24S	NS	NS	NS	NS	NS	C/C	G
425	-	25S	NS	NS	NS	NS	NS	NS	C^m/C^m
426	-	26S	NS	NS	NS	NS	C^m/C^m	C/C^m	NS
430	+	30S	NS	C^m/C^m	C^m/C^m	C/C	C^m/C^m	C/C	C^m/C^m
434	+	34S	A	A	C^m/C	NS	C/C	A	C^m/C^m
436	-	36S	NS	A	C^m/C	NS	C/C	NS	NS